**FUNCTIONAL EVALUATION OF CIRCULATING ENDOTHELIAL
PROGENITOR CELLS FOR VASCULAR TISSUE ENGINEERING**

A Dissertation
Presented to
The Academic Faculty

by

Ann Elizabeth Ensley

In Partial Fulfillment
Of the Requirements for the Degree
Doctor of Philosophy in Bioengineering

Georgia Institute of Technology

May 2006

FUNCTIONAL EVALUATION OF CIRCULATING ENDOTHELIAL PROGENITOR CELLS FOR VASCULAR TISSUE ENGINEERING

Approved by:

Dr. Robert M. Nerem, Advisor
School of Mechanical Engineering
Georgia Institute of Technology

Dr. Suzanne G. Eskin
School of Biomedical Engineering
Georgia Institute of Technology

Dr. Gary G. Gibbons
Cardiovascular Research Institute
Morehouse School of Medicine

Dr. Stephen R. Hanson
Department of Biomedical Engineering
Oregon Health & Sciences University

Dr. Raymond P. Vito
School of Mechanical Engineering
Georgia Institute of Technology

Date Approved: March 28, 2006

For my parents, Neal and Barbara Ensley

and for my best friend, Kaj Miller

TABLE OF CONTENTS

CHAPTER VI: MICROARRAY ANALYSIS OF GENE EXPRESSION PROFILES OF ENDOTHELIAL PROGENITOR CELLS AND VASCULAR ENDOTHELIAL CELLS IN STATIC AND FLUID FLOW ENVIRONMENTS 83

LIST OF TABLES

LIST OF FIGURES

LIST OF ABBREVIATIONS

3-D   three-dimensional

acLDL   acetylated low density lipoprotein

ANOVA   analysis of variance

BOEC   blood outgrowth endothelial cells

cAMP   cyclic adenosine monophosphate

CDC   centers for disease control

cDNA   complementary DNA

CEC   circulating endothelial cell

DMSO   dimethyl sulphoxide

DNA   deoxyribonucleic acid

EC   endothelial cell

EGF   epidermal growth factor

ELISA   enzyme-linked immunosorbent assay

eNOS   endothelial nitric oxide synthase

EPC   endothelial progenitor cell

ePTFE   expanded polytetrafluoroethylene

F3   factor three

FGF-β   fibroblast growth factor beta

FITC   flourescein

flt-1   fms-related tyrosine kinase 1

HAEC   human aortic endothelial cell

HBSS	hanks balanced salt solution
HPP-ECFC	high proliferative potential-endothelial colony forming cells
HUVEC	human umbilical vein endothelial cells
ICAM-1	intercellular adhesion molecule 1
IGF	insulin growth factor
IL1-β	interleukin one beta
iNOS	inducible nitric oxide synthase
KDR	kinase insert domain receptor
LDL	low density lipoprotein
LPP-ECFC	low proliferative potential-endothelial colonly forming cells
MAPC	multipotent adult progenitor cell
MCAM	melanoma cell adhesion molecule
MESF	molecules of equivalent soluble flourescence
mRNA	messenger RNA
NaOH	sodium hydroxide
NO	nitric oxide
NOS3	nitric oxide synthase 3 (endothelial)
OEC	outgrowth endothelial cell
PAI-1	plasminogen activator inhibitor
PBMC	peripheral blood mononuclear cell
PBS	phosphate buffered saline
PECAM-1	platelet endothelial cell adhesion molecule 1
RNA	ribonucleic acid

RT-PCR	reverse-transcription polymerase chain reaction
SEM	scanning electron microscopy
SMA	smooth muscle actin
SMC	smooth muscle cell
TF	tissue factor
TFPI	tissue factor pathway inhibitor
THBD	thrombomodulin
TNF-α	tumor necrosis factor alpha
TPA	tissue plasminogen activator
UCB	umbilical cord blood
VCAM-1	vascular cell adhesion molecule 1
VEGF	vascular endothelial growth factor
VEGFR1	vascular endothelial growth factor receptor 1
VEGFR2	vascular endothelial growth factor receptor 2
vWF	von willebrand factor
WHO	world health organization

SUMMARY

One critical barrier to the success of vascular tissue engineering strategies is the need for appropriate endothelial cell sources. Adult stem and progenitor cells have emerged as a potentially promising cell source but very little is known about their functional potential. The endothelial cell (EC) resides on the vascular wall at the interface with flowing blood and is a key mediator of hemostasis and thrombosis. These studies investigated the use of endothelial progenitor cells (EPCs) derived from peripheral blood as a vascular lining on an engineered blood vessel substitute. Models were developed to investigate two aspects of the vascular environment, shear stress and substrate on EPC response at the gene, protein and functional levels. Isolation of EPC colonies from peripheral blood gave rise to cells which displayed an endothelial-like phenotype with expression of many EC specific markers and functions. Through the use of transcriptional profiling, results demonstrated that EPC gene expression was generally less sensitive to shear stress than ECs but shear stress preconditioning did result in upregulation of the EPC antioxidant defense system and promoted anticoagulant function. When co-cultured on a model of the vascular wall, EPCs altered their gene expression and favored a response more similar to mature vascular ECs. In a baboon arteriovenous shunt, shear stress preconditioned EPCs were able to resist platelet deposition and provided a non-thrombogenic lining on an engineered blood vessel substitute. Although significantly more research needs to be done, this work has provided an understanding of EPC function in the shear stress environment and provides evidence that EPCs are a viable endothelial cell source for vascular tissue engineering.

CHAPTER I: INTRODUCTION

Creation of a living blood vessel substitute has the potential to revolutionize the treatment of coronary heart disease, now the leading cause of death worldwide [1]. In the United States alone, there are over 71 million people suffering from one or more types of cardiovascular disease (including hypertension, coronary heart disease, heart failure, stroke, and congenital cardiovascular defects) with a cost burden exceeding 403 billion in 2006 [2]. The World Health Organization (WHO) states that "coronary heart disease…is on the rise and has become a true pandemic that respects no boarders" [1]. This increasing burden of disease combined with an increasing shortage of organs for transplant have heightened the need for alternative therapeutic strategies [3, 4]. Tissue engineering is the development of biological substitutes and/or strategies for regeneration that can be used to replace, enhance, repair, and/or regenerate tissue/organ function. Tissue engineering has emerged as a science and as a technology which aims to address the clinical problems of chronic disease and the transplantation crisis [5].

Scientific advances in recent years have moved cardiovascular tissue engineering from bench research into initial human studies [6, 7]. While these early studies are promising, identifying appropriate cell sources for tissue engineering still remains a critical issue. In the tissue engineering of a blood vessel substitute, creating a functional, non-thrombogenic endothelium is essential to ensure clinical success, yet the choice of endothelial cell source presents a major barrier. Issues such as availability, immune acceptance and function are important considerations for tissue engineering strategies.

Adult stem and progenitor cells have emerged as a promising autologous supply of cells but very little is known about their functional potential for use in tissue engineering.

The peripheral blood is a repository of circulating progenitor cells and may be a useful resource for tissue engineers. The research presented in this dissertation investigates the use of postnatal bone marrow derived circulating endothelial progenitor cells (EPCs) as an endothelial cell source for tissue engineering. These studies focus on the potential for EPCs to provide a functional endothelial lining on a living engineered blood vessel substitute. The endothelial cell resides in a dynamic environment at the interface between the vascular wall and blood where it is uniquely positioned to regulate hemostasis and while remaining poised to respond to vascular injury. In model systems designed to mimic the arterial environment, these studies probed EPCs response to local hemodynamic forces with a specific focus on understanding how the shear stress environment influences EPC ability to modulate hemostasis and thrombosis.

Tissue engineering offers the potential to address the overwhelming clinical need for new therapeutic options to treat cardiovascular disease. It is anticipated that these studies will contribute to the field of tissue engineering by providing insights into the potential of EPCs as a cell source for vascular applications.

CHAPTER II: HYPOTHESIS AND SPECIFIC AIMS

The critical need for appropriate endothelial cell sources for vascular tissue engineering combined with the emergence of scientific evidence that a circulating progenitor cell exists in adult peripheral blood with endothelial-like characteristics led to the central hypothesis of this work.

Central Hypothesis

The central hypothesis of this work is that endothelial progenitor cells (EPCs), derived from peripheral blood, may be a useful cell source for tissue engineering of blood vessel substitutes due to their ability to maintain hemostasis and provide a suitable non-thrombogeneic luminal lining on engineered vascular constructs.

To address the central hypothesis, four specific aims were defined.

Specific Aim 1

To isolate and characterize endothelial progenitor cells derived from peripheral blood and compare them to mature vascular endothelial cells through evaluation of receptor expression and endothelial specific cellular function.

EPCs were isolated from peripheral blood of a relevant preclinical model (baboon) and were characterized according to cell surface marker expression and functional assays. These results are presented in Chapter V.

Specific Aim 2

   To compare the phenotypic characteristics of endothelial progenitor cells to mature vascular endothelial cells when exposed to a physiologically relevant shear stress and three-dimensional engineered tissue substrate.

   The phenotypic response of EPCs to fluid shear stress was quantified at the gene and protein level and compared to mature vascular endothelial cells. A transcriptional profile analysis using microarray technology is presented in Chapter VI. In Chapter VII, focusing on a subset of coagulation associated genes, EPCs on both absorbed collagen and on an engineered tissue were compared to ECs in response to flow.

Specific Aim 3

   To develop an engineered vascular tissue appropriate for ex vivo study including characterization of the material properties, matrix organization and cellular function.

   An engineered vascular tissue model, appropriate for baboon *ex vivo* studies, was created by combining baboon vascular smooth muscle cells with naturally derived matrix materials. The characterization of this engineered tissue is presented in Chapter VIII.

Specific Aim 4

To evaluate endothelial dependent hemostasis on engineered tissue constructs in an ex vivo baboon arteriovenous shunt model.

EPCs functional capacity to maintain hemostasis and to provide a non-thrombogenic luminal lining was investigated using a femoral artery to femoral vein shunt in the baboon. Results of these studies are presented in Chapter VIII.

CHAPTER III: BACKGROUND

Cardiovascular Disease and Current Treatment Options

The World Health Organization (WHO) in combination with the Centers for

Disease Control (CDC) recently published "The Atlas of Heart Disease and Stroke"

which compiled data on the global burden of cardiovascular disease. In 2002, there were

11.2 million deaths globally from various forms of heart disease including coronary heart

disease, peripheral arterial disease, and congenital heart disease [1]. In the United States

alone, it is estimated that one in three adults has some type of cardiovascular disease [2].

Treatment of cardiovascular disease often necessitates surgical intervention for

the replacement of diseased arteries or reconstruction of congenital malformations.

Clinically, there are more than 460,000 coronary bypass procedures performed annually

and out of an estimated 36,000 babies born each year in the United States with congenital

heart defects, it is estimated that 9,200 will require invasive treatment [2]. Unfortunately,

there is a lack of appropriate surgical materials for both applications. Thrombosis and

anastomotic intimal hyperplasia compromise the clinical usefulness of smaller diameter

(<6mm) non-autologous blood conduits [8]. In small diameter applications, surgeons

must turn to autologous artery or vein grafting which is associated with inadequate

supplies of healthy tissue and donor site morbidity. In congenital repair, synthetic

substrates or chemically preserved homografts may be applicable but those materials do

not provide potential for growth or remodeling therefore requiring repeat surgical

interventions as the child matures.

Bypass procedures treating peripheral artery disease can often utilize synthetic graft materials for applications ≥6mm but these interventions are limited in long term durability. For example, 5-year patency rates for femoral-popliteal grafts are approximately 66%. In critical ischemia, results are even less encouraging with patencies of 47% above-the-knee and 33% for below-the-knee grafts [9]. For the more than 100,000 patients that are currently on chronic hemodialysis, patency rates for dialysis access grafts are usually measured in months [10]. For these applications, expanded polytetrafluoroethylene (ePTFE) grafts are most frequently used, although there has been only modest improvement in overall patency rates since these grafts were introduced in 1972 [11, 12].

Consequently, a great deal of research has been directed towards the identification of graft materials that will prevent thrombosis and limit the development of intimal hyperplasia. While early studies with polymers (e.g., polyurethanes, silicones) often showed favorable results on the basis of *in vitro* tests of biocompatibility, such testing has not been predictive of clinical graft outcomes [13]. To more closely simulate properties of native blood vessels, biologic and bioactive molecular coatings (e.g. heparin, phosphorylcholine) have also been applied to graft materials such as ePTFE [14, 15]. While such coatings may modestly attenuate early blood reactions and healing responses, only a limited benefit may be achievable in terms of late outcome events.

The Vascular Wall: Anatomy and Physiology

The native blood vessel is composed of three main structural layers containing distinct cell and matrix compositions. The inner most layer of the blood vessel is the tunica intima which is composed of a single layer of endothelial cells (ECs) with an underlying basement membrane consisting of Type IV collagen, glycosaminoglycans, elastin and laminin [16]. The middle layer of the natural blood vessel is the tunica media which is composed of concentric sheets of smooth muscle cells (SMCs) encased in a fibrillar matrix of Type I and Type III collagen, elastin and proteoglycans. The medial layer provides most of the artery's strength. The collagen fibers, aligned both circumferentially and helically along the axis of the vessel, are important in resisting tension created by pulsatile blood flow while elastin provides elastic compliance to the vessel wall. The outermost layer of the blood vessel, the tunica adventitia, forms a connective sheath around the vessel consisting of loosely arranged Type I and Type III collagen, elastin and fibroblasts. The adventitia functions to stabilize and anchor the blood vessel *in vivo*, maintaining longitudinal tension. In larger vessels, the adventitia is infiltrated by a vascular blood supply (vaso vasorum) and nerves [17].

The Native Endothelial Cell

Endothelial Cell Function

The endothelium is more than a passive barrier between blood and tissues. Rather, it is a biocompatible and physiological container that maintains blood fluidity by localizing platelet and coagulation reactions to sites of vessel injury while regulating the functions and caliber of blood vessels in response to changing hemodynamic and other

environmental conditions [18]. Other endothelial cell (EC) functions broadly include the transfer of metabolic substances, synthesis of regulatory substances, thromboresistance, vascular repair and wound healing, and cellular immunity [16]. One of these functions, endothelial thromboresistance, includes passive mechanisms (surface phospholipids, heparins and proteoglycans) and active mechanisms such as the synthesis of prostacyclin and nitric oxide (NO), secretion of plasminogen activator, membrane ADPase (CD39) activity, degradation of vasoactive amines, inactivation of thrombin, and thrombomodulin activation of protein C [19]. Stimulated ECs can be both procoagulant and proinflammatory. Activated ECs express tissue factor, which iniates the extrinsic pathway of coagulation. Stimulated ECs also secrete plasminogen activator inhibitor (PAI-1) and release von Willebrand factor from Weibel-Palade bodies within the cell [20]. A schematic of the endothelial cell's role in hemostasis is shown in Figure 3.1
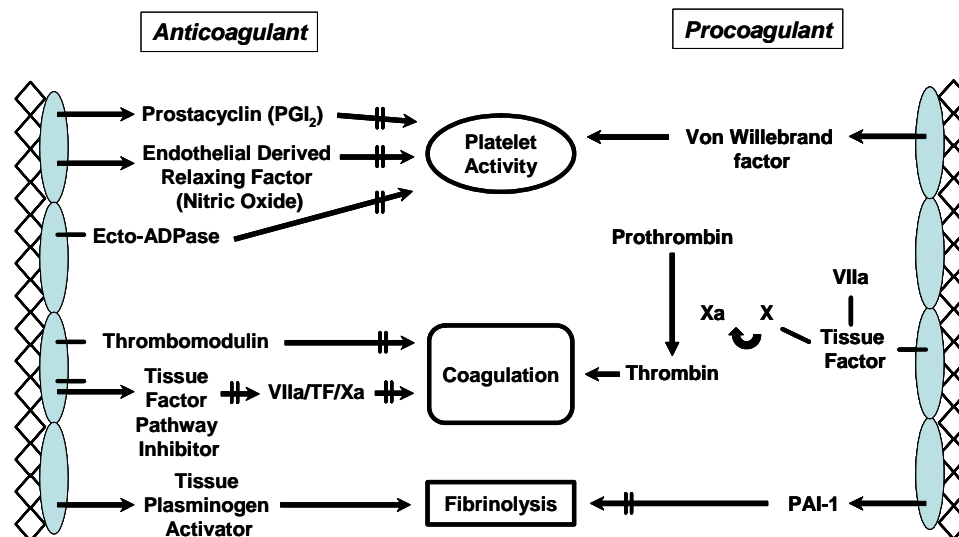
Figure 3.1: Participation of the vascular endothelial cell in the coagulant properties of the vessel wall. Adapted from [20].

The regulation of endothelial nitric oxide (NO) (decreased NO synthesis or increased NO degradation), is of particular interest to EC function since NO has multiple effects on the vessel wall. Nitric oxide produced by the endothelial isoform of nitric oxide synthase (eNOS) mediates a variety of physiological functions *in vivo* including neovascularization, regulation of blood vessel tone (vessel wall tension), vascular permeability and leukocyte-endothelial interaction [21]. eNOS represents an integral part of vascular hemostasis. In addition to effects as a vasodilator, NO also prevents the adhesion of platelets and white cells to endothelium, inhibits the aggregation of platelets, and induces the disaggregation of platelets. Basal release of NO can also decrease the rolling and adhesion of polymorphonuclear leukocytes to the endothelium [22]. The capacity of ECs to liberate NO has correlated with the severity of endothelial dysfunction (e.g., coronary artery disease) and with patency rates following surgical coronary bypass with internal mammary artery and saphenous vein grafts [23, 24].

The Role of Hemodynamic Environment in Modulating Endothelial Cell Function

Through decades of research, we now appreciate the endothelium as a multifunctional organ whose health can be the determinant between normal physiology and the development of vascular disease. The endothelium is exposed to three types of mechanical forces *in vivo*; tensile stress acting along the vessel wall due to circumferential deformations, normal stress acting radially on the vessel due to hydrostatic pressure and tangential stress or shear stress acting along the length of the vessel wall due to the flow of blood along its surface [25]. Early *in vivo* observations that arteriosclerosis was a focal disease and subsequent correlations drawn between the local hemodynamic forces and disease prevalence launched a field of research into the role of

physical forces in EC function [26]. Detailed study of endothelial cell function first

became possible following the development of techniques to culture ECs *in vitro* [27-29].

With collaborations between clinicians, scientists and engineers, *in vitro* tools were

developed to precisely control the fluid shear environment on the surface of the

endothelium in order to study EC response. These simplified flow systems included

capillary tubes, concentric cylinders, parallel plate flow chambers and cone and plate

viscometers [30]. Studies first reported morphological alterations in ECs in response to

shear [31-34]. EC morphology becomes more elongated with increasing shear stress *in*

vitro, a finding consistent with *in vivo* observations. More detailed study of the

cytoskeleton has shown that actin containing stress fiber expression is associated with

shear exposure. Increased stress fiber assembly is found in cells exposed to higher shear

stresses. Additionally, numerous studies have reported changes in the metabolic and

synthetic activities of endothelial cells following exposure to shear stress including

production of prostacyclin, growth factors, coagulation and fibrinolytic components,

extracellular matrix production and vasoactive mediators [35-37]. We now know that

unidirectional blood flow generates a constant shear stress which maintains the

endothelium in a quiescent phenotype, promoting an antiinflammatory, antithrombotic,

anticoagulative, profibrinolytic and antihypertrophic state. In contrast, areas of low mean

shear stress and oscillatory flow with reversal are characterized by endothelium prone to

vascular disease. In these "atheroprone" areas, decreased shear stress is associated with

increases in reactive oxygen species (ROS), endothelial cell permeability to lipoproteins,

leukocyte adhesion, apoptosis, smooth muscle cell proliferation and collagen deposition.

Low and oscillatory shear stress are also associated with reduction in eNOS production and endothelial cell repair [38-40].

There have been a number of endothelial flow sensitive mechanotransducers suggested but the exact mechanisms of how a mechanical stress is converted into a biochemical signal are not fully understood and still require further study. Theories on mechanotransduction can be generally grouped into either localized models where the signal is generated in close proximity to the plasma membrane or a more decentralized model (tensegrity model) where forces applied at the cell surface are transmitted to other locations via the cytoskeleton. Integrins, which are membrane associated glycoproteins, may provide some intersection between the two models. Integrins are composed of two subunits each with a large extracellular domain, a transmembrane region and a short cytoplasmic domain. The integrin alpha subunit determines binding to the extracellular matrix and the beta subunit initiates intracellular signaling. It has been documented that shear stress can sequentially activate mechanosensors, intracellular signaling pathways, specific transcription factors and the expression of genes and proteins. Potential endothelial cell membrane mechanosensors such as ion channels (e.g. K+ channel, nonselective cation channel and/or voltage-gated Na+ channel), protein kinases, G proteins, reactive oxygen species, intracellular junctional proteins and membrane lipids have also been suggested [35, 38, 40-42].

EC functional properties related to hemostasis and thrombosis are also influenced by fluid shear stress. Prostacyclin was the first inhibitor of platelet aggregation shown to be released from endothelial cells on exposure to shear stress [43, 44]. Since then, numerous investigators have demonstrated that shear stress is one of the most powerful

stimuli for release of nitric oxide, which also possesses strong anti-platelet aggregation properties [45-47]. In addition, enhanced expression of tissue plasminogen activator (TPA) [48, 49] and tissue factor pathway inhibitor (TFPI) [50] result from shear stress exposure. There have been conflicting reports about thrombomodulin expression in cultured cells. Malek et al. [51] reported that steady shear stress (15 dynes/cm^2) results in a time–dependent decrease in THBD mRNA in bovine aortic endothelial cells measured by northern blot analysis of total RNA. In contrast, Takada et al. [52] demonstrated that cultured human umbilical vein endothelial cells (HUVEC) respond to shear stress (15 dynes/cm^2) with a time-dependent increase in THBD using RT-PCR, flow cytometry, and ELISA methods. The reason for this disparity in species response is unclear but these studies provided evidence that mechanical hemodynamic forces such as shear stress are associated with alterations in thrombomodulin expression.

The interaction between thrombomodulin and shear stress has been demonstrated to have clinical relevance. Clinically, early vein graft occlusion by thrombosis occurs more often than in arterial grafts [53]. This has been partly attributed to the loss of endothelial thromboresistance and reductions in thrombomodulin expression once vein grafts have been placed in the arterial circulation [54]. Although inflammatory processes are clearly active in this setting, several groups have established links between thrombomodulin expression and the local mechanical environment including shear stress and pressure associated changes in vessel wall tension. Using a rabbit model to perform interpositional grafting of jugular vein segments into the carotid circulation, Sperry et al [55] demonstrated that decreases in THBD mRNA and protein correlated with increases in wall tension and were independent of shear stress changes up to 8.2 dynes/cm^2. Again,

13

conflicting data exists using human saphenous veins in an *ex vivo* flow circuit. Consistent with Sperry's results, Gosling et al.[56] saw decreases in thrombomodulin immunostaining after saphenous veins were exposure to arterial flow (4 dynes/cm^2), but by limiting circumferential distension in their model system, the authors attributed the THBD decrease to shear stress rather than circumferential deformation.

Endothelin-1, a potent vasoconstrictor and mitogen for SMCs, is unregulated in the minutes following exposure to shear but decreased when shear stress is applied for six hours or more [57, 58]. In ECs, shear stress has also been shown to regulate tissue factor, a membrane bound glycoprotein that triggers extrinsic blood coagulation at the gene, protein, and functional levels [50, 59, 60].

Strategies for Engineering a Vascular Graft

Considerable evidence suggests that there is no simple biomaterials-based solution to the problems of small caliber graft thrombosis and intimal hyperplasia, presumably because no synthetic biomaterial or acellular coating can exhibit the anti-thrombotic, anti-arteriosclerotic, and self-renewing functional properties of the living vessel wall. More promising, therefore, are cellularized devices that have been engineered to exhibit specific and durable biological activities for modulating graft thrombosis and healing *in vivo*. Central to this strategy is a functional endothelium for long-term inhibition of blood coagulation and graft intimal thickening.

The earliest attempts at vascular tissue engineering have seeded autologous vascular endothelial cells, harvested from either veins or adipose tissue, onto the surface of a graft made from a synthetic material [61-63]. This elective graft endothelialization with mature ECs can increase synthetic graft patency in animals [64-66]. In humans,

14

vascular grafts seldom undergo complete endothelialization [67]. For grafts electively endothelialized *in vitro*, the reported clinical experience is still quite limited [68-70]. The most extensive clinical results are those reported by Meinhart et al. [9] who show a primary patency rate of 62.8% after 7 years in 6 and 7mm infrainguinal grafts.

There have been a number of biologic strategies to engineer a blood vessel substitute. These started with the work of Weinberg and Bell [71] who used collagen gel technology to create a blood vessel substitute that had an intima, a media, and an adventia. Others have continued to work with this naturally derived matrix and have made incremental improvements in construct fabrication to increase collagen fiber alignment [72], in enhancing the material properties (including strength and compliance) through exogenous biochemical stimulation [73], natural crosslinking [74], reinforcement strategies [75, 76], and the application of dynamic mechanical strain during *in vitro* culture [77, 78]. In addition to collagen gel technology, decellularized natural tissue matrices, which contain the intact extracellular matrix and associated attachment proteins have been used to create vascular conduits [79, 80]. More recently, the blood clotting protein fibrin has also been investigated as a vascular tissue-engineering matrix [81, 82]. However, in general the blood vessel substitutes created with these technologies have been limited by their ultimate strength.

The seeding of polymeric scaffolds has been used as a vascular engineering approach which led to excellent burst pressures [83]. Although promising, challenges are still associated with achieving the necessary cell proliferation and matrix synthesis needed. In addition, there is the problem of polymer degradation products altering the

local cellular environment and as a result cell function [84, 85]. Interestingly, there also appears to be significant variation in mechanical strength among different species.

Another approach is one that might be called cell-secreted structures. This includes the approach of L'Heureux et al. [7, 86] in which a blood vessel substitute is fabricated by the layering of *in vitro* cultured cell sheets. In this approach, sheets are created though the production of extracellular matrix by native vascular cells, and these then can be rolled around a mandrel to form multicellular tubular blood vessel analogs. In a second "cell-secreted" approach, the harnessing of the body's natural foreign body response and associated generation of granulation tissue has been used to create completely autologous vascular structures by implanting silicone tubing into the peritoneal cavity [87]. Following two weeks of implantation, the silicone can be removed and the resulting tubular tissue implanted.

Cell Sources for Vascular Tissue Engineering

There is a critical need for appropriate endothelial cell sources in vascular tissue engineering. There are a variety of endothelialization strategies currently being pursued including the autologous cell seeding approaches already discussed, as well as the potential use of genetically engineered cells and embryonic stem cells [88-90]. Adult bone marrow derived cells, termed endothelial progenitor cells (EPCs) have also emerged as a promising endothelial cell source for tissue engineering and are the subject of this disseratation.

Endothelial Progenitor Cells (EPCs)

The established paradigms for the formation of new blood vessels (vasculogenesis and angiogenesis) have been challenged in recent years following Asahara et al.'s [91] ground breaking report that there was a population of human circulating cells that could differentiate *ex vivo* into cells with endothelial-like characteristics. This circulating cell population, termed "endothelial progenitor cells" or EPCs was reported to contribute to the formation of new blood vessels in the adult which Asahara and colleagues termed "postnatal vasculogenesis" [92]. Since the first report in 1997, there has been an explosion in research related to the isolation, characterization, mobilization and function of these mysterious circulating progenitor cells. To date there are more than 1400 peer reviewed publications related to endothelial progenitors [93]. Subsequent studies have now demonstrated that these cells are bone marrow derived, they circulate in peripheral blood and they are recruited or home to sites of new blood vessel formation including ischemic tissues and tumor microenvironments (reviewed in [94-100]). It has also become apparent that they are rare events. Estimates are that EPCs make up 0.0001% of peripheral blood cells depending on the age, sex and health status of the individual [95].

Published reports of circulating angiogenic/endothelial-like cells in blood date back at least 40 years [101]. Over the years, surgeons and/or pathologists have provided evidence that there are circulating cells which contribute to vascular healing and neoendothelialization [102-105]. Today, there is tremendous excitement about the therapeutic potential of such a progenitor cell population but along with the excitement there are "unresolved questions" about how to appropriately define the endothelial progenitor cell. Emerging evidence suggests that peripheral blood contains a

heterogeneous population of cells that posses the ability to differentiate into cells with endothelial-like characteristics. Various culture techniques have generated endothelial like-cells from a number of cell types present in peripheral blood. Circulating hemangioblasts which share multi-lineage potential for both primitive hematopoietic and endothelial progenitors have been identified [106, 107] as well as monocyte/macrophage derived cells [108] and detached mature endothelial cells [109].

Endothelial Progenitor Cell Isolation and Culture

There have been numerous reports of different culture methods for isolation of "EPCs". These diverse methodologies have increased our understanding and knowledge of the circulating progenitor population but have also lead to results which are difficult to compare and interpret. Asahara's first report [91] used a magnetic separation technique to isolate specific cell populations using two antigens that are shared by angioblasts and hematopoietic stem cells; CD34 and flk-1, a vascular endothelial growth factor (VEGF) receptor. Use of cell selection techniques has allowed studies of a number of specific cell populations within peripheral blood. In addition to sorting for CD34 and flk-1 (also known as KDR or VEGFR2) [110], a more specific stem cell marker termed CD133 (also called AC133) has also been used to select a subpopulation of cells which are thought to be more "immature stem cells" [111]. CD133 expression has been reported to diminish during differentiation and is quickly lost once cells have been removed from the circulation and established in *in vitro* culture. None-the-less, these cell populations have been shown to develop into endothelial-like cells with endothelial marker expression and endothelial specific function [112-115]. Another CD133 positive cell population which may or may not be related to the cells obtained from peripheral blood sorting is what

Reyes et al [116] term multipotent adult progenitor cells (MAPCs). These cells which can be induced to differentiate into an endothelial-like cell are described as "nonendothelial bone marrow stem cells". In an effort to understand the origins of EPCs, additional research using separation of peripheral blood cells based on surface markers has been used to suggest that certain EPC populations are derived from CD14 positive monocytes [108, 117-121].

Blood Outgrowth

It has become apparent that a population, or more likely, multiple populations of cells exists in peripheral blood which can offer therapeutic potential. Without the use of selection based techniques, EPCs have been observed from "blood outgrowth" when the mononuclear fraction of blood is cultured on specific substrates (fibronectin, collagen, or gelatin) with medium which contains growth factors: VEGF and/or EGF, FGF-β and IGF.

Cell selection based on specific markers as described previously or "preplating" techniques to remove all adherent low density mononuclear cells have been performed in an effort to avoid possible contamination of EPC cultures with monocytes, hematopoietic progenitors, and/or mature circulating endothelial cells (termed CECs) [122]. Through ground breaking work, Lin et al [123] used human patients who received sex-mismatched bone marrow transplants to determine that in the outgrowth population (without specific cell selection procedures), there were cells which had both recipient and donor genotype. They found CECs appeared early in culture and were derived from the recipient but they also reported a population of cells they termed blood outgrowth endothelial cells (BOECs) [124] which persisted in cultures greater than six weeks and were bone marrow

derived (having donor genotype). With increasing culture duration, the majority of the culture was donor genotype bone marrow derived cells. These outgrowth cells had remarkable proliferative capacity (1023-fold expansion during 4 weeks of culture) and were positive for flk-1, VWF, CD36 (collagen type 1/thrombospondin receptor indicating microvascular phenotype [125]), and ve-cadherin. The outgrowth cells were also negative for CD14 (monocyte marker). Since this study, many groups have used the blood outgrowth method to establish cultures of endothelial-like cells [120, 123, 126-140].

<u>What's in the name?</u>

There is currently considerable debate in the literature about what is an EPC and how do we appropriately define it. When should we use the terms EPC, CEC, OEC, BOEC or others? Ingram et al [135] has proposed that endothelial progenitors be named the way that hematopoietic cell progenitors are defined based on differences in proliferative and/or differentiation potential. Using single cell assays, they propose that cells giving rise to microscopic colonies that form secondary and tertiary colonies upon replating would be termed HPP-ECFCs (high proliferative potential-endothelial colony forming cells) in contrast to more differentiated low proliferative potential-endothelial colony forming cells (LPP-ECFCs) which form small colonies but do not form secondary colonies when replated.

There is new evidence which may help clarify some of the mystery associated with different reports about "EPCs". Recently, several studies have identified two populations of cells that emerge from peripheral blood outgrowth cultures, termed early EPCs and late EPCs [133, 140] (or late outgrowth endothelial cells (OECs) in other

studies [123, 130]). Early EPCs are similar to the progenitor cells first reported by Asahara et al. [91] and have been used in therapeutic angiogenesis trials [141, 142]. These cells appear to be of monocyte/macrophage origin [120, 130], capable of secreting angiogenic peptides [120] and shown to have limited proliferative potential [143]. Late EPCs, named after their late outgrowth potential, form homogenous cobblestone morphologies and have high proliferative capacity [130, 133, 140] (similar to the description of BOECs by Lin et al. [123]). Ingram et al [134, 135] have extended beyond these observations in peripheral blood, suggesting that these populations also exist in umbilical cord blood and possibly in vascular tissue. New data also suggests that there may be synergistic angiogenic effects of both early and late EPCs when delivered to ischemic tissue as a mixed population [140].

In a September 2005 editorial in *Circulation*, Gulati and Simari [144] summarized the current knowledge about EPCs in their statement: "…*in vitro* studies confirm the emerging paradigm that early EPCs are monocyte derived (and not truly endothelial) and of limited proliferative potential (and not progenitors), but are capable of assuming endothelial features (uptake of acetylated low-density lipoprotein and binding of Bandeiraea simplicfolia-lectin) and producing and secreting potent cytokines and growth factors. Thus, the term EPC is significant only in an historical rather than literal sense. The true endothelial precursor cell population (capable of generating OECs *in vitro*) is rare within the circulation and likely originates from a subset of CD14–/CD34+/KDR+ cells that is not fully defined…"

The Role of the Hemodynamic Environment in Endothelial Progenitor Cell Function

There is very little data available on the effect of shear stress in EPC phenotype and function. Low levels of shear stress exposure (0.1-2.5 dynes/cm^2) altered EPC proliferation, differentiation, and ability to form *in vitro* vascular networks [145]. Higher levels of shear stress (15-25 dynes/cm^2) have been reported to enhance EPC maturation [146] and increase tissue plasminogen activator (tPA) secretion and mRNA expression [147].

Endothelial Progenitor Cells in Tissue Engineering

Recently, there has been increasing interest in using EPCs in tissue engineering strategies. EPCs have been seeded onto synthetic polyurethane [148-150] and PGA/P4HB substrates [151] and used for the engineering of microvascular networks [152, 153]. EPCs have also been tested in vascular graft applications [129, 154-160]

Grafts endothelialized using EPCs have shown promise for reducing intimal hyperplasia and preserving patency in animal models [156-158]. For example, Kaushal et al. demonstrated a dramatic increase in carotid artery graft patency using decellularized porcine iliac vessels that were endothelialized with ovine EPCs [157]. The ability of the grafts to undergo NO-mediated relaxation was also noted. Matsuda et al. seeded both human and canine EPCs onto segmented polyurethane grafts with success [156, 158]. While the human EPCs had a profile of tPA expression that was similar to human umbilical vein endothelial cells (HUVECs), the expression levels of eNOS and PGI2 (prostacyclin or prostaglandin I2) were significantly reduced compared to HUVECs [158]. Canine EPCs, seeded onto Type I collagen gel within a polyurethane support, were positive for acLDL uptake, Factor VIII-related antigen, Flk-1 and intracellular NO

production. When implanted as carotid grafts, these surfaces remained fully

endothelialized for up to 3 months [156].

CHAPTER IV: MATERIALS AND METHODS

General Cell and Tissue Culture Procedures

Cell Isolation and Culture

Cells used in the following studies were all obtained by primary isolation from juvenile male baboons (*Papio anubis*) weighing approximately 10-20kg. These studies were conducted under approval of the Institutional Animal Care and Use Committees of Emory University and Georgia Institute of Technology in accordance with related university policies.

Baboon Vascular Endothelial Cells

Baboon carotid artery endothelial cells (ECs) and baboon carotid artery smooth muscle cells (SMCs) were isolated from fresh carotid arteries obtained just prior to sacrifice from animals enrolled in other chronic implantation studies. The arteries were rinsed using sterile Hanks Balanced Salt Solution (HBSS) containing a 2X concentration of antibiotic-antimycotic solution (Gibco/Invitrogen, Carlsbad, CA)) and transported on ice from the surgery or necroscopy suite to the cell culture laboratory. In an aseptic environment, the adventitial layer was removed by dissection and the artery lumen was exposed. The endothelial cells were removed by gentle scraping following a five minute exposure to 600 U/mL collaganase (type CLS 2, Worthington Biochemical Corp. Lakewood, NJ) and plated onto a 6-well tissue culture treated dish precoated for at least one hour with either human fibronectin (50μg/mL) (Gibco/Invitrogen) or 0.1% gelatin

(porcine skin gelatin, Sigma-Aldrich, St. Louis, MO). ECs were expanded in a complete

growth medium containing MCDB 131 supplemented with 5% fetal bovine serum (FBS),

1% L-glutamine, 1% penicillin-streptomycin, 50μg/mL ascorbic acid, 0.01μg/mL hEGF,

0.002μg/mL hFGF-basic, 0.002μg/mL IGF-1, 0.001μg/mL VEGF, and 0.001mg/mL

hydrocortisone (Table 4.1).

Table 4.1: Endothelial Cell Complete Media Formulation

Component	Manufacturer/Supplier	Media Final Concentration
Base: MCDB-131	Mediatech cellgro, catalog number 15-100-CV	1X
Fetal Bovine Serum (Heat-Inactivated)	Mediatech cellgro, catalog number 35-011-CV	5%
L-Glutamine	Mediatech cellgro, catalog number 25-005-CI, L-Glutamine, Liquid 200mM solution (29.23 mg/mL with 8.5g/L NaCl),	1%
Penicillin-Streptomycin	Mediatech cellgro, catalog number 30-002-CI, Penicillin-Streptomycin Solution, 100X, 10,000 I.U. Penicillin/mL, 10,000 μg/mL Streptomycin	1%
L-Ascorbic acid 2-phosphate	SIGMA, catalog number A-8960	50 g/mL
Epidermal Growth Factor (human, recombinant)	Gibco, catalog number 13247-051	0.01 g/mL
Fibroblast Growth Factor-basic (human, recombinant)	PeproTech, catalog number 100-18B	0.002 g/mL
Insulin-Like Growth Factor-I (human, recombinant)	Gibco, catalog number 13245-063	0.002 g/mL
Vascular Endothelial Growth Factor (human, recombinant)	SIGMA, catalog number V-7259	0.001 g/mL
Hydrocortisone	SIGMA, catalog number H-4001	0.001mg/mL

Baboon Smooth Muscle Cells

Following removal of the adventitia and endothelium as described above, smooth

muscle cells were isolated from the vascular media using a facilitated migration method

[161]. This method combined the enzymatic digestion method used by some groups [162] and the explant outgrowth method which has also been described previously [163] to obtain a population of SMCs from the vascular media cross-section. The medial tissue was rinsed in HBSS containing 2X antibiotic-antimycotic solution and dissected into 1-2mm pieces. The tissue chunks were transferred to a solution of 300 U/mL collagenase (type CLS 2) dissolved in MCDB-131 and incubated at 37ºC with gentle agitation for 16-19 hours. Following incubation in collagenase, the partially digested tissue was centrifuged and resuspended in MCDB 131 supplemented with 10% fetal bovine serum (FBS), 1% L-glutamine and 1% penicillin-streptomycin. The adherent cells were designated passage zero. SMCs were expanded in complete SMC growth media (Table 4.2) and cryopreserved for future use.

Table 4.2: Smooth Muscle Cell Complete Media Formulation

Component	Manufacturer/Supplier	Media Final Concentration
Base: MCDB-131	Mediatech cellgro, catalog number 15-100-CV	1X
Fetal Bovine Serum (Heat-Inactivated)	Mediatech cellgro, catalog number 35-011-CV	10%
L-Glutamine	Mediatech cellgro, catalog number 25-005-CI, L-Glutamine, Liquid 200mM solution (29.23 mg/mL with 8.5g/L NaCl),	1%
Penicillin-Streptomycin	Mediatech cellgro, catalog number 30-002-CI, Penicillin-Streptomycin Solution, 100X, 10,000 I.U. Penicillin/mL, 10,000 µg/mL Streptomycin	1%

Baboon Endothelial Progenitor Cells

Fresh blood was collected from baboons by venipuncture and anticoagulated with buffered sodium citrate. The anticoagulated blood was diluted 1:2 with HBSS containing 1 mM EDTA and 0.5% bovine serum albumin. Density gradient centrifugation was performed using Histopaque-1077 (Sigma-Aldrich, St. Louis, MO) following the manufacture's instructions. Baboon mononuclear cells were isolated from the buffy coat and washed three times in MCDB 131 supplemented with 1% L-glutamine and 1% penicillin-streptomycin. Buffy coat mononuclear cells from 50-250mL of blood were resuspended in EGM-2 endothelial cell growth media (Cambrex, East Rutherford, NJ)) and placed in 1-3 wells of a 6-well tissue culture plate precoated for at least one hour with human fibronectin (50μg/mL) (Gibco/Invitrogen). The plate was incubated at 37°C in a humidified incubator with 5% CO_2. After 24 hours, unattached cells and debris were removed by exchange of the culture medium. The culture medium was changed every other day for up to 4 weeks. Cell colonies were passaged using 0.05% Trypsin-0.53mM EDTA (Gibco/Invitrogen) and further expanded in fibronectin coated tissue culture flasks. Cells were cryopreserved for future use. Following cryopreservation, cells were thawed and expanded in endothelial cell complete medium (Table 4.1) for use in specific experimental protocols.

Cryopreservation

All primary cells were cryopreserved at early passages and were stored in liquid nitrogen until needed for experimental procedures. Following trypsinization, cells were pelleted via centrifugation and resuspended in a freezing medium containing 10%

dimethyl sulfoxide (DMSO), 40% fetal bovine serum and 50% cell specific complete culture medium. Cells were transferred to cryogenic screw cap vials (Nalgene Nunc) and frozen in Nalgene™ freezing canisters containing room temperature isopropyl alcohol and incubated in a -70°C freezer for 24 hours. After 24 hours, vials were transferred to a liquid nitrogen tank for long term storage.

<div align="center">**Engineered Vascular Tissue Fabrication**</div>

Two types of engineered vascular tissues were fabricated as part of this research. SMCs were embedded within a type I collagen hydrogel with or without an intact elastin scaffold. The type I collagen was purchased as a lyophilized product (type I collagen from calf skin, MP Biomedicals, Irvine, CA) which was dissolved in 0.02N acetic acid via gentle stirring at 4°C. Following the techniques first described by Weinberg and Bell [71], reconstitution of the collagen into a fibrillar form was achieved by changing the pH and temperature of the solution. SMCs were suspended in the collagen solution and became entrapped in the collagen fiber network during collagen fibrillogenesis.

Three-Dimensional Collagen Hydrogel Engineered Tissues

SMCs were trypsinized with 0.05% Trypsin-0.53mM EDTA (Gibco/Invitrogen) following expansion in standard tissue culture treated flasks. The cells were counted and the appropriate number of cells (final concentration 1x10^6 cells/mL) was resuspended in SMC complete medium. For a typical batch of 8 constructs including 10% excess, SMCs were suspended in 16.5mL of complete medium. In a separate tube, the remaining reagents were mixed over ice. 6.6mL 5X MCDB-131, 24.6mL acid solublized bovine dermal type I collagen and 3.3mL 0.1N NaOH solution were mixed thoroughly being

careful not to introduce air bubbles into the solution. The cell suspension was then added to the neutralized collagen solution and mixed thoroughly, again being careful to avoid bubbles. A 6.0mL volume of this collagen solution was injected into a glass mandrel assembly to form a tubular geometry. The assembly consists of a glass capillary tube mandrel outfitted with rubber end stoppers and a glass test tube mold. The constructs were placed in an incubator at 37°C for one hour to promote gel formation. The mandrel and construct were then removed from the test tube and cultured in a 150mm suspension culture dish containing SMC complete medium. The reagent volumes could be scaled to fabricate any given number or size engineered tissue. Using the tubular assembly described, original construct dimensions were typically 60mm in length with an 11.6mm outer diameter and a 3mm inner diameter.

Isolation of an Intact Elastin Scaffold

The isolation of elastin was performed as described previously [164] using a series of enzymatic, chemical and thermal treatments aimed at removing cells and nonelastin matrix components. Fresh porcine carotid arteries (3-5mm inner diameter) were obtained from a local slaughter house (Holifield Farms, Conyers, GA) or purchased from an animal tissue supplier (Animal Technologies, Tyler, TX). The arteries were incubated in a sodium phosphate buffer solution for three twenty-four hour cycles to thoroughly clean each vessel. Excess adventitia is then removed using surgical scissors and forceps, and the arteries were cut into approximately 4-6cm segments and loaded onto glass capillary tube mandrels with rubber stoppers placed on each end. Arterial segments were immersed in 100mL of deionized (DI) water and autoclaved for five cycles (60 minutes, 120°C). Upon completion of each autoclave cycle, the water was

removed while still hot and replaced with clean DI water. Arterial segments are then

incubated in a trypsin-tris buffer solution (0.1M trizma base, 0.02M $CaCl_2$, and 900

BAEE units/L trypsin (Sigma)) at 37°C for 18 hours. Following the enzymatic digestion,

the artery segments are rinsed five times in DI water and further digested for 18 hours in

a β-mercaptoethanol-urea solution (0.05M trizma base, 6M urea, and 0.5% 2-

mercaptoethanol). Following five DI water rinses, elastin segments were incubated in

absolute ethanol for 60 minutes to help remove contaminant lipids. Finally, at least three

24 hour rinses were performed in DI water at 4°C to remove residual ethanol. At this

point, the isolated elastin scaffolds were sterilized in an autoclave cycle (25 minute,

120°C) and were ready to be incorporated into engineered tissue constructs.

Fabrication of an Elastin-Collagen Hybrid Engineered Tissue

Following the methodology described for fabrication of 3-D collagen hydrogels

above, SMCs were mixed with a bovine dermal type I collagen solution and poured into

glass test tube molds. Intact elastin scaffolds were incorporated into the engineered tissue

by inserting the elastin on the glass capillary tube into the SMC-collagen solution (as

shown in Figure 4.1A). As described above, the constructs were placed in an incubator at

37°C for one hour to promote gel formation followed by removal from the test tube for

static culture in 150mm suspension culture dishes containing SMC complete medium (as

shown in Figure 4.1B). While the majority of the SMC-collagen gel resides exterior to

the elastin scaffold, small gaps between the elastin and mandrel permitted some of the

SMC-collagen solution to infiltrate the inner lumen of the scaffold. Constructs were

cultured in SMC complete medium for up to eight days.
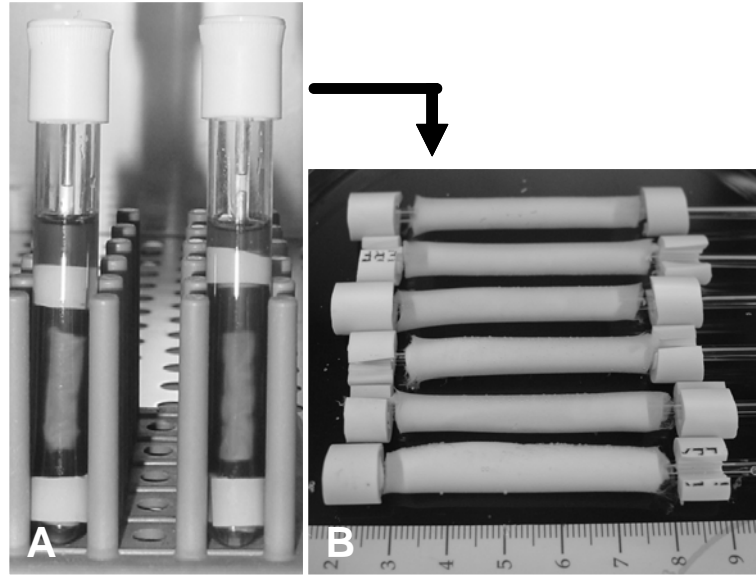
Figure 4.1: Elastin-collagen hybrid engineered tissues in culture. (A) An intact elastin scaffold was combined with a SMC-collagen solution to create an elastin-collagen hybrid engineered tissue. Following one hour incubation at 37°C, the tissues were removed from the glass test tube mold and culture *in vitro*. (B) Elastin-collagen hybrid constructs following several days in culture.

Application of Shear Stress

In order to study the effect of steady laminar shear stress on cellular phenotype, the fluid mechanic environment was controlled using two bioreactor geometries. A parallel plate flow chamber based on a rectangular channel flow and a tubular bioreactor configured to simulate fully developed pipe flow were both used to expose cells to controlled magnitudes of fluid shear stress.

Parallel Plate Flow Chamber with 2-D and 3-D Substrates

A parallel plate flow chamber device was used to expose cell monolayers to fluid shear stress as previously described [34]. The device was designed such that cells could either be grown on glass slides (typically coated with an extracellular matrix protein) or could be cultured on an *in vitro* fabricated engineered tissue slab as shown in Figure 4.2. The flow chamber consisted of a polycarbonate flow block which directed fluid to the surface, a spacer which defined the flow channel height, two stainless steel plates and a rubber gasket to seal the chamber. Cells will be seeded onto a glass slide coated with 50μg/mL absorbed collagen or onto 3-D engineered tissue constructs which have been opened longitudinally and embedded into agar.

The culture medium used for all flow studies was MCDB 131 supplemented with 5% fetal bovine serum (FBS), 1% L-glutamine, 1% penicillin-streptomycin, 0.0005μg/mL hEGF and 0.002μg/mL hFGF-basic (Table 4.3).

The experimental protocol for shear experiments using the parallel plate flow chamber was to embed and seed cells on day zero. Twenty-four hours later, the flow medium was removed and fresh flow medium was added to the Petri dish. At 48 hours,

Table 4.3: Flow Media Formulation

Component	Manufacturer/Supplier	Media Final Concentration
Base: MCDB-131	Mediatech cellgro, catalog number 15-100-CV	1X
Fetal Bovine Serum (Heat-Inactivated)	Mediatech cellgro, catalog number 35-011-CV	5%
L-Glutamine	Mediatech cellgro, catalog number 25-005-CI, L-Glutamine, Liquid 200mM solution (29.23 mg/mL with 8.5g/L NaCl),	1%
Penicillin-Streptomycin	Mediatech cellgro, catalog number 30-002-CI, Penicillin-Streptomycin Solution, 100X, 10,000 I.U. Penicillin/mL, 10,000 µg/mL Streptomycin	1%
Epidermal Growth Factor (human, recombinant)	Gibco, catalog number 13247-051	0.0005 g/mL
Fibroblast Growth Factor-basic (human, recombinant)	PeproTech, catalog number 100-18B	0.002 g/mL

slides or constructs were transferred into the parallel plate flow chamber. The chamber

was connected to a recirculation flow loop containing 110mL of fresh flow medium

(shown in Figure 4.2B) and flow was initiated. The flowrate was controlled to maintain a

laminar shear stress of 15 dynes/cm^2 for an additional 24 hours. Sheared samples were

then compared to static controls which had been incubated in the same volume of

medium and in the same incubator environment. The wall shear stress was determined

using the following equation: $\tau_w = (6\mu Q/bh^2)$ where μ is the viscosity, Q is the

volumetric flowrate, b is the channel width (2.54cm) and h is the channel height

determined by the spacer thickness minus the cell height (0.0505cm).

Embedding a 3-D Engineered Tissue for Application of Laminar Shear Stress

  Following five days in static culture, tubular constructs were removed from the

glass mandrel, cut longitudinally and gently transferred to a glass slide, lumen side down

as shown in Figure 4.3. The construct was trimmed on either end using a scalpel to create a clean rectangular surface. A polycarbonate mold was placed around the construct and the mold was filled with a 3.5% agar solution maintained at 48°C in a temperature controlled waterbath. A second glass slide was quickly placed on top of the molten agar and pressure was applied to "sandwich" the construct and force excess agar outside of the mold. The agar was allowed to cool and solidify for approximately 3-4 minutes ($\approx$37°C) and the embedded construct was turned over (lumen side up) before growth medium was added to the culture dish containing the embedded construct. The glass slide was gently removed exposing the luminal surface to growth medium. ECs or EPCs were seeded onto the construct surface using 50,000 cells/cm^2 in approximately 400µL of media. Cells were allowed to adhere to the surface for one hour before media was gently added to the Petri dish and constructs were transferred to an incubator at 37°C.
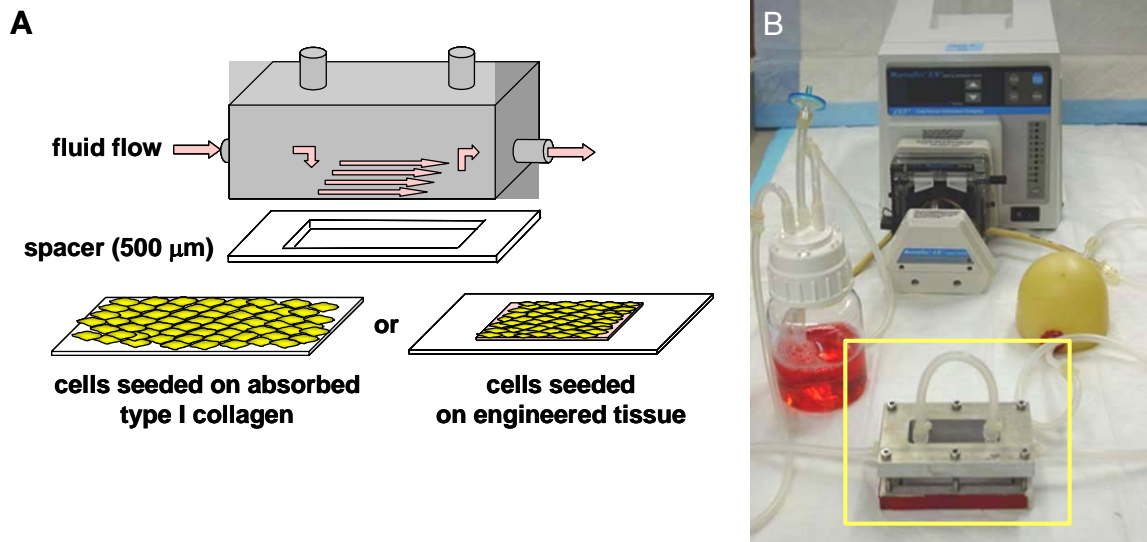
Figure 4.2: Application of shear stress using a parallel plate flow chamber and recirculation flow loop (A) A channel flow geometry was used to create a laminar shear stress on the cell surface. Cells were seeded onto glass slides coated with absorbed collagen or onto collagen hydrogel engineered tissues. (B) A recirculation flow loop provides steady flow through the parallel plate flow chamber (highlighted with a yellow box).
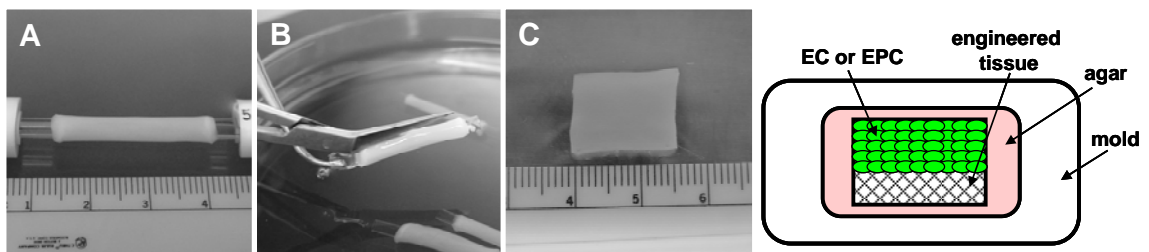
Figure 4.3: Preparation of an engineered tissue for application of shear stress. (A) An engineered tissue is grown *in vitro* in a tubular configuration on an inner silicon membrane. (B) Using sterile scissors, the silicone membrane and engineered tissue are cut longitudinally and (C) positioned lumen side down on a glass slide. Using a polycarbonate mold, the engineered tissue is embedded in agar and flipped over to expose the construct lumen. ECs or EPCs could then be seeded onto the luminal surface.

Cylindrical Bioreactor

A rudimentary bioreactor system was designed to allow EPC seeding and shear stress preconditioning on tubular constructs prior to interposition into the baboon *ex vivo* shunt. The system was designed to allow for an easy transition from an *in vitro* flow system directly into the *ex vivo* shunt without the requirement for any tissue manipulation. The tubular elastin-collagen hybrid constructs which were cultured between 4 and 8 days, were sutured to Teflon connectors (9 gauge, 20mm long, wall thickness 0.250mm, Small Parts, Miami Lakes, FL). The constructs were encased in an outer covering of 3.5% agar inside of a heat shrink Teflon outer covering (1 gauge,10cm long). The thin walled Teflon connectors were inserted into the glass mandrel containing the construct and the construct was gently pulled onto the connector. A suture was tied around the outer construct surface to secure the construct to the connectors. The outer Teflon casing was inserted into a glass cylinder capped on one end. The glass cylinder apparatus was positioned vertically in a container of ice. The construct and Teflon connectors, still on the glass mandrel were positioned inside the larger glass cylinder. A molten 3.5% agar solution (48°C) was poured around the exterior surface of the construct inside of the outer Teflon casing. The agar solidified and cooled within 3-4 minutes. The tissue, now encased in agar and an outer Teflon sleeve, was removed from the vertical glass cylinder and transferred to a Petri dish. The inner glass mandrel was gently removed and silicon tubing was attached to the thin walled Teflon connectors. The outer Teflon sleeve was heat shrunk around the silicon tubing and additionally sealed with another piece of heat shrink rubber being careful to keep the heat distal to the engineered

tissue. Media was added to this rudimentary bioreactor prior to EPC seeding onto the construct surface.

EPC Seeding Inside the Cylindrical Bioreactor

Medium was drained from the bioreactor and 500uL of EC complete medium containing approximately 100,000 EPC cells/cm^2 were injected into the bioreactor. The cell solution was confined to the area of the construct surface by capping both ends of the reactor. The bioreactor containing the cell solution was transferred to an incubator at 37°C and rotated 45 degrees every 15 minutes to ensure uniform cell coverage on the construct surface. After 1.5 hours, the media and unattached cells were drained from the bioreactor and a second bolus injection of EPCs was added to the bioreactor. Again the cell solution was confined to the construct surface and incubated for an additional 1.5 hours with rotation every 15 minutes. After a total of three hours of static cell seeding, the bioreactor was incorporated into the same recirculation flow loop shown in Figure 4.2B. The exception to Figure 4.2B was that the bioreactor was positioned in place of the parallel plate flow chamber (highlighted in the yellow box). The flow loop was primed with flow medium prior to addition of the bioreactor. Once the bioreactor containing the EPC seeded engineered tissue was incorporated into the flow loop, the flow was gradually increased to 15 dynes/cm^2 over the course of forty minutes and maintained for a total of 20 hours (time 0-20 minutes 79.5cm^3/min or 6.0 dynes/cm^2; 20-40 minutes 139.1cm^3/min or 10.5 dynes/cm^2, 40 minutes to 20 hours 198.7cm^3/min or 15.0 dynes/cm^2). A schematic drawing of the bioreactor is shown in cross-section in Figure 4.4.

      The bioreactor was designed based on assumptions of fully developed flow in a straight rigid pipe of circular cross section where the wall shear stress was determined

using the following equation: $\tau_w = (4\mu Q/\pi R^3)$ where μ is the viscosity, Q is the volumetric flowrate and R is the radius. The flow channel was based on the internal dimensions of the engineered tissue which was 3mm in diameter and 60 to 80mm in length depending on the specific tissue fabrication. A shear stress of 15 dynes/cm^2 was achieved at a flow rate of 198.7cm^3/min using a working fluid (culture medium) with a viscosity of 0.012 dyne s/cm^2. While this methodology did not exactly duplicate the *in vivo* environment, it did allow for precise control of the shear environment on a confluent monolayer of cells lining the engineered tissue lumen. Care was taken to ensure that the luminal surface, on which the ECs and EPCs resided, was as smooth as possible and that there was minimal flow disturbance at the connectors.
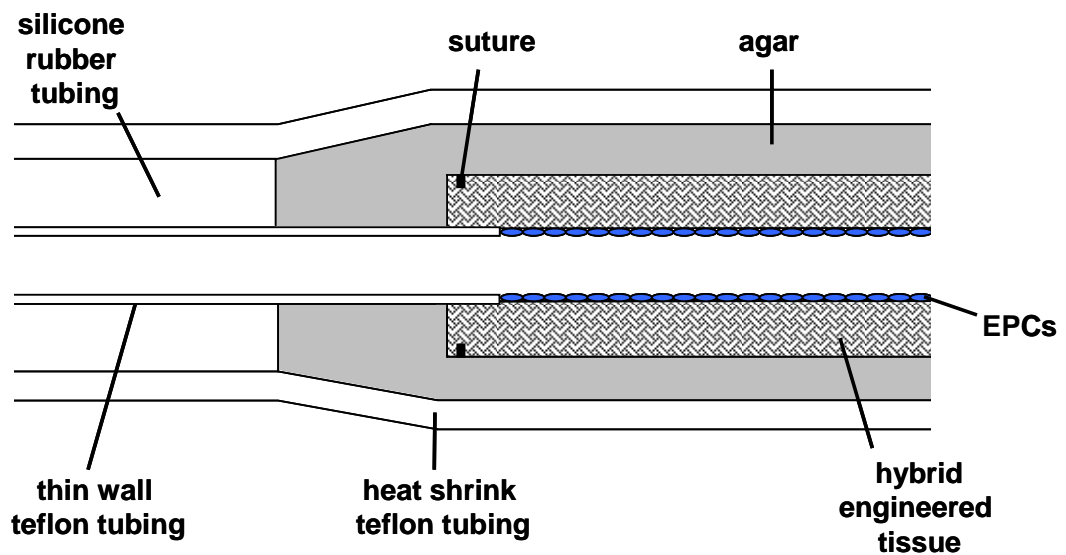
Figure 4.4: Schematic drawing of cylindrical bioreactor crosssection

Microscopy

<u>Cell Viability</u>

The construct cellular viability was determined using two different methods: LIVE/DEAD® viability/cytotoxicity assay (Molecular Probes, Carlsbad, CA) or a trypan blue exclusion assay (Sigma). The LIVE/DEAD assay was performed on small (approximately 5mm) ring samples of the construct. Tissues were removed from culture, rinsed in PBS and incubated with 4μM calcein AM and 4μM ethidium homodimer-1 for 45 minutes. The constructs were then rinsed in PBS prior to imaging on a LSM 510 laser scanning confocal microscope (Zeiss). The confocal microscopy was used to acquire images from at least five microscope fields at varying depths in the tissue ($\approx$0-100μm) as well as at least five fields covering the cross-section were used to quantify average cell viability in the engineered tissues. Image analysis based on threshold measurements was performed using ImagePro Plus to quantify the number of viable and non-viable cells in the constructs.

A Trypan blue exclusion assay was also used in select cases to verify the LIVE/DEAD assay results. For Trypan blue exclusion, construct samples were rinsed in PBS and then incubated with 600 U/mL collagenase (type CLS2, Worthington Biochemical Corporation) at 37ºC until the matrix was completely dissolved (generally 1 hour was required). The collagenase was diluted by addition of SMC complete medium (5X the collagenase volume). A small volume of digested construct solution was incubated with trypan blue (0.4%) as previously described [165]. A hemocytometer was

used to count the number of viable cells, those that exclude the trypan blue, and the number of non-viable cells, those that retain the blue stain.

F-actin Localization Using Phalloidin

Following exposure to shear stress, intracellular F-actin was stained using rhodamine phalloidin (Molecular Probes, Carlsbad, CA). The cells adhered to glass slides were fixed in 4% formaldehyde (Tousimis, Rockville, MD) for five minutes. Slides were rinsed with PBS, permeabilized with 0.1% Triton X-100 for five minutes and stained with rhodamine phalloidin (1:40 in 400μL/slide) for 20 minutes. Hoechst 33258 (1:400) was used for nuclear visualization. Slides were rinsed in PBS followed by distilled water and sealed using 1.0 glass coverslips with aqueous mounting medium (Faramount, DakoCytomation, Carpinteria, CA). A fluorescent microscope (Nikon) or the LSM510 (Zeiss) was used for imaging.

General Immunofluorescent Staining

Immunofluorescent staining techniques were used for cell characterization of ECs, EPCs and SMCs. Adherent monolayers of cells were fixed in 4% formaldehyde (Tousimis, Rockville, MD) for five minutes and rinsed with PBS. For intracellular staining, cells were permeabilized for five minutes using 0.1% triton-X. Blocking was performed using 5% normal goat serum (Sigma) or 5% donkey serum (Sigma) for one hour at 37°C. Primary (1:100) and secondary antibody (1:40) incubations were performed for 40 minutes each at 37°C. Table 4.4 lists specific antiobodies which were used with success in this research. Hoechst 33258 (1:400) was used for nuclear counterstaining. Slides were rinsed in PBS followed by distilled water and sealed using

1.0 glass coverslips with aqueous mounting medium (Faramount, DakoCytomation,

Carpinteria, CA). A fluorescent microscope (Nikon) or the LSM510 (Zeiss) was used for

imaging.

Table 4.4: Primary and secondary antibodies

Primary Antibody	Supplier	Description	Product Information
Acetylated LDL	Molecular Probes	acetylated low-density lipoprotein from human plasma, DiI complex (DiI AcLDL)	L3484
Alpha smooth muscle actin	Sigma	FITC conjugated monoclonal anti-alpha-smooth muscle actin (clone 1A4)	F 3777
Calponin	DakoCytomation	monoclonal mouse anti-human calponin (clone CALP)	M3556
CD14	Beckman Coulter	monoclonal mouse anti-human (clone RM052)	IMO643
Endoglin (CD105)	Research Diagnostics Inc.	FITC conjugated monoclonal mouse anti-human (clone 8E11)	RDI-CBL418FT
eNOS (NOS Type Ⅲ)	Santa Cruz Biotechnology	polyclonal rabbit anti-human (N-20)	sc-653
Flk-1 (VEGFR2)	Research Diagnostics Inc.	polyclonal rabbit anti-mouse Flk-1	RDI-MFLK1abrX
Flt-1 (VEGFR1)	Alpha Diagnostic International	polyclonal rabbit anti-human	FLT11-A
Myosin heavy chain (MHC)	Santa Cruz Biotechnology	monoclonal mouse anti-rat full length myosin heavy chain	sc-6956
Myosin heavy chain (MHC)	Santa Cruz Biotechnology	PE conjugated monoclonal mouse anti-rat full length myosin heavy chain	sc-6956 PE
PECAM-1 (CD31)	BD Pharmingen	FITC conjugated monoclonal mouse anti-human (clone WM59)	555445
Thrombomodulin (CD141)	DakoCytomation	monoclonal mouse anti-thrombomodulin (clone 1009)	M0617
Tissue Factor (CD142)	American Diagnostica Inc.	monoclonal mouse anti-human tissue factor	4508
Tissue Factor (CD142)	American Diagnostica Inc.	FITC conjugated monoclonal mouse anti-human tissue factor	CJ4508
Ulex europaeus lectin	Sigma	FITC conjugate	L 9006
VE-cadherin (CD144)	Santa Cruz Biotechnology	polyclonal goat anti-human (C-19)	sc-6458
Von Willebrand factor	DakoCytomation	polyclonal rabbit anti-human	A0082
Secondary Antibody	**Supplier**	**Description**	**Product Information**
	DakoCytomation	FITC conjugated polyclonal swine anti-rabbit	F0205
	DakoCytomation	FITC conjugated polyclonal rabbit anti-mouse	F0313
	Jackson Immuno Research	FITC conjugated polyclonal donkey anti-rabbit	711-095-152
	Jackson Immuno Research	FITC conjugated polyclonal donkey anti-goat	705-095-147

Cell Separation from Engineered Vascular Tissues

In order to investigate the EC or EPC specific mRNA expression, a sorting strategy was developed to remove the cells from the engineered tissue surface followed by positive selection for ECs and EPCs to ensure removal of possible SMC contamination. FITC conjugated CD31 (BD Pharmingen) was used to label ECs and EPCs followed by indirect magnetic cell labeling with anti-FITC MACS microbeads (Miltenyi Biotec, Auburn, CA). A MACS magnetic column was used to sort for EC and EPC specific populations based on CD31 expression as shown schematically in Figure 4.5. Validation of this technique is presented in Chapter VII.

At the conclusion of the experiment, ECs or EPCs were removed form the surface of the engineered tissue. 600 U/mL collagenase (Type II, Worthington) was added to the surface and incubated for 4 minutes. Media was added to the surface to stop the action of collagenase and the surface was scraped gently with a flat cell scraper. The entire procedure was performed as quickly as possible and all solutions from this point forward were kept on ice and incubations were performed at 4°C. The surface was rinsed with PBS and the cell suspension collected. The cell pellet was incubated with a FITC-CD31 antibody (10μL) for 5 min at 4°C followed by secondary incubation with anti-FITC microbeads (20μL) following the manufacturer's instructions. ECs or EPCs were eluted in the positive effluent and immediately used for analysis.
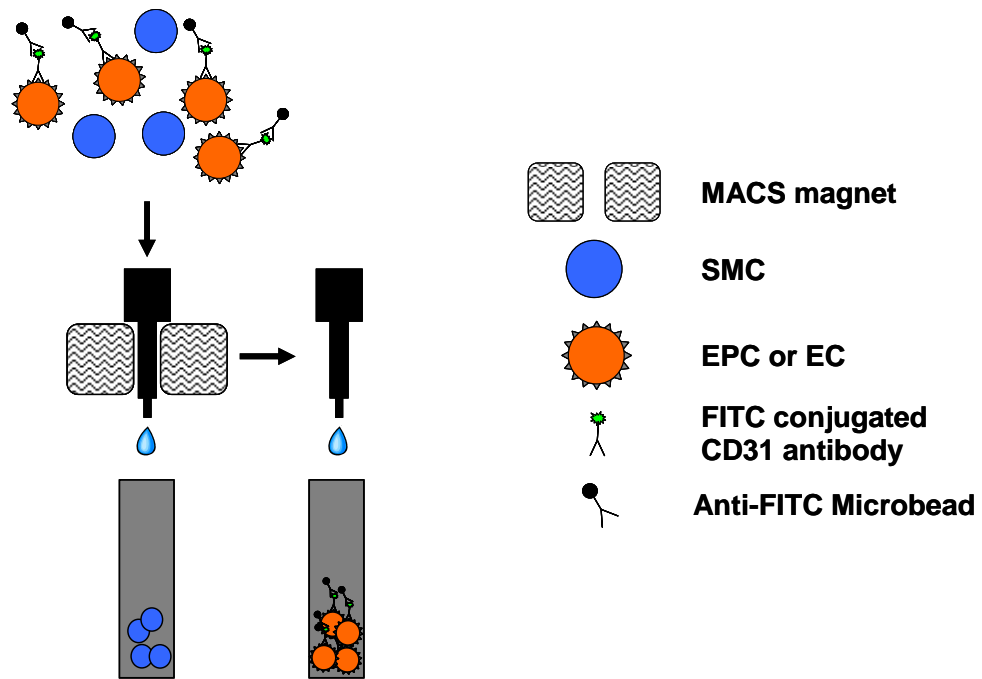
Figure 4.5: EC and EPC positive selection using the MACS® cell separation system. ECs and EPCs were separated from cell suspensions using a positive selection for CD31 (FITC) followed by indirect magnetic cell labeling with anti-FITC microbeads. CD31 positive cells were retained in the MACS® column and unlabeled cells pass through (negative effluent). The column was removed from the magnet separator and the retained cells were eluted as the positively selected cell fraction (positive effluent).

Gene Expression

RNA Isolation and Assessing Quantity and Quality of RNA

Endothelial cells were lysed and total RNA extracted using the RNeasy Mini kit (Qiagen, Valencia, CA) following the manufacture's recommendations. Samples were lysed in 350µL lysis buffer and stored at -70°C. Total RNA extraction was performed along with analysis of quantity and quality immediately prior to cDNA synthesis to minimize the number of freeze thaw cycles and preserve the RNA quality.

Quality of RNA was assessed using the RNA 6000 Nano LabChip (Agilent, Palo Alto, CA) on an Agilent Bioanalyzer 2100 by evaluating degradation of ribosomal RNA peaks. An example of a high quality RNA sample is shown in Figure 4.6. Quantity of high quality RNA was assessed by absorbance at 260nm.
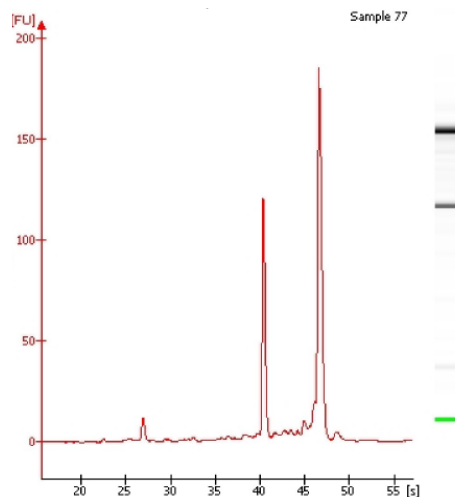
Figure 4.6: Example result from Agilent 2100 Bioanalyzer. This example shows a high quality RNA sample used for cDNA synthesis for qRT-PCR

Quantitative Real Time Reverse-Transcriptase Polymerase Chain Reaction (qRT-PCR)

qRT-PCR was performed as previously described [166, 167]. cDNA synthesis was performed on DNaseI-treated total RNA (1 μg) by oligo(dT) priming using the Superscript First Strand Synthesis System for RT-PCR (Invitrogen). qRT- PCR using SYBR Green intercalating dye was performed with the ABI Prism 7700 Sequence Detection System (Applied Biosystems, Foster City, CA; 40 cycles, melting: 20s at 95°C, annealing and extension: 120s at 60°C). qRT-PCR oligonucleotide primers (Table 4.5) were designed using ABI Primer Express software and purchased from IDTDNA (Coralville, IA). Primer specificity was confirmed by agarose gel electrophoresis and ABI Prism 7700 Dissociation Curve Software. Standards for each gene were amplified from cDNA using oligonucleotide primers, purified using a Qiagen PCR Purification kit and diluted over a functional range of concentrations. Transcript concentration in template cDNA solutions was quantified from a linear standard curve, normalized to 1 μg of total RNA, and expressed as femtomoles of transcripts per μg of total RNA. Detection limits for each gene were determined by reactions without cDNA and were at least an order of magnitude below the most dilute sample.

Table 4.5: Oligonucleotide primers for real time RT-PCR

Target		Sense primer	Antisense primer
THBD	thrombomodulin	5'-GCATTCGGGCTTGCTCATAG-3'	5'-CAAAAGCGCCACCACCA-3'
TFPI	tissue factor pathway inhibitor (lipoprotein-associated coagulation inhibitor)	5'-GACTCCGCAATCAACCAAGGT-3'	5'-TGCTGGAGTGAGACACCATGA-3'
NOS3	nitric oxide synthase 3 (endothelial cell)	5'-ATCTCCGCCTCGCTCATG-3'	5'-AGCCATACAGGATTGTCGCCT-3'
F3	coagulation factor III (thromboplastin, tissue factor)	5'-CACCGACGAGATTGTGAAGGAT-3'	5'-TTCCCTGCCGGGTAGGAG-3'
VWF	von Willebrand factor	5'-CCTATTGGAATTGGAGATCGCTA-3'	5'-CTTCGATTCGCTGGAGCTTC-3'

DNA Microarray Analysis

DNA microarray analysis was performed in collaboration with the genomics core laboratory at Morehouse School of Medicine. 500ng of total RNA from experimental samples and 500ng Universal Human Reference RNA (Stratagene, La Jolla, CA) were prepared for competitive microarray hybridization. Samples were amplified using the Agilent Low RNA Input Flourescent Linear Amplification Kit and labeled with Cy-3 and Cy-5 CTP (Perkin-Elmer, Wellesley, MA). Hybridization was performed using the Agilent In Situ Hybridization Plus kit to Human Whole Genome Oligo Microarrays (Agilent). Arrays were scanned using the Agilent dual laser DNA microarray scanner with SureScan technology. Image extraction was conducted using Agilent Feature Extraction software 7.5.1.

Gene expression was analyzed using GeneSpring software. A one-way analysis of variance (ANOVA) was performed using a Student-Newman-Keuls post hoc test and the Benjamini and Hochberg False Discovery Rate multiple testing correction. P-values <0.05 were considered significant. Pairwise comparisons were performed using a

student's t-test. The specific comparisons were: EC: shear versus static, EPC: shear versus static, Static: EPC versus EC and Shear: EPC versus EC.

Ingenuity Pathways Analysis (IPA) was used to interpret the microarray data in the context of pathways and biological systems. All genes with significant expression (ANOVA $p<0.05$) in the microarray dataset were imported into IPA. IPA used the Genbank gene ID in the dataset to map the imported data against the Ingenuity Pathways Knowledge Base (IPKB) which is the world's largest curated database of biological networks including coverage of over 23,900 mammalian genes [168]. All genes within the imported dataset which map to the IPKB and interact with at least one other gene in the IPKB were considered focus genes. Focus genes were established for the dataset from genes which were significant in the pairwise comparisons ($p<0.05$).

Measurement of Protein Expression

Flow Cytometry

Cell samples were collected for flow cytometry and were fixed in a 4% formaldehyde/2% sucrose solution for fice minutes, rinsed in PBS and incubated in 20mM glycine for 15 minutes. Blocking was performed in 5% normal goat serum (NGS) for one hour at 37°C followed by incubation with primary antibody diluted in 1% NGS for one hour at 37°C. In cases where preconjugated antibodies were not available, a separate incubation with fluorescently labeled secondary antibodies was performed for one hour at 37°C. For intracellular molecules, cells were permeabilized prior to the blocking step in 0.1% Triton X-100.

Functional Assessments

Matrigel Assay

An *in vitro* tube formation assay was perfomed on Matrigel™ basement membrane. Matrigel™ (BD Biosciences) was added to a chamber slide and allowed to gel at room temperature for one hour. 1×10^4 cells/cm^2 were added to the chamber slide in 500μL of EGM-2 medium (Cambrex). Following 18 and 24 hours of culture at 37°C, samples were imaged using a LSM510 confocal microscope (Zeiss).

Intracellular Nitric Oxide

Diamino-fluorescein-2-diacetate (DAF-2DA, Cayman Chemicals, Ann Arbor, MI), a membrane permeable intracellular nitric oxide (NO)-specific fluorescent indicator, was used to detect NO expression. Cells grown in chamber slides (Lab-Tek II, Nunc) were rinsed twice with PBS and then immersed in MCDB-131 containing 10μM DAF-2DA. Following 60 minute incubation at 37°C, cells were rinsed with PBS and fixed in 4% formaldehyde (Tousimis) for five minutes. Slides were rinsed in PBS followed by distilled water and sealed using 1.0 glass coverslips with aqueous mounting medium (Faramount, DakoCytomation, Carpinteria, CA).

Baboon *Ex Vivo* Shunt

Normal male juvenile baboons (*Papio anubis*) were used with approval of the Institutional Animal Care and Use Committee in compliance with the National Institutes of Health guidelines. Shunt studies were performed as previously described [169]. Chronic exteriorized arteriorvenous (AV) access shunts were surgically placed between

the femoral artery and vein to permit interposition of the engineered tissue constructs. Engineered tissue constructs were interposed into the exteriorized AV shunts of awake immobilized animals and blood flow in the shunt was maintained at 100mL/min by real time measurement of flow using an ultrasonic flow probe. Thrombus accumulation on engineered tissues was quantified by measuring the deposition of platelets. Autologous baboon platelets are labeled with 111 Indium chloride (Mallinckrodt Inc., St. Louis, MO) and reinjected prior to experimentation. Gamma camera imaging of the test segments was performed at five minute intervals for up to 35 minutes to quantify 111In-labeled platelet deposition.

111 Indium Chloride Labeling of EPCs

In order to quantify cell retention on the graft surface during whole blood exposure in the *ex vivo* shunt, EPCs were radiolabeled using a radiopharmaceutical Indium (In) 111 Chloride (Mallinckrodt Inc., St. Louis, MO) prior to seeding onto the engineered tissue. EPCs were trypsinized from tissue culture flasks and counted using a hemocytometer. Up to $4x10^6$ cells were resuspended in 0.5mL DPBS (without CaCl and MgCl) plus 10μL of labeling buffer and incubated at 37°C for 10 minutes. The labeling buffer was prepared fresh and consisted of 50μL of Indium 111 chloride solution (calibrated to be 500μCi), 1.3μL of 0.2M tropolone (Sigma) and 50μL carbonate buffer. Immediately following incubation in the labeling buffer, 2mL of fresh growth media was added. The cell solution was centrifuged at 250 RCF, excess labeling buffer was removed and cells were resuspended in fresh growth media. Labeling efficiency was quantified using a 1480 Wizard Automatic Gamma Counter (PerkinElmer). Radiolabeled

cells suspended in growth media were then seeded onto the engineered tissue grafts in two administrations of approximately 100,000 cells/cm^2 each.

Construct Material Property Testing

Mechanical characterization is conducted on a ring testing apparatus that was developed and implemented in our laboratory [75, 77, 164].

Sample Preparation

Tubular constructs were removed from the culturing medium and rinsed in PBS (pH 7.4) under gentle agitation. Each construct was divided into ≈5mm ring sections using a razor blade, and four small black beads were attached to the cut ends of the rings with a cyanoacrylate-based adhesive. Specimens were handled using surgical instruments and care was taken in all steps to minimize incidental damage.

Uniaxial Tensile Testing and Analysis

Uniaxial tensile tests were performed on ring samples of the engineered vascular tissue. Ring samples were loaded onto the hooks of the testing apparatus and preconditioned through three cyclic loading sequences (0.2 mm/sec) to approximately 20% of the strain at rupture. Samples are then stretched at a constant rate to failure (0.2 mm/sec). Cauchy stresses and Eularian strains were used to determine the stress-strain profiles.

Cauchy stresses were determined as:

$$\sigma\{t\} = \frac{F\{t\}}{A_o} = \frac{F\{t\}}{2TW}$$

where $\sigma(t)$ is the stress as a function of time, $F(t)$ is the force as a function of time, A_o is the original cross-sectional area, T is the wall thickness, and W is the width of each ring sample. Since both construct walls are assessed at the same time in the ring specimen testing format, the dimensions are multiplied by a factor of two to obtain the cross-sectional area. Strain was determined from the hook positions from the linear motor position voltage output. The voltage displacement information was converted to Lagrangian strain data using the following equation:

$$\varepsilon\{t\} = \frac{L\{t\} - L_o}{L_o}$$

where $\varepsilon(t)$ is the strain as a function of time, $L(t)$ is the distance between the hooks as a function of time, and L_o is the original distance between the hooks.

Ultimate tensile stress (UTS) was defined by the peak stress attained during the testing procedure. Linear moduli were defined by best fit regressions of the regions spanning 25 to 75% of the UTS.

CHAPTER V: CELL ISOLATION AND CHARACTERIZATION

Introduction

The overall motivation for this study comes from the clinical setting where patients present with vascular disease and require medical intervention. Ultimately the disease pathology results in a reduction in blood flow and therefore reduction in oxygen transport to the surrounding tissues. One of the current clinical treatment options is to bypass the diseased vessel, thereby providing a new conduit for blood and nutrients to reach the tissues. While a patient's own vessels may be transplanted as the bypassing conduit, there remains an insufficient supply of autologous tissue in a significant number of patients. Tissue engineering approaches aim to provide an engineered alternative to autologous vessel transplant by providing a blood vessel substitute which will function as the needed conduit for blood and nutrient transport.

There are a number of tissue engineering strategies directed at emulating the native blood vessel function (a detailed presentation of current tissue engineering strategies can be found in Chapter II: Background). It has been our approach to build an engineered tissue using naturally derived matrix materials and cells which can be modulated *in vitro* to ultimately produce a functional blood vessel substitute. The native vessel is structured as a tri-layer unit composed of a blood contacting intima supported by a smooth muscle rich media and anchored to the surrounding tissue by an adventitia infiltrated with vaso vasorum. *In vitro*, we are able to create an engineered tissue which structurally mimics the native vessel with the use of donor vascular cells and natural

matrix materials. This approach is able to create a physiologic model of the vascular wall *in vitro* but in order to create clinically viable strategies, current research is aimed at identifying appropriate cells sources which are readily available and can replicate the functions of the native vascular cells.

The vascular endothelial cell (EC) provides a barrier between blood and the remainder of the vascular wall. Extensive research has shown that the EC is a gatekeeper for many biological processes including normal hemostasis and it is considered a critical cell type needed for engineered blood vessel substitutes. While it may be possible to use allogeneic SMCs in a tissue engineering approach, an autologous or immune privileged source of ECs will be required. The earliest vascular tissue engineering approaches isolated autologous endothelial cells and through *in vitro* expansion, created a neointima on synthetic substrates [61-63]. These approaches have made it into clinical application but have not gained widespread use due to a number of factors, including their limited applicability to large diameter applications (>6mm internal diameter) [9]. Finding appropriate endothelial cell sources for tissue engineering remains a challenge but the recent discovery of endothelial progenitor cells (EPCs) in bone marrow and peripheral blood [91] is a potentially promising addition to the tissue engineer's toolbox. To date, several "proof of concept" studies have incorporated EPCs into tissue engineering strategies [149-153, 157, 158] but a lot of research remains to understand their true therapeutic potential.

The research presented in this dissertation includes specific aims which rely on the use of primary vascular cells. Vascular smooth muscle cells were used for the fabrication of an engineered blood vessel substitute mimicking the medial layer of a

native vessel. This engineered tissue serves as an *in vitro* model of the vascular wall and provides a physiologic substrate on which new endothelial cell sources can be investigated. Endothelial progenitor cells were isolated, characterized and further studied in the context of providing a vascular lining. This newly discovered cell population holds promise for many applications including tissue engineering of vascular grafts and vascular networks as well as in cell therapies and induction of endogenous repair mechanisms. Vascular endothelial cells were isolated and served as species specific age and sex matched controls for many of the studies with EPCs.

For the scope of this research, three primary cell types were isolated and cultivated in culture. This chapter highlights the isolation results and phenotype characterization for vascular smooth muscle cells (SMCs), vascular endothelial cells (ECs), and peripheral blood derived endothelial progenitor cells (EPCs). In this study, primary cells were obtained from juvenile baboon (*Papio anubis*) tissues and expanded *in vtiro* to sufficient numbers for subsequent experimental protocols. The baboon is an established non-human primate animal model for cardiovascular and thrombosis studies and is considered the gold standard in replicating human physiology for pre-clinical studies. The rheology of baboon blood has been extensively validated against the human and is considered a premier model for investigating blood biomaterial interactions *in vivo* [169-173].

Experimental Design

SMCs, ECs and EPCs were isolated from juvenile male baboons (*Papio anubis*) weighing approximately 10-15kg as described in detail in Chapter IV: Materials and Methods. The baboon species was chosen because of the similarity with human

physiology which facilitates the translation of these results into predictors for human application. These studies were conducted under approval of the Institutional Animal Care and Use Committee (Emory University and Georgia Institute of Technology) in accordance with related university policies. Briefly, fresh carotid artery specimens and blood samples were obtained just prior to sacrifice from animals enrolled in other chronic implantation studies. ECs were isolated from the carotid artery lumen using a brief enzymatic digestion followed by manual scraping of the surface. Following dissection and removal of the adventitia, SMCs were obtained from the carotid artery media. The vascular tissue was treated overnight in a collagenase solution and then plated into standard culture flasks for SMC isolation. Through the course of this research, we were able to perform eight successful SMC isolations.

EPCs were isolated from the mononuclear fraction of anti-coagulated baboon blood and cultivated on fibronectin coated tissue culture plastic in endothelial specific growth media enriched with VEGF, EGF, FGF-β and IGF. Within 9-23 days after plating, colonies of adherent cells with cobblestone morphology grew out of the buffy coat cultures. Using standard culture techniques, these outgrowth colonies were expanded through passaging and characterized. This project started as collaboration between the laboratory of Dr. Robert Nerem and Dr. Stephen Hanson of Emory University (now at Oregon Health and Science University). Dr. Hanson's group had experience with isolation of baboon peripheral blood EPCs. Initial studies were performed with cells generously donated from Dr. Hanson but as the project progressed an additional four successful isolations were performed. The results presented in this chapter are results from the later isolations.

The cell phenotype was characterized using light and confocal microscopy in addition to flow cytometry to investigate protein expression and cell specific functions.

Results

Baboon Arterial Smooth Muscle Cells (SMCs)

Phase Contrast Microscopy

Phase contrast microscopy images in Figure 5.1 show the spindle morphology of baboon carotid artery smooth muscle cells in culture. The collagenase digestion resulted in a heterogeneous slurry of partially digested tissue and single cells which were plated onto tissue culture flasks. As shown in Figure 5.1A, following five days in culture adherent pieces of partially digested tissue were visible surrounded by an abundance of spindle shaped cells. In other areas of the culture flask, single adherent cells were visible (Figure 5.1B). Remnants of tissue could be seen in the cultures for 1-2 passages. SMCs were expanded in culture and used for experiments between passages 6-8. As SMCs reached confluence, SMC morphology took on a "hill and valley" appearance as shown in Figure 5.1C.
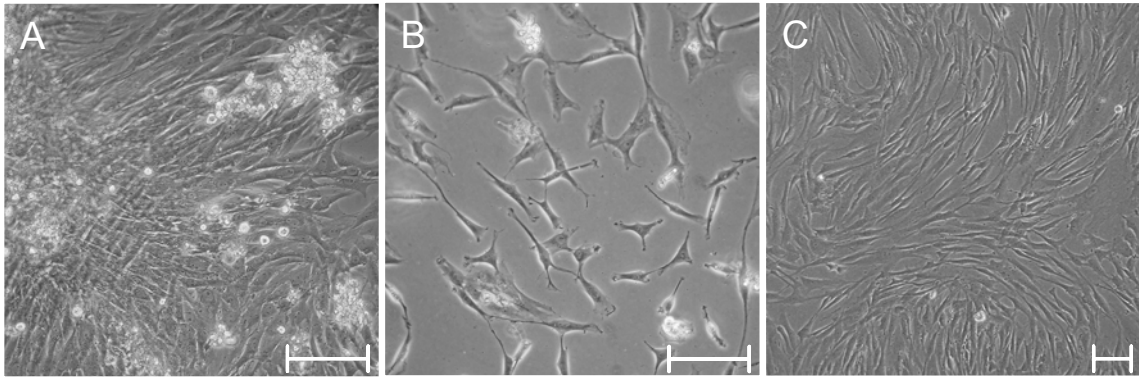
Figure 5.1: Phase contrast microscopy of SMCs. (A,B) Baboon carotid artery smooth muscle cells (SMCs, passage 0) five days after enzymatic digestion of native tissue (C) SMC expanded on tissue culture plastic (passage 7). Scale bar = 100μm.

Contractile Protein Expression

Immunofluorescence

Using immunofluorescence, SMC monolayers were stained with antibodies to

proteins associated with the smooth muscle cell cytoskeleton and contractile apparatus.

As shown in Figure 5.2, staining was performed for the major contractile proteins, actin

(alpha smooth muscle isoform) and myosin (full length including SM-1 and SM-2

isoforms) as well as for the regulator protein, calponin. The baboon carotid artery

smooth muscle cells (SMCs) showed strong expression of alpha smooth muscle actin and

weaker expression of calponin (Figure 5.2A,B). Myosin heavy chain expression was not

detected using immunofluorescence (Figure 5.2C).

Flow Cytometry

Flow cytometry was used as a semi-quantitative method to characterize SMC

phenotype. Figure 5.3 shows representative histograms and quantification of protein

expression for alpha smooth muscle actin, calponin and myosin heavy chain in SMCs.

Expression was quantified as the percentage of cells which had fluorescence greater than

95% of the negative control. The large majority of SMCs were positive for alpha smooth

muscle actin (99.9%) and calponin (86.2%) but showed negligible expression of myosin

heavy chain (4.6%).
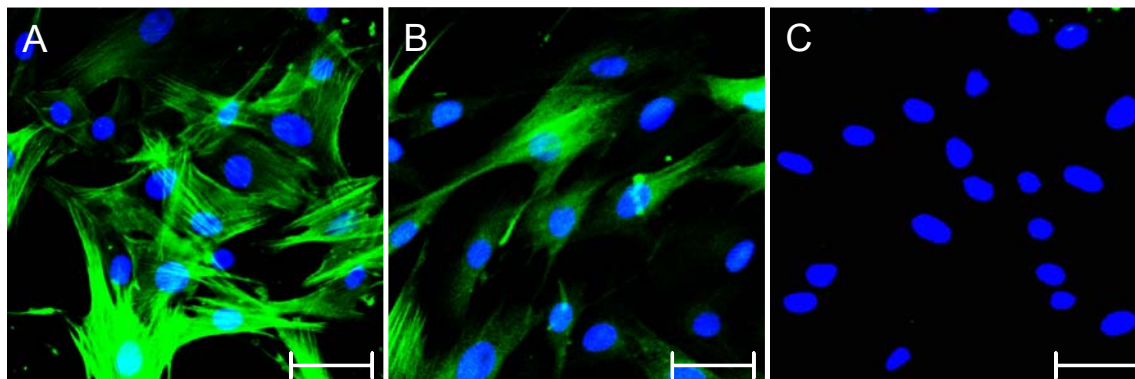
Figure 5.2: Confocal microscopy of contractile protein expression in SMCs. (A) Baboon carotid artery smooth muscle cells (SMCs, passage 2) stained for expression of alpha smooth muscle actin, (B) calponin, (C) smooth muscle myosin heavy chain. Scale bar = 50μm.
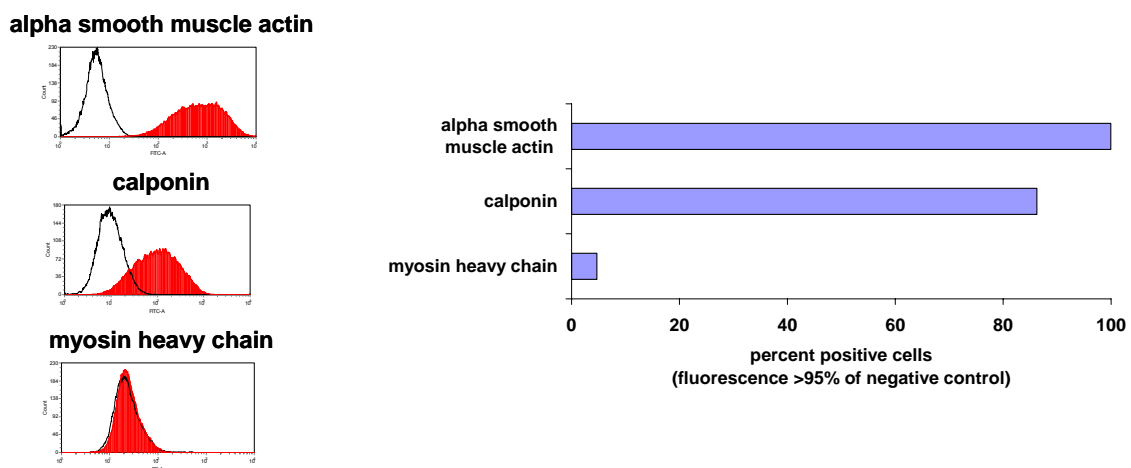
Figure 5.3: Characterization of SMC protein expression using flow cytometry. Representative flow cytometry histograms are shown for each of the proteins investigated in baboon carotid artery smooth muscle cells (SMCs, passage 2) (left panel). Black outlines the negative control. Red histograms are the fluorescently labeled cell samples. Protein expression was quantified from flow cytometry histograms (right panel). Cells with fluorescence values >95 percent of the negative control were considered positive.

Baboon Arterial Endothelial Cells (ECs)

Phase Contrast Microscopy

Baboon carotid artery endothelial cells were isolated from fresh carotid artery specimens using a brief enzymatic (collagenase and/or typsin) digestion followed by manual scraping of the luminal surface. The lumen was rinsed and the solution was plated onto tissue culture plastic coated with either 50ug/mL Type I collagen or human fibronectin. Figure 5.4 shows phase contrast microscopy images of adherent carotid artery endothelial cells five days after initial plating. ECs showed cobblestone morphology and grew into contact inhibited confluent monolayers. Occasionally, sheets of endothelial cells removed from the native artery surface during scraping or small pieces of extracellular matrix could be seen in the culture dishes (Figure 5.4A). Individual cells as well as multi-cellular sheets adhered to the culture flask and began to proliferate within the first few days of culture.
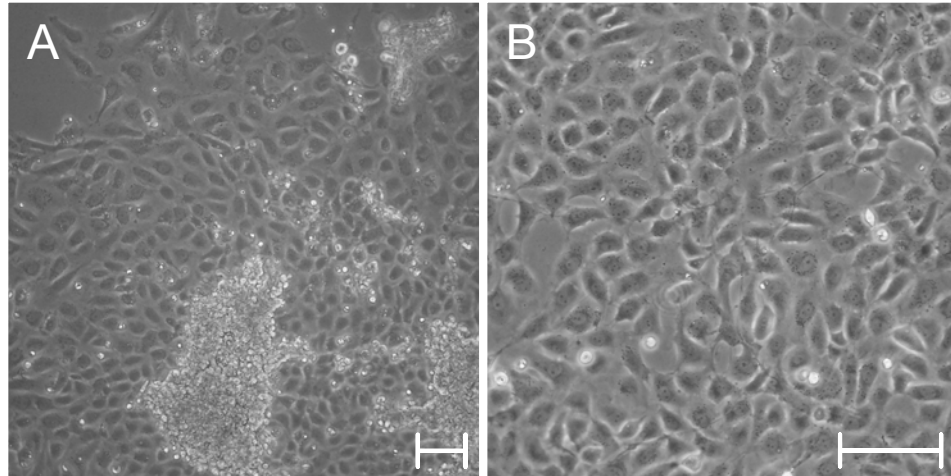
Figure 5.4: Phase contrast microscopy of ECs. (A,B) Baboon carotid artery endothelial cells (ECs, passage 0) five days after isolation from native tissue. Scale bar = 100μm.

Receptor Expression and Cellular Function

Receptor Expression – Immunofluorescence

Figure 5.5 shows representative images of fluorescent staining for alpha smooth muscle actin (SMA), nitric oxide synthase 3 (NOS3), *Ulex europaeus* agglutinin I (ulex lectin) and ve-cadherin in baboon carotid artery ECs. Hoechst 33258 was used as a nuclear counterstain. ECs displayed no detectable expression of SMA but were positive for expression of NOS3 and ve-cadherin. Additionally, ECs bound FITC conjugated ulex lectin to their cell surface.

Cellular Function

Two markers of endothelial cell specific function were assayed using fluorescent microscopy. Cellular uptake of Dil labeled acetylated LDL (acLDL) and intracellular nitric oxide (NO) production (shown with a NO specific fluorescence indicator, DAF-2DA) is shown in Figure 5.6. ECs readily took up Dil acLDL into intracellular storage pools as indicated by the bright red staining in individual cells. In panel B of Figure 5.6, EC also stained positive for DAF-2DA indicating the presence of intracellular nitric oxide.

Baboon Circulating Endothelial Progenitor Cells (EPCs)

Fresh anti-coagulated blood (50-250mL) was diluted 1:2 in HBSS+1mM EDTA+0.5%BSA, layered onto Histopaque-1077 (Figure 5.7A) and centrifuged following the manufacturer's instructions. This gradient centrifugation resulted in aggregation and sedimentation of the erythrocytes and granulocytes to the bottom of the centrifuge tube. The mononuclear cell fraction of the blood remained at the plasma-

Histopaque-1077 interface (Figure 5.7B) and could be separated, washed and plated onto

fibronectin coated tissue culture plastic.
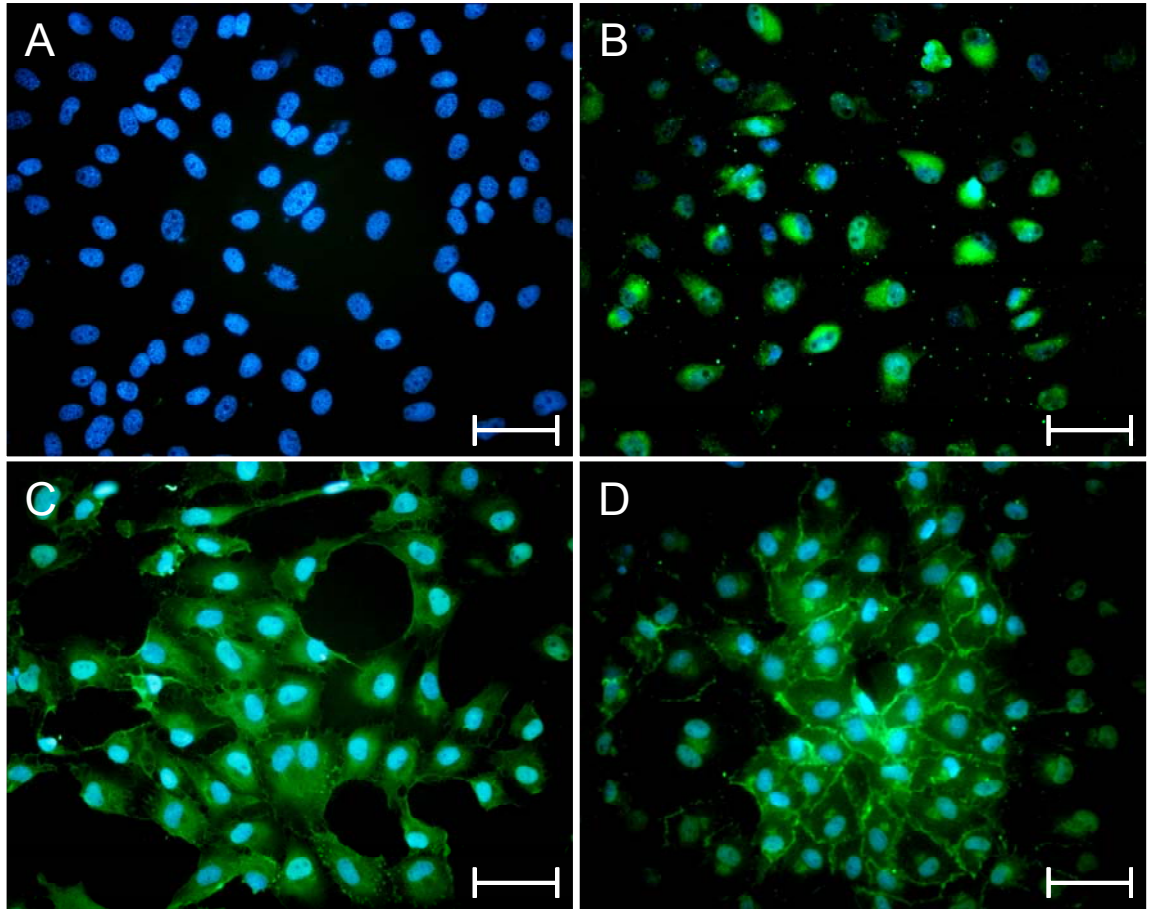
Figure 5.5: Fluorescent microscopy of surface markers in ECs. Immunofluroescent staining of baboon carotid artery endothelial cells (ECs, passage 5) for expression of (A) alpha smooth muscle actin (SMA), (B) nitric oxide synthase 3 (NOS3), (C) *Ulex europaeus* agglutinin I (ulex lectin) and (D) ve-cadherin. Hoechst 33258 was used as a nuclear counterstain. Scale bar = 50μm.
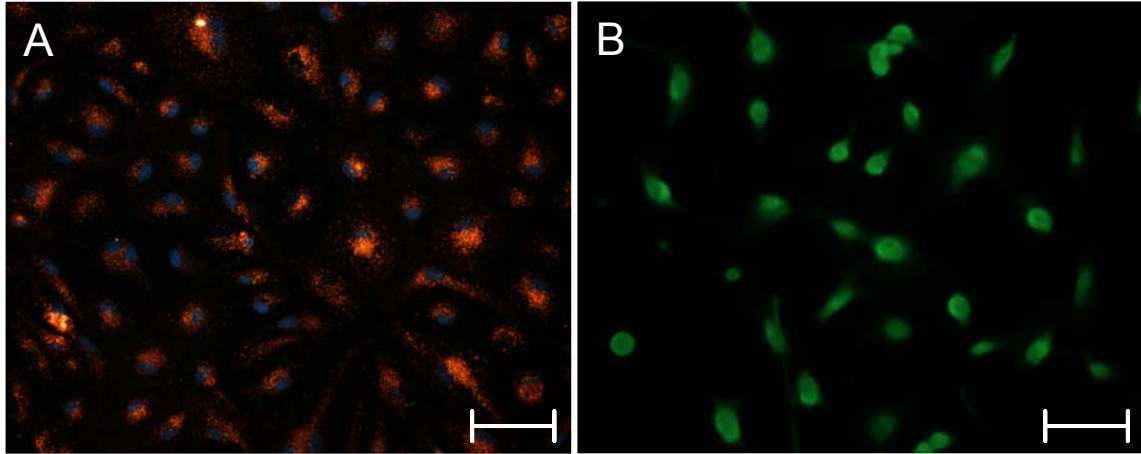
Figure 5.6: Fluorescent microscopy of markers of cellular function in ECs.
Fluorescent microscopy images show baboon carotid artery endothelial cells (ECs, passage 5) were positive for (A) uptake of Dil-labeled acetylated LDL and (B) intracellular nitric oxide (NO) production as shown with a NO specific fluorescence indicator, DAF-2DA. (A) Hoechst 33258 was used as a nuclear counterstain. Scale bar = 100μm.
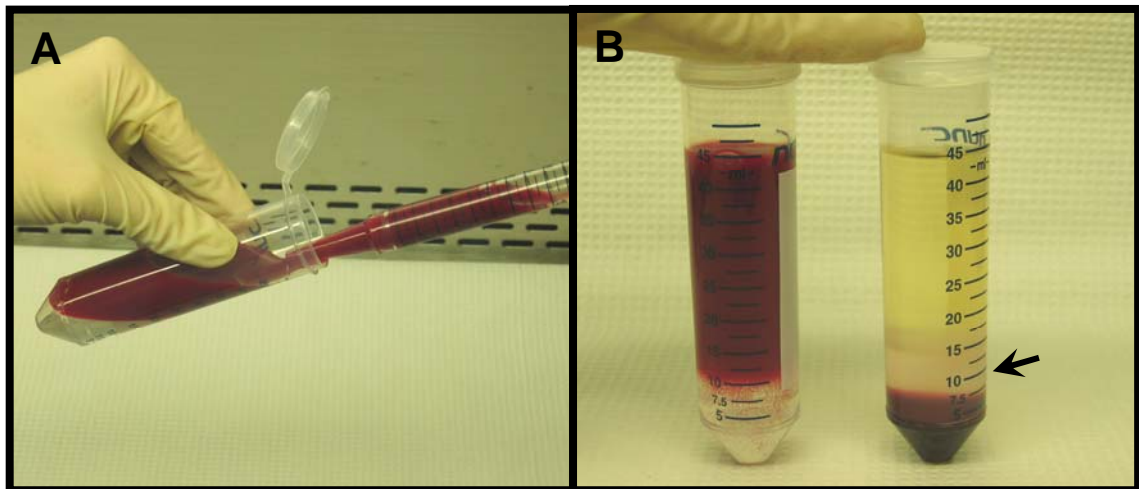
Figure 5.7: Buffy coat preparation from baboon peripheral blood. (A) Blood collected in 3.8% sodium citrate or acid citrate dextrose (ACD) solution was diluted 1:2 in HBSS+1mM EDTA+0.5%BSA and layered onto Histopaque-1077. (B) Following centrifugation, arrow indicates mononuclear cell fraction plated for endothelial progenitor cell isolation. Photograph by TLJ.

After 24 hours, unattached cells and debris were removed by exchange of the culture medium. Figure 5.8 shows representative phase contract microscopy images of the mononuclear cell culture in the days following plating. The adherent cells had a heterogenous morphology. There were many round, monocyte-like cells as well as a number of flattened cells mixed with spindle-like cells. Media was changed every other day and the number of rounded monocyte-like cells diminished over the course of approximately 4 weeks. Cultures were monitored daily and between 9 and 23 days of culture, small outgrowth colonies of approximately 30-100 cells were observed. The colonies had cobblestone morphology as shown in Figure 5.9 and rapidly proliferated. Colonies were selectively trypsinized and replated in separate culture dishes. This rapid proliferation continued allowing for exponential expansion of the cells. Cells were cryopreserved in 10% dimethyl sulfoxide (DMSO) using standard techniques and thawed as needed for characterization and further study.

Receptor Expression and Cellular Function

Receptor Expression – Immunofluorescence

EPCs were stained for a panel of markers using immunofluorescent techniques. Figure 5.10 shows representative images investigating EPCs expression of both smooth muscle and endothelial specific markers. EPCs were negative for expression of SMA. EPCs showed positive expression of VEGR1, NOS3, ve-cadherin and von willebrand factor (VWF). EPCs also bound FITC conjugated ulex lectin.

Cellular Function

As indicators of endothelial cell specific function, the uptake of acLDL, the production of intracellular nitric oxide (NO) and the ability to form *in vitro* vascular network structures was investigated. EPCs readily took up Dil labeled acLDL and also stained positive for intracellular NO using a NO specific fluorescence indicator, DAF-2DA as shown in Figure 5.11.

Figure 5.12 shows representative images of EPCs which have been labeled with a fluorescent cell tracker (CellTracker Orange CMTMR, Molecular Probes) to enhance visualization prior to seeding onto Matrigel™ plugs in multiwell culture dishes. EPCs formed extensive multicellular branching networks when seeded onto Matrigel™ for 18-24 hours. By 18 hours, EPCs had formed substantial tube like structures covering the Matrigel™ surface which were essentially unchanged at 24 hours. Additional studies performed with unlabeled EPCs showed similar results (data not shown).

Receptor Expression – Flow Cytometry

Flow cytometry was used as a semi-quantitative method to investigate EPC protein expression. Figure 5.13 shows representative histograms of EPCs labeled for expression of VWF, ve-cadherin, ulex lectin, thrombomodulin, pecam (CD31), flt-1 (VEGFR1), flk-1 (VEGFR2), eNOS (NOS3), endoglin (CD105), and CD14. In addition, quantification of flow cytometry data from independent experiments is compiled in Figure 5.14. Cells with fluorescence values greater than 95% of the negative control were considered positive. EPCs were strongly positive for VWF, ve-cadherin, ulex lectin, CD31, VEGFR1, eNOS, and CD105 with more than 90% of the cells positive for

66

each of these markers. EPCs were weakly positive for thrombomodulin and VEGR2

(23% and 36%, respectively) and showed minimal expression of the monocytic marker,

CD14 (9%).
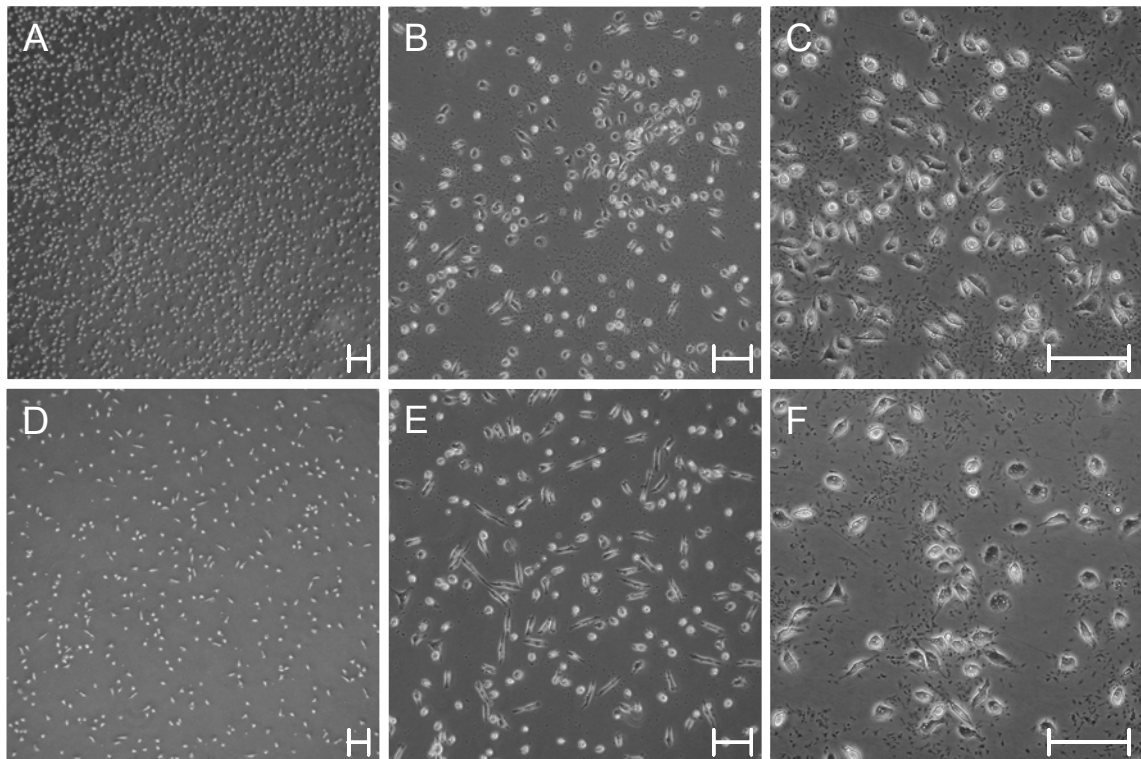
Figure 5.8: Phase contrast microscopy of mononuclear cells plated onto fibronection coated tissue culture plastic. Two representative images are shown for 5X (A,D), 10X (B,E), and 20X (C,F) magnifications. Images were taken on days 2-9 of culture. Scale bar = 100μm.
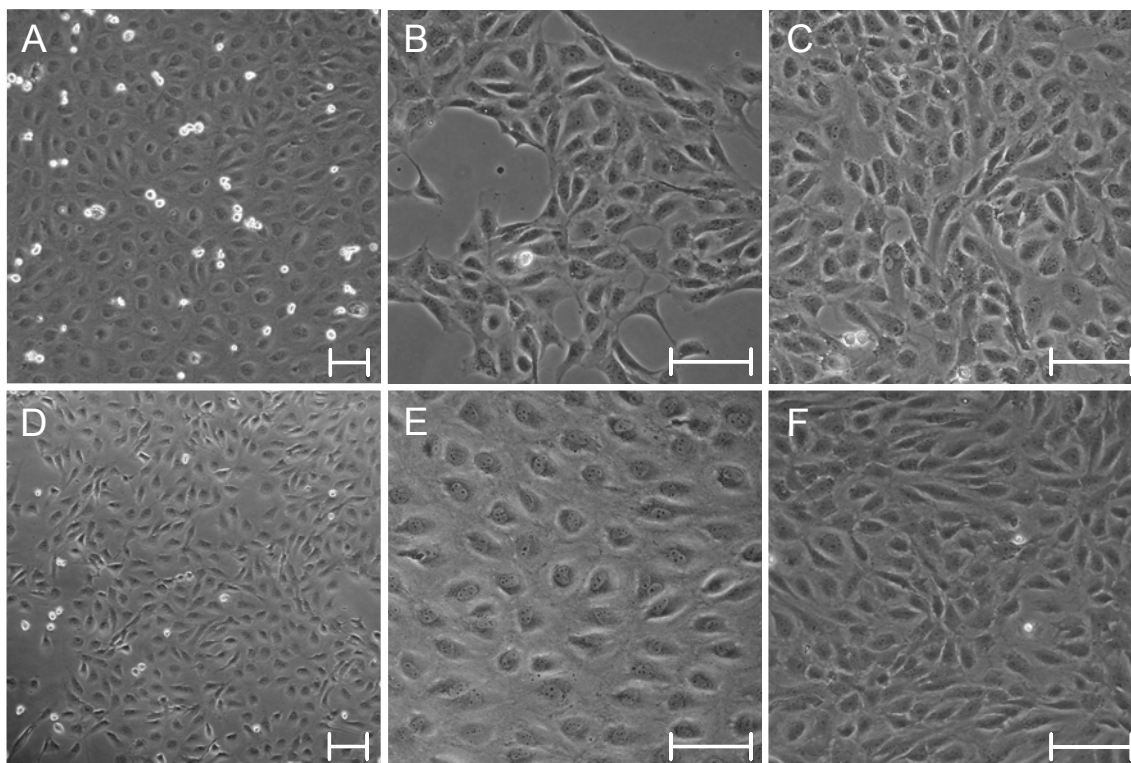
Figure 5.9: Phase contrast microscopy of endothelial progenitor cell (EPC) outgrowth from peripheral blood buffy coat cultures. Representative images are shown for 10X (A,D) and 20X (B,C,E,F) magnifications. Outgrowth colonies were observed after 9 to 23 days in culture. Scale bar = 100μm.
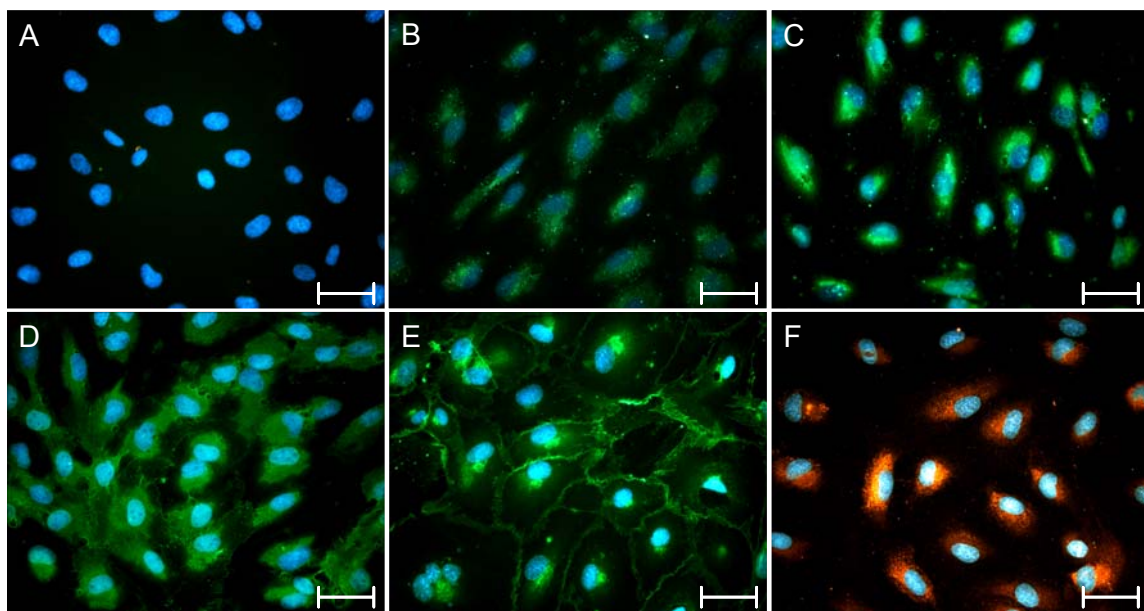
Figure 5.10: Fluorescent microscopy of markers in EPCs. Immunofluorescent staining of baboon endothelial progenitor cells (EPCs, passage 3) for expression of (A) alpha smooth muscle actin (SMA), (B) flt-1 / VEFR1 (C) nitric oxide synthase 3 (NOS3), (D) *Ulex europaeus* agglutinin I (ulex lectin), (E) ve-cadherin and (F) von Willebrand factor (VWF). Hoechst 33258 was used as a nuclear counterstain. Scale bar = 50μm.
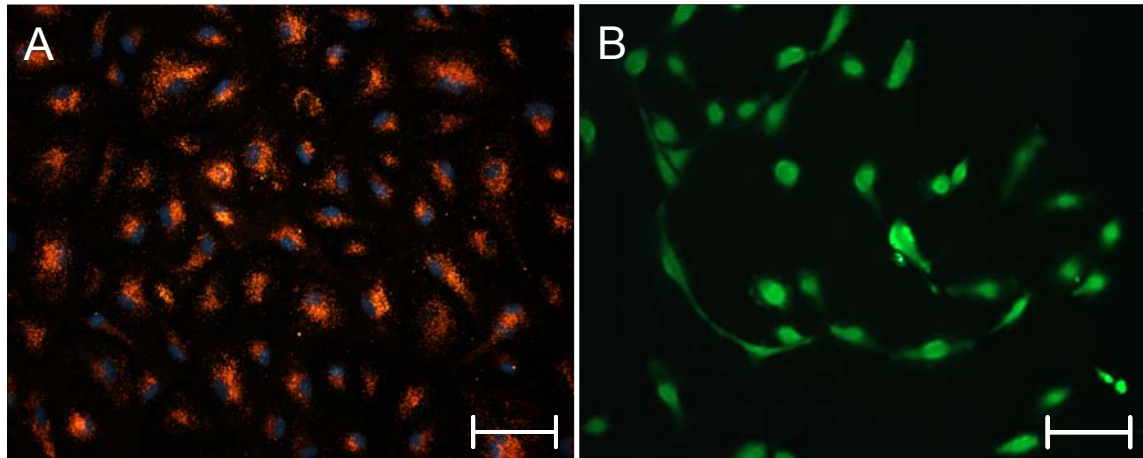
Figure 5.11: Fluorescent microscopy of markers of cellular function in EPCs.
Fluorescent microscopy images show baboon endothelial progenitor cells (EPCs, passage 3) were positive for (A) uptake of Dil-labeled acetylated LDL and (B) intracellular nitric oxide (NO) production as shown with a NO specific fluorescence indicator, DAF-2DA. Hoechst 33258 was used as a nuclear counterstain. Scale bar = 100μm.
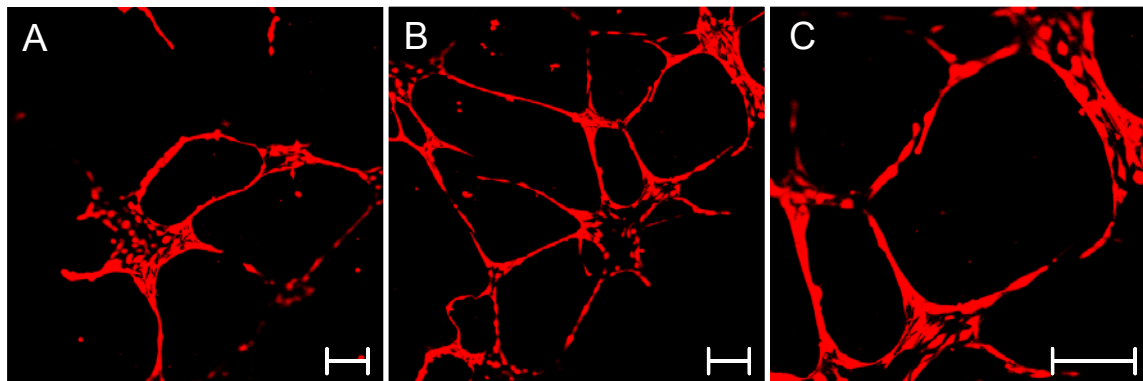
Figure 5.12: Confocal microscopy of EPC capillary tube formation on Matrigel™.
Endothelial progenitor cells were labeled with a fluorescent cell tracker and seeded onto Matrigel basement membrane matrix. Following (A) 18 hours and (B,C) 24 hours of culture, EPCs readily formed extensive multi-cellular branching networks. Scale bar = 200μm.
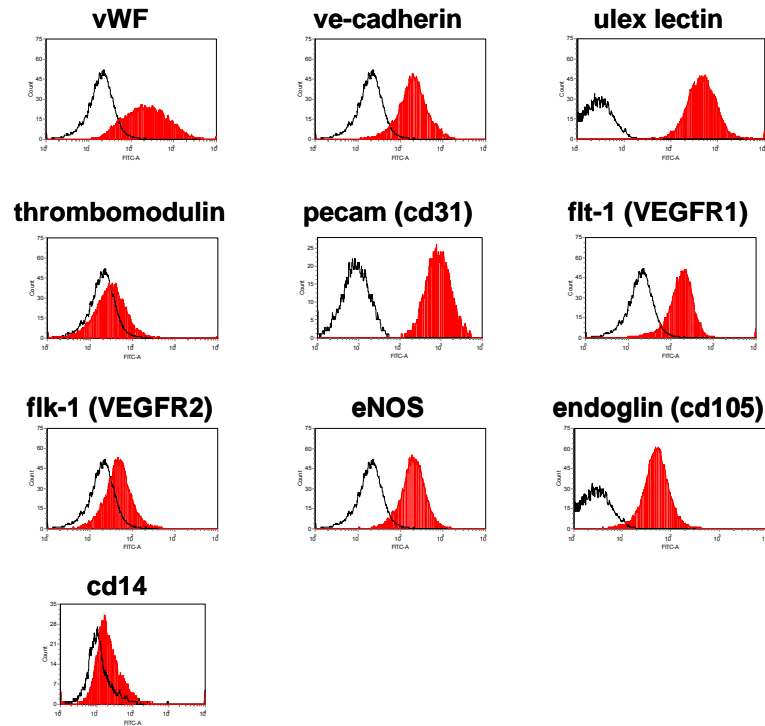
Figure 5.13: Characterization of EPC protein expression using flow cytometry.
Representative flow cytometry histograms are shown for each of the proteins
investigated in EPCs (passage 3). Black outlines the negative control. Red histograms
are the fluorescently labeled cell samples.

EPC Characterization
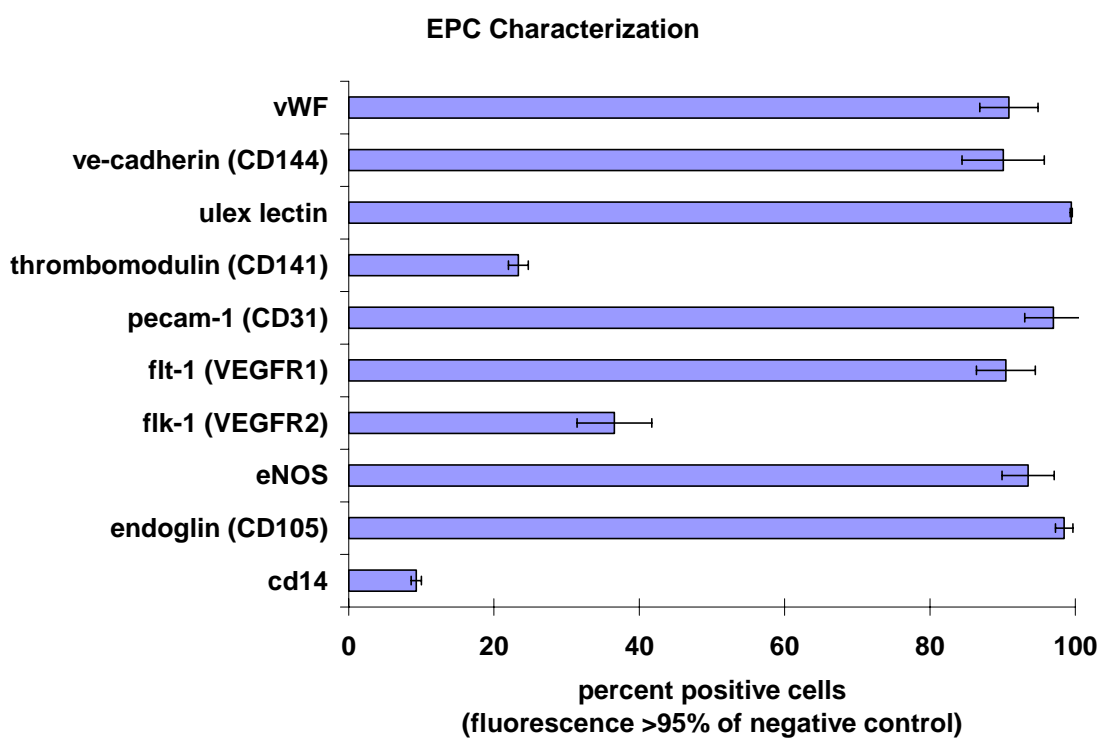
Figure 5.14: Quantification of EPC protein expression using flow cytometry.
Protein expression was quantified from flow cytometry histograms. Cells with
fluorescence values >95 percent of the negative control were considered positive. Data
are expressed as mean ± standard deviation.

Discussion

Limitations of the Experimental Approach

There are several limitations of this study. In order to isolate cells for *in vitro* culture, the cells were removed from their *in vivo* native environment of the vascular wall or blood. *In vivo,* the cells are surrounded by a local milieu of extracellular matrix proteins, neighboring cells, soluble or bound factors and a three-dimensional (3-D) environment which may or may not be recreated *in vitro*. The advantages of this *in vitro* culture approach is that the local environment of the cells is now more easily controlled allowing for study of numerous isolated independent variables (i.e. cytokines, substrate, local shear stress) on the cellular response. The disadvantage of this approach may be that in the simplified *in vitro* culture environment, cells could alter their phenotype and may not "react" exactly as would be seen *in vivo*. Our understanding of vascular biology has advanced significantly since the advancement of routine cell culture owing to the fact that *in vitro* culture allows the researcher a mechanism to "probe" specific cellular functions. Culture techniques have begun to advance, incorporating multiple facets of the *in vivo* environment into *in vitro* platforms. For example, specialized growth medium cocktails are used and co-culture with multiple cell types as well as incorporation of extracellular matrix proteins are now often reported in published research. In addition to these advances, we have also incorporated more physiologic *in vitro* culture methods in our own research. The primary smooth muscle cells described in this study were used as building blocks in the generation of an engineered tissue which mimics the medial layer of the native vascular wall. By combining the SMCs with the natural extracellular matrix

73

protein, Type I collagen in a 3-D environment we have created an *in vitro* model which mimics the *in vivo* blood vessel. In the research presented in this dissertation, a combination of culture approaches will be presented and their advantages and disadvantages discussed. In this study, we have removed SMCs, ECs and EPCs from their native environment to allow for detailed characterization of their phenotype and function.

Baboon Arterial Smooth Muscle Cells

In this study, baboon carotid artery smooth muscle cells (SMCs) were successfully isolated and cultured *in vitro* and maintained for up to 10 passages. Since the first reports describing smooth muscle cells culture [174, 175], there have been significant advances in vascular biology research performed with cultured SMCs. The use of baboon derived primary cells was chosen in preparation for future pre-clinical studies where the non-human primate is an established model. Isolation of the SMCs from the vascular media was performed using a facilitated migration method [161]. This method combined the enzymatic digestion method used by some groups [162] and the explant outgrowth method which has also been described previously [163] to obtain a population of SMCs from the vascular media cross-section. Smooth muscle cells are capable of expressing a continuous spectrum of phenotypes ranging from exclusively "contractile" on one end to exclusively "synthetic" on the other end [176]. In this study, immunofluorescence and flow cytometry were used to positively identify the cell population as SMCs which lie somewhere along the spectrum between "contractile" and "synthetic". The baboon cells expressed SMA and calponin but were negative for myosin heavy chain. It has been previously reported that once SMCs are plated in

culture, they rapidly loose their "contractile" phenotype which also corresponds to a dramatic decrease in staining for myosin isoforms [177]. This is consistent with our own data and may explain why myosin heavy chain expression was not detected using either immunofluorescence or flow cytometry. Unless otherwise stated, SMCs were used between passages 6-8 for experimental protocols.

Baboon Arterial Endothelial Cells

Baboon carotid artery endothelial cells were isolated and cultured from fresh vascular tissues. The ECs were characteristic of normal large vessel endothelial cells forming contact inhibited confluent monolayers with cobblestone morphology. In early isolation attempts to obtain a homogeneous population of ECs, some cultures were "contaminated" with a mixed cell population containing spindle shaped SMCs or fibroblast-like cells which would quickly "take over" the culture. These cultures were abandoned and only cultures containing a uniform polygonal morphology were expanded and characterized. Immunofluorescence showed that the cell populations were negative for SMA and were positive for a number of endothelial specific antigens including NOS3, ulex lectin and ve-cadherin. Endothelial specific functions; the uptake of acLDL and nitric oxide production, were also confirmed in baboon carotid artery ECs. When the lysine residues of LDL's apoprotein are acetylated, the modified LDL is taken up by specialized scavenger receptors on endothelial cells and can be easily visualized using a fluorescently labeled acLDL [178]. Intracellular NO was visualized in the ECs using DAF-2DA (4,5-diaminofluorescein diacetate). The diacetate indicator easily enters cells allowing the ester bonds to be hydrolyzed by intracellular esterases. This modification results in generation of the relatively nonfluorescent, membrane impermeable DAF-2.

75

DAF-2 reacts rapidly and irreversibly in solution with NO and NO-derived reactive

species in a concentration dependent manner to produce the highly fluorescent

triazolofluorescein (DAF-2T). This method has been used to investigate NO pathways

and is sensitive to varying concentrations of intracellular NO [179-181].

Consistent with other ongoing research in our laboratory, baboon SMCs and ECs

showed very similar morphology and growth to human aortic and human coronary artery

cells (data not shown). Primary ECs were expanded in culture and cryopreserved as

needed. Unless otherwise stated, ECs were used between passages 5-7 for all subsequent

studies.

Baboon Circulating Endothelial Progenitor Cells

The work described in this dissertation used a blood outgrowth method to

establish EPC cultures. Using a modification of the method described by Lin et al. [123]

(culture of mononuclear cells on culture dishes coated with fibronectin rather than type I

collagen), we established cultures which have been expanded for greater than 9 passages.

This cell population, derived from baboon peripheral blood, most resembles the "late

EPC" phenotype described in recent literature. For the remainder of this thesis, this cell

population will be termed peripheral blood derived endothelial progenitor cells or EPCs.

Table 5.1 summarizes the results obtained for characterization of the baboon

peripheral blood derived EPCs. The EPCs had an endothelial-like phenotype with a

cobblestone morphology and positive expression of CD105, NOS3, VEGFR1, VEGFR2,

CD31, THBD, ve-cadherin, and VWF. The cell population did not express alpha smooth

muscle actin, one of the contractile proteins expressed by vascular smooth muscle cells

and they showed minimal expression of CD14, a known monocyte marker. The EPCs

additionally displayed endothelial-like functions by forming capillary tubes structures on Matrigel™ basement membrane, taking up Dil labeled acLDL, and staining positive for intracellular nitric oxide.

These results compare well with many studies published in the literature. Table 5.2 provides a summary of recent literature which has reported characterization of blood outgrowth colonies maintained beyond 9 days in culture. In this study, we reported the emergence of outgrowth colonies between 9-23 days of culture in growth factor supplemented medium. This is also consistent with other investigators who have reported the appearance of colonies between 5 and 22 days after plating the peripheral blood mononuclear cell (PBMC) fraction onto protein (fibronectin, collagen or gelatin) coated culture dishes [129, 130, 132, 133, 135, 138, 158].

Flow cytometry was used to obtain a semi-quantitative evaluation of the marker expression in EPCs. Figure 5.15 shows representative histograms of protein expression measured using flow cytometry for EPCs compared to age and sex matched baboon carotid artery ECs. Both cell types show very similar expression profiles for all of the markers investigated (CD105, NOS3, VEGFR1, VEGFR2, CD31, THBD, ulex lectin, ve-cadherin, VWF and CD14). Yoon et al [140] compared human blood outgrowth endothelial cells (OECs) with gastroepiploic artery endothelial cells (GEAECs) obtained from age-matched donors and also saw very similar flow cytometry expression profiles for AC133, CD34, KDR, ve-cadherin, CD31, CD14 and CD45. Using reverse-transcriptase polymerase chain reaction (RT-PCR), Hur et al. [133] demonstrated that human late EPCs after 5 weeks in culture exhibited strong expression of endothelial genes, ve-cadherin, KDR, FLT-1, eNOS, and VWF at the same level as human umbilical

vein endothelial cells (HUVECs). At the protein level, Hur et al also showed very similar flow cytometry expression profiles between the late EPCs and HUVEC for CD31, KDR, ve-cadherin, and CD45. Vascular endothelial cells have not only been compared to peripheral blood outgrowth EPCs but also to EPCs derived from the umbilical cord blood (UCB) of full term newborns. Ingram et al. [134] used flow cytometry to perform immunophenotype analysis of UCB derived EPCs, HUVECs and human aortic endothelial cells (HAECs) and showed that their expression of CD31, CD141, CD105, CD146, CD144, VWF, flk-1, CD45, and CD14 were almost identical.

At least three surface markers reported by other investigators using late blood outgrowth culture methods as part of EPC characterization were not included in this study. CD34 expression in baboon EPCs, a known marker of early hematopoietic progenitors, was investigated in preliminary studies but due to concerns with antibody cross-reactivity and lack of good control samples, it was not investigated further. At least three studies have shown positive CD34 expression [135, 138, 140] and at least one reported that EPCs were negative for CD34 [127]. CD133 or hematopoietic stem cell antigen and CD117 (c-kit) also known as mast/stem cell growth factor receptor have been investigated by others. Again, mixed results were seen for blood outgrowth EPC expression of CD133, one report found low levels of expression [135] and two studies report the cells were CD133 negative [127, 140]. Ingram et al. reported the outgrowth cells were CD117 positive [135]. Each of these antigens are considered "early" markers and have been reported more frequently in studies using cell selection or from mononuclear fractions early in culture (usually only a few days). As mentioned previously, CD133 has been shown to decrease with differentiation and time in culture
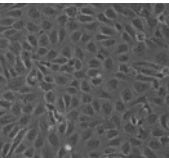
[116] which may explain these results. Discrepancies could be due to the culture

conditions (medium and/or growth factor supplements) and time of analysis (from fresh

blood or following *in vitro* culture) or may be due to different "differentiation states".

Thinking of cellular differentiation as a continuum from completely undifferentiated or

uncommitted to fully differentiated; maybe the EPC populations described by separate

researches are at different points along the continuum. Additional research in this area

will be needed to better define EPC biology.

In this study, we collaborated with the lab of Dr. Stephen Hanson to obtain

baboon tissue and blood for cell isolations. In addition, the early studies in this

dissertation were performed with EPCs generously donated by Dr. Hanson's laboratory.

The isolations performed in this study used the same methodology for isolation and

culture as Hanson's group. Dr. Minhui Ma, working with Dr. Hanson performed

extensive characterization of the baboon EPCs isolated in their laboratory. Ma and

Hanson found that EPCs had the following marker profile: VWF++, ve-cadherin++,

CD31++, CD34-, VEGFR2++, CD146+, THBD+, E-selectin+, ICAM1-, VCAM1- and

NOS3+ using immunocytochemistry. Drs. Ma and Hanson also found very similar

expression profiles for ECs. This data shows strong agreement with the characterization

presented as part of this dissertation and therefore no future distinction will be made

between studies using EPC isolations performed prior to or during these studies.

Through this work, a population of endothelial-like cells has been isolated from

peripheral blood and maintained in culture. The results are significant because we have

demonstrated in a non-human primate model, an autologous population of cells can be

derived from a minimally invasive blood draw. The therapeutic potential of this cell

population still remains unknown, but as presented in the following chapters, additional research will focus on their potential for providing a non-thrombogenic vascular lining in tissue engineering strategies.

Table 5.1: Summary: Baboon peripheral blood derived EPC phenotype

Morphology	**polygonal/cobblestone**
Growth pattern in vitro	late outgrowth observed after 9-23 days in culture
Antigen expression	SMA-, CD14-, CD105++, NOS3++, VEGFR2+, VEGFR1++, CD31++, THBD+, Ve-cadherin++, VWF++
AcLDL uptake and lectin binding	positive
Tube formation	yes
NO production	positive
Responsive to fluid shear stress	cytoskeletal regorganization, gene, and protein changes

++ expression in > 90% of cells
+ expression in > 20% of cells
- expression in < 10% of cells

Table 5.2: Characteristics of late blood outgrowth EPCs reported by other investigators

Characteristic		Literature Reference
Cobblestone morphology		[123, 129, 130, 132, 133, 135, 138, 158]
Antigen Expression	SMA negative	[136]
	CD14 negative	[123, 130, 135, 138, 140]
	endoglin (CD105) positive	[127, 135, 138, 146]
	eNOS (NOS3) positive	[130, 132, 133, 158]
	flk-1 (VEGFR2) positive	[123, 127, 129, 132, 133, 135, 140, 158]
	flt-1 (VEGFR1) positive	[130, 133]
	pecam-1 (CD31) positive	[130, 132, 133, 135, 136, 138, 140, 157]
	thrombomodulin (CD141) positive	[135]
	ve-cadherin (CD144) positive	[123, 127, 129, 130, 132, 133, 135, 136, 140, 146]
	vWF positive	[123, 129, 132, 133, 135, 136, 146, 157, 158]
AcLDL uptake and lectin binding		[123, 127, 129, 130, 132, 133, 135, 138, 157, 158]
Tube formation		[129, 130, 133, 135, 140]
NO production		[130, 132, 133, 158]
Responsive to fluid shear stress		[145, 146, 148, 149, 157, 158]
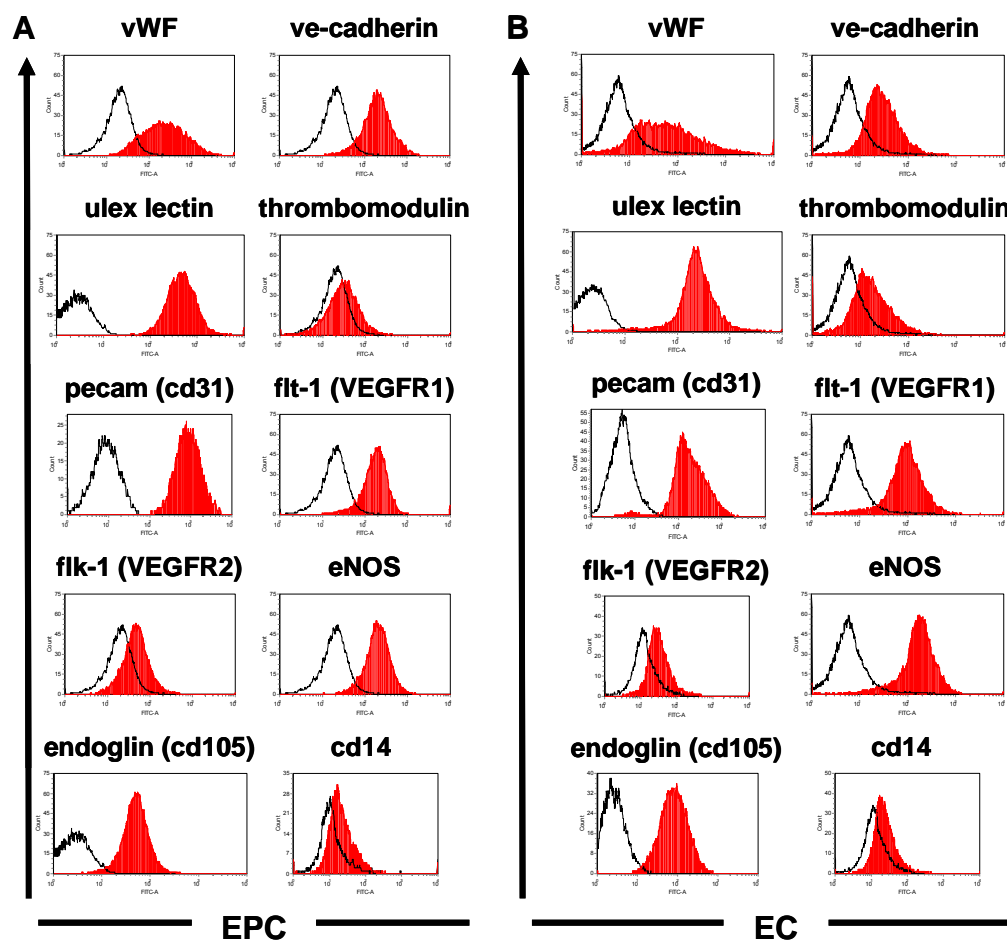
Figure 5.15: Comparison of EPC and EC protein expression using flow cytometry analysis. EPCs (A) and ECs (B) were subjected to flow cytometry following immunofluorescence labeling. Representative flow cytometry histograms are shown for each of the proteins investigated in EPCs (passage 3) and ECs (passage 5). Black outlines the negative control. Red histograms are the fluorescently labeled cell samples.

CHAPTER VI: MICROARRAY ANALYSIS OF GENE EXPRESSION PROFILES OF ENDOTHELIAL PROGENITOR CELLS AND VASCULAR ENDOTHELIAL CELLS IN STATIC AND FLUID FLOW ENVIRONMENTS

Introduction

An alteration in gene expression marks the cell's earliest response to a stimulus and initiates a cascade of events which lead to alterations in protein expression and cellular function. The advent of high throughput screening technologies such as DNA microarrays, enables researchers to probe thousands of genes simultaneously without the time and labor required using other candidate gene approaches such as reverse transcription-polymerase chain reaction (RT-PCR), Northern blot analysis or in situ hybridization. DNA microarrays have already been used to advance the study of endothelial cell (EC) biology. Through the use of these methodologies, advancements have also been made in understanding cellular response to the local mechanical environment, including EC response to fluid shear stress. DNA microarray approaches allow investigations to probe clusters of genes related to specific high level functions as well to as understand individual gene responses to a given stimulus. In tissue engineering there continues to be an ongoing challenge of identifying cell sources which will provide appropriate functions in an engineered therapy. DNA microarrays may offer the possibility of "screening" promising new cell sources with hopes of predicting therapeutic potential.

Endothelial progenitor cells (EPCs) derived from peripheral blood have emerged as an "endothelial-like" cell which can be isolated from blood outgrowth cultures. The

ability to isolate and expand this cell population from a minimally invasive blood draw makes these cells a potentially important autologous source of cells for tissue engineering and other therapeutic strategies. Since the first report of EPCs in the adult circulation [91], there has been a significant amount of research into the origin, phenotype and therapeutic potential of this heterogeneous cell population. Although there are many reports confirming that EPCs express a number of endothelial specific cell markers, very little known about how EPCs respond to stress compared to their mature vascular endothelial cell counterparts. One possible application of EPCs in tissue engineering would be as a vascular lining on an engineered blood vessel substitute. In this application, EPCs would be exposed to a complex mechanical environment dominated by fluid shear stresses imposed by the flowing blood. In order to study the response of EPCs to this hemodynamic environment, DNA microarray technology offers an excellent tool for capturing the entire transcriptional profile and allows comparisons to be made investigating both cell type and shear stress dependent responses.

ECs perform many specialized functions including maintaining hemostasis, responding to oxidative modifications in the circulation and contributing to neovascularization *in vivo*. Fluid shear stress has been shown to be a potent stimulus for ECs and has also been implicated in endothelial inflammation and atherosclerosis. Therefore developing an understanding of EPC's response to shear stress will provide a foundation for exploiting their therapeutic potential in this environment. The objective of this study was to characterize the similarities and differences between EPCs and ECs though transcriptional profiles in static and shear conditions in order to identify

mechanosensitive proteins that may be important for application of EPCs in tissue engineering.

Experimental Design

ECs and EPCs were isolated from juvenile male baboons (*Papio anubis*) as described in detail in Chapter IV: Materials and Methods. ECs from fresh carotid artery tissue and EPCs from peripheral blood samples were shown to be positive for endothelial receptor expression and cellular function (see detailed analysis in Chapter V: Cell Isolation and Characterization). ECs and EPCs were seeded onto collagen coated glass slides at confluence and allowed to adhere for 48 hours. A parallel plate flow chamber was used to expose ECs and EPCs to steady laminar shear stress (15 dynes/cm^2) for 24 hours. At the end of 24 hours of shear exposure, cells were removed from the substrate and lysed for extraction of total RNA. Statically cultured slides served as controls. This experimental timeline is displayed graphically in Figure 6.1. Total RNA was pooled from two identical and independent experiments. Quality of RNA was assessed using an Agilent Bioanalyzer 2100 by evaluating degradation of ribosomal RNA peaks. Quantity of high quality RNA was assessed by absorbance at 260nm. Competitive microarray hybridization was performed between experimental samples and Universal Human Reference RNA (Stratagene) labeled with Cy3 and Cy5 fluorophores. Figure 6.2 shows a schematic of the microarray experimental design where each of the four conditions; EC shear, EC static, EPC shear and EPC static, were hybridized against human reference RNA on one microarray slide. For each of the four conditions, three replicate microarrays were analyzed.

Figure 6.3 outlines the analysis procedure that was performed for the microarray studies. The microarray area was scanned using the Agilent Microarray Scanner System and image extraction was performed using Agilent Feature Extraction Image Analysis software. GeneSpring software was used to perform statistical analysis of gene expression from the 12 microarrays (3 replicates for each of the 4 conditions). A one-way analysis of variance (ANOVA) was performed using a Student-Newman-Keuls post hoc test and the Benjamini and Hochberg False Discovery Rate multiple testing correction. P-values <0.05 were considered significant. Pairwise comparisons were performed using a student's t-test. The four comparisons which will be discussed are the effect of shear on each cell type (EC: Shear vs. Static and EPC: Shear vs. Static) and a comparison of each cell type in static and shear environments (Static: EPC vs. EC and Shear: EPC vs. EC).

Ingenuity Pathways Analysis (IPA) software was used to query significantly expressed genes against the Ingenuity Knowledge Base, a comprehensive database of published biological information. This software allowed investigation of relevant networks and biological functions for each of the comparisons.

Confirmation of microarray results was performed using quantitative real time reverse transcription-polymerase chain reaction (qRT-PCR) to quantify mRNA for three genes significantly expressed in the microarray comparisons; tissue factor (F3), tissue factor pathway inhibitor (TFPI) and thrombomodulin (THBD).
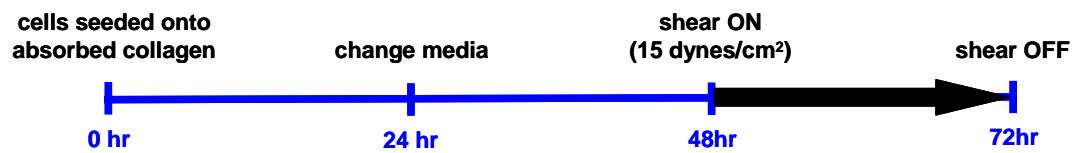
Figure 6.1: Outline of experimental time course. Cells were exposed to 15 dynes/cm^2 steady laminar shear stress for 24 hours following a 48 hour static incubation.
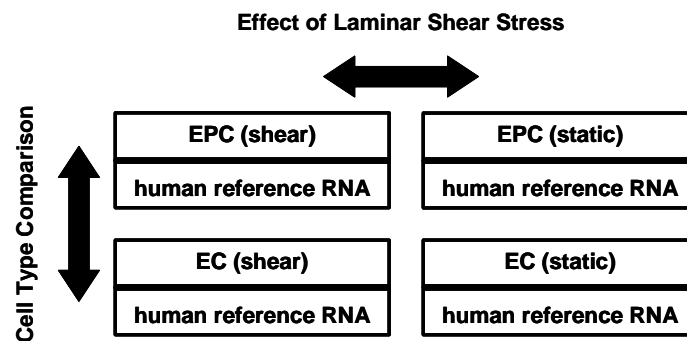
Figure 6.2: Microarray experimental design

```
┌─────────────────────────────────────────────────────────────────────┐
│        Agilent Whole Human Genome Microarray with 44,290 features / microarray │
│                       (~41,000 genes / microarray)                    │
│        Microarray area scanned using Agilent Microarray Scanner System │
└─────────────────────────────────────────────────────────────────────┘
                                    │
                                    ▼
┌─────────────────────────────────────────────────────────────────────┐
│      Image Extraction:  Agilent Feature Extraction Image Analysis software │
└─────────────────────────────────────────────────────────────────────┘
                                    │
                                    ▼
┌─────────────────────────────────────────────────────────────────────┐
│                          GeneSpring Analysis                          │
│      Imported expression data for 12 microarrays (3 replicates of each condition) │
│          Four conditions:  EC static, EC shear, EPC static, EPC shear │
└─────────────────────────────────────────────────────────────────────┘
                                    │
                                    ▼
┌─────────────────────────────────────────────────────────────────────┐
│                    1-way Analysis of Variance (ANOVA)                 │
│  Multiple Testing Correction (MTC):  Benjamini and Hochberg False Discovery Rate │
│                 Post hoc test:  Student-Newman-Keuls                   │
│                     p<0.05 condsidered significant                    │
└─────────────────────────────────────────────────────────────────────┘
                                    │
                                    ▼
┌─────────────────────────────────────────────────────────────────────┐
│              Pairwise Comparison:  Student's t-test                    │
│                                    EC: Shear vs Static                 │
│       Four comparisons:            EPC: Shear vs Static                │
│   p<0.05 condsidered significant   Static: EPC vs EC                   │
│                                    Shear: EPC vs EC                    │
└─────────────────────────────────────────────────────────────────────┘
```

Figure 6.3: Microarray analysis methods

Results

Overview of Transcriptional Profile Analysis

Microarray studies were performed using sheared and static control samples of ECs and EPCs. An ANOVA was performed using GeneSpring with p-values <0.05 considered significant. Table 6.1 provides a summary of the total number of genes regulated based on significance criteria in this study. Following outlier subtraction based on Agilent microarray internal controls, there were a total of 40,324 gene probes investigated. Using an ANOVA p-value cutoff of p<0.05, there were 5854 genes which were significantly regulated across all array comparisons. All further analysis only considered this pool of genes which met ANOVA significance criteria.

Pairwise comparisons were made investigating the effect of shear stress and cell type on gene expression using a student's t-test. As shown in Table 6.1, between 2811 and 4256 genes of the 5824 genes were up or downregulated based on pairwise comparison significance (p<0.05). Of those genes which met pairwise significance, shear stress regulated 939 and 625 genes more than 1.5 fold in ECs and EPCs, respectively. When comparing EPCs versus ECs, 1247 genes were differentially regulated more than 1.5 fold in static conditions and 1528 genes were altered by shear. Comparisons of gene expression are shown as a fold change ratio and therefore ratios of >1.5 or <0.666 are included in these numbers.

Focusing on genes which met the three criteria (ANOVA p<0.05, pairwise t-test p<0.05 and fold change >1.5 or <0.666), Figure 6.4 uses venn diagrams to project the overlap of genes regulated similarly by shear in ECs and EPCs (283 genes) and the genes

regulated similarly in both cell types (782 genes) under static and shear conditions. Shear exposure upregulated 428 and 319 genes in ECs and EPCs, respectively and of those, 122 were common to both cell types. On the other hand, shear exposure downregulated expression of 511 and 306 genes in ECs and EPCs, respectively with 152 genes common to both cell types. A total of 579 and 795 genes were expressed more in EPCs compared to ECs in static and shear conditions, respectively. Conversely, 668 and 733 genes were expressed more in ECs under the same conditions. Table 6.2 lists a detailed summary of the number of genes which met the three criteria (ANOVA p<0.05, pairwise t-test p<0.05 and fold change >1.5 or <0.666) in each comparison. There were a total of 57 genes which were expressed in all four comparisons, six of which were upregulated in all comparisons and eight of which were downregulated.

qRT-PCR Validation of Microarray Data

Quantitative real time RT-PCR (qRT-PCR) was used to validate select genes within the microarray data. We chose three genes which met the ANOVA significance criteria (p<0.05) in the microarray results and were differentially regulated across the four comparisons. Tissue factor (F3), tissue factor pathway inhibitor (TFPI) and thrombomodulin (THBD) expression was quantified using qRT-PCR methods. All qRT-PCR analyses were performed on n≥3 samples from at least three independent experiments. Data are reported as fold change ratios with significance p-values. Statistical comparisons were based on ANOVA and Tukey's test for pairwise comparisons with a p-value < 0.05 considered significant. In order to make the variance independent of the mean, statistical analysis of qRT-PCR data was performed following logarithmic transformation of the raw data.

90

Table 6.1: Microarray data statistical analysis summary. Microarray data was filtered based on significance criteria. The number of genes significantly regulated for each of the four comparisons is shown.

Microarray Summary		EC: Shear vs. Static	EPC: Shear vs. Static	Static: EPC vs. EC	Shear: EPC vs. EC
Total gene probes investigated (following outlier subtraction)		40324	40324	40324	40324
Data filters applied in series:	ANOVA with MTC p<0.05	5854	5854	5854	5854
	Pairwise comparison (Students t-test) p<0.05	3323	2811	3835	4256
	Total number of genes satisflying ANOVA MTC p<0.05, t-test p<0.05 and fold change criteria (>1.5 or <0.666)	939	625	1247	1528
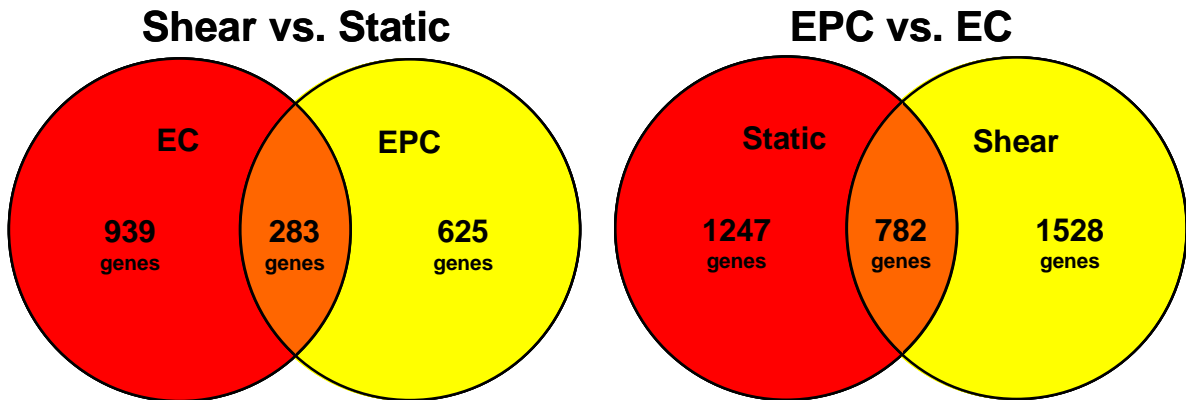
Figure 6.4: Venn diagram illustration of Shear vs. Static and EPC vs. EC microarray results. The number of genes which met significance criteria (ANOVA p<0.05, t-test<0.05 and fold change >1.5 or <0.666) for each comparison. (left panel) shear vs. static for ECs and EPCs, (right panel) EPC vs. EC for static and shear. Red and yellow circles represent the total number of genes significantly expressed for the specified condition. The orange overlapping region represents the number of genes common between the two conditions.

Table 6.2: Microarray analysis investigating the effect of cell type and shear stress on gene expression. The number of genes significantly regulated (ANOVA p<0.05, t-test<0.05 and fold change >1.5 or <0.666) for each of the four comparisons is shown in the table below.

Comparisons		EC: Shear vs. Static	EPC: Shear vs. Static	Static: EPC vs. EC	Shear: EPC vs. EC
Total number of genes satisflying ANOVA MTC p<0.05, t-test p<0.05 and fold change criteria (>1.5 or <0.666)		939	625	1247	1528
Fold change >1.5		428	319	579	795
Fold change <0.666		511	306	668	733
Shear vs. Static	Genes present in BOTH EC and EPC	283			
	Genes present in EC NOT in EPC	656			
	Genes present in EPC NOT in EC		342		
	EC up AND EPC up	122			
	EC down AND EPC down	152			
	EC up AND EPC down	4			
	EC down AND EPC up	5			
EPC vs. EC	Genes present in BOTH Static and Shear			782	
	Genes present in Static NOT in Shear			465	
	Genes present in Shear NOT in Static				746
	Static up AND Shear up			360	
	Static down AND Shear down			414	
	Static up AND Shear down			4	
	Static down AND Shear up			4	
Genes present in all comparisons		57			
Genes with fold change >1.5 in all four comparisons		6			
Genes with fold change <0.666 in all four comparisons		8			

Microarray and qRT-PCR data comparisons are presented graphically and in tabular form in Tables 6.3 and 6.4 and in Figure 6.5. qRT-PCR confirmed the microarray data in 6 of 7 comparisons where microarray results showed a significant difference in expression (EC: shear vs. static (F3 and TFPI), EPC: shear vs. static (THBD) and Shear: EPC vs. EC (F3, TFPI and THBD)). In comparing EPC to EC expression of THBD in static conditions, the microarray data suggests a 1.7 fold greater expression in EPCs while the qRT-PCR results shown no significant difference in expression between the two cell types. In two comparisons (Static: EPC vs. EC (F3 and TFPI)), microarray data did not show a significant difference between EPC and EC expression but qRT-PCR results indicated less expression in ECs compared to EPCs.

Regulation of High Level Biological Functions

Ingenuity Pathways Analysis (IPA) was used to interpret the microarray data in the context of pathways and biological systems. All genes with significant expression (5854 genes, ANOVA $p<0.05$) in the microarray dataset were imported into IPA. IPA used the Genbank gene ID in the dataset to map the imported data against the Ingenuity Pathways Knowledge Base (IPKB) which is the world's largest curated database of biological networks including coverage of over 23,900 mammalian genes [168]. All genes within the imported dataset which map to the IPKB and interact with at least one other gene in the IPKB were considered focus genes. Focus genes were established for the dataset from genes which were significant in the pairwise comparisons ($p<0.05$). Of the 5854 genes imported into IPA, 964 genes were eligible for generating networks and were considered focus genes. Those that were not determined to be focus genes either did not meet pairwise significance criteria ($p<0.05$), the gene ID did not correspond to a

known gene product, or there was insufficient findings in the literature regarding the gene.

IPA was used to perform a global analysis of high level functions. Two specific functional categories revealed differences between EC and EPC response to shear stress. Those categories: (1) Molecular and Cellular Functions and (2) Physiological System Development and Function were compared for ECs and EPCs in shear vs. static conditions. Each of these high level functional categories includes a number of specific functional subsets as shown in Figures 6.6 and 6.7. There were obvious differences in the EC and EPC response to shear in both Molecular and Cellular Functions (Figure 6.6) and also in Physiologic System Development and Functions (Figure 6.7). In these graphs, the significance is expressed as a p-value using the right-tailed Fisher's Exact Test. This methodology generates a p-value by comparing the number of imported genes that can participate in a function, relative to the total number of occurrences of these genes in all functional annotations stored in the IPKB. The threshold value line shown on each graph marks a threshold of 1:20 meaning that at that level there is a 1 in 20 chance that the listed functions were associated with the genes from the imported dataset by random chance alone. The IPA of Molecular and Cellular Functions (Figure 6.6) showed that both cell types had genes associated with cell to cell signaling and interaction but that the effect of shear stress altered genes which mapped to different functional groups depending on cell type. Shear in ECs was associated with regulation of genes in the broad functional categories of cell cycle, cell signaling, cellular function and maintenance, molecular transport, and vitamin and mineral metabolism. In contrast, shear on EPCs was associated with differential regulation of genes in the broad functional

categories of cell death, cell morphology, cellular movement and post-translational modification. Table 6.5 lists the number of genes associated with each of these functional categories. IPA also identified differences between EC and EPC response to shear in the Physiological System Development and Function area. As shown in Figure 6.7, both cell types regulated genes associated with nervous system development and function and the hematological system development and function with exposure to shear stress. IPA also demonstrated that there were functional categories which contained genes specifically regulated by either ECs or EPCs. In ECs, shear exposure was associated with organismal survival while in EPCs, shear modulated genes related to embryonic development, immune and lymphatic system development, organ development, tissue development, tissue morphology, and visual system development and function.

Shear Stress Responsive Gene Expression

Mature vascular endothelial cells have been shown in numerous studies to be responsive to their shear stress environment at the gene, protein and functional levels. In this study we were able to investigate the mechanosensitivity of EPCs and compare the EPC response to mature vascular ECs in a controlled *in vitro* environment. Table 6.6 lists 26 genes across multiple functional groups which have been shown in other studies to be significantly regulated by shear in vascular ECs. The EPC response to shear was compared to age and sex matched baboon carotid artery ECs using microarray studies. Two genes (SOD1 and CAV1) are listed twice because they represent the same gene at two different locations on the microarray area (noted by different Agilent probe IDs).

95

Table 6.3: qRT-PCR confirmation of microarray data (shear vs. static) Red boxes are used to highlight significant ratios >1 (p<0.05) and blue boxes highlight significant ratios <1 (p<0.05). Data which were not significantly different (p>0.05) are left without color.

Gene Name	Gene Symbol	Systematic Name	ANOVA P-value	EC: Shear vs Static				EPC: Shear vs Static			
				Microarray		qRT-PCR		Microarray		qRT-PCR	
				Fold change	P-value	Fold change	P-value	Fold change	P-value	Fold change	P-value
coagulation factor III (thromboplastin, tissue factor)	F3	NM_001993	0.003	3.628	0.000	6.540	0.000	0.864	0.539	1.285	0.156
tissue factor pathway inhibitor (lipoprotein-associated coagulation inhibitor)	TFPI	NM_006287	0.004	1.357	0.005	1.301	0.041	0.924	0.450	1.516	0.003
thrombomodulin	THBD	NM_000361	0.001	0.999	0.996	1.187	0.084	1.404	0.033	3.313	0.000

p<0.05 considered significant

Table 6.4: qRT-PCR confirmation of microarray data (EPC vs. EC) Red boxes are used to highlight significant ratios >1 (p<0.05) and blue boxes highlight significant ratios <1 (p<0.05). Data which were not significantly different (p>0.05) are left without color.

Gene Name	Gene Symbol	Systematic Name	ANOVA P-value	Static: EPC vs EC				Shear: EPC vs EC			
				Microarray		qRT-PCR		Microarray		qRT-PCR	
				Fold change	P-value	Fold change	P-value	Fold change	P-value	Fold change	P-value
coagulation factor III (thromboplastin, tissue factor)	F3	NM_001993	0.003	1.147	0.350	0.629	0.008	0.273	0.003	0.124	0.000
tissue factor pathway inhibitor (lipoprotein-associated coagulation inhibitor)	TFPI	NM_006287	0.004	0.798	0.082	0.412	0.000	0.543	0.000	0.481	0.000
thrombomodulin	THBD	NM_000361	0.001	1.787	0.003	0.939	0.846	2.511	0.002	2.620	0.000

p<0.05 considered significant
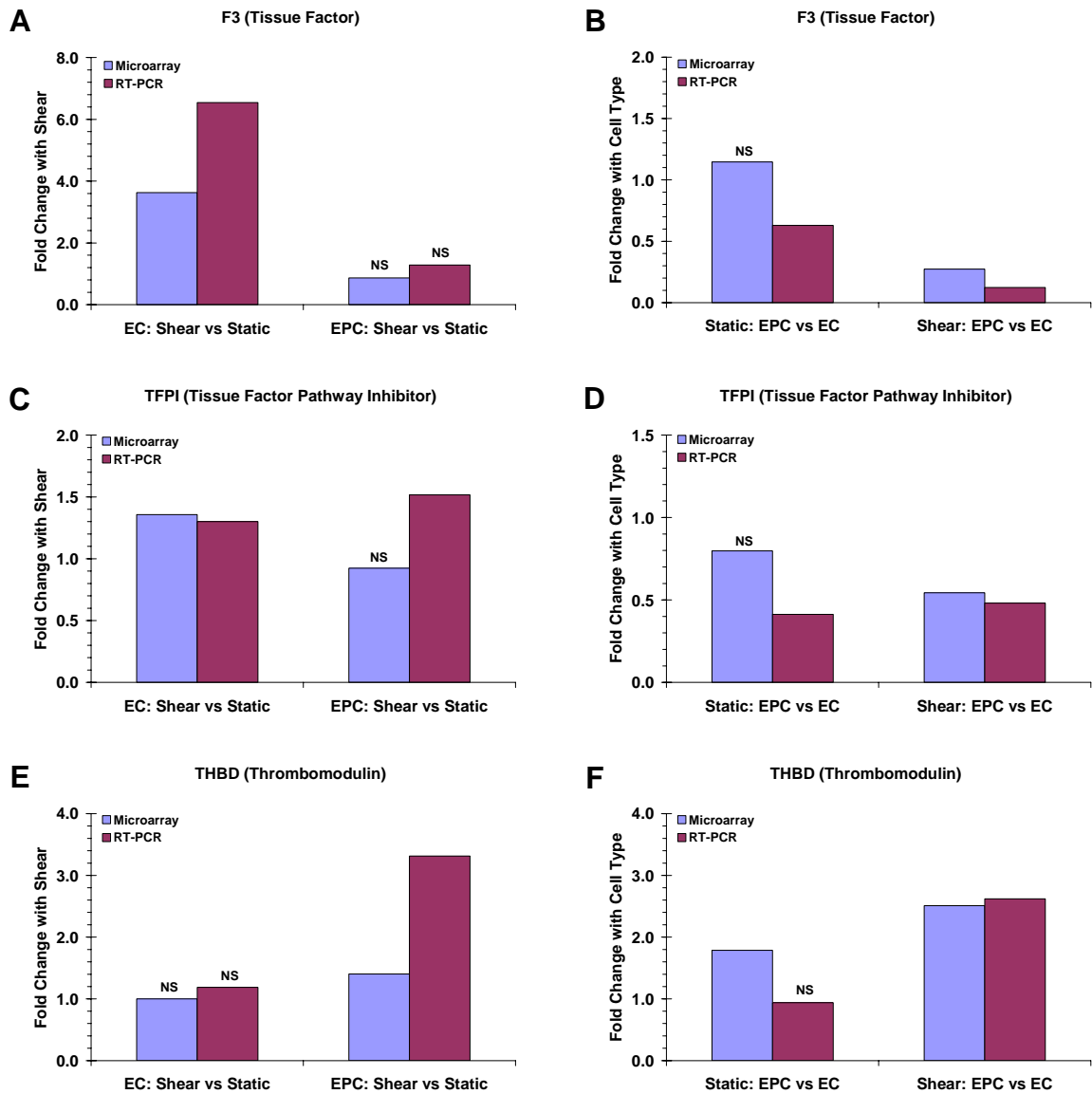
Figure 6.5: Confirmation of microarray data by qRT-PCR. NS denotes not significantly changed. All other fold expressions are significantly different (p<0.05). (A) F3 fold change with shear, (B) F3 fold change with cell type, (C) TFPI fold change with shear, (D) TFPI fold change with cell type, (E) THBD fold change with shear, (F) THBD fold change with cell type
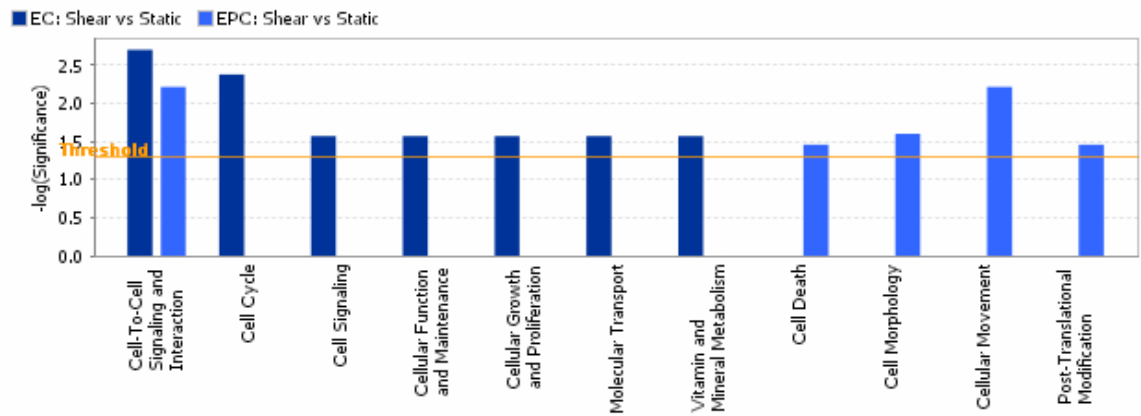
FIgure 6.6: Ingenuity Pathways Analysis of Molecular and Cellular Functions for Shear vs. Static
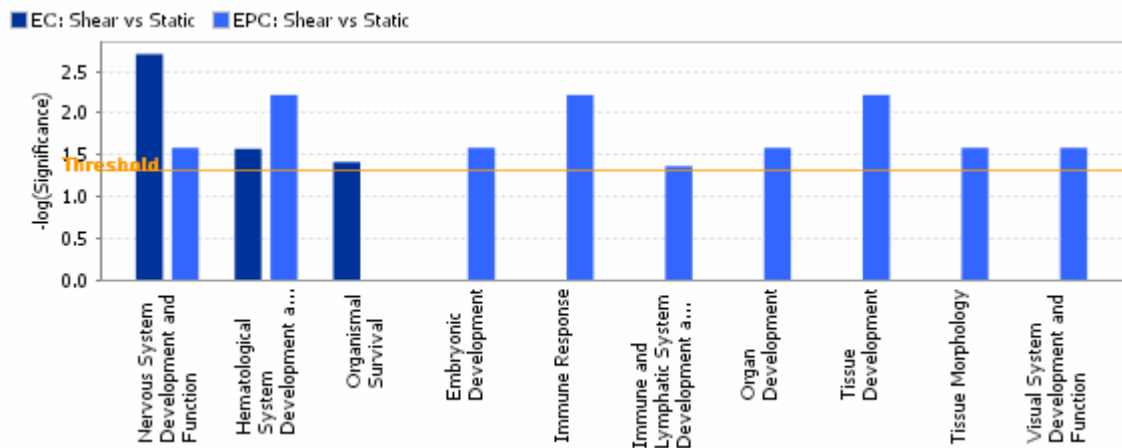
FIgure 6.7: Ingenuity Pathways Analysis of Physiological System Development and Functions for Shear vs. Static

Table 6.5: Ingenuity Pathways analysis of high level functions. The following table provides a summary of the number of genes associated with each high level function.

Number of genes associated with each high level function:

Molecular and Cellular Functions	EC: Shear vs. Static	EPC: Shear vs. Static
Cell-To-Cell Signaling and Interaction	31	15
Cell Cycle	13	--
Cell Signaling	4	--
Cellular Function and Maintenance	4	--
Cellular Growth and Proliferation	9	--
Molecular Transport	4	--
Vitamin and Mineral Metabolism	4	--
Cell Death	--	14
Cell Morphology	--	9
Cellular Movement	--	24
Post-Translational Modification	--	13

Physiological System Development and Function	EC: Shear vs. Static	EPC: Shear vs. Static
Nervous System Development and Function	29	7
Hematological System Development and Function	4	28
Organismal Survival	12	--
Embryonic Development	--	8
Immune Response	--	26
Immune and Lymphatic System Development and Function	--	8
Organ Development	--	11
Tissue Development	--	19
Tissue Morphology	--	5
Visual System Development and Function	--	9

Table 6.6: Genes shown to be shear stress responsive in other systems. Red boxes are used to highlight significant ratios >1 (p<0.05) and blue boxes highlight significant ratios <1 (p<0.05). Data which were not significantly different (p>0.05) are left without color.

Genes shown to be shear stress responsive in other systems

Gene Name	Gene Symbol	Systematic Name	Functional Group	EC: Shear vs Static Fold change	EC: Shear vs Static P-value (pairwise)	EPC: Shear vs Static Fold change	EPC: Shear vs Static P-value (pairwise)	Static: EPC vs EC Fold change	Static: EPC vs EC P-value (pairwise)	Shear: EPC vs EC Fold change	Shear: EPC vs EC P-value (pairwise)	ANOVA	Agilent Probe ID
cytochrome P450, family 1, subfamily A, polypeptide 1	CYP1A1	NM_000499	antioxidant	1.693	0.016	1.206	0.194	0.337	0.000	0.240	0.001	0.000	A_23_P163402
heme oxygenase (decycling) 1	HMOX1	NM_002133	antioxidant	8.866	0.000	6.020	0.000	1.224	0.139	0.831	0.216	0.000	A_23_P120883
heme oxygenase (decycling) 2	HMOX2	NM_002134	antioxidant	1.332	0.001	1.051	0.624	0.805	0.042	0.635	0.003	0.006	A_23_P100501
superoxide dismutase 1, soluble (amyotrophic lateral sclerosis 1 (adult))	SOD1	NM_000454	antioxidant	1.192	0.010	1.412	0.001	1.009	0.830	1.195	0.008	0.001	A_23_P154840
superoxide dismutase 1, soluble (amyotrophic lateral sclerosis 1 (adult))	SOD1	NM_000454	antioxidant	1.288	0.008	1.379	0.008	1.060	0.453	1.136	0.046	0.009	A_24_P151464
cyclin A2	CCNA2	NM_001237	cell cycle	0.442	0.000	0.584	0.004	1.204	0.019	1.589	0.007	0.000	A_23_P58321
cyclin B1	CCNB1	NM_031966	cell cycle	0.354	0.000	0.403	0.003	1.340	0.012	1.523	0.033	0.000	A_23_P122197
cyclin B2	CCNB2	NM_004701	cell cycle	0.326	0.000	0.434	0.003	1.069	0.434	1.423	0.036	0.000	A_23_P65757
thrombomodulin	THBD	NM_000361	coagulation	0.999	0.996	1.404	0.033	1.787	0.003	2.511	0.002	0.001	A_23_P91390
matrix metalloproteinase 1 (interstitial collagenase)	MMP1	NM_002421	extracellular matrix / remodeling	1.136	0.008	1.365	0.086	5.890	0.000	7.076	0.000	0.000	A_23_P1691
matrix metalloproteinase 2 (gelatinase A, 72kDa gelatinase, 72kDa type IV collagenase)	MMP2	NM_004530	extracellular matrix / remodeling	1.424	0.037	1.112	0.273	0.838	0.018	0.655	0.034	0.032	A_23_P163787
matrix metalloproteinase 9 (gelatinase B, 92kDa gelatinase, 92kDa type IV collagenase)	MMP9	NM_004994	extracellular matrix / remodeling	1.896	0.040	0.685	0.029	0.760	0.090	0.275	0.003	0.006	A_23_P40174
gap junction protein, alpha 1, 43kDa (connexin 43)	GJA1	NM_000165	gap junction	0.938	0.614	0.693	0.002	0.644	0.001	0.476	0.003	0.002	A_24_P55295
gap junction protein, alpha 4, 37kDa (connexin 37)	GJA4	NM_002060	gap junction	1.462	0.019	1.168	0.250	0.195	0.000	0.156	0.000	0.000	A_23_P1083
gap junction protein, alpha 5, 40kDa (connexin 40)	GJA5	NM_005266	gap junction	0.843	0.546	1.035	0.873	0.323	0.001	0.396	0.035	0.018	A_23_P371729
bone morphogenetic protein 4	BMP4	NM_001202	inflammation	0.439	0.006	0.834	0.249	0.607	0.030	1.153	0.363	0.022	A_23_P54144
intercellular adhesion molecule 1 (CD54), human rhinovirus receptor	ICAM1	NM_000201	inflammation	1.057	0.790	1.069	0.591	2.466	0.005	2.514	0.004	0.005	A_23_P153320
intercellular adhesion molecule 3	ICAM3	NM_002162	inflammation	1.445	0.000	1.028	0.700	0.985	0.815	0.700	0.001	0.003	A_23_P164691
interleukin 1, alpha	IL1A	NM_000575	inflammation	11.973	0.009	3.746	0.041	1.678	0.245	0.525	0.324	0.028	A_23_P72096
jagged 1 (Alagille syndrome)	JAG1	NM_000214	proliferation / differentiation	1.988	0.001	0.711	0.015	1.645	0.010	0.589	0.000	0.003	A_23_P210763
jagged 2	JAG2	NM_002226	proliferation / differentiation	1.586	0.000	1.113	0.430	1.056	0.644	0.741	0.013	0.034	A_23_P106024
transforming growth factor, beta 2	TGFB2	NM_003238	proliferation / differentiation	0.774	0.010	0.813	0.280	3.243	0.001	3.409	0.000	0.000	A_24_P402438
vascular endothelial growth factor B	VEGFB	NM_003377	proliferation / differentiation	0.939	0.141	0.903	0.221	0.781	0.004	0.752	0.013	0.010	A_23_P1594
vascular endothelial growth factor C	VEGFC	NM_005429	proliferation / differentiation	2.426	0.003	1.266	0.073	0.869	0.439	0.453	0.000	0.002	A_23_P167096
caveolin 1, caveolae protein, 22kDa	CAV1	NM_001753	signal transduction	0.769	0.003	0.831	0.003	1.139	0.010	1.231	0.007	0.001	A_23_P134454
caveolin 1, caveolae protein, 22kDa	CAV1	NM_001753	signal transduction	0.757	0.007	0.792	0.016	0.987	0.820	1.032	0.622	0.017	A_24_P12626
kinase insert domain receptor (a type III receptor tyrosine kinase)	KDR	NM_002253	signal transduction	1.154	0.027	1.147	0.246	1.506	0.013	1.497	0.001	0.006	A_24_P71973
Kruppel-like factor 2 (lung)	KLF2	NM_016270	transcription factor	4.219	0.000	3.315	0.003	0.906	0.546	0.711	0.121	0.001	A_23_P119196

This replicate data was consistent for SOD1 across all 4 comparisons and for 2 of 4 comparisons for CAV1. In comparing EPC vs. EC in static and shear, one of the two replicates (A_24_P12626) did not meet pairwise significance criteria (p>0.05) while the second replicate (A_23_P134454) suggested more expression in EPCs compared to ECs (1.1 and 1.2 fold for static and shear, respectively).

Consistent with other studies, microarray results demonstrated the mechanosensitve nature of vessel wall ECs. EPCs were also mechanosensitive. In EPCs, shear exposure resulted in altered expression of approximately one half (11 of 21) of the genes responsive to shear in ECs. In these shear responsive genes which were common for both cell types, EPCs showed similar regulation (up or down) compared to ECs. In only two cases (MMP9 and JAG1) shear resulted in different regulation in EPCs compared to ECs. In both cases, shear resulted in an increase in MMP9 and JAG1 expression in ECs with a contrasting decrease in EPCs. Like vascular ECs, shear caused a general increase in antioxidant genes (HMOX1 and SOD1) and decrease in cell cycle associated genes (CCNA2, CCNB1 and CCNB2) in EPCs. Shear caused several genes to be upregulated by more than two fold in ECs (HMOX1, IL1A, KLF2 and VEGFC). EPCs also responded to shear by upregulating these genes but to a lesser extent than seen with ECs. (Shear vs. Static -- HMOX1: EC 8.9 fold, EPC 6.0 fold; IL1A: EC 12.0 fold, EPC 3.7 fold; KLF2: EC 4.2 fold, EPC 3.3 fold; VEGFC: EC 2.4 fold, EPC not significantly altered). Shear also caused three genes to be downregulated by more than double (ratio < 0.5) in both ECs and EPCs. The same trend was seen where the EPC response was attenuated compared to the EC response to shear (Shear vs. Static --

101

CCNA2: EC 0.4 fold, EPC 0.6 fold; CCNB1: EC 0.3 fold, EPC 0.4 fold; CCNB2: EC 0.3 fold, EPC 0.4 fold)

Thrombosis and Hemostasis

One of the primary functions of vascular ECs which line blood vessels is the maintenance of hemostasis, providing pro and anti-coagulant function in response to the appropriate cues. ECs lining the vessel are constantly exposed to hemodynamic stresses. In this study, we have investigated the effect of unidirectional laminar shear stress on gene expression in blood derived EPCs and compared the response to vessel wall derived ECs. Table 6.7 lists 16 genes related to pro and anticoagulant function which were significantly regulated (ANOVA p<0.05) in the microarray results. Two genes (PTGS2 and THDS2) are listed twice due to duplicate spots on the Agilent array area. These genes serve as technical replicates on the same array slide. The data for the two replicates was consistent across six of eight comparisons. In two cases (PTGS2 – Static: EPC vs. EC and THSD2 – EPC: Shear vs. Static), one data point indicated upregulation and the second data point was not significantly changed (p>0.05). The majority of coagulation associated genes (pro and anticoagulant function) were shear stress responsive in ECs (12 of 15) while less than one half of those genes were altered by shear in EPCs (5 of 12). Compared to ECs, EPCs showed a similar response to shear in four (PLAT, PTGIS, F13B and THSD1) of the five genes. For one gene (PLAU), ECs showed an increase in expression while EPCs displayed a shear depended decrease in expression. Shear resulted in an overall increase in anticoagulant gene expression (7 of 8 genes) in ECs, a finding that was not consistent with the EPC response to shear. In EPCs, only thrombomodulin (THBD) expression was significantly upregulated (1.4 fold) with

Table 6.7: Genes related to coagulation. Red boxes are used to highlight significant ratios >1 (p<0.05) and blue boxes highlight significant ratios <1 (p<0.05). Data which were not significantly different (p>0.05) are left without color.

Genes related to coagulation

Gene Name	Gene Symbol	Systematic Name	Coagulant Effect	EC: Shear vs Static Fold change	EC: Shear vs Static P-value (pairwise)	EPC: Shear vs Static Fold change	EPC: Shear vs Static P-value (pairwise)	Static: EPC vs EC Fold change	Static: EPC vs EC P-value (pairwise)	Shear: EPC vs EC Fold change	Shear: EPC vs EC P-value (pairwise)	ANOVA	Agilent Probe ID
annexin A5	ANXA5	NM_001154	anti	1.512	0.000	1.148	0.220	1.088	0.370	0.826	0.025	0.019	A_23_P69720
plasminogen activator, tissue	PLAT	NM_000930	anti	0.424	0.000	0.378	0.000	1.311	0.008	1.166	0.045	0.000	A_23_P82868
plasminogen activator, urokinase	PLAU	NM_002658	anti	1.580	0.029	0.669	0.020	1.828	0.004	0.774	0.144	0.039	A_23_P24104
plasminogen activator, urokinase receptor	PLAUR	NM_001005377	anti	4.409	0.008	0.837	0.452	4.676	0.002	0.888	0.719	0.012	A_23_P16469
prostaglandin I2 (prostacyclin) synthase	PTGIS	NM_000961	anti	0.363	0.000	0.590	0.007	0.605	0.004	0.982	0.873	0.001	A_24_P48723
prostaglandin-endoperoxide synthase 2 (prostaglandin G/H synthase and cyclooxygenase)	PTGS2	NM_000963	anti	2.854	0.000	1.197	0.306	1.272	0.174	0.534	0.001	0.002	A_24_P250922
prostaglandin-endoperoxide synthase 2 (prostaglandin G/H synthase and cyclooxygenase)	PTGS2	NM_000963	anti	3.253	0.001	1.099	0.162	1.319	0.025	0.446	0.001	0.000	A_24_P77008
protein C receptor, endothelial (EPCR)	PROCR	NM_006404	anti	1.242	0.001	0.803	0.238	4.158	0.000	2.669	0.000	0.000	A_23_P80040
tissue factor pathway inhibitor (lipoprotein-associated coagulation inhibitor)	TFPI	NM_006287	anti	1.357	0.005	0.924	0.450	0.798	0.082	0.543	0.000	0.004	A_23_P17095
thrombomodulin	THBD	NM_000361	anti	0.999	0.996	1.080	0.448	1.787	0.003	2.511	0.002	0.001	A_23_P91390
coagulation factor II (thrombin)	F2	NM_000506	pro	0.973	0.569	0.864	0.539	1.422	0.001	1.578	0.008	0.006	A_23_P94879
coagulation factor III (thromboplastin, tissue factor)	F3	NM_001993	pro	3.628	0.000	1.323	0.035	1.147	0.350	0.273	0.003	0.003	A_23_P126782
coagulation factor VII (serum prothrombin conversion accelerator)	F7	NM_000131	pro	0.969	0.610	1.097	0.348	1.132	0.130	1.546	0.006	0.016	A_23_P117298
coagulation factor VIII-associated (intronic transcript) 1	F8A1	NM_012151	pro	1.014	0.593	0.578	0.008	0.743	0.009	0.803	0.028	0.025	A_23_P11262
coagulation factor XIII, B polypeptide	F13B	NM_001994	pro	0.335	0.007	1.707	0.001	1.053	0.681	1.819	0.046	0.007	A_23_P46549
thrombospondin, type I, domain containing 1	THSD1	NM_018676	pro	1.325	0.006	0.951	0.585	0.792	0.031	1.020	0.693	0.002	A_23_P14184
thrombospondin, type I, domain containing 2	THSD2	NM_032784	pro	1.168	0.364	0.896	0.495	0.272	0.001	0.221	0.000	0.000	A_23_P111402
thrombospondin, type I, domain containing 2	THSD2	NM_032784	pro	1.929	0.013	0.896	0.495	0.642	0.046	0.298	0.001	0.003	A_24_P106542

shear stress. In contrast, ECs showed no significant ($p > 0.05$) alteration in THBD expression with shear.

In static conditions, EPCs expressed six anticoagulant genes to a greater extent than ECs. In fact, EPCs expressed three anticoagulant genes at greater than 1.5 times the EC expression (Static: EPC vs. EC -- PLAU 1.8 fold; PLAUR 4.7 fold; PROCR 4.2 fold). In addition, EPCs expressed three procoagulant genes (F8A1, THSD1 and THSD2) to a lesser extent than ECs in static culture. When both cell types were exposed to shear stress, the balance of expression of pro and anticoagulant genes in EPCs vs. ECs was more heterogeneous in nature.

Oxidative and Inflammatory Gene Expression

The pathological basis of a number of diseases has been linked to oxidative modifications. In the cardiovascular system, atherosclerosis has been associated with both oxidative stress and inflammation [182]. EPCs are a promising cell source for a number of therapeutic strategies in the cardiovascular system and therefore investigating the regulation of oxidative and inflammatory genes may be important for predicting the therapeutic potential of EPCs. Table 6.8 shows 36 genes related to oxidation for each of the four comparisons investigated. As presented earlier, SOD1 is listed twice because it appears in two different spots on the Agilent microarray. These two data points which are technical replicates showed consistent results across the comparisons.

Shear resulted in an upregulation of a large number of antioxidant genes in both ECs and EPCs (18 and 16, respectively). Additionally, there were only four genes with antioxidant function downregulated in EPCs following shear exposure compared to eight genes downregulated in ECs. In comparing the EPC and EC gene expression under static

conditions, there appeared to be a heterogeneous mixture of antioxidant genes which are expressed to a greater extent in each cell type. In the shear stress environment, EPCs expressed more antioxidant genes (12 genes) to a greater extent than ECs. EPCs expressed four antioxidant genes at levels more than 1.5 times the level found in ECs (ALDH1A1 8.6 fold; GLRX 3.0 fold; GLRX2 3.0 fold; GPX4 2.0 fold).

Antioxidant enzymes are largely cell associated proteins whose function is to maintain a reducing tone within cells. There were 12 enzymatic antioxidants regulated in the microarray results including superoxide dismutase, glutathione peroxidase, glutathione reductase and transferase, and peroxiredoxin (noted with * in Table 6.8). Shear promoted an upregulation of these genes in EPCs and when compared to ECs in the shear environment, EPCs expressed these antioxidant enzymes to a greater extent (1.1-2.0 fold). In only one case did EPCs express less of the antioxidant enzyme (GSTM3) compared to ECs in the shear environment.

Genes with important pro and antiinflammatory function are shown in Table 6.9. In this study, shear promoted an increase in expression of a number of proinflammatory mediators in ECs combined with decreased expression of antiinflammatory molecules. Shear had less of a proinflammatory effect in EPCs, increasing expression of only 2 of 11 proinflammatory genes and reducing expression of three others. When comparing the two cell types, EPCs had less expression of inflammatory genes (both pro and anti) compared to ECs in both shear and static conditions.

Table 6.8: Genes related to oxidation. Red boxes are used to highlight significant ratios >1 ($p<0.05$) and blue boxes highlight significant ratios <1 ($p<0.05$). Data which were not significantly different ($p>0.05$) are left without color. * indicates ROS scavenging and detoxifying enzymes [183, 184].

Genes related to oxidation				EC: Shear vs Static		EPC: Shear vs Static		Static: EPC vs EC		Shear: EPC vs EC			
Gene Name	Gene Symbol	Systematic Name	Oxidation Effect	Fold change	P-value (pairwise)	Fold change	P-value (pairwise)	Fold change	P-value (pairwise)	Fold change	P-value (pairwise)	ANOVA	Agilent Probe ID
NADPH oxidase 4	NOX4	NM_016931	pro	0.840	0.147	0.789	0.114	1.758	0.003	1.651	0.015	0.008	A_24_P739344
aldehyde dehydrogenase 1 family, member A1	ALDH1A1	NM_000689	anti	0.208	0.000	1.594	0.001	1.128	0.145	8.635	0.000	0.000	A_23_P83098
cytochrome P450, family 1, subfamily A, polypeptide 1	CYP1A1	NM_000499	anti	1.693	0.016	1.206	0.194	0.337	0.000	0.240	0.001	0.000	A_23_P163402
ferritin, heavy polypeptide 1	FTH1	NM_002032	anti	1.749	0.001	1.967	0.004	0.966	0.787	1.087	0.118	0.002	A_24_P58337
ferritin, light polypeptide	FTL	NM_000146	anti	1.645	0.003	1.480	0.002	1.160	0.079	1.044	0.567	0.002	A_23_P50504
glutamate-cysteine ligase, catalytic subunit	GCLC	NM_001498	anti	1.152	0.161	1.420	0.001	0.955	0.456	1.178	0.085	0.023	A_23_P145114
glutaredoxin (thioltransferase)	GLRX	NM_002064	anti	2.287	0.000	2.310	0.002	2.998	0.001	3.029	0.000	0.000	A_23_P69908
glutaredoxin 2	GLRX2	NM_016066	anti	0.777	0.061	1.268	0.018	1.863	0.000	3.042	0.000	0.000	A_23_P160503
*glutathione peroxidase 4 (phospholipid hydroperoxidase)	GPX4	NM_002085	anti	0.454	0.003	0.741	0.086	1.248	0.117	2.036	0.007	0.004	A_23_P28075
*glutathione peroxidase 7	GPX7	NM_015696	anti	0.676	0.001	0.968	0.764	0.812	0.014	1.162	0.194	0.046	A_23_P73972
*glutathione reductase	GSR	NM_000637	anti	1.423	0.011	1.556	0.021	1.201	0.054	1.313	0.097	0.017	A_23_P146084
*glutathione S-transferase M3 (brain)	GSTM3	NM_000849	anti	0.864	0.040	0.732	0.003	0.800	0.012	0.678	0.001	0.001	A_24_P914434
*glutathione S-transferase theta 2	GSTT2	NM_000854	anti	0.752	0.010	1.086	0.165	0.881	0.082	1.273	0.013	0.033	A_23_P357571
guanylate cyclase 1, soluble, alpha 3	GUCY1A3	NM_000856	anti	1.530	0.021	0.903	0.155	0.944	0.567	0.557	0.003	0.012	A_23_P69573
heme oxygenase (decycling) 1	HMOX1	NM_002133	anti	8.866	0.000	6.020	0.000	1.224	0.139	0.831	0.216	0.000	A_23_P120883
heme oxygenase (decycling) 2	HMOX2	NM_002134	anti	1.332	0.001	1.051	0.624	0.805	0.042	0.635	0.003	0.006	A_23_P100501
leukotriene B4 12-hydroxydehydrogenase	LTB4DH	NM_012212	anti	1.985	0.005	1.144	0.416	0.844	0.302	0.486	0.005	0.012	A_23_P157809
monoamine oxidase A	MAOA	NM_000240	anti	0.967	0.743	1.028	0.667	0.585	0.002	0.622	0.004	0.003	A_23_P83857
monoamine oxidase B	MAOB	NM_000898	anti	1.138	0.026	0.965	0.387	0.851	0.021	0.721	0.000	0.002	A_23_P85008
microsomal glutathione S-transferase 2	MGST2	NM_002413	anti	0.953	0.320	0.768	0.020	0.630	0.000	0.508	0.001	0.000	A_23_P110167
microsomal glutathione S-transferase 3	MGST3	NM_004528	anti	1.260	0.000	1.144	0.071	1.122	0.029	1.018	0.722	0.012	A_23_P51548
methionine sulfoxide reductase A	MSRA	NM_012331	anti	1.075	0.332	1.033	0.648	1.416	0.004	1.360	0.012	0.010	A_23_P61426
methionine sulfoxide reductase B3	MSRB3	NM_198080	anti	1.456	0.021	1.240	0.005	1.154	0.247	0.982	0.534	0.028	A_24_P273726
metallothionein 1B (functional)	MT1B	NM_005947	anti	1.292	0.010	1.268	0.015	1.097	0.071	1.077	0.355	0.016	A_23_P37983
protein disulfide isomerase family A, member 3	PDIA3	NM_005313	anti	1.019	0.759	0.929	0.386	1.360	0.012	1.240	0.027	0.032	A_32_P63182
protein disulfide isomerase family A, member 5	PDIA5	NM_006810	anti	0.799	0.004	0.766	0.013	1.527	0.003	1.464	0.000	0.001	A_23_P167040
P450 (cytochrome) oxidoreductase	POR	NM_000941	anti	1.553	0.009	1.234	0.148	0.845	0.254	0.671	0.008	0.024	A_24_P29723
*peroxiredoxin 1	PRDX1	NM_002574	anti	1.650	0.001	1.640	0.000	0.943	0.224	0.937	0.281	0.000	A_23_P11995
*peroxiredoxin 2	PRDX2	NM_005809	anti	0.817	0.005	0.924	0.113	1.209	0.003	1.368	0.002	0.001	A_23_P142045
*peroxiredoxin 3	PRDX3	NM_006793	anti	0.761	0.013	0.891	0.016	0.851	0.077	0.996	0.855	0.017	A_23_P63751
*peroxiredoxin 5	PRDX5	NM_012094	anti	1.097	0.083	1.136	0.027	1.083	0.125	1.122	0.032	0.037	A_23_P12989
*peroxiredoxin 6	PRDX6	NM_004905	anti	1.038	0.242	1.204	0.001	0.899	0.003	1.043	0.246	0.006	A_23_P983
*superoxide dismutase 1, soluble (amyotrophic lateral sclerosis 1 (adult))	SOD1	NM_000454	anti	1.192	0.010	1.412	0.001	1.009	0.830	1.195	0.008	0.001	A_23_P154840
*superoxide dismutase 1, soluble (amyotrophic lateral sclerosis 1 (adult))	SOD1	NM_000454	anti	1.288	0.008	1.379	0.008	1.060	0.453	1.136	0.046	0.009	A_24_P151464
*superoxide dismutase 2, mitochondrial	SOD2	NM_000636	anti	0.946	0.589	1.129	0.156	1.250	0.039	1.492	0.012	0.034	A_23_P134176
thioredoxin	TXN	NM_003329	anti	1.395	0.002	1.295	0.000	1.082	0.010	1.004	0.934	0.001	A_23_P60248
thioredoxin reductase 1	TXNRD1	NM_003330	anti	1.388	0.004	1.344	0.001	1.123	0.077	1.087	0.138	0.002	A_23_P204581

* ROS scavenging and detoxifying enzymes

Table 6.9: Genes related to inflammation. Red boxes are used to highlight significant ratios >1 ($p<0.05$) and blue boxes highlight significant ratios <1 ($p<0.05$). Data which were not significantly different ($p>0.05$) are left without color.

Genes related to inflammation

Gene Name	Gene Symbol	Systematic Name	Inflammatory Effect	EC: Shear vs Static		EPC: Shear vs Static		Static: EPC vs EC		Shear: EPC vs EC		ANOVA	Agilent Probe ID
				Fold change	P-value (pairwise)	Fold change	P-value (pairwise)	Fold change	P-value (pairwise)	Fold change	P-value (pairwise)		
follistatin	FST	NM_013409	anti	0.247	0.001	0.679	0.045	0.243	0.000	0.668	0.077	0.000	A_23_P110531
gap junction protein, alpha 5, 40kDa (connexin 40)	GJA5	NM_005266	anti	0.843	0.546	1.035	0.873	0.323	0.001	0.396	0.035	0.018	A_23_P371729
heterogeneous nuclear ribonucleoprotein R	HNRPR	NM_005826	anti	0.695	0.005	0.916	0.146	0.894	0.088	1.177	0.059	0.014	A_23_P45726
prostaglandin I2 (prostacyclin) synthase	PTGIS	NM_000961	anti	0.363	0.000	0.590	0.007	0.605	0.004	0.982	0.873	0.001	A_24_P48723
activated leukocyte cell adhesion molecule	ALCAM	NM_001627	pro	1.133	0.419	2.147	0.001	1.418	0.001	2.688	0.004	0.002	A_23_P41227
bone morphogenetic protein 4	BMP4	NM_001202	pro	0.439	0.006	0.834	0.249	0.607	0.030	1.153	0.363	0.022	A_23_P54144
gap junction protein, alpha 1, 43kDa (connexin 43)	GJA1	NM_000165	pro	0.938	0.614	0.693	0.002	0.644	0.001	0.476	0.003	0.002	A_24_P55295
gap junction protein, alpha 4, 37kDa (connexin 37)	GJA4	NM_002060	pro	1.462	0.019	1.168	0.250	0.195	0.000	0.156	0.000	0.000	A_23_P1083
interleukin 1, alpha	IL1A	NM_000575	pro	11.973	0.009	3.748	0.041	1.678	0.245	0.525	0.324	0.028	A_23_P72096
interleukin 8	IL8	NM_000584	pro	1.159	0.352	0.602	0.038	3.577	0.001	1.859	0.023	0.003	A_32_P87013
matrix metalloproteinase 2 (gelatinase A, 72kDa gelatinase, 72kDa type IV collagenase)	MMP2	NM_004530	pro	1.424	0.037	1.112	0.273	0.838	0.018	0.655	0.034	0.032	A_23_P163787
syndecan 2 (heparan sulfate proteoglycan 1, cell surface-associated, fibroglycan)	SDC2	NM_002998	pro	1.512	0.003	0.961	0.479	0.523	0.001	0.332	0.000	0.000	A_24_P380734
tyrosyl-tRNA synthetase 2 (mitochondrial)	YARS2	NM_015936	pro	0.781	0.016	0.841	0.051	1.254	0.022	1.351	0.008	0.007	A_23_P151093
chemokine (C-X-C motif) receptor 4	CXCR4	NM_001008540	pro	1.486	0.001	1.219	0.090	0.500	0.000	0.411	0.001	0.000	A_23_P102000
tumor necrosis factor receptor superfamily, member 21	TNFRSF21	NM_014452	pro	1.236	0.005	1.024	0.281	1.090	0.008	0.904	0.059	0.010	A_23_P30666

Neovascularization

Asahara et al.'s [91] first report of EPCs in adult circulation claimed that these circulating cells contributed to neoangiogenesis in the adult species by incorporating into active sites of vascular growth and by delivering pro-angiogenic agents. This work has been further confirmed in many additional publications. The area of neovascularization of tissues has enormous potential for clinical benefit. In this study, we investigated the effect of shear stress on a subset of 14 genes related to neovascularization (shown in Table 6.10). Fibroblast growth factor 12 was found on two different spots of the Agilent microarray (see different Agilent probe ID numbers) and is listed in the table twice. This technical replicate showed agreement in three of the four comparisons. The one difference was in the Static: EPC vs. EC comparison where A_23_P211727 showed a significant increase while A_23_P334300 did not show a significant difference. Shear exposure resulted in a complex and heterogeneous regulation of the genes associated with neovascularization in both ECs and EPCs. When comparing the two cell types in both shear and static environments, EPCs expressed genes related to neovascularization to a greater extent than ECs. In static culture, EPCs expressed 1.1 to 3.6 fold more of seven angiogenic genes compared to ECs. Following shear, 9 of 14 genes were more highly expressed in EPCs than ECs (1.1 to 3.4 fold).

Table 6.10: Genes related to neovascularization. Red boxes are used to highlight significant ratios >1 ($p<0.05$) and blue boxes highlight significant ratios <1 ($p<0.05$). Data which were not significantly different ($p>0.05$) are left without color.

Genes related to neovascularization

Gene Name	Gene Symbol	Systematic Name	EC: Shear vs Static		EPC: Shear vs Static		Static: EPC vs EC		Shear: EPC vs EC		ANOVA	Agilent Probe ID
			Fold change	P-value (pairwise)	Fold change	P-value (pairwise)	Fold change	P-value (pairwise)	Fold change	P-value (pairwise)		
cathepsin H	CTSH	NM_148979	0.443	0.000	0.906	0.342	1.686	0.005	3.447	0.000	0.000	A_23_P14774
cathepsin L	CTSL	NM_001912	1.263	0.003	0.870	0.327	3.284	0.000	2.264	0.001	0.000	A_23_P94533
endothelial cell growth factor 1 (platelet-derived)	ECGF1	NM_001953	1.037	0.226	0.864	0.099	1.355	0.005	1.129	0.065	0.016	A_23_P91802
fibroblast growth factor 12	FGF12	NM_004113	0.983	0.852	0.825	0.092	2.128	0.000	1.787	0.005	0.001	A_23_P211727
fibroblast growth factor 12	FGF12	NM_004113	0.642	0.090	1.236	0.211	1.211	0.443	2.330	0.001	0.047	A_24_P334300
interleukin 1, alpha	IL1A	NM_000575	11.973	0.009	3.748	0.041	1.678	0.245	0.525	0.324	0.028	A_23_P72096
interleukin 24	IL24	NM_006850	1.093	0.629	1.372	0.058	1.613	0.055	2.025	0.003	0.022	A_24_P222740
interleukin 32	IL32	NM_001012631	1.149	0.081	1.217	0.035	1.145	0.030	1.214	0.064	0.036	A_23_P15146
interleukin 5 (colony-stimulating factor, eosinophil)	IL5	NM_000879	1.545	0.027	1.262	0.070	0.863	0.120	0.705	0.067	0.038	A_24_P209047
interleukin 8	IL8	NM_000584	1.159	0.352	0.602	0.038	3.577	0.001	1.859	0.023	0.003	A_32_P87013
platelet derived growth factor D	PDGFD	NM_025208	0.387	0.005	0.504	0.065	1.347	0.335	1.754	0.030	0.027	A_24_P124349
stromal cell derived factor 4	SDF4	NM_016176	1.254	0.001	1.183	0.052	1.168	0.073	1.103	0.010	0.011	A_23_P201338
transforming growth factor, beta 2	TGFB2	NM_003238	0.774	0.010	0.813	0.280	3.243	0.001	3.409	0.000	0.000	A_24_P402438
vascular endothelial growth factor B	VEGFB	NM_003377	0.939	0.141	0.903	0.221	0.781	0.004	0.752	0.013	0.010	A_23_P1594
vascular endothelial growth factor C	VEGFC	NM_005429	2.426	0.003	1.266	0.073	0.869	0.439	0.453	0.000	0.002	A_23_P167096

<center>**Discussion**</center>

Hemodynamic force is a well recognized modulator of vascular endothelial cell (EC) phenotype and has been implicated in both vascular function and dysfunction. Endothelial progenitor cells (EPCs) are derived from bone marrow and circulate in the adult circulation. These cells can be cultured from peripheral blood outgrowth colonies and express a number of endothelial specific markers. Very little is known about the role of hemodynamics in EPC biology. In this study, a comprehensive transcriptional profile analysis was performed to investigate the effect of fluid shear stress on EPCs in the context of vascular endothelial cell response to shear. Several high throughput technologies have been employed to investigate the effect of varying hemodynamic factors in EC mRNA expression [185-195] but to our knowledge, this is the first microarray study investigating the effects of shear on EPCs.

Limitations of the Experimental Approach

There are several limitations associated with this study. First, microarray analysis was performed on cells in *in vitro* culture. While *in vitro* culture allows precise control of the local microenvironment, it is difficult to exactly simulate the *in vivo* situation and conclusions must be made with caution when trying to predict the true *in vivo* response. A second limitation relates to the vascular endothelial cell choice. Endothelial cells from different anatomical locations in the body have been shown to have diverse phenotypes, presumably related to their *in vivo* functional requirements and local mileu [196]. Juvenile male baboon carotid artery endothelial cells were chosen as the cell type for microarray studies because they represented an age and sex matched control for the

<center>110</center>

baboon peripheral blood derived EPCs. The carotid artery was an accessible tissue sample which yielded sufficient endothelial cell numbers at isolation so that excessive expansion was not necessary for experimental protocols. The carotid artery also represented a large artery endothelial cell which experiences mean arterial shear stresses in the range of 10-15 dynes/cm^2 *in vivo*. We chose to investigate the effect of steady laminar shear stress on EC and EPC response at 24 hours. This represented a "chronic" exposure to shear where time dependent alterations in gene expression would be minimized resulting in stable genetic profiles. Static culture controls were used to compare to the shear environment and represented a "baseline" zero shear stress state. There is a significant amount of data that exists on endothelial cells in steady laminar shear stress compared to other more complex flow regimes. This enabled us to make more conclusive comparisons to the work of others. Finally, baboon cells were chosen because of the possibility to quickly move into a gold standard and physiologically relevant pre-clinical model for functional evaluations. The microarray system used was the Agilent Whole Human Genome microarray. The baboon is considered one of the Old World monkeys which are the closest non-ape relative to humans. While the baboon and human genome are certainly not identical, their genome is highly conserved with human [197]. Human cDNA microarrays have been validated with success in at least one other study with baboon cells [198]. Baboon specific arrays were not available and therefore the human microarray provided a relevant platform for studying transcriptional profile changes with a stimulus (shear) compared to species matched controls.

EPCs are Shear Stress Responsive

Microarray analysis has demonstrated that EPCs are mechanosensitive to fluid shear stress, altering expression of 1.5% (625 of 40324) of the total gene probes investigated by more than 1.5 fold. Compared to vascular ECs, the EPCs response to shear was attenuated both in the number of genes regulated by shear and the extent of regulation (up or down). Investigating a subset of genes commonly associated with endothelial response to shear demonstrated that although EPCs regulated almost all of these genes similar to ECs, the EPCs generally altered the expression to a lesser extent (lower fold changes). Shear resulted in altered EC expression by ≥ 1.5 fold in more of the total gene probes investigated (2.3% or 939 of 40324) with only 0.7% (283 of 40324) of the genes being similarly regulated by both cell types.

There have only been a few reports of blood derived EPC response in a shear environment at the molecular level. Several studies have reported morphological changes in EPCs in the presence of shear [149, 157, 158, 160] but few have investigated alterations in gene or protein expression. Rossig et al. [146] recently suggested that physiological shear stress (15 dynes/cm^2) was capable of promoting the commitment of progenitor cells to an endothelial phenotype and that HoxA9 was a critical regulator in that process. HoxA9 is a member of the Hox family of homeodomain transcription factors which are known to play important roles in the embryonic development of the cardiovascular system. In our dataset, nine of the Hox transcription factors had altered expression across the four comparisons but HoxA9 did not meet ANOVA significance criteria ($p < 0.05$). Yamamoto et al. [145] reported that low levels of fluid shear (0.1-2.5 dynes/cm^2) increased mRNA levels of the VEGF receptors (KDR and Flt-1) and vascular

endothelial (VE) cadherin. In our microarray results with 15 dynes/cm^2 shear stress,

KDR and Flt-1 expression was not significantly altered (p>0.05) by shear based on

pairwise comparisons and VE-cadherin (CDH5) did not meet ANOVA significance

criteria (p<0.05).

While EPCs and ECs demonstrated similar regulation of specific individual genes

known to be shear responsive in vascular ECs, Ingenuity Pathways Analysis (IPA) of

global function identified some interesting differences in EPC and EC response to shear.

When broken down into specific functional groups, the genes regulated by shear in each

cell type aligned with different functional categories. ECs responded to shear with

alterations in genes associated with more molecular and cellular functions while EPCs

altered expression of more genes associated with physiological systems development and

function. These differences may relate to the origin of these cells. The fact that EPCs are

derived from a bone marrow progenitor source may inherently confer the EPCs with

expression of genes associated with development which are altered in the presence of

shear stress. In vascular ECs, this global functional analysis is consistent with previous

reports that shear causes alterations in categories such as cell cycle, cell signaling and

cellular growth and proliferation.

Coagulation

As one of the primary endothelial functions, we were keenly interested in how

shear would modulate EPC genes associated with coagulation. Shear clearly upregulated

a number of anticoagulant associated genes in ECs while EPCs were less responsive to

shear exposure in this system. One anticoagulant protein, thrombomodulin, stood out as

being differentially upregulated by shear in EPCs and not in ECs. Thrombomodulin

binds thrombin serving as a co-factor which dramatically accelerates the rate of protein C activation. Through this action, thrombomodulin causes a net loss of coagulant effect and an enhancement of anti-coagulant function.

When comparing the two cell types in the static environment, EPCs appear to display an anticoagulant phenotype with more expression of anticoagulant molecules and less expression of procoagulant genes than ECs. When exposed to shear, the ECs were more responsive and therefore the regulation of coagulation associated genes was heterogenous. This study demonstrates that EPCs respond to shear differently than ECs when considering genes associated with coagulation but further study will be needed to understand how these complex changes in gene expression translate to protein expression and ultimately coagulant function.

EPC Antioxidant and Antiinflammatory Capacity

For many years, research in atherosclerosis localization and progression has demonstrated that the endothelium, the hemodynamic environment, oxidative modifications and inflammation all play critical roles [182, 199, 200]. One overriding hypothesis associated with the hemodynamic environment and atherosclerosis is that areas of unidirectional laminar shear stress produce a quiescent, antithrombotic, and antioxidant phenotype in vascular endothelial cells [201, 202]. Consistent with many other studies, our microarray data support this hypothesis in baboon carotid artery ECs. In contrast to disease localization and progression, antioxidant capacity in EPCs has recently been suggested to have other import functions. Two recent publications have suggested that there exists a set of general stem cell features or "stemness" genes, a subset of which provides increased resistance to stress [203, 204]. This high resistance to

114

stress has been proposed as one of the mechanisms which EPCs need to aid in recreating a perfusion network in any post-ischemic environment where exceptionally high levels of reactive oxygen species (ROS) are known to accumulate [205]. In this study, shear exposure resulted in an overall upregulation of antioxidant function in EPCs between 1.1 and 6.0 fold. When compared to ECs in the shear environment, EPCs had greater antioxidant gene expression including more expression of superoxide dismutase and glutathione peroxidase which are believed to be the primary antioxidant defense systems in the mitocondria [206]. Recently, two other *in vitro* studies demonstrated that EPCs express higher levels of these two enzymes compared to HUVEC and coronary artery ECs or human microvascular ECs [132, 207]. Our microarray results demonstrate that shear stress upregulated redundant antioxidant defense mechanisms in EPCs. This data combined with EPCs overall low expression of genes related to inflammation may have important implications for EPC's *in vivo* function and clinical utility.

Neovascularization

EPCs normally found in the bone marrow may be mobilized into the circulation and have been shown to physically integrate into newly forming vasculature or promote *de novo* vessel formation by supplying appropriate cytokines and growth factors (reviewed in [100]). In a subset of genes related to neovascularization including the cathepsin proteases, cytokines and growth factors, the microarray data clearly showed that EPCs expressed higher levels of these key proteins compared to ECs but that shear did not appear to have a significant effect. EPC enhanced expression is consistent with recent reports investigating the both soluble factors and protease activity in EPCs compared to mature vascular ECs [208, 209].

115

Study Validation

qRT-PCR was used as an independent experimental method/technique to "check" the mRNA expression results obtained from DNA microarray analysis. Investigating three genes (F3, TFPI and THBD) in the four comparisons (EC: Shear vs. Static, EPC: Shear vs. Static, Static: EPC vs. EC and Shear: EPC vs. EC), mRNA expression was regulated similarly (up or down) in 8 of 12 cases. In four cases, one technique showed no significant change in expression where the second method suggested either more (2 cases) or less (2 cases) expression. There were no instances where the two methods suggested opposite regulation (e.g. up vs. down).

Concluding Remarks

This work has contributed to our knowledge of EPC biology related to vascular endothelial cells and provides significant new data on how EPCs response to the hemodynamic environment. These microarray studies provide a transcriptional profile of EPC gene modulation and provide a foundation for many additional studies needed to more clearly define the role of EPCs in tissue engineering and regenerative medicine.

CHAPTER VII: ENDOTHELIAL PROGENITOR CELL PHENOTYPE IN RESPONSE TO FLOW – COMPARISON TO VASCULAR ENDOTHELIAL CELLS ON ABSORBED COLLAGEN AND ON AN ENGINEERED VASCULAR TISSUE

Introduction

The normal endothelium, composed of a single layer of endothelial cells (ECs), maintains blood fluidity by producing inhibitors of blood coagulation and platelet aggregation, providing a barrier separating hemostatic blood components from reactive subendothelial structures, and by modulating vascular tone and permeability. This system maintains blood fluidity under physiologic conditions but is primed to react to vascular injury by quickly sealing any vascular wall defect. Shear stresses produced by flowing blood are imposed on the apical surface of ECs and are an important stimulus for vascular remodeling. These local mechanical forces cause documented alterations in many aspects of EC biology including cell shape, metabolism and gene expression and are often linked to disease pathologies. Additionally, the local mechanical environment alters the ECs role in hemostasis by modulating a number of key molecules critical to both pro- and anti-coagulant function. (A detailed review of endothelial cell response to flow can be found in Chapter II: Background.)

Endothelial progenitor cells (EPCs) have been shown to exhibit many of the same cellular markers and functions as vascular ECs [94], yet very little is known about how these cells respond to local mechanical forces such as fluid shear stress. EPCs have

emerged as a promising autologous cell source for tissue engineering strategies. For example, EPCs could be used as a luminal lining on an engineered blood vessel substitute or as a vascular stent coating. For applications such as these and others where EPCs are attached to surfaces exposed to flow, it is critical that the EPC response to fluid shear stress be investigated.

Depending on the specific therapeutic application, EPCs may be required to adhere and function on a variety of substrates. In vascular applications, it is likely that EPCs will interface with neighboring vascular SMCs as well as the native extracellular matrix proteins. A number of *in vitro* coculture models have been developed which incorporate both ECs and SMCs influences. Approaches have used porous membranes [210-214], collagen gels containing SMCs [215, 216], microcarrier/spheroid-bound ECs or SMCs [217, 218], conditioned media [213, 219], and direct culture of ECs on SMCs [220-222]. These studies have shown that the presence of SMCs may alter EC morphology, proliferation, growth factor expression, and inflammatory status. To investigate the role of substrate in this study, EPC response to fluid flow was investigated on two surfaces. EPCs were seeded onto absorbed type I collagen slides or onto an engineered vascular tissue. The engineered tissue, composed of a type I collagen hydrogel with embedded carotid artery SMCs, mimicked the medial layer of the native blood vessel and served as a more physiologic vascular substrate.

One of the most striking responses visualized when mature vascular endothelial cells are exposed to fluid shear stress is the morphological shape change which occurs in a time and shear dependent manner [34]. These characteristic changes in cell morphology including spatial reorganization of cytoskeletal structures have been shown

to be important in many downstream signal transduction pathways related to EC functions [223]. In order to investigate EPCs gross morphological response to the shear environment, this study used fluorescent confocal microscopy to quantify alterations in F-actin organization as a function of cell type and shear environment.

In addition to morphological changes, understanding of how EPCs regulation of hemostasis may be influenced by the local mechanical environment and/or substrate is important for many applications including their potential use in cardiovascular substitutes. Hemostasis involves a complex cascade or series of events that involve zymogens or cofactors, the transformation of these zymogens to proteolytic enzymes, and protease inhibitors that limit the reactions at each step [224]. In this study, several key molecules central to hemostasis have been investigated to characterize the thrombotic potential of EPCs in response to fluid shear stress and on both absorbed collagen and on an engineered tissue. Starting with the cell's earliest response to a given stimulus, gene expression changes with known pro- and anti-coagulant function were investigated using quantitative real time RT-PCR. This study focused on three molecules with known anti-coagulant function: thrombomodulin (THBD), tissue factor pathway inhibitor (TFPI) and endothelial nitric oxide synthase 3 (NOS3) as well as two molecules with known pro-coagulant function: tissue factor (F3) and von Willebrand factor (VWF).

While variations in mRNA expression represent the cell's first response to a stimulus, translation of gene expression into alterations in protein expression is also important in assessing cell phenotype. Using flow cytometry, cell surface THBD and F3 protein expression were quantified. F3 protein is the initiator of the extrinsic coagulation cascade which leads directly to fibrin rich clot formation. In contrast, THBD has

significant anti-coagulant function binding thrombin and therefore inhibiting thrombin's ability to cleave fibrinogen and activate platelets and factors Va and VIIIa. In addition, THBD enhances thrombin's ability to activate protein C and therefore to inhibit thrombogenesis.

To characterize EPC phenotype, this study uses a combination of approaches to quantify gross morphological changes and measure specific alterations in gene and protein expression in both static and fluid shear stress environments on two model substrates. Furthermore, using the baboon model, this study compared the response of blood derived EPCs to age and sex matched native vascular wall ECs. These findings provide an improved understanding of EPC response to fluid shear stress and allow us to make predictions about the anti-thrombotic potential of EPCs when exposed to a flow environment.

Experimental Design

The detailed methods for this study are described in Chapter IV: Materials and Methods. Briefly, an engineered tissue was fabricated with baboon carotid artery smooth muscle cells embedded in a type I collagen hydrogel. The tissue was statically cultured for five days to allow for initial SMC mediated remodeling prior to EPC or EC seeding. Confluent monolayers of baboon carotid artery endothelial cells or baboon peripheral blood derived endothelial progenitor cells were seeded onto glass slides coated with absorbed collagen or onto the engineered tissue and allowed to adhere for 48 hours. Following this static incubation, both cell types were exposed to steady laminar shear stress using a parallel plate flow chamber system. Cells were exposed to 15 dynes/cm^2 of steady laminar shear stress for 24 hours and compared to static controls.

120

Cell morphology was assessed using light and fluorescent microscopy combined with F-actin localization. mRNA was extracted from cell lysates and used for quantitative real time RT-PCR analysis of five genes: THBD, TFPI, NOS3, F3, and VWF. For flow cytometry, cells were removed from the slide substrate immediately upon completion of the experiment and paraformaldehyde fixed for subsequent immunofluroescent labeling of cell surface proteins: THBD and F3.

All analyses were performed on n≥3 samples from at least three independent experiments. Data are reported as mean ± standard error of the mean (SEM) and statistical comparisons were based on ANOVA and Tukey's test for pairwise comparisons with a p-value < 0.05 considered significant. In order to make the variance independent of the mean, statistical analysis of real time RT-PCR data was performed following logarithmic transformation of the raw data.

Results

Monolayer Culture on Absorbed Collagen

<u>Cell Morphology</u>

At confluence, ECs and EPCs displayed very similar polygonal or "cobblestone" morphology, a distinct nuclear region and clearly visible cell borders as shown in Figure 7.1. Following exposure to fluid shear stress, rhodamine phalloidin was used to visualize F-actin distribution within the cells of both static and shear samples. As shown in Figure 7.2, both cell types subjected to 15 dynes/cm^2 altered their morphology in response to flow. Static ECs and EPCs had dense peripheral bands of F-actin which reorganized to

elongated fibers found throughout the cells and oriented parallel to the flow axis following 24 hours of shear exposure.

Using image analysis, confocal microscopy images were analyzed to quantify morphological changes in ECs and EPCs. Angle of orientation and shape index were quantified following 24 hours of shear stress exposure as shown in Figure 7.3. Angle of orientation or the degree of alignment of the cells was characterized by measuring the deviation of the primary cell axis direction from the flow direction. If the orientation of the cells was completely random, the mean angle would be 45 degrees. As cells align with the flow direction, the mean approaches 0 degrees. ECs and EPCs each had a statistically significant decrease ($p < 0.05$) in the angle of orientation following 24 hours in a steady laminar shear stress environment but there was not a significant ($p > 0.05$) difference between the two cell types. Shape index is defined as $4(\pi)(area/perimeter^2)$. As defined, this parameter has a circular shape when the shape index = 1.0 and in the limiting case, a straight line, when the shape index = 0.0. Therefore the more elongated a cell becomes, the smaller the value for its shape index. Shown quantitatively in Figure 7.3, both cells types had a significant ($p < 0.05$) decrease in shape index when exposed to shear stress for 24 hours but ECs elongated to a greater extent than EPC ($p < 0.05$).

Cytoskeletal reorganization occurred as a function of the number of hours of shear stress exposure. Figure 7.4 shows the angle of orientation for ECs and EPCs as a function of shear duration. While shear stress exposure caused both cells types to orient parallel with the flow direction, at 6 and 12 hours, ECs exposed to shear stress displayed a smaller angle of orientation ($p < 0.05$) than sheared EPCs. By 24 hours, both sheared samples appeared to have reached a minimum angle of orientation and were not statically

different from each other (p>0.05). At 6 and 12 hours, EPC static samples had a

significantly larger angle of orientation than EC static samples (p<0.05) but the

interaction of cell type and condition (shear versus static) was not significant (p>0.05)

indicating that neither cell type was significantly more sensitive to shear exposure at

these early time points.
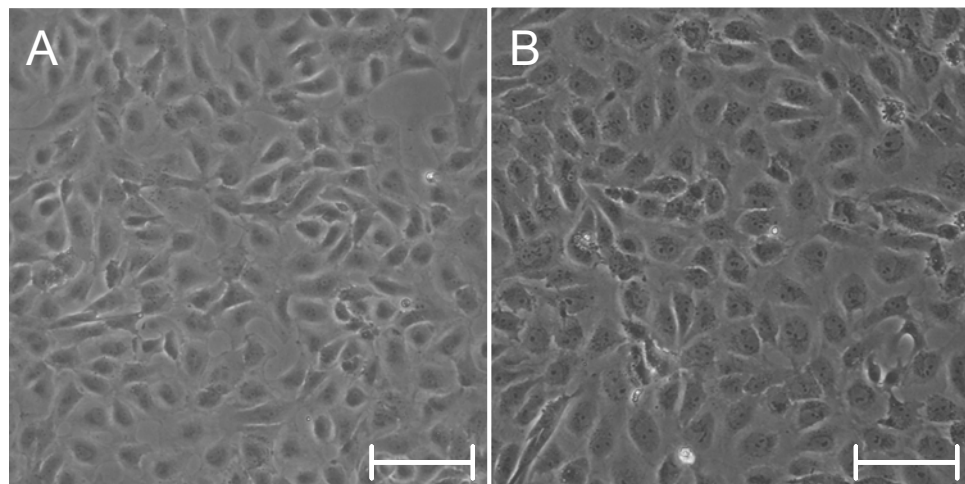
Figure 7.1: Phase contrast microscopy of EC and EPC. (A) Baboon carotid artery
endothelial cells (EC, passage 1); (B) Baboon peripheral blood derived endothelial
progenitor cells (EPC, passage 1). Scale bar = 100μm.
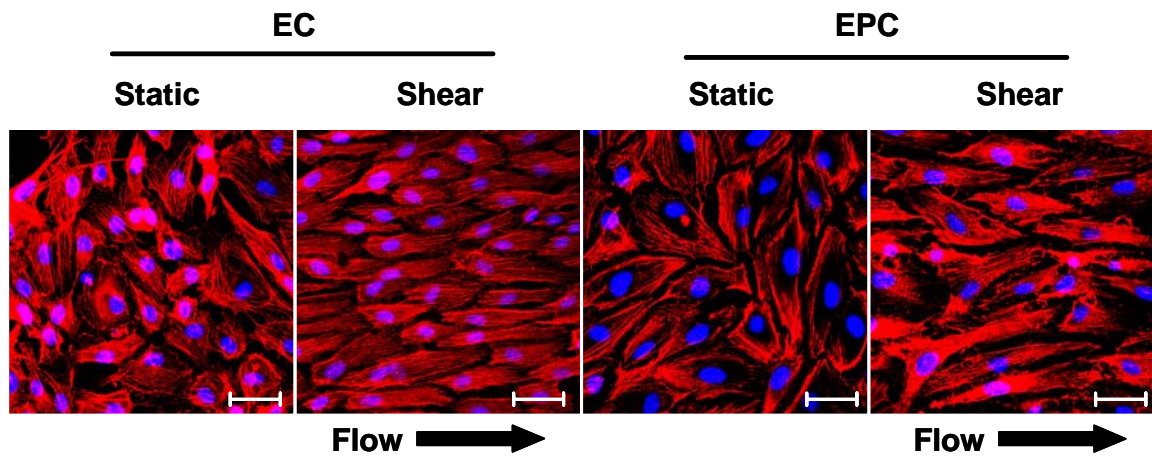
Figure 7.2: Visualization of cytoskeletal reorganization in EC and EPC using confocal microscopy. Rhodamine phalloidin was used to stain F-actin of cells exposed to steady laminar shear stress (15 dynes/cm^2, 24 hours) compared to static controls. Flow direction was left to right in pictured shear samples. Hoechst 33258 was used as a nuclear counterstain. Scale bar = 50μm.
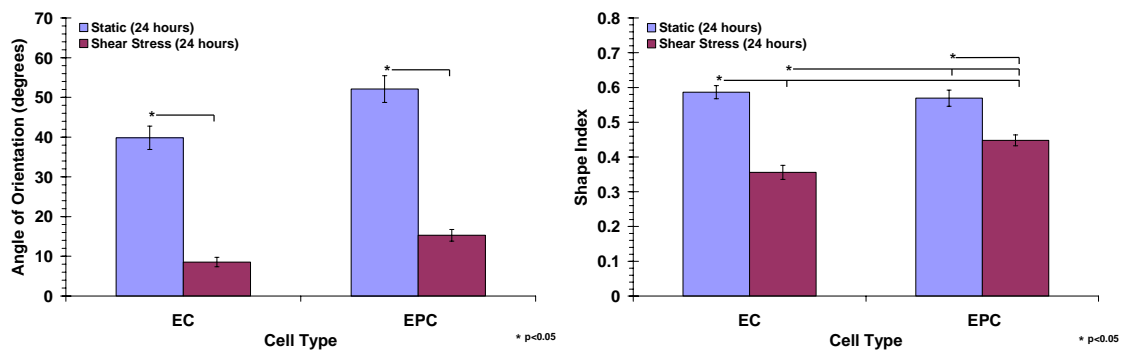
Figure 7.3: Quantification of cytoskeletal reorganization in EC and EPC. Angle of orientation (left panel) and shape index (right panel) was quantified in cells exposed to steady laminar shear stress (15 dynes/cm^2, 24 hours) and compared to static controls (mean ± SEM, n≥40). ANOVA showed differences in groups (p<0.0001). Pairwise comparisons: *(p<0.05).
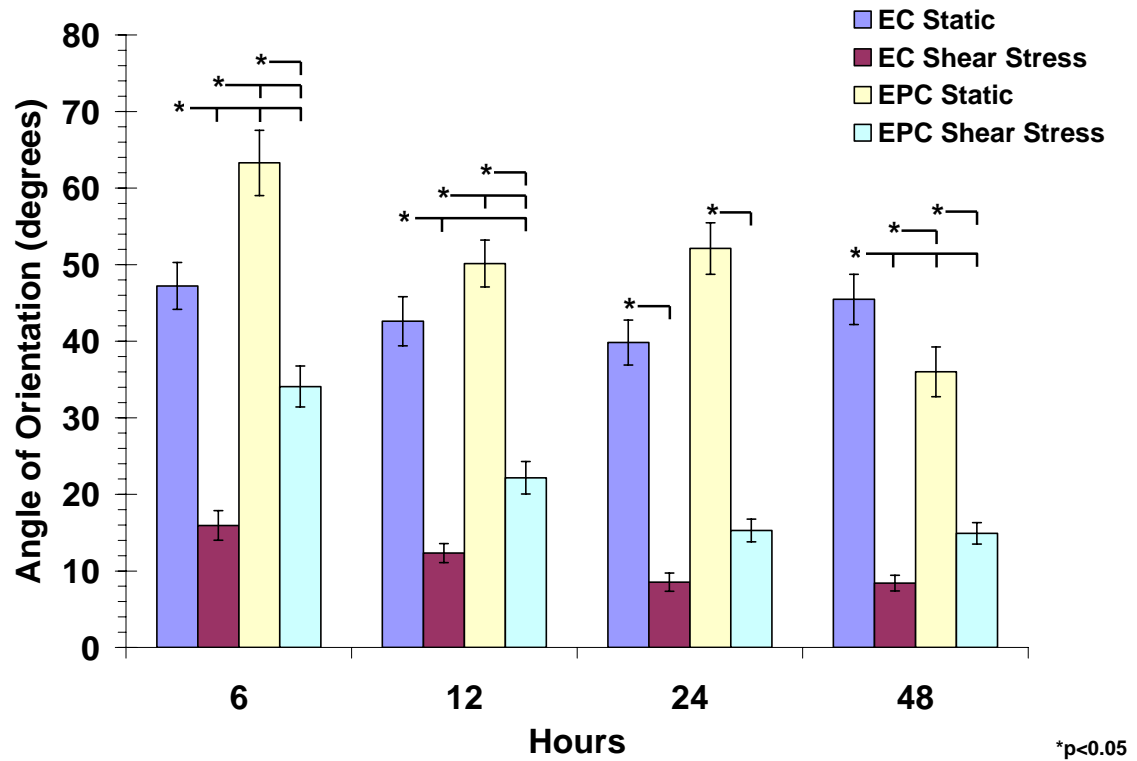
Figure 7.4: Quantification of cytoskeletal reorganization in EC and EPC. Angle of orientation was quantified in cells exposed to steady laminar shear stress (15 dynes/cm^2 for 6,12, 24 and 48 hours) and compared to static controls (mean ± SEM, n≥40). ANOVA showed differences in groups (p<0.0001). Pairwise comparisons: *(p<0.05).

Quantitative real time RT-PCR was used to quantify gene expression of select hemostasis associated genes in ECs and EPCs. As shown in Table 7.1, five genes (THBD, TFPI, NOS3, F3 and VWF) with known pro- or anti-coagulant function were investigated.

Table 7.1: Quantitative real-time RT-PCR of select hemostasis associated genes.

Primary Function	Systematic Name	Gene Symbol	Gene Name
Anti-Coagulant	NM_000361	THBD	Homo sapiens thrombomodulin
	NM_006287	TFPI	Homo sapiens tissue factor pathway inhibitor (lipoprotein-associated coagulation inhibitor)
	NM_000603	NOS3	Homo sapiens nitric oxide synthase 3 (endothelial cell)
Pro-Coagulant	NM_001993	F3	Homo sapiens coagulation factor III (thromboplastin, tissue factor)
	NM_000552	VWF	Homo sapiens von Willebrand factor

Thrombomodulin (THBD)

Thrombomodulin gene expression is shown in Figure 7.5 for ECs and EPCs. Thrombomodulin is transmembrane protein presented on the surface of endothelial cells. Thrombomodulin binds to thrombin serving as a co-factor which dramatically accelerates the rate of protein C activation. Thrombomodulin binding of thrombin also inhibits thrombin's ability to cleave fibrinogen and activate platelets and factors Va and VIII. Therefore when thrombomodulin is bound to thrombin, there is a net loss of coagulant effect and an enhancement of anti-coagulant effect through the activated protein C pathway [225]. Under static conditions, ECs and EPCs both have similar ($p > 0.05$) levels

of THBD expression. When exposed to shear stress, ECs responded with a slight but not significant ($p>0.05$) increase in THBD transcripts while EPCs responded with a greater than 3-fold ($p<0.05$) increase in THBD expression.

Tissue Factor Pathway Inhibitor (TFPI)

Tissue factor pathway inhibitor has anti-coagulant effect by acting on the extrinsic system of coagulation. TFPI is a protein that in association with factor VIIa and factor Xa inhibits the tissue factor (TF)/factor VIIa complex. The result is a fully inhibited tetramolecular complex (TF:VIIa:TFPI:Xa) which not only blocks the enzymatic activity of TF:VIIa, it also promotes the internalization and degradation of TF:VIIa complexes on the cell surface [226]. RT-PCR results (Figure 7.6) show that in vascular ECs there is significantly more TFPI expression ($p<0.05$) than in EPCs under static conditions. When both cell types were exposed to shear stress, the TFPI mRNA expression was unregulated ($p<0.05$) in both cell types but even with the increased expression following shear stress exposure, EPCs still showed significantly less TFPI than ECs ($p<0.05$).

Nitric Oxide Synthase 3 (NOS3)

NOS3, the endothelial isoform of nitric oxide synthase, has been extensively studied because the nitric oxide (NO) produced by eNOS mediates a variety of physiological functions *in vivo* including neovascularization, regulation of blood vessel tone (vessel wall tension), vascular permeability and leukocyte-endothelial interaction [21]. NOS3 represents an integral part of vascular hemostasis. In addition to effects as a vasodilator, NO also prevents the adhesion of platelets and white cells to endothelium, inhibits the aggregation of platelets, and induces the disaggregation of platelets. Basal

release of NO can also decrease the rolling and adhesion of polymorphonuclear leukocytes to the endothelium [22]. Figure 7.7 shows the NOS3 mRNA expression for ECs and EPCs under static and shear conditions. In static cell culture conditions, EPC expression levels of NOS3 were lower than ECs ($p<0.05$). Following 24 hours of shear stress, both EPC and EC NOS3 mRNA expression increased ($p<0.05$). EPCs message levels nearly doubled in the presence of shear stress resulting in expression which equaled the EC static expression but still at levels significantly lower than in ECs following shear exposure ($p<0.05$).

Tissue Factor (F3 or TF)

There are two main pathways for triggering the coagulation cascade, the intrinsic or "contact" pathway and the extrinsic or "tissue factor" pathway. The extrinsic pathway is triggered when plasma comes in contact with cells that express tissue factor. Presentation of tissue factor can be a physiological response to injury or can be caused by a pathologic activation. Tissue factor is a transmembrane protein which serves as a co-factor to a serine protease, factor VIIa. Tissue factor (TF) can bind factor VII or VIIa with high affinity but once the TF:VIIa complex has assembled on the cell surface, it is the most potent know activator of the clotting cascade [227]. In vascular ECs, Figure 7.8 shows that shear stress caused a significant up-regulation (6.5-fold) of F3 mRNA ($p<0.05$) while shear stress did not augment EPC F3 expression over static levels ($p>0.05$). ECs had a slightly more F3 expression in static conditions than static EPC samples ($p<0.05$).

Von Willebrand Factor (VWF)

VWF has a pro-coagulant function primarily in supporting the adhesion of platelets to damaged blood vessels but it also has post-synthetic association with factor VIII which protects factor VIII from proteolysis [228]. VWF is synthesized in both the megakaryocyte and the endothelial cell. Endothelial cells and platelets are known to store VWF in secretory granules called Weibel-Palade bodies in ECs and α-granules in platelets. Following stimulation by an appropriate agonist, platelets and ECs can release VWF both luminally into plasma and abluminally into the subendothelial cell matrix. VWF bound to the subendothelial matrix can interact with circulating platelets, initiating platelet adhesion and subsequent platelet activation [229]. Figure 7.9 shows the VWF gene expression of both ECs and EPCs in static and following shear stress exposure. Shear stress caused a significant down-regulation of VWF mRNA in ECs compared to ECs under static conditions ($p<0.05$). EPC VWF mRNA under static conditions was not different than EC static levels ($p<0.05$) and following shear stress exposure, although EPCs mRNA levels rose slightly, there was not a significant difference compared to static controls ($p<0.05$).
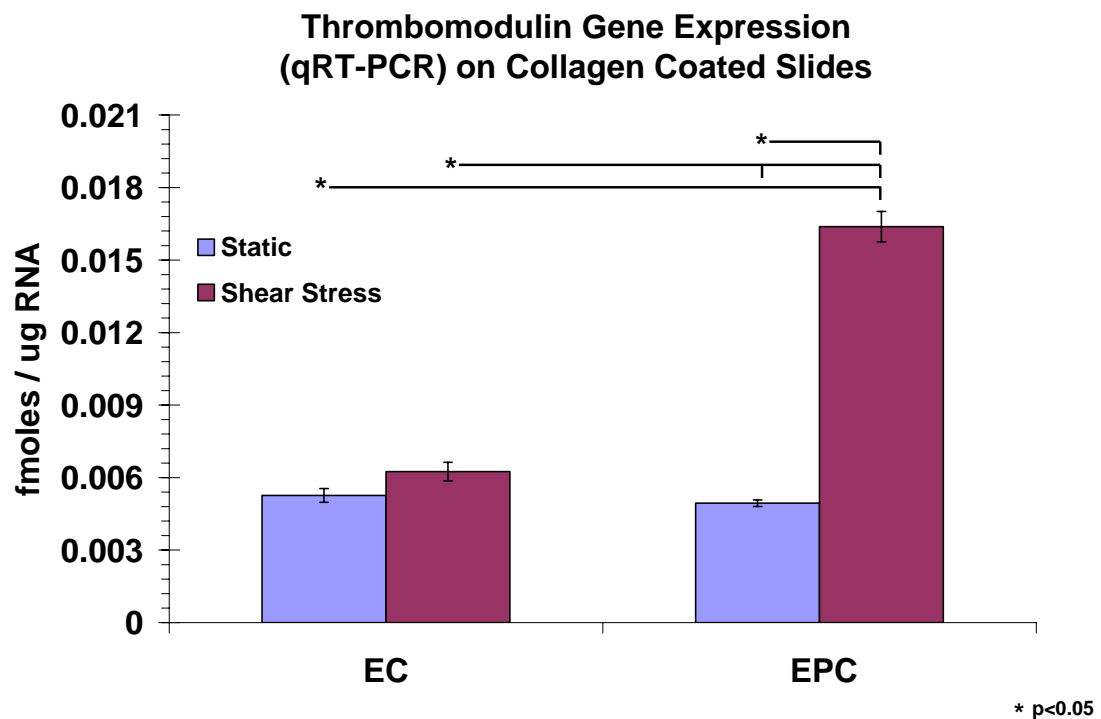
Figure 7.5: Thrombomodulin (THBD) gene expression in EC and EPC determined by real-time RT-PCR. mRNA expression was quantified in cells exposed to steady laminar shear stress (15 dynes/cm^2, 24 hours) and compared to static controls (mean ± SEM, n=9). ANOVA showed differences in groups (p<0.0001). Pairwise comparisons: *(p<0.05).
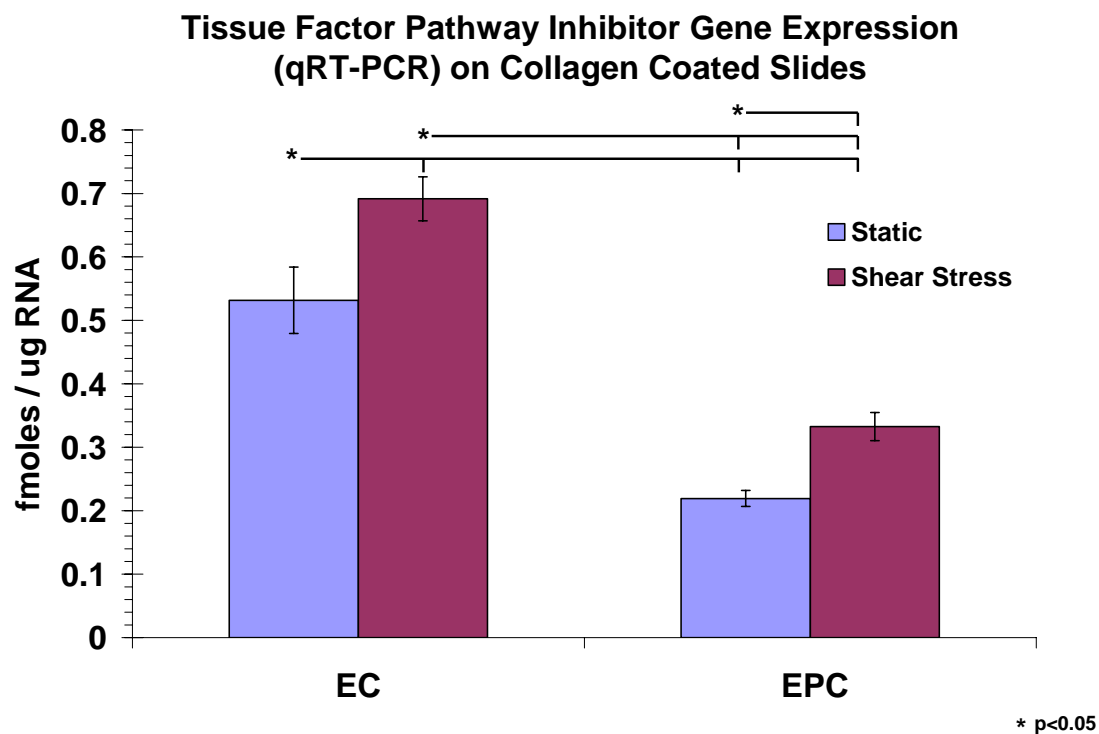
Figure 7.6: Tissue factor pathway inhibitor (TFPI) gene expression in EC and EPC determined by real-time RT-PCR. mRNA expression was quantified in cells exposed to steady laminar shear stress (15 dynes/cm^2, 24 hours) and compared to static controls (mean $\pm$ SEM, n=9). ANOVA showed differences in groups (p<0.0001). Pairwise comparisons: *(p<0.05).

NOS3 Gene Expression (qRT-PCR) on Collagen Coated Slides

* p<0.05
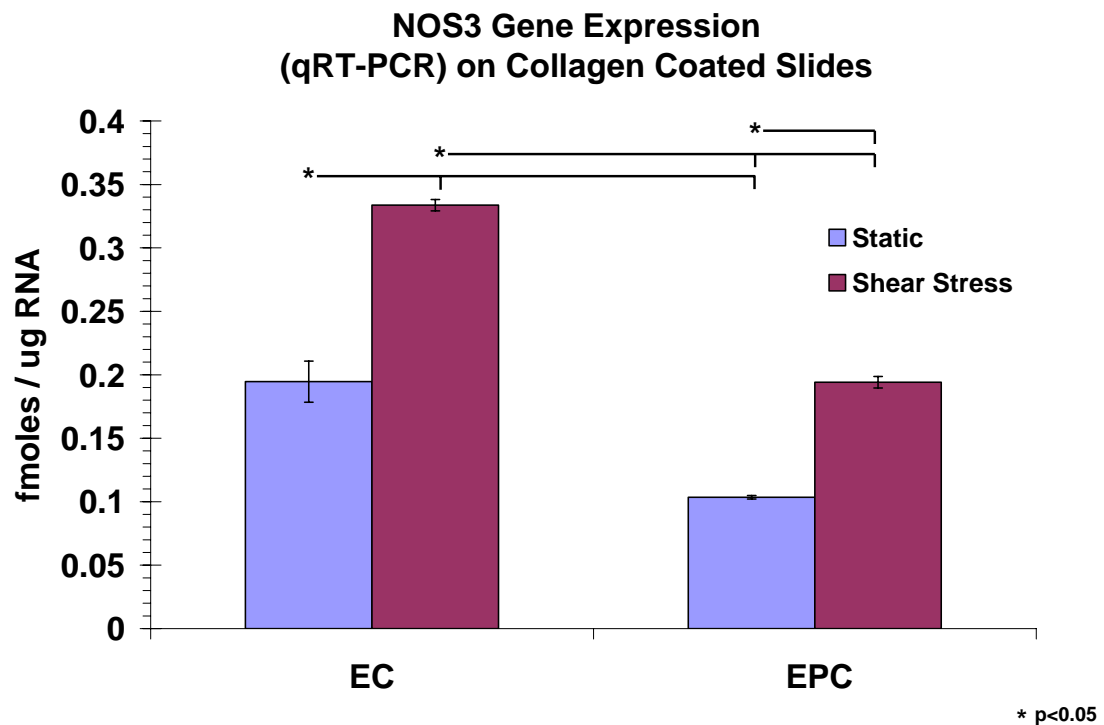
Figure 7.7: Nitric Oxide Synthase 3 (NOS3) gene expression in EC and EPC determined by real-time RT-PCR. mRNA expression was quantified in cells exposed to steady laminar shear stress (15 dynes/cm^2, 24 hours) and compared to static controls (mean ± SEM, n=9). ANOVA showed differences in groups (p<0.0001). Pairwise comparisons: *(p<0.05).
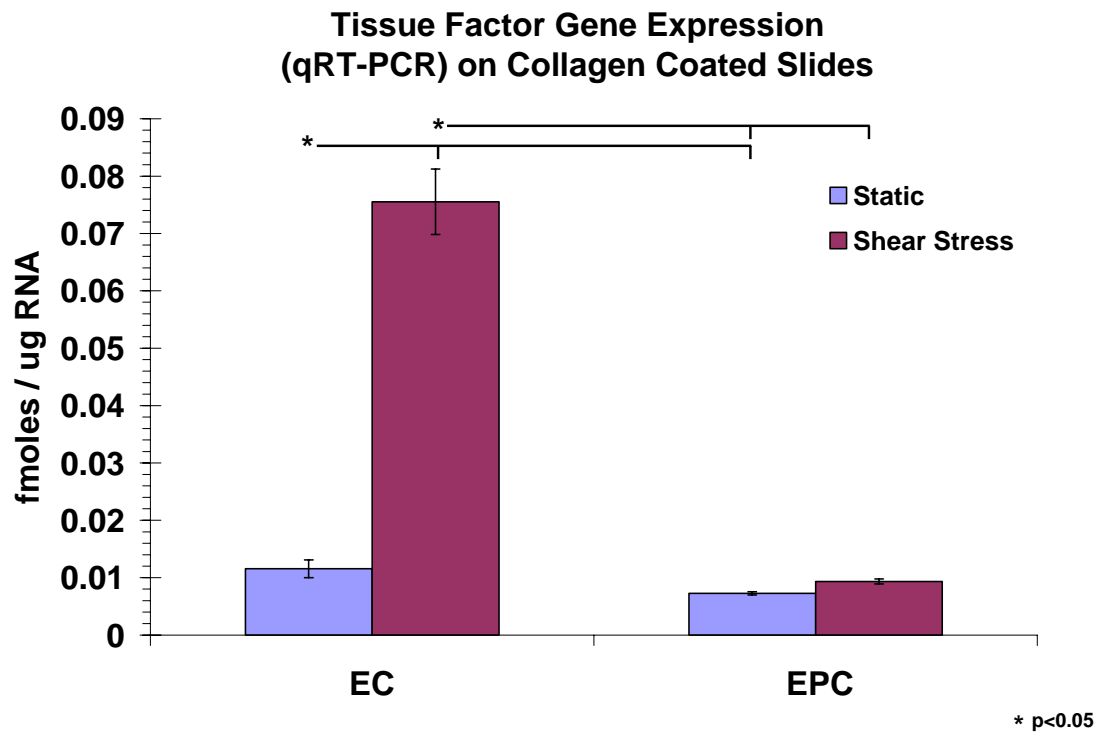
Figure 7.8: Tissue factor (F3) gene expression in EC and EPC determined by real-time RT-PCR. mRNA expression was quantified in cells exposed to steady laminar shear stress (15 dynes/cm^2, 24 hours) and compared to static controls (mean ± SEM, n=9). ANOVA showed differences in groups (p<0.0001). Pairwise comparisons: *(p<0.05).

von Willebrand Factor Gene Expression (qRT-PCR) on Collagen Coated Slides

* p<0.05
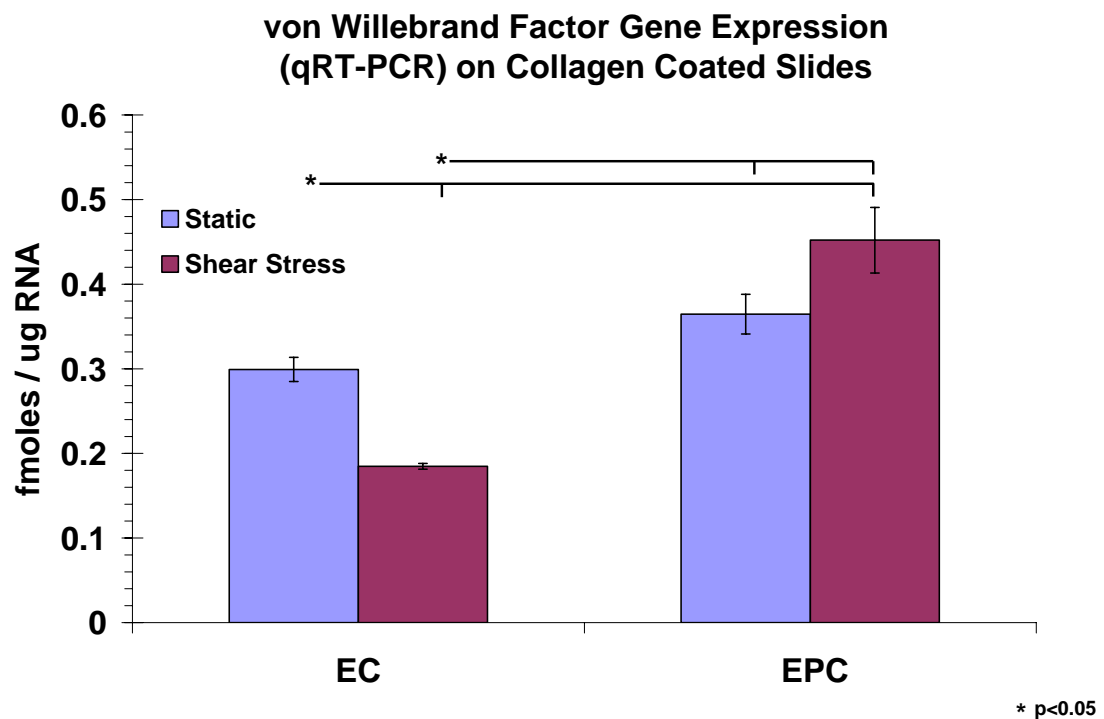
Figure 7.9: Von Willebrand factor (VWF) gene expression in EC and EPC determined by real-time RT-PCR. mRNA expression was quantified in cells exposed to steady laminar shear stress (15 dynes/cm^2, 24 hours) and compared to static controls (mean ± SEM, n=9). ANOVA showed differences in groups (p<0.0001). Pairwise comparisons: *(p<0.05).

Protein Expression

Using flow cytometry, levels of cellular protein expression were investigated in ECs and EPCs under static and shear stress conditions. Antibodies specific to THBD and F3 were used to independently label the protein expressed on the cell surface followed by quantification relative to fluorescent standards.

Thrombomodulin (THBD)

Figure 7.10 shows the cell surface protein expression of THBD for both ECs and EPCs under static and shear conditions. There was not a significant difference in THBD protein expression between ECs and EPCs in static conditions ($p > 0.05$). This basal level of expression was unchanged in ECs exposed to shear ($p > 0.05$) but in EPCs, shear caused a significant 3.9 fold increase in THBD protein ($p < 0.05$).

Tissue Factor (F3 or TF)

At the protein level, Figure 7.11 shows flow cytometry results for F3 expression. The opposite trend was seen in F3 protein expression compared to THBD protein. Similarly under static conditions, there was not a significant difference in ECs and EPCs basal F3 protein expression ($p > 0.05$). Following shear stress exposure, EPC F3 protein remained unchanged from static conditions ($p < 0.05$) while EC F3 protein levels increased more than double the static level ($p < 0.05$).
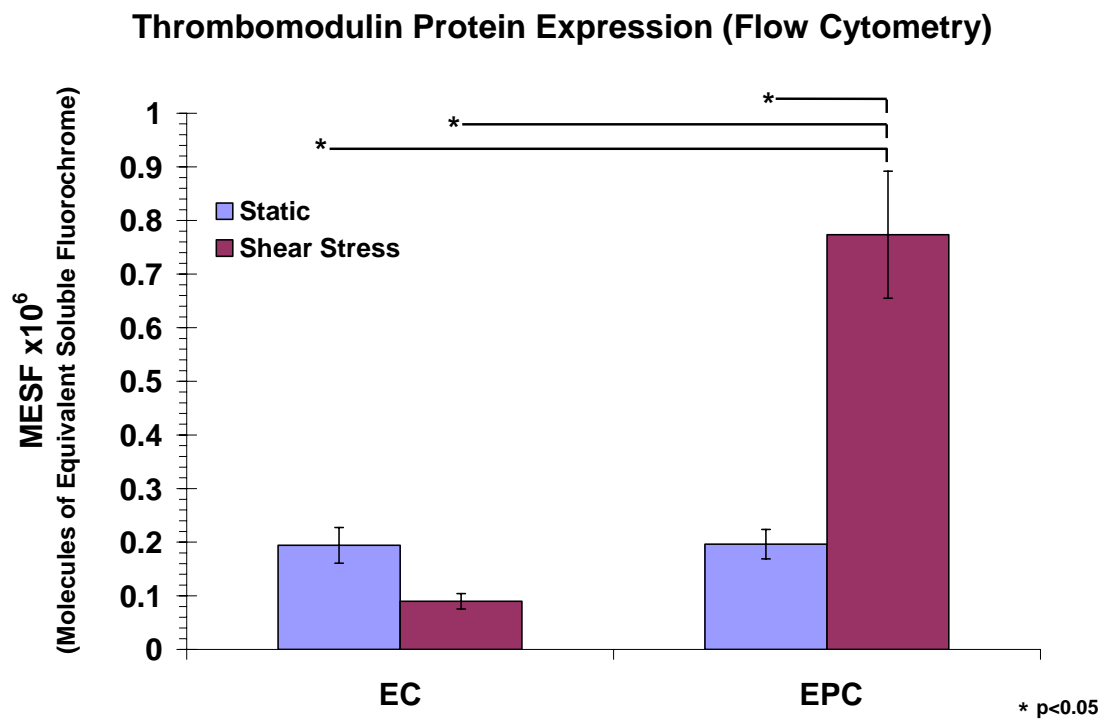
Figure 7.10: Thrombomodulin (THBD) protein expression in EC and EPC determined by flow cytometry. Cell surface protein expression was quantified in cells exposed to steady laminar shear stress (15 dynes/cm^2, 24 hours) and compared to static controls (mean ± SEM, n≥9). ANOVA showed differences in groups (p<0.0001). Pairwise comparisons: *(p<0.05).

Tissue Factor Protein Expression (Flow Cytometry)
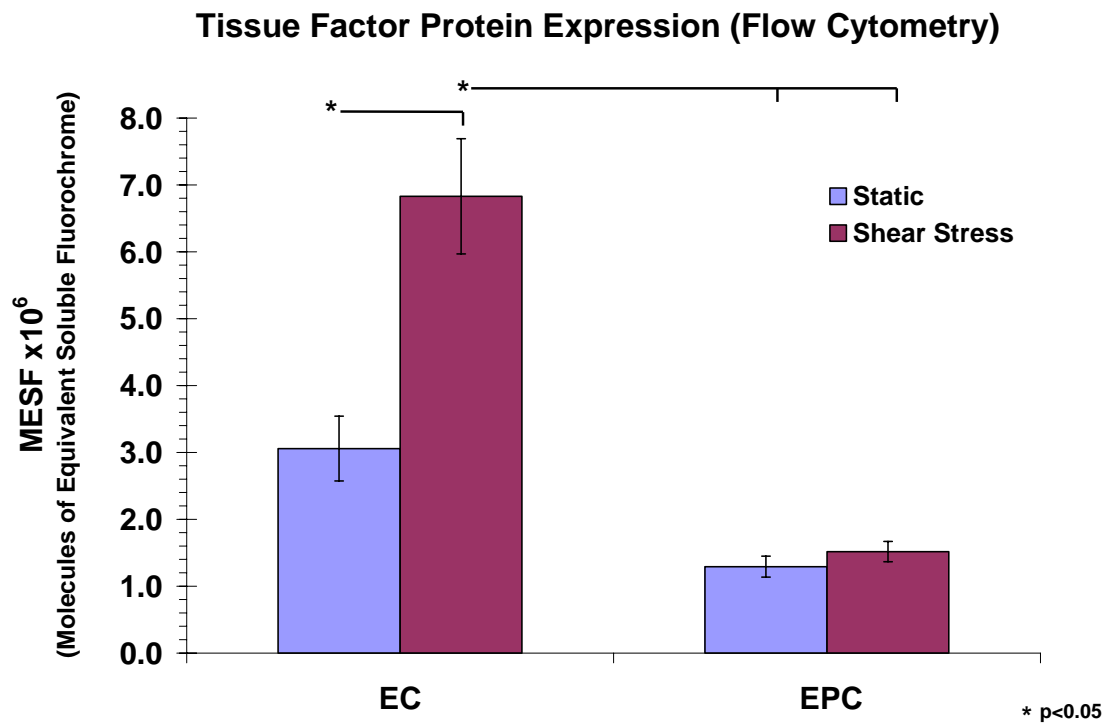
Figure 7.11: Tissue Factor (F3) protein expression in EC and EPC determined by flow cytometry. Cell surface protein expression was quantified in cells exposed to steady laminar shear stress (15 dynes/cm^2, 24 hours) and compared to static controls (mean ± SEM, n≥9). ANOVA showed differences in groups (p<0.0001). Pairwise comparisons: *(p<0.05).

Coculture on an Engineered Tissue

Cell Morphology

Studies were performed to investigate EC and EPC gene expression when cultured on the surface of an engineered tissue hydrogel composed of type I collagen embedded with SMCs. Tubular engineered vascular tissue constructs were cut longitudinally and embedded in agar exposing the luminal surface as described in Chapter IV: Methods and Materials. Following the same procedures used for the absorbed collagen substrate, ECs and EPCs were seeded onto the engineered tissue, allowed to adhere for 48 hours and then exposed to either shear or static conditions for an additional 24 hours. A modification of the parallel plate flow chamber was used to expose cells on the coculture model to a steady laminar shear stress of 15 dynes/cm^2.

To visualize cell attachment ECs and EPCs were labeled with a fluorescent cell tracker (Orange CMTMR, Molecular Probes) and then seeded onto the construct surface. Figure 7.12 shows the morphology of ECs and EPCs using confocal microscopy following 48 hours of static culture. Both cell types formed a confluent monolayer on the construct surface and a more elongated morphology than was seen on the absorbed collagen slides where the morphology was a more defined cobblestone appearance (Figure 7.1 and Figure 7.2). The cell morphology appeared to be influenced by the topography of the random collagen fiber network in the underlying engineered tissue. Following the initial 48 hours of static culture, EC and EPCs on the engineered tissue were exposed to steady laminar shear stress and compared to static controls. Figure 7.13 shows representative images of the EC and EPC morphology with or without shear
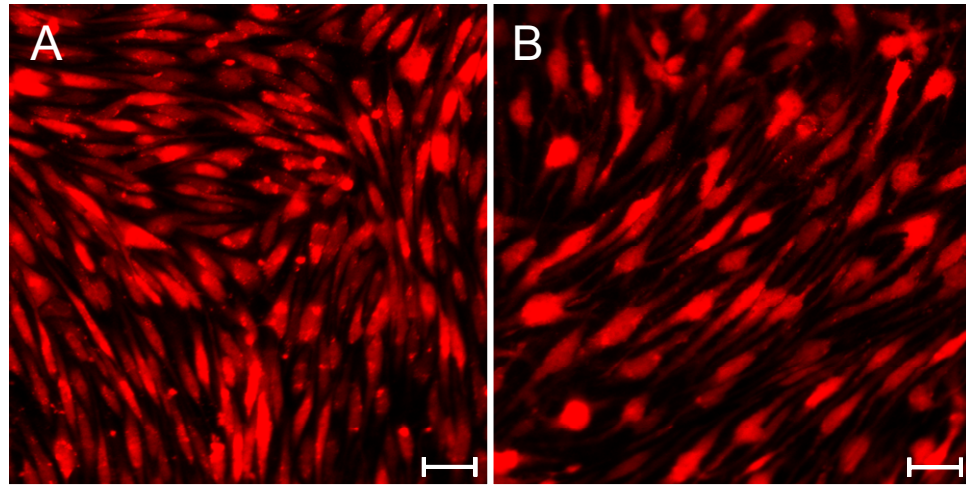
Figure 7.12: Confocal microscopy of fluorescently labeled EC and EPC on a 3-D engineered vascular tissue. Cells were labeled with a fluorescent cell tracker (Orange CMTMR, Molecular Probes) and seeded onto the engineered tissue. (A) Baboon carotid artery endothelial cells (ECs) and (B) baboon peripheral blood derived endothelial progenitor cells (EPCs) after 48 hours of static culture. Scale bar = 50μm.
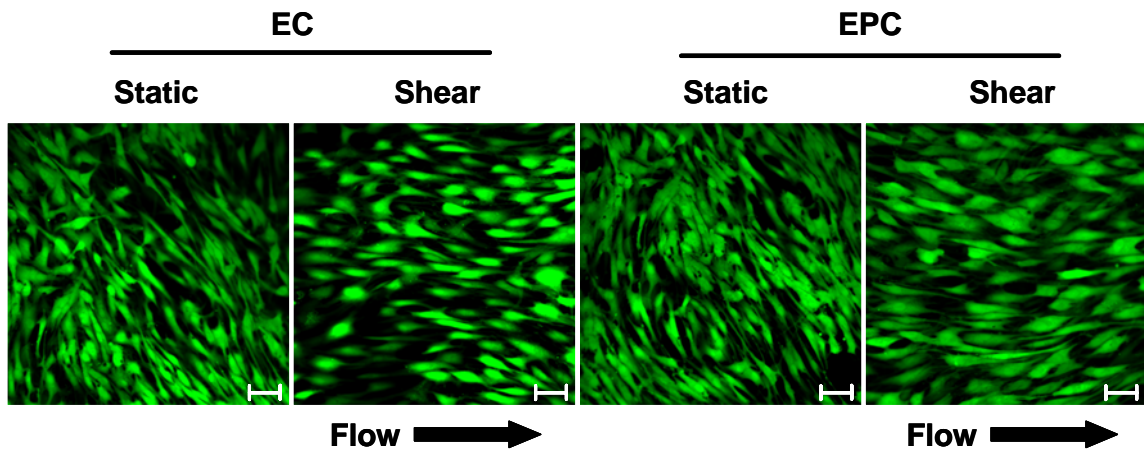
Figure 7.13: Visualization of cell morphology on a 3-D engineered vascular tissue using confocal microscopy. Calcein AM was used to visualize viable ECs and EPCs on the engineered tissue in static conditions and following exposure to steady laminar shear stress (15 dynes/cm^2, 24 hours). Scale bar = 50μm.

exposure. Calcein AM was used to label viable ECs and EPCs on the construct surface and clearly showed a confluent lining with and without shear exposure. Morphological alterations were evident in samples exposed to fluid shear stress. Both cell types responded to fluid flow by aligning parallel to the direction of flow and elongating after 24 hours of *in vitro* stimulation.

Cell Separation

In order to investigate the EC or EPC specific mRNA expression, a sorting strategy was developed to remove the cells from the engineered tissue surface followed by positive selection for ECs and EPCs to ensure removal of possible SMC contamination. CD31 or platelet/endothelial cell adhesion molecule (PECAM1) was investigated as a candidate selection molecule based on cell surface expression. The flow cytometry histograms of CD31 expression in ECs, EPCs and SMCs are shown in Figure 7.14. ECs and EPCs showed strong expression of CD31 while SMCs were negative for CD31 expression.

Indirect magnetic cell labeling was used to sort for EC and EPC specific populations based on CD31 expression as shown schematically in Figure 7.15. Validation of this technique to yield EC and EPC populations free of SMCs was performed using an additional labeling procedure. In independent experiments, ECs and EPCs were labeled with a cytoplasmic cell tracker molecule (Orange CMTMR, Molecular Probes), seeded onto engineered tissues and following 72 hours were removed using the CD31 indirect magnetic labeling procedure. Flow cytometry analysis was performed on both the negative and positive effluents. Figure 7.16 shows the flow cytometry results for fluorescence detected in the range of 565nm (the emission
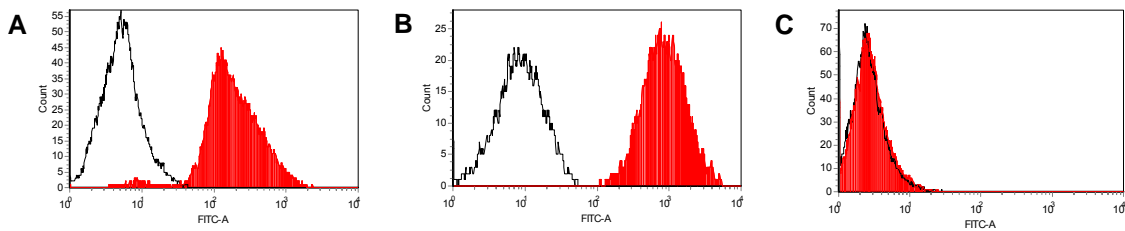
Figure 7.14: Flow cytometry analysis of CD31 (PECAM-1) expression in ECs, EPCs and SMCs. Cells were labeled with FITC conjugated anti-CD31 antibody (BD Pharmingen, clone WM59) and analyzed using flow cytometry. Black outline is cell only negative control. Red filled histogram is cells plus antibody. (A) ECs, (B) EPCs and (C) SMCs. At least 10,000 events were recorded.
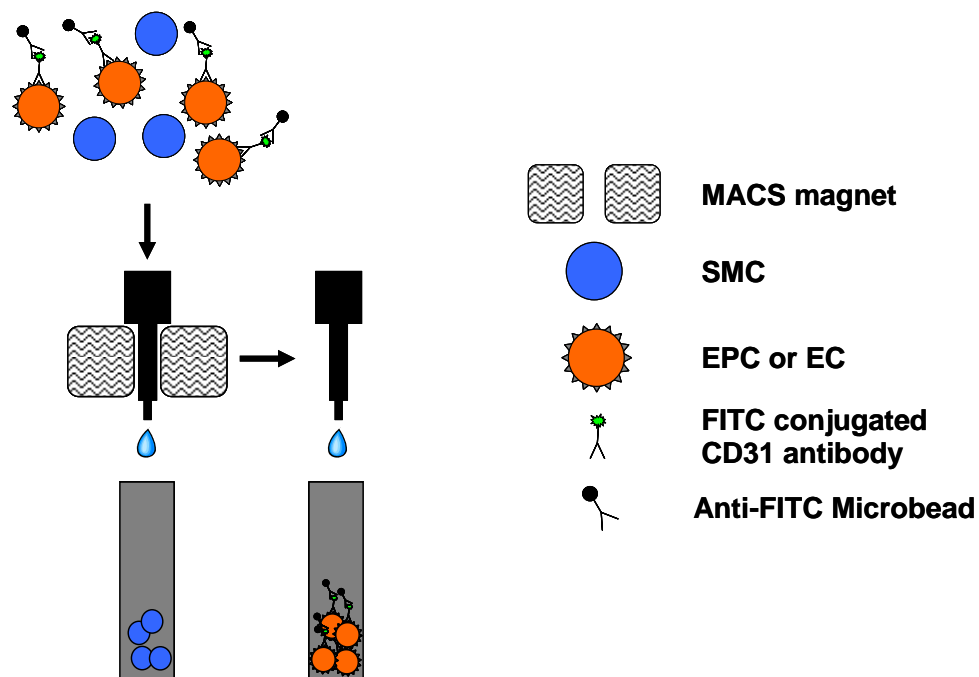
Figure 7.15: EC and EPC positive selection using the MACS® cell separation system. ECs and EPCs were separated from cell suspensions using a positive selection for CD31 (FITC) followed by indirect magnetic cell labeling with anti-FITC microbeads. CD31 positive cells were retained in the MACS® column and unlabeled cells pass through (negative effluent). The column was removed from the magnet separator and the retained cells were eluted as the positively selected cell fraction (positive effluent).

141
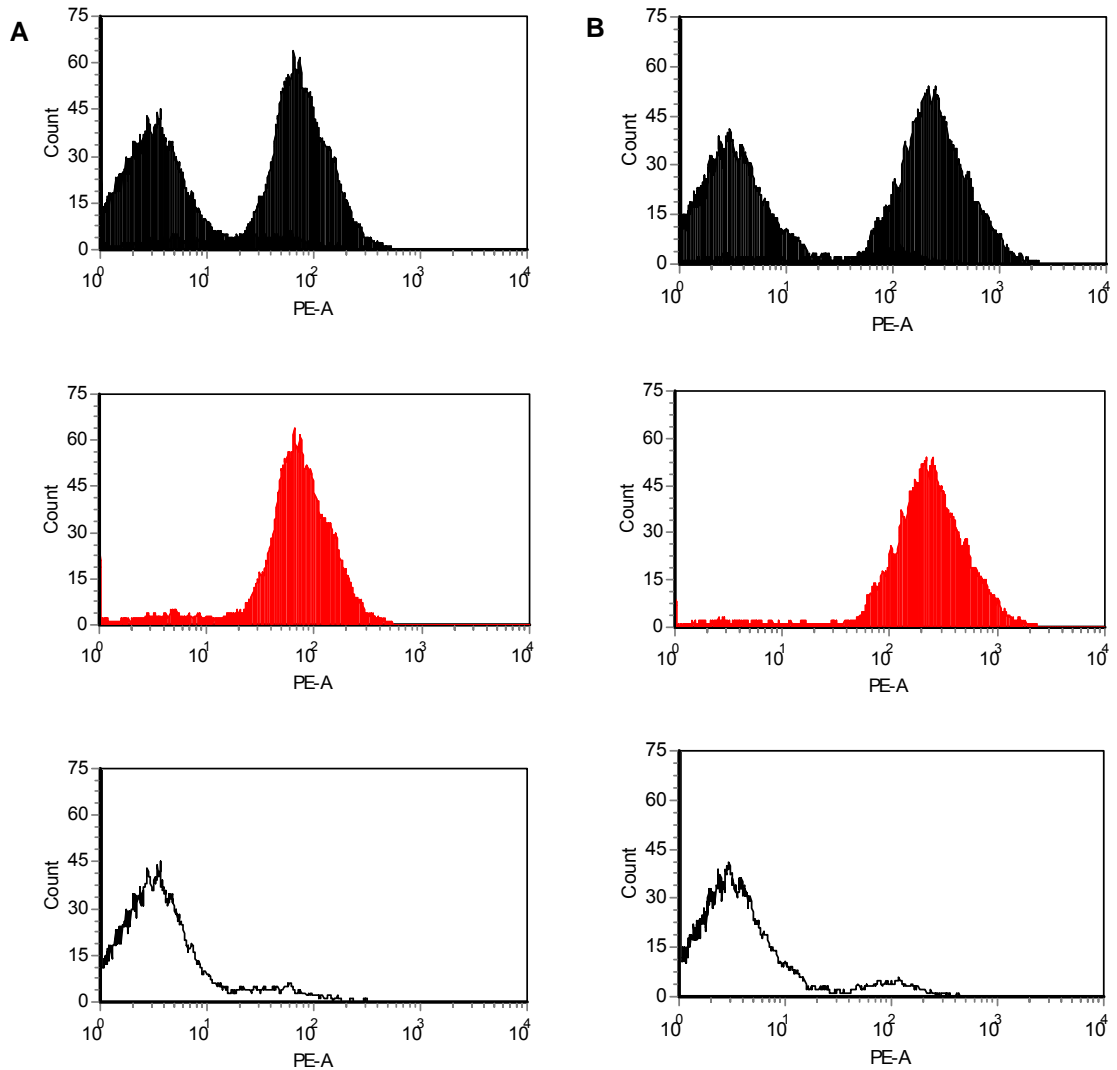
Figure 7.16: Validation of EC and EPC positive selection using flow cytometry.
ECs or EPCs were labeled with a fluorescent cell tracker (Orange CMTMR, Molecular
Probes) prior to seeding onto the engineered tissue. At the completion of the
experiment, cells were then removed from the construct surface using a collagenase
treatment. ECs and EPCs were separated from contaminating SMCs using a positive
selection for CD31. The flow cytometry histograms are shown for the positive and
negative effluent from MACS separation for both (A) ECs and (B) EPCs. The x-axis
(labeled PE) is the fluorescence detection covering 565nm, the emission of cell tracker
orange CMTMR. The top panel is the combined negative and positive effluents. The
middle panel (red filled histogram) is the positive effluent (CD31 positive fraction).
The bottom panel shows the negative effluent (CD31 negative fraction) as a black
outlined histogram.

wavelength of the cell tracker orange) for both ECs and EPCs. The top panel of Figure

7.16A and B shows the mixed population of cell tracker positive and negative cells which

corresponded to labeled ECs or EPCs and unlabeled SMCs. In the middle panel, the red

solid histogram is the fluorescence of the positive effluent (CD31 positive fraction) from

the magnetic sorting procedure which demonstrates that the positive effluent contained a

uniform population of ECs (Figure 7.16A) and EPCs (Figure 7.16B) without SMC

contamination. In the lower panel, the black line, which is the fluorescence of the

negative effluent collected from the MACS column (CD31 negative fraction), shows a

uniform population of SMCs which were not labeled with the cell tracker dye.

Quantification of Gene Expression

mRNA for ECs and EPCs was obtained from the positive effluent of the magnetic

separation procedure. This study focused on three genes having both anti and

procoagulant function. The expression of thrombomodulin (THBD), NOS3 and tissue

factor (F3) was investigated in both cell types on the engineered tissue in static and shear

environments.

Thrombomodulin (THBD)

ECs and EPCs had comparable expression of THBD on the coculture model under

static conditions as shown in Figure 7.17 Following exposure to shear stress, there was a

significant reduction in THBD expression in both cell types ($p<0.05$), with EPCs

showing less THBD expression than ECs on the engineered tissue ($p<0.05$).

Nitric Oxide Synthase 3 (NOS3)

In contrast to the down regulation of THBD, shear stress exposure resulted in an upregulation of NOS3 in both cell types (shown in Figure 7.18). In static conditions, ECs demonstrated significantly more NOS3 mRNA than EPCs on the engineered construct ($p<0.05$). When exposed to shear stress, there was a significant upregulation of NOS3 in ECs and EPCs ($p<0.05$), but EPCs on the engineered tissue still showed significantly less NOS3 expression than the ECs ($p<0.05$).

Tissue Factor (F3 or TF)

The procoagulant molecule F3 was investigated in ECs and EPCs on the engineered tissue. Quantification of mRNA expression is shown in Figure 7.19. In the static environment, ECs had significantly more F3 expression than EPCs ($p<0.05$). When the cells were exposed to shear stress, F3 mRNA expression was enhanced. ECs and EPCs both showed increases in F3 mRNA with shear ($p<0.05$) but ECs still showed significantly more F3 expression than the EPCs ($p<0.05$).
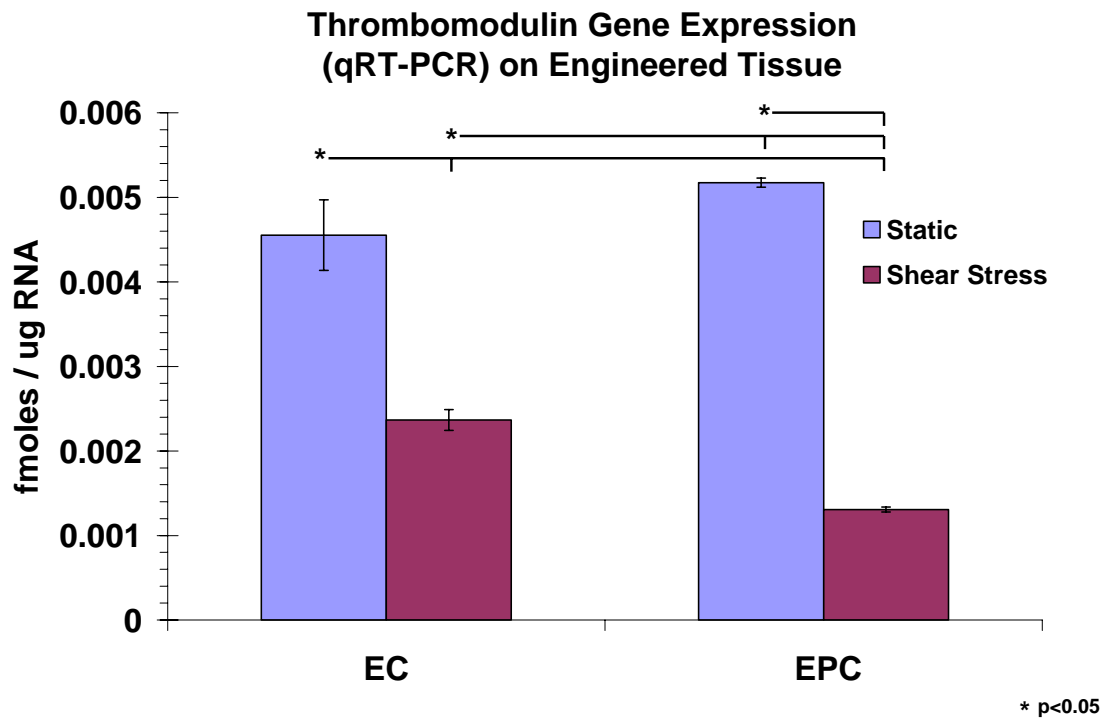
Figure 7.17: Thrombomodulin (THBD) gene expression in EC and EPC on a 3-D engineered vascular tissue determined by real-time RT-PCR. mRNA expression was quantified in cells exposed to steady laminar shear stress (15 dynes/cm^2, 24 hours) and compared to static controls (mean ± SEM, n=3). ANOVA showed differences in groups (p<0.0001). Pairwise comparisons: *(p<0.05).

NOS3 Gene Expression (qRT-PCR) on Engineered Tissue
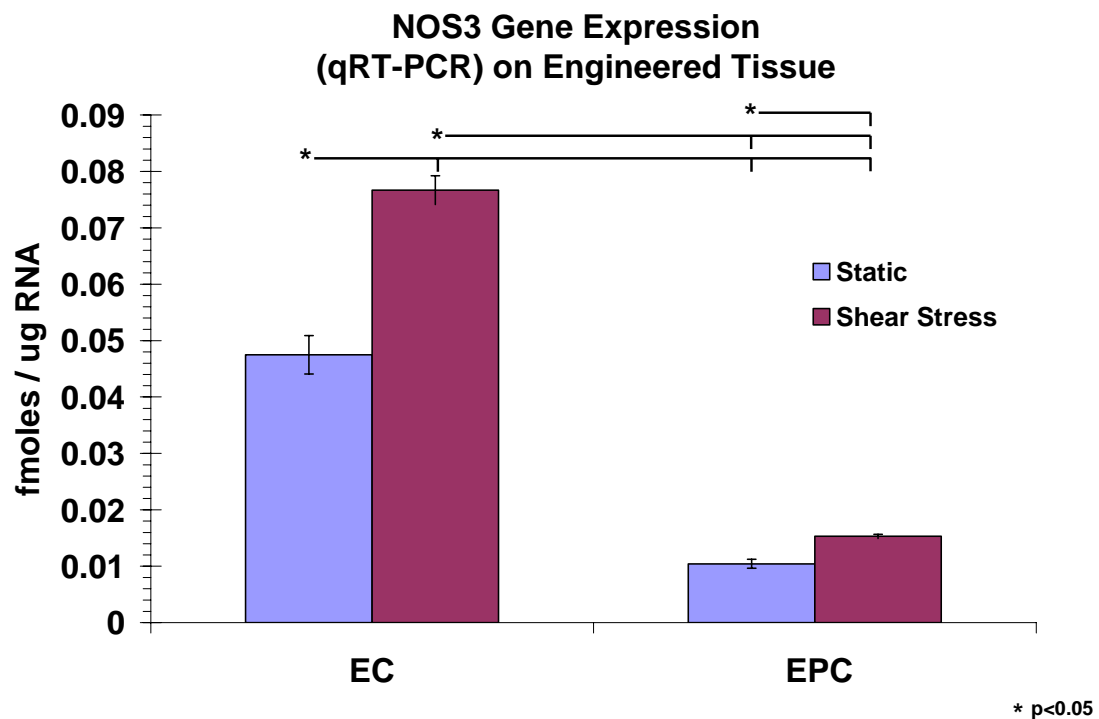
Figure 7.18: Nitric Oxide Synthase 3 (NOS3) gene expression in EC and EPC on a 3-D engineered vascular tissue determined by real-time RT-PCR. mRNA expression was quantified in cells exposed to steady laminar shear stress (15 dynes/cm^2, 24 hours) and compared to static controls (mean $\pm$ SEM, n=3). ANOVA showed differences in groups (p<0.0001). Pairwise comparisons: *(p<0.05).
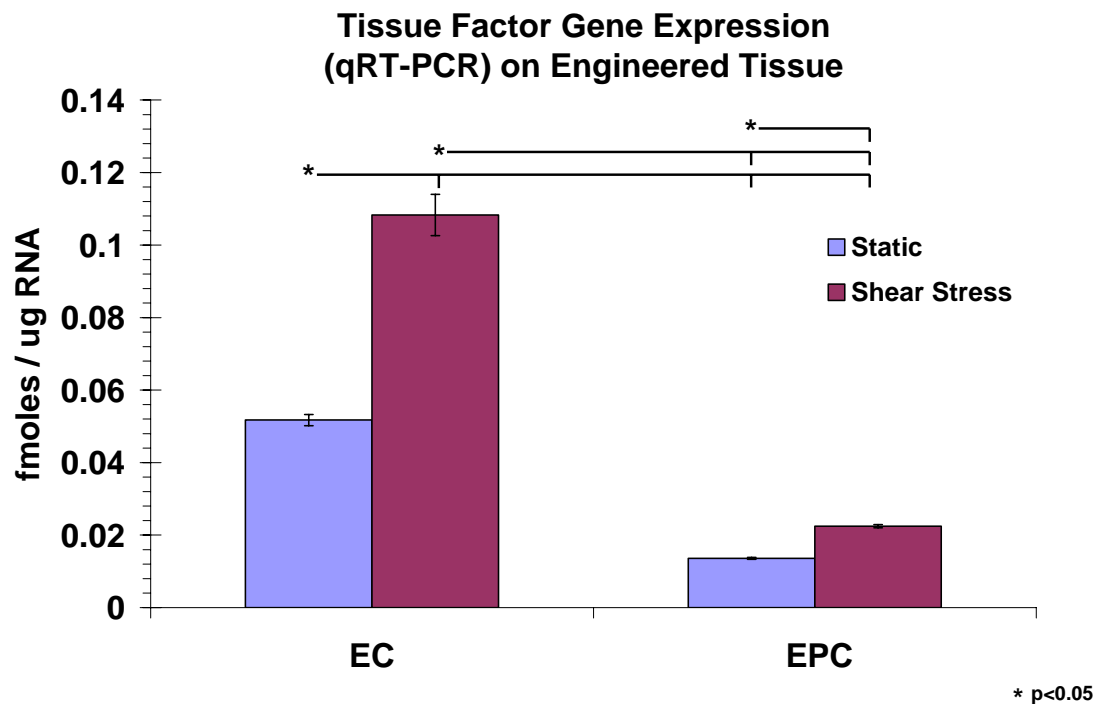
Figure 7.19: Tissue Factor (F3) gene expression in EC and EPC on a 3-D engineered vascular tissue determined by real-time RT-PCR. mRNA expression was quantified in cells exposed to steady laminar shear stress (15 dynes/cm^2, 24 hours) and compared to static controls (mean ± SEM, n=3). ANOVA showed differences in groups (p<0.0001). Pairwise comparisons: *(p<0.05).

Discussion

Limitations of the Experimental Approach

This study has several limitations. Due to the *in vitro* nature of this study, ECs and EPCs were removed from their normal extracellular environment for investigation and subsequently expanded through routine cell culture techniques. These studies were performed with ECs and EPCs between passages 5-7. There were no observed differences in growth or morphology of either cell type in this passage range. While *in vitro* culture could affect cellular response, samples were kept in identical culture conditions to isolate the effect of shear stress and substrate on cellular response.

This study used a parallel plate flow chamber to expose cells to a steady laminar shear stress as previously described [34]. The parallel plate flow chamber was designed using channel flow geometry where the channel is a rectangular crosssection whose height (h) is much less than either its length (L) or its width (b). In these studies the flow channel dimensions were L=6.20cm, b=2.54cm and h=0.05cm. Based on an estimated entrance length of 0.11cm, a fully developed velocity profile was expected over 98% of the chamber length. A shear stress of 15 dynes/cm^2 was achieved at a flow rate of 1.3cm^3/s using a working fluid (culture medium) with a viscosity of 0.012 dyne s/cm^2. The resulting Reynolds number was 44, the shear rate was 1250s^{-1} and the pressure drop was 368 Pa. While this methodology did not exactly duplicate the *in vivo* environment, it did allow for precise control of the shear environment on a confluent monolayer of cells. Incorporation of an engineered tissue into the parallel plate flow chamber was performed

148

as previously described.[216, 230]. Care was taken to ensure that the luminal surface, on which the ECs and EPCs resided, was as flat as possible.

This study focused on a number of genes and proteins related to coagulation. The regulation of hemostasis and thrombosis and the involvement of the endothelium is complex and requires regulation of a number of molecules not included in these investigations. This study has attempted to investigate an important subset of the known essential factors.

The Role of Shear Stress and Substrate in EPC Phenotype

EPC response to fluid shear stress was evaluated on two substrates; absorbed collagen slides and on an engineered vascular tissue. The engineered tissue mimicked the medial layer of the native blood vessel with baboon carotid artery SMCs embedded within an extracellular matrix of type I collagen fibrils. On both substrates, peripheral blood derived EPCs were compared to mature vascular ECs derived from the vascular wall of the carotid artery. A significant amount of research has shown that fluid shear stress is an important determinant of vascular EC phenotype and more recently, studies have also suggested that neighboring SMCs and the extracellular matrix also play an important role. Our current research demonstrates that not only are EPCs responsive to the mechanical environment but that the response is dependent on the specific substrate.

EPCs responded to shear stress by elongating and orienting parallel to the direction of flow when exposed to 15 dynes/cm^2 steady laminar shear stress for up to 48 hours. This finding was consistent whether EPCs were seeded onto a simplified absorbed collagen slide or on a more complex engineered tissue coculture model. Quantification of cytoskeletal reorganization on absorbed collagen showed that EPCs demonstrate a

time dependant cytoskeletal reorganization and alignment which mimicked the response of baboon carotid artery ECs in the same system. Following 24 and 48 hours of shear stress, the angle of orientation demonstrated increasing alignment of the cells parallel to the direction of flow and was not significantly different between EPCs and ECs. This data was consistent with previous reports using bovine aortic ECs and human umbilical vein ECs on simplified two-dimensional substrates [31, 32, 34, 231]. as well as with reports of porcine aortic ECs and human aortic ECs on a three-dimensional hydrogel coculture model [216, 230] in response to steady laminar shear stress

Hemodynamic forces have been shown to regulate many of the coagulation controlling properties of endothelial cells. Prostacyclin was the first inhibitor of platelet aggregation shown to be released from endothelial cells on exposure to shear stress [43, 44]. Since then, numerous investigators have demonstrated that shear stress is one of the most powerful stimuli for release of nitric oxide, which also possesses strong anti-platelet aggregation properties [45-47]. In addition, enhanced expression of tissue plasminogen activator (TPA) [48, 49] and tissue factor pathway inhibitor (TFPI) [50] result from shear stress exposure. There have been conflicting reports about thrombomodulin expression in cultured cells. Malek et al. [51] reported that steady shear stress (15 dynes/cm^2) results in a time–dependent decrease in THBD mRNA in bovine aortic endothelial cells measured by northern blot analysis of total RNA. In contrast, Takada et al. [52] demonstrated that cultured human umbilical vein endothelial cells (HUVEC) respond to shear stress (15 dynes/cm^2) with a time-dependent increase in THBD using RT-PCR, flow cytometry, and ELISA methods. The reason for this disparity in species response is

unclear but these studies provided evidence that mechanical hemodynamic forces such as shear stress are associated with alterations in thrombomodulin expression.

The interaction between thrombomodulin and shear stress has been demonstrated to have clinical relevance. Clinically, early vein graft occlusion by thrombosis occurs more often than in arterial grafts [53]. This has been partly attributed to the loss of endothelial thromboresistance and reductions in thrombomodulin expression once vein grafts have been placed in the arterial circulation [54]. Although inflammatory processes are clearly active in this setting, several groups have established links between thrombomodulin expression and the local mechanical environment including shear stress and pressure associated changes in vessel wall tension. Using a rabbit model to perform interpositional grafting of jugular vein segments into the carotid circulation, Sperry et al [55] demonstrated that decreases in THBD mRNA and protein correlated with increases in wall tension and were independent of shear stress changes up to 8.2 dynes/cm^2. Again, conflicting data exists using human saphenous veins in an *ex vivo* flow circuit. Consistent with Sperry's results, Gosling et al.[56] saw decreases in thrombomodulin immunostaining after saphenous veins were exposure to arterial flow (4 dynes/cm^2), but by limiting circumferential distension in their model system, the authors attributed the THBD decrease to shear stress rather than circumferential deformation.

In our own study with primary cultured baboon carotid artery ECs cultured on absorbed collagen, there was not a significant alteration in THBD mRNA or protein with exposure to 15 dynes/cm^2 steady laminar shear stress for 24 hours (see summary Table 7.2). Yet, in sharp contrast to ECs, EPCs increased THBD mRNA levels 3.3 fold and protein levels 3.9 fold in response to flow. The cell's response to flow changed when

cultured on an engineered tissue. In the coculture model, ECs showed a two fold

reduction in THBD mRNA and EPCs responded with over a three fold decrease in

THBD. These results mimic the findings of both Sperry et al. [55] and Gosling et al. [56]

who used *in vivo* and *ex vivo* experimental methodologies, respectively.

The impact of substrate on EC and EPC expression of THBD is summarized in

Figure 7.20A. Each cell's mRNA expression on the engineered tissue was divided by the

mRNA expression on the absorbed collagen slide and reported as a fold change. Ratios

less than one are reported as negative fold change (in the form of -1/(ratio less than one)).

In static conditions, there was very little effect of coculture on the THBD expression in

ECs and EPCs but shear stress caused a reduction in THBD expression which was more

pronounced in EPCs. When focused on THBD expression, EPCs are clearly responding

differently than ECs to local changes in fluid shear stress and that response is heavily

dependent on the substrate (absorbed collagen versus engineered tissue).

Shear stress is only one factor that has previously been reported to alter

thrombomodulin expression. THBD has been shown to increase in response to

stimulants such as tumor-promoting phorbol esters [232], histamine [233], retinoic acid

and other agents that increase intracellular cyclic adenosine monophosphate (cAMP)

[234, 235] but decrease in the presences of endotoxin and cytokines such as TNFα or

IL1-β [236-238]. Heterogeneous levels of thrombomodulin expression can also be found

in different vascular beds possibly playing a role in vascular bed-specific prothrombotic

potential [239]. THBD is not only constituently expressed in vascular endothelium, but it

Table 7.2: RT-PCR and flow cytometry data summary. Four comparisons were made with the RT-PCR (mRNA) and flow cytometry (protein) data investigating the effect of shear on each cell type (EC and EPC) and investigating the differences between cell types for a given condition (static or shear) on both the absorbed collagen and engineered tissue substrate. The data are presented as ratios for the comparisons that were statistically significant ($p<0.05$). Dashed lines indicate comparisons which did not meet significance criteria ($p>0.05$). Grey boxes indicate experiments were not performed for that specific comparison.

| | | EC: Shear vs. Static | | | EPC: Shear vs. Static | | | Static: EPC vs. EC | | | Shear: EPC vs. EC | | |
| | | Absorbed Collagen | | Engineered Tissue | Absorbed Collagen | | Engineered Tissue | Absorbed Collagen | | Engineered Tissue | Absorbed Collagen | | Engineered Tissue |
		mRNA	Protein	mRNA	mRNA	Protein	mRNA	mRNA	Protein	mRNA	mRNA	Protein	mRNA
Anti-Coagulant Function	THBD	—	—	0.5	3.3	3.9	0.3	—	—	—	2.6	8.6	0.6
	TFPI	1.3			1.5			0.4			0.5		
	NOS3	1.7		1.6	1.9		1.5	0.5		0.2	0.6		0.2
Pro-Coagulant Function	F3	6.5	2.2	2.1	—	—	1.7	0.6	—	0.3	0.1	0.2	0.2
	VWF	0.6			—			—			2.4		

A Thrombomodulin Gene Expression (qRT-PCR)
Engineered Tissue Compared to Slide

B NOS3 Gene Expression (qRT-PCR)
Engineered Tissue Compared to Slide

C Tissue Factor Gene Expression (qRT-PCR)
Engineered Tissue Compared to Slide
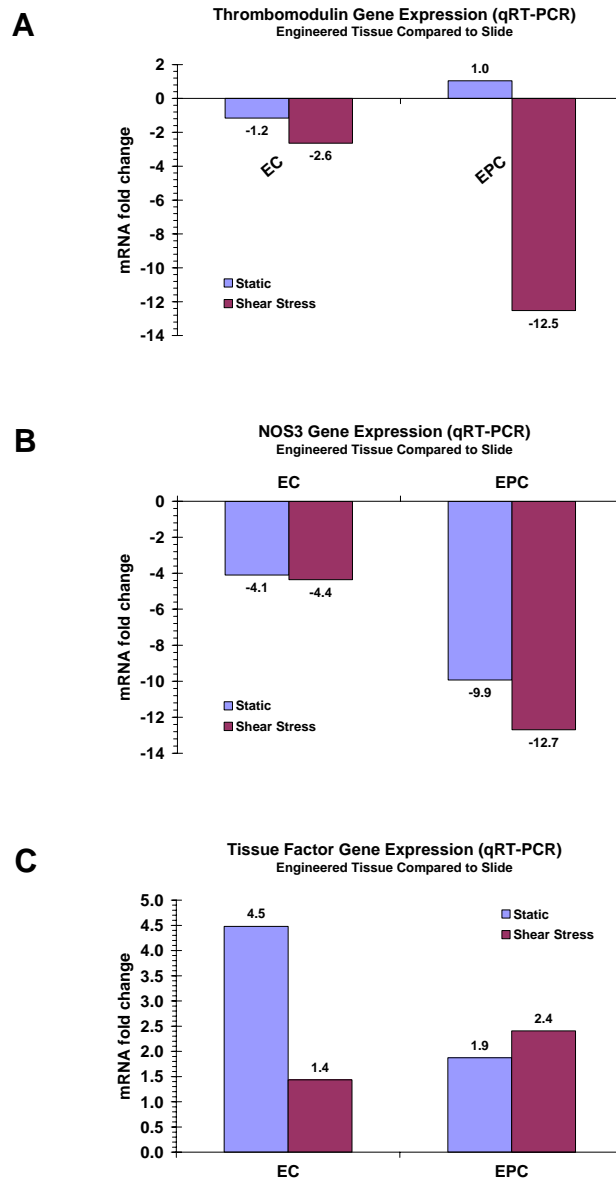
Figure 7.20: The effect of a substrate on gene expression in EC and EPC. The mRNA expression on the engineered tissue was divided by the mRNA expression on the absorbed collagen slide and reported as a fold change. Ratios less than one are reported as negative fold change (-1/(ratio less than one)) for (A) thrombomodulin, (B) NOS3 and (C) tissue factor.

154

has also been detected in human platelets[240], smooth muscle cells [241] and monocytes (unstimulated monocytes surface THBD activity represents ~20% of early passage HUVECs) [242, 243]. It is clear that THBD is required for survival because its absence causes embryonic lethality in mice prior to embryonic day 9.5 [244]. While the anti-coagulant function of thrombomodulin has been established, studies of murine development have suggested that THBD may also exert different or related functions in locations other than the vascular endothelium [245].

The biology of EPCs including their origin, differentiation, and functions are currently an active area of world-wide research. Static cultures of EPCs have been shown to express THBD [246], consistent with their "endothelial-like" phenotype but to our knowledge this is the first demonstration that THBD expression in EPCs is modulated by fluid shear stress -- a finding which may have important implications for applications where EPCs line a blood contacting surface.

TFPI, another molecule with known anticoagulant function, was significantly up-regulated by chronic shear exposure (15 dynes/cm^2, 24 hours) in both ECs and EPCs on both absorbed collagen (see Table 7.2). These results with ECs are consistent with previous reports that shear stress induces upregulation of synthesis and release of TFPI resulting in enhanced anti-coagulant activity [50, 60, 247]. Previously unreported, this study showed that EPCs express TFPI in static culture with elevated expression following exposure to shear stress.

NOS3, a multifunctional mediator of anticoagulant function was similarly upregulated by fluid shear stress in ECs and EPCs on both the absorbed collagen and engineered tissue substrate. Consistent with the results of this study, NOS3 expression in

EPCs under static culture conditions has been reported by a number of investigators [130, 133, 156, 158]. Functionally, evidence is emerging that NOS3 is not only important for EPC function but it is also critical for the initial mobilization of EPCs from the bone marrow into peripheral circulation [248, 249]. EPCs isolated from adult human peripheral blood have been shown to participate in neovascularization after ischemic insults, often referred to as postnatal vasculogenesis [92, 250, 251]. Recently, EPCs were shown to not only preserve the microcirculation in ischemic myocardium, by incorporation into the host vascular structures, but to also rapidly deliver cytokines to the injured tissue [252]. EPCs were shown to be active repositories of NOS activities (i.e. eNOS and iNOS) as well as vascular endothelial growth factor (VEGF). Flow dependent regulation of NOS3 in mature vascular endothelial cells is well established (reviewed in [253]), but shear induced upregulation of NOS3 in EPCs may have additional important biological implications even beyond its known importance in platelet interactions with the endothelium.

Comparing NOS3 expression on an engineered tissue to expression when cells were cultured on absorbed collagen showed dramatic decreases in NOS3 mRNA with coculture. Figure 7.20B summarizes the substrate influence on NOS3 expression in ECs and EPCs with and without shear stress exposure. When ECs were cultured on the engineered tissue, NOS3 mRNA was prominently decreased compared to culture on absorbed collagen. These results are consistent with several other studies using different types of *in vitro* EC/SMC coculture [211, 254, 255]. Interestingly, EPCs also responded to coculture with an obvious down regulation of NOS3 gene expression. While EPCs

overall showed less NOS3 expression than ECs, culture on the engineered tissue heighten that difference.

When cultured on absorbed collagen, shear stress did not significantly alter EPC expression of tissue factor or von Willebrand factor, the two prothrombotic factors investigated in this study. As summarized in Table 7.2, EPCs expressed VWF and F3 at levels comparable (F3 protein and vWF mRNA) or slightly lower (F3 mRNA) than ECs in static conditions. In contrast to the EPC response to shear on absorbed collagen, shear exposure did have a significant effect on F3 and VWF expression in ECs. Shear stress resulted in an increase in F3 mRNA in ECs (6.5-fold) with a corresponding increase in F3 protein (2.2-fold). Shear stress exposure resulted in a modest (1.6-fold) decrease in EC VWF mRNA. Shear stress plays many roles in modulating the pro-coagulant function of VWF from alterations in cellular expression and storage to structural modifications which occur once VWF is circulating in the plasma [256]. In this study, we investigated the effect of shear stress on mRNA expression. It may be difficult to draw direct conclusions about the pro-coagulant effect of VWF mRNA changes due to the large intracellular pools of VWF that exist in ECs. Shear stress has been reported to modulate local VWF concentrations by stimulating an enhanced release of VWF from Weibel-Palade bodies, the ECs' intraceulluar storage organelles, without significantly altering *de novo* synthesis [257]. Here we have reported the cell's first response to shear stress at the message level.

Several hemodynamic factors including shear stress [59, 247, 258-261], pressure [262], and cyclic strain [263] have been shown to alter F3 expression in vascular ECs. Normally, quiescent vascular endothelium does not favor coagulation and thrombosis resulting in undetectable levels of tissue factor *in vivo* [264-266]. However, cultured

human umbilical vein endothelial cells (HUVEC) produce low levels of F3 mRNA [267, 268] consistent with the findings of this study. Shear stress has been reported to cause induction of the tissue factor gene with transient increases in F3 transcripts and activity [261]. Based on studies with HUVEC exposed to shear for up to 15 hours, F3 expression continued to decrease with increasing exposure to constant shear stress [258]. Our study with baboon carotid artery ECs shows a significant increase in TF mRNA and protein following 24 hours of shear stress compared to static controls. Because we did not quantify F3 expression in ECs as a function of shear duration, it is difficult to predict how the response of the baboon arterial endothelial cells may change in response to either longer or shorter durations of shear stress.

F3 expression in EPCs was sensitive to changes in substrate. Not only did EPC F3 mRNA increase when cultured on the engineered tissue compared to absorbed collagen (Figure 7.20C), but in the coculture environment, fluid shear stress caused a 1.7 fold increase in F3 mRNA (Table 7.2). This sensitivity to substrate was also evident in the ECs. ECs also showed increases in F3 mRNA on the engineered tissue compared to absorbed collagen (Figure 7.20C) and that expression was increased further by exposure to fluid shear stress (Table 7.2). Several studies have previously reported that *in vitro* coculture of ECs with SMCs resulted in enhanced expression of F3 in both static [219, 269] and shear [254] environments, consistent with our own data.

Figure 7.21 summarizes a comparison of EPC to EC gene expression for the three molecules studies when ECs and EPCs were cultured on the engineered tissue substrate. In the method described for Figure 7.20, the ratio of mRNA expression is presented as a positive or negative fold change. The mRNA expression of EPCs was divided by the

mRNA expression of ECs for the given comparison (absorbed collagen slide or

engineered tissue, ± shear stress) and reported as a fold change. Ratios less than one

were reported as a negative fold change (in the form of -1/(ratio less than one)). As

shown in Figure 7.21, THBD was heterogeneously regulated in EPCs compared to ECs

as a function of shear and substrate. EPCs showed overall lower expression of both

NOS3 (Figure 7.21B) and F3 (Figure 7.21C) compared to ECs.
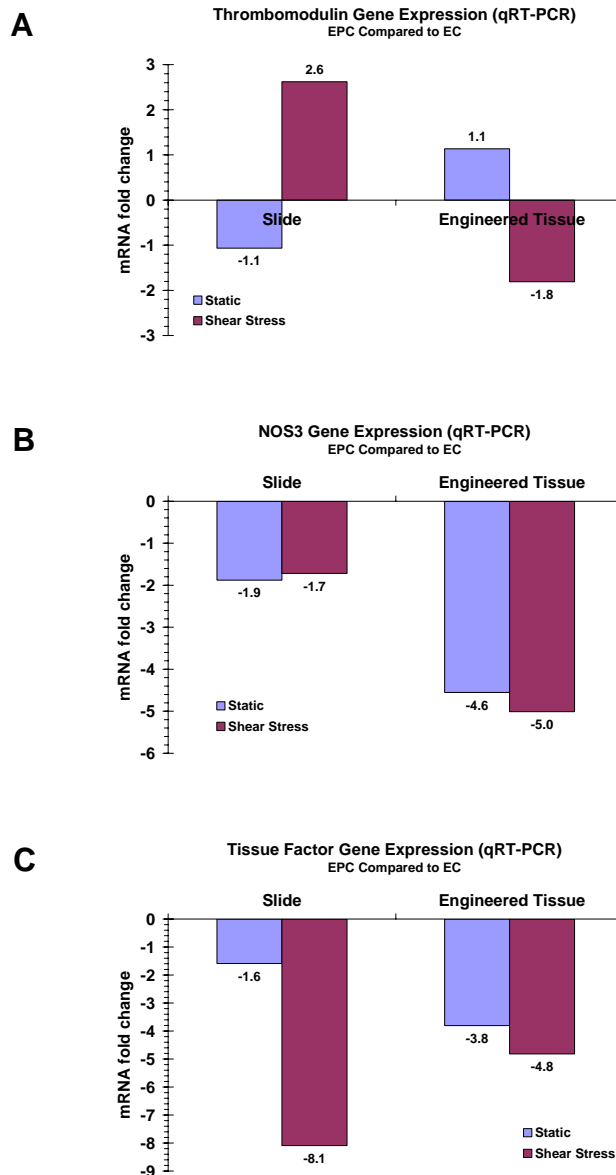
Figure 7.21: Gene expression in EPCs compared to ECs on a slide and on a 3-D engineered vascular tissue under static and fluid flow conditions. The mRNA expression of EPCs was divided by the mRNA expression of ECs and reported as a fold change. Ratios less than one are reported as negative fold change (-1/(ratio less than one)) for (A) thrombomodulin, (B) NOS3 and (C) tissue factor.

Conclusions

The results presented here demonstrate that EPCs derived from peripheral blood are responsive to the local shear stress environment. The mechanosensitive nature of EPCs results in morphological changes (cytoskeletal reorganization) as well as alterations in their transcriptional profile and antigen presentation. When cultured on an absorbed collagen substrate, fluid shear stress promoted an anti-coagulant phenotype in EPCs by upregulating the anti-coagulant factors: THBD, TFPI, and NOS3 without significantly altering basal expression of pro-coagulant factors: F3 and VWF. In static culture, EPCs mimic the expression patterns of mature vascular endothelial cells with respect to THBD and VWF mRNA as well as THBD and F3 protein expression but have lower levels of TFPI, NOS3, and F3 mRNA. In comparing how each cell type responds to the shear stress environment, we found obvious differences in both THBD and F3. EPCs significant upregulation of THBD mRNA and protein with shear was in contrast to the ECs response which did not change from static levels. There was no change in F3 mRNA or protein expression in EPCs following shear exposure while ECs upregulation of F3 indicated they were activated by the local mechanical environment.

Culture on an engineered tissue in the presence of neighboring SMCs caused dramatic changes in the gene expression patterns for both EPCs and ECs. In the static environment, there was a general decrease in NOS3 expression and upregulation of F3 in both cell types. These gene expression results suggest that coculture with SMCs in a static environment may cause EPCs and ECs to exhibit a prothrombogenic phenotype compared to cells cultured on absorbed collagen. Additionally, EPC response to shear stress more closely mimicked the expression of ECs when cultured on the engineered

tissue compared to culture on absorbed collagen, although the EPC response to shear was generally attenuated. EPCs and ECs showed differential regulation of anticoagulant function (downregulation of THBD, upregulation of NOS3) and upregulation of procoagulant function (F3) with shear on the engineered tissue. It is clear that coculture with SMCs altered EPC phenotype and response to shear stress but the mechanism is unclear at this time. ECs and SMCs have been shown to communicate through paracrine mechanisms [254, 270] as well as though direct gap junction communication at myoendothelial junctions [271-273]. It is certainly possible that EPCs may communicate with SMCs in similar mechanisms. Although beyond the scope of the current study, SMC coculture may have also effected the differentiation of EPCs, possibly resulting in a more mature EC phenotype.

The results of this study may have clinical relevance. The emerging evidence that adult tissues possess repair and regenerative capacity through the mobilization of stem and progenitor cells from endogenous stores has transformed how engineers and clinicians develop treatment strategies in all areas of disease management. In the present study we have shown how application of fluid shear stress can be used to modulate the phenotype of a potentially autologous cell source obtained from minimally invasive peripheral blood samples. Manipulation of EPC phenotype using control of the local mechanical environment may be important in the development of non-thrombogenic surfaces on engineered blood vessel substitutes and other cardiovascular implants.

CHAPTER VIII: ENDOTHELIAL PROGENITOR CELLS AS A FUNCTIONAL VASCULAR LINING ON AN ELASTIN-COLLAGEN HYBRID VASCULAR TISSUE MODEL

Introduction

Tissue engineered small diameter vascular grafts have been considered the holy grail in vascular research for a number of years [274]. Tissue engineering has been faced with a number of challenges including the need for advances in three core enabling technology areas: cell source, construct fabrication and integration into the living system [5]. This work contributes in each of these three areas.

The need for a nonthrombogeneic surface on an engineered blood vessel substitute is paramount. In the native vessel, vascular endothelial cells (ECs) provide this unique surface but in recent years, other cells sources have emerged as possible alternatives to the EC. Endothelial progenitor cells (EPCs), which were first identified in the adult circulation in 1997 [91], are one such possible alternative but very little is known about their hemostatic function or their response to the arterial mechanical environment. We use an arteriovenous shunt model to test the application of EPCs in creating a vascular lining on an engineered tissue and investigate the role of the mechanical environment in EPC functional outcome.

In the area of construct fabrication, many strategies have been pursued using natural [75, 77, 80-82, 86, 164, 275, 276] and synthetic materials [9, 76, 83] as well as the body's own regeneration capacity [87] to create a suitable vascular substitute. In this

study, we focus on the use of natural extracellular matrix components which can (theoretically) be remodeled by donor and/or host cells. This natural hybrid approach provides a physiologically relevant substrate for the investigation of EPC function.

Experimental Design

This study discusses the development of an elastin-collagen hybrid vascular tissue which serves as a substrate for endothelial progenitor cells (EPCs). EPCs were seeded as a luminal vascular lining and preconditioned with steady laminar shear stress prior to functional evaluation of thrombogenicity in a baboon *ex vivo* arteriovenous shunt. Chapter IV: Methods and Materials provides a detailed description of the methodology used in these studies.

Results

Elastin-Collagen Hybrid Vascular Tissue Model

Elastin Isolation and Characterization

An intact elastin scaffold was isolated from fresh porcine carotid arteries following the methods described by Berglund et al. [164]. Figure 8.1 shows a macroscopic view of the original undigested artery and the resulting intact elastin scaffold. Undigested artery segments with inner diameters between three and five millimeters were acquired from either a local slaughterhouse or were purchased from a fresh tissue distribution company (Animal Technologies, Tyler, TX). Artery segments were cut to the desired length depending on application. As described previously, a series of thermal and chemical procedures resulted in an elastin scaffold which met

published criteria for elastin purity based on amino acid analysis and was absent of type I collagen immunostaining [164]. The elastin scaffold displayed significant autofluorescence and could be imaged using confocal microscopy. As shown in Figure 8.2, the scaffold was composed of multiple concentric lamellar ring structures encased by a loosely arranged networks of adventical fibers. Using scanning electron microscopy, the structure was more clearly elucidated. Figure 8.3A shows a cross-section of the scaffold displaying the multilayered structure with unique morphology on both the interior and exterior surface. At higher magnification, the luminal surface is dominated by fibers organized into a fenestrated sheet-like morphology (Figure 8.3B). These thin sheets of elastic tissue are termed fenestrated lamellae [277] and were organized into the concentric sheets which are predominant in the medial layer of medium size arteries (Figure 8.2). The exterior surface of the elastin scaffold (Figure 8.3C) was structured as a three-dimensional meshwork of elastic fibers lacking any significant organized pattern.

Elastin-Collagen Hybrid Tissue Fabrication and Characterization

Intact elastin scaffolds were combined with a solublized type I collagen and baboon SMC suspension and allowed to gel in tubular molds. Using the approach first described by Weinberg and Bell [71], a collagen hydrogel was formed entrapping the SMCs and the elastin scaffold within a collagen fiber network. Collagen hydrogels containing SMCs were also fabricated in the same way without the intact elastin scaffold and were cultured on glass mandrels in baths of nutrient rich media for eight days (shown in Figure 8.4). In the elastin-collagen hybrid tissue, the opaque elastin scaffold can easily
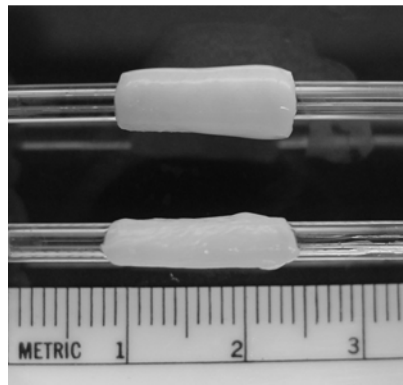
Undigested Porcine Carotid Artery

Intact Elastin Scaffold

Figure 8.1: Intact elastin scaffold. (top image) Freshly isolated native porcine carotid artery. (bottom image) Intact elastin scaffold following thermal and chemical digestion procedures.
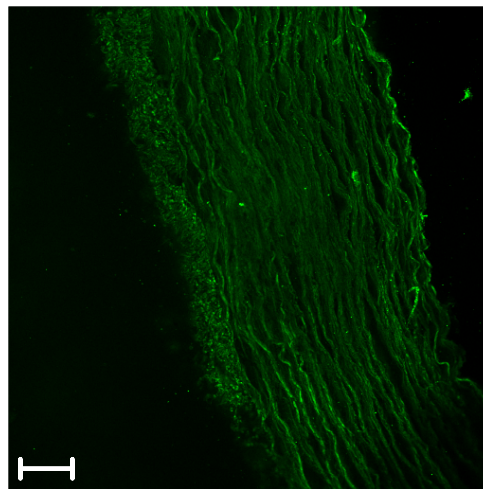
Figure 8.2: Confocal microscopy of intact elastin scaffold autofluorescence.
Scale bar = 100μm.
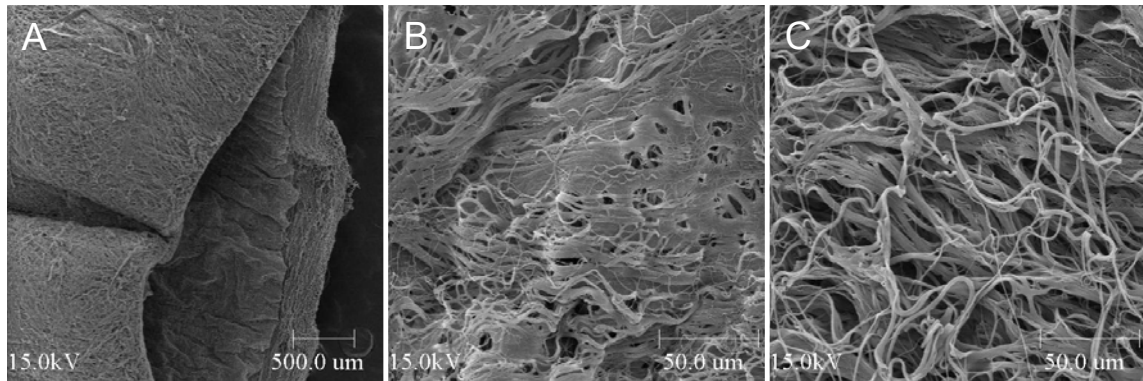
Figure 8.3: Scanning electron microscopy of an intact elastin scaffold. A) the cross-sectional view of the intact elastin scaffold B) the luminal surface C) the exterior (abluminal) surface. Scale bars are shown in each image.

elastin hybrid →

collagen →

elastin hybrid →
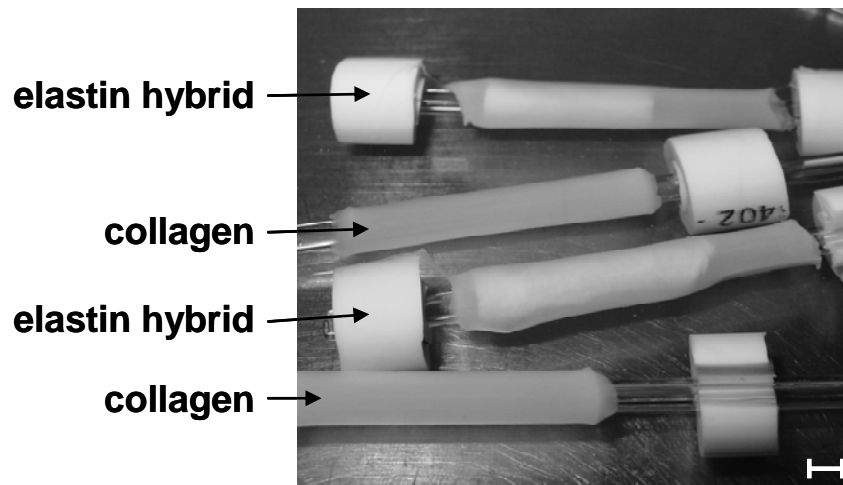
collagen →

Figure 8.4: Engineered vascular tissues in culture. (elastin hybrid) Engineered tissues fabricated with an intact elastin scaffold, baboon carotid artery smooth muscle cells (SMCs) and Type I collagen following 8 days in static culture. (collagen) Engineered tissue fabricated from SMCs embedded inType I collagen. Scale bar = 3mm.

be seen within the more transparent collagen matrix. Constructs were released from the rubber stoppers at each end on day one in culture and were allowed to compact constrained only by the inner glass mandrel for the remaining seven days in culture.

Cell Viability

Many of the chemicals used during the isolation procedure are cytotoxic and require complete removal from the intact elastin scaffold prior to fabrication of the hybrid tissue. Phosphate buffered saline washes were used as the final isolation steps to ensure cytotoxic chemical removal. Once the elastin scaffold was combined with collagen and cells, investigations of cell viability were performed using a two-color fluorescence-based staining method containing calcein AM and ethidium homodimer-1 (LIVE/DEAD® kit, Molecular Probes, Carlsbad, CA). These molecules allow measurement of two recognized parameters of cell viability, intracellular esterase activity and plasma membrane integrity [278]. Figure 8.5 shows representative images from LIVE/DEAD® staining in elastin-collagen hybrid tissues after eight days in static culture. The cells were generally distributed throughout the collagen matrix as individual cells with the majority of cells fluorescing green indicating positive viability. In rare instances, cell clusters could be found in the collagen matrix and probably resulted from poor mixing or inhomogeneous suspensions at the time of fabrication (Figure 8.5A). The elastin scaffold autofluorescence could also be seen in the confocal microscopy images (Figure 8.5A). Confocal images from at least five microscope fields at varying depths in the tissue (≈0-100µm) as well as at least five fields covering the cross-section were used to quantify average cell viability in the engineered tissues. Using image analysis (ImagePro Plus), the ratio of live/dead cells was quantified as described for constructs fabricated in six

independent experiments. As shown in Figure 8.6, the cell viability was greater than 73% for both collagen hydrogels and the elastin hybrid tissue. There was not a significant difference in cell viability ($p > 0.05$) between constructs fabricated with or without the elastin scaffold indicating that there was not residual toxicity associated with the scaffold isolation. An additional experiment with the elastin hybrid used a collagenase digestion (CLS2 600U/mL for 2 hours at 37°C) followed by trypan blue exclusion to verify the LIVE/DEAD$^®$ staining results. Trypan blue exclusion showed an average of 81% cell viability providing confirmation of the confocal microscopy results.

Matrix Compaction and Organization

Elastin-collagen hybrid constructs were subjected to histological assessment using hematoxylin and eosin (H&E) staining. As shown in Figure 8.7, the construct was organized in a composite fashion with the elastin scaffold located at the lumen and the SMC rich collagen hydrogel forming an outer covering. Cells were distributed throughout the collagen with a layer of cells along the outer wall. Very few cells were seen within the elastin scaffold after eight days of static culture.

Creation of an elastin-collagen hybrid tissue was first reported by Berglund et al. [164] using rat aortic smooth muscle cells (RASMCs) and human dermal fibroblasts (HDFs). In this research, early studies were performed with RASMC prior to isolation of baboon SMCs. This work aimed to develop an engineered tissue model appropriate for future *in vivo* studies in the nonhuman primate (baboon) and therefore later studies incorporated baboon carotid artery SMCs into the engineered tissues. It is common for
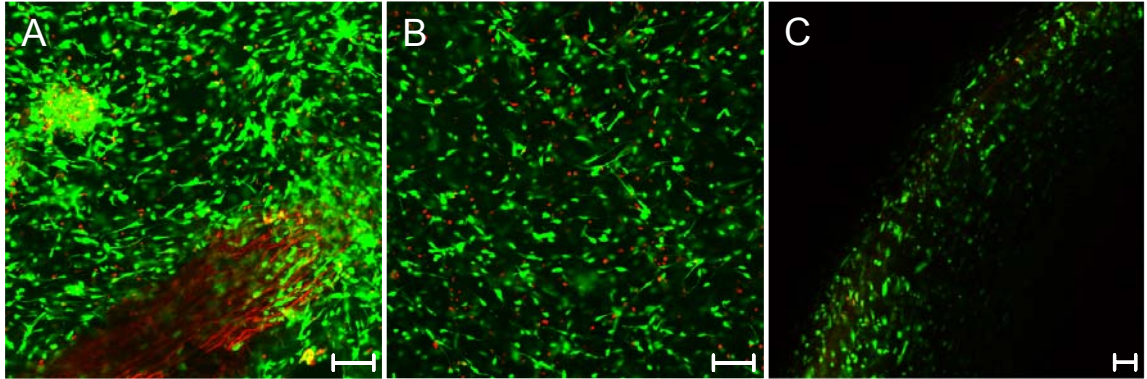
Figure 8.5: Confocal microscopy using a LIVE/DEAD® viability/cytotoxicity stain.
(A) cross-sectional view of the hybrid tissue midsection including elastin scaffold autofluorescence following 8 days in static culture; (B) view of external (abluminal) surface; (C) cross-sectional view of the hybrid tissue. Scale bar = 100μm.
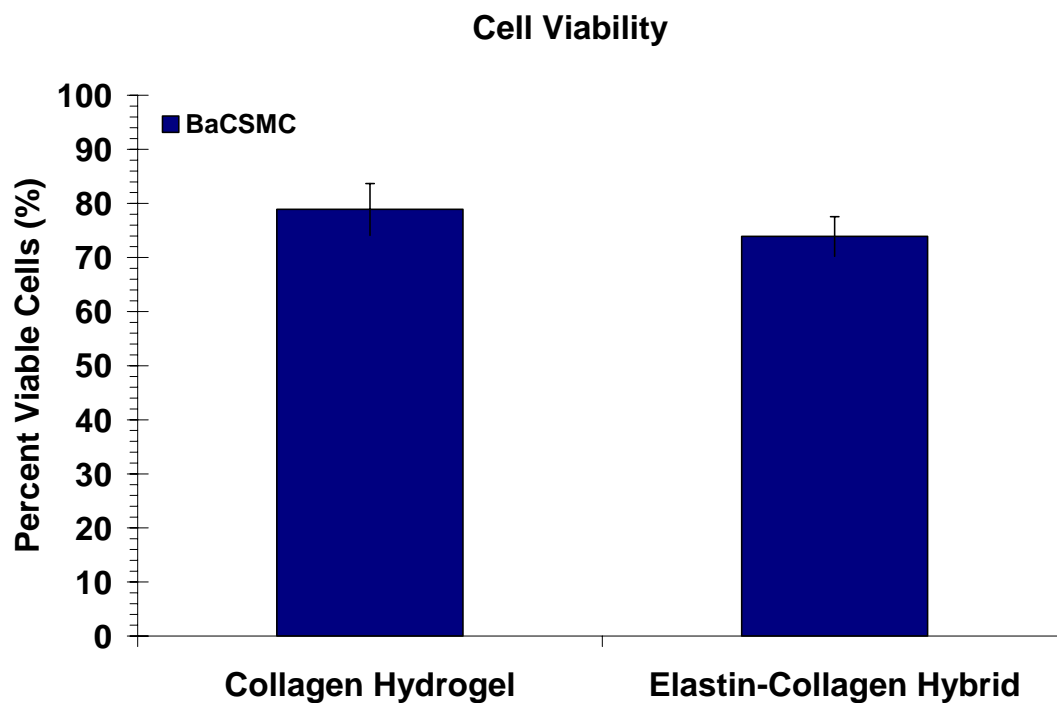
Figure 8.6: Quantification of cell viability. Image analysis was used to quantify the ratio of live/dead cells in engineered tissues fabricated with and without an intact elastin scaffold following 8 days in static culture. At least ten fields in each sample were acquired using confocal microscopy with a LIVE/DEAD® viability/cytotoxicity stain. Data presented as mean ± SEM, n=6. ANOVA showed no significant difference (p>0.05).
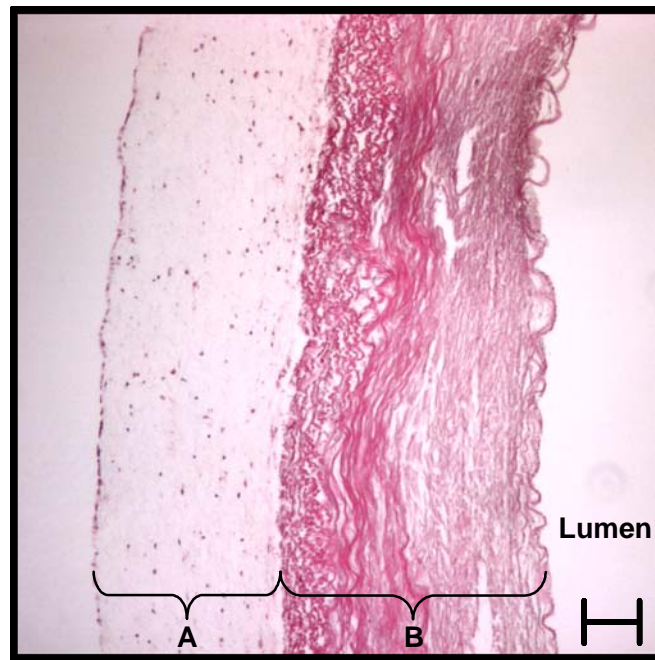
Figure 8.7: Hematoxylin and eosin (H&E) section. H&E was used to identify cell and matrix components in the elastin-collagen hybrid tissue cross-section following 8 days in static culture. The hybrid construct was a composite of a SMC-collagen layer (A) combined with an elastin (B) inner layer. Scale bar = 100μm.

there to be species specific differences in growth and remodeling and therefore the remaining engineered tissue characterization will be presented for both RASMCs and baboon carotid artery smooth muscle cells (BaCSMCs).

Cells were able to rapidly reorganize and compact their surrounding matrix during *in vitro* culture. Constructs were typically fabricated 60mm in length with an 11.6mm outer diameter and a 3mm inner diameter. Following eight days in culture, both cell types had compacted their matrix to less than 25% of the original volume (Figure 8.8). Cell seeded constructs without an elastin scaffold compacted more (occupied less volume) than elastin hybrid constructs ($p<0.05$). RASMC and BaCSMCs compacted the collagen hydrogels to the same extent but RASMC compacted the elastin hybrids slightly more than the BaCSMCs ($p<0.05$). Changes in wall thickness followed the same trend as seen in the compaction results with collagen hydrogels having slightly thinner walls (average wall thickness 0.89mm and 0.92mm for RASMC and BaCSMC, respectively) than elastin-collagen hybrid constructs (1.12mm and 1.37mm for RASMC and BaCSMC, respectively).

Uniaxial Tensile Material Properties

Material properties of the two engineered tissues were evaluated by testing ring samples to failure in a uniaxial tensile testing apparatus. The ultimate tensile stress of constructs is presented in Figure 8.9. Incorporation of an elastin scaffold into the construct significantly increased the ultimate tensile strength of engineered tissues using either RASMC or BaCSMCs ($p<0.05$). The cell type did not significantly impact the strength of either collagen hydrogels or elastin collagen hybrid constructs ($p>0.05$).

Cell Mediated Construct Compaction
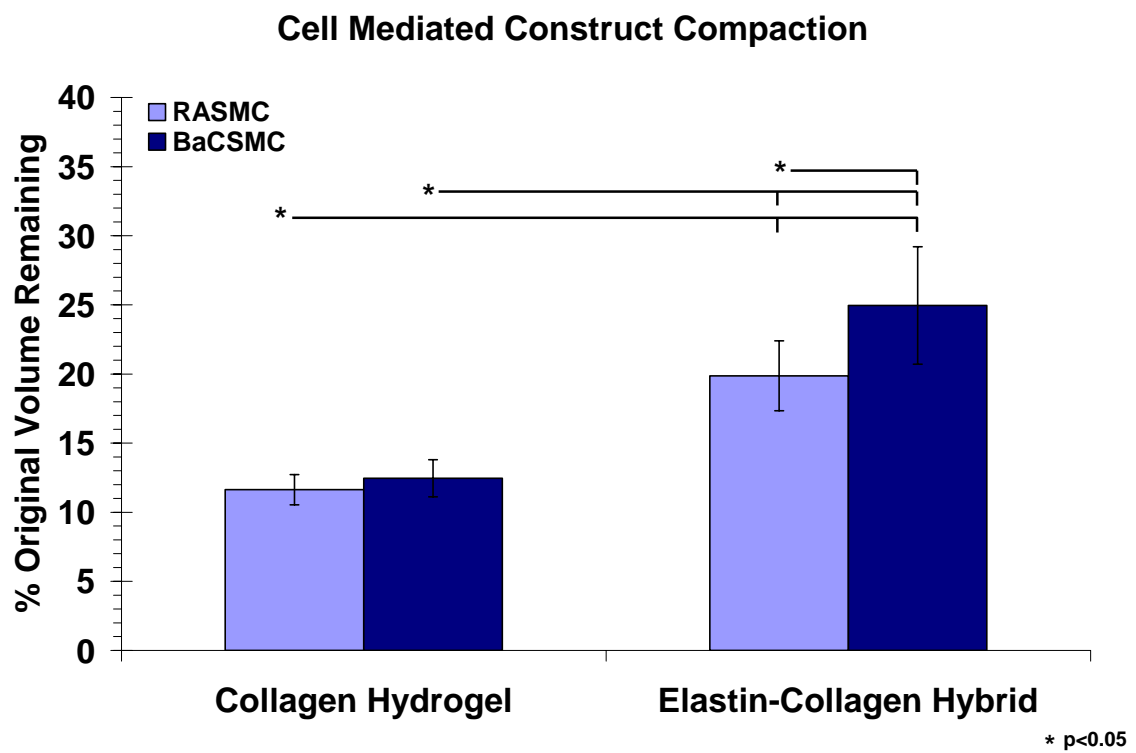
Figure 8.8: Quantification of SMC mediated construct compaction. Construct volume was quantified following eight days in static culture and shown as a percentage of the original construct volume on day 0 (mean ± SEM, n=6). ANOVA showed differences in groups (p<0.0001). Pairwise comparisons: *(p<0.05).
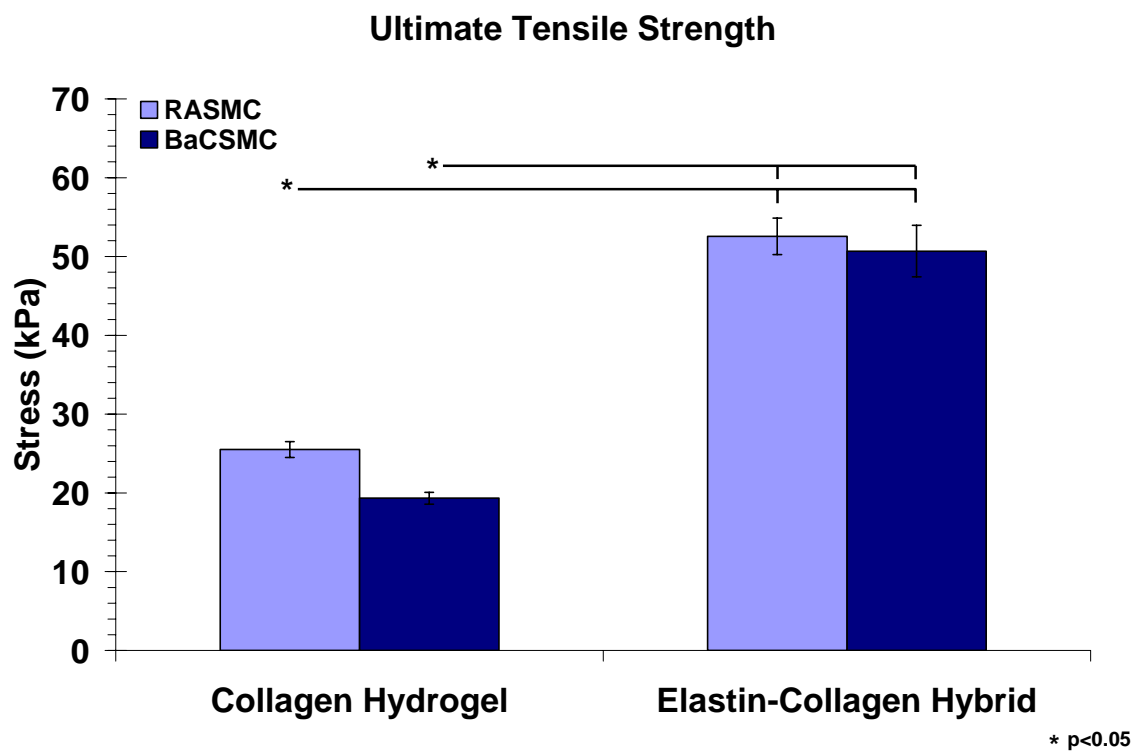
Figure 8.9: Elastin-collagen hybrid tissue material properties: ultimate tensile strength. Ultimate tensile strength was quantified in ring samples of hybrid tissue following eight days in static culture. Data presented as mean ± SEM, n=6. ANOVA showed differences in groups (p<0.0001). Pairwise comparisons: *(p<0.05).
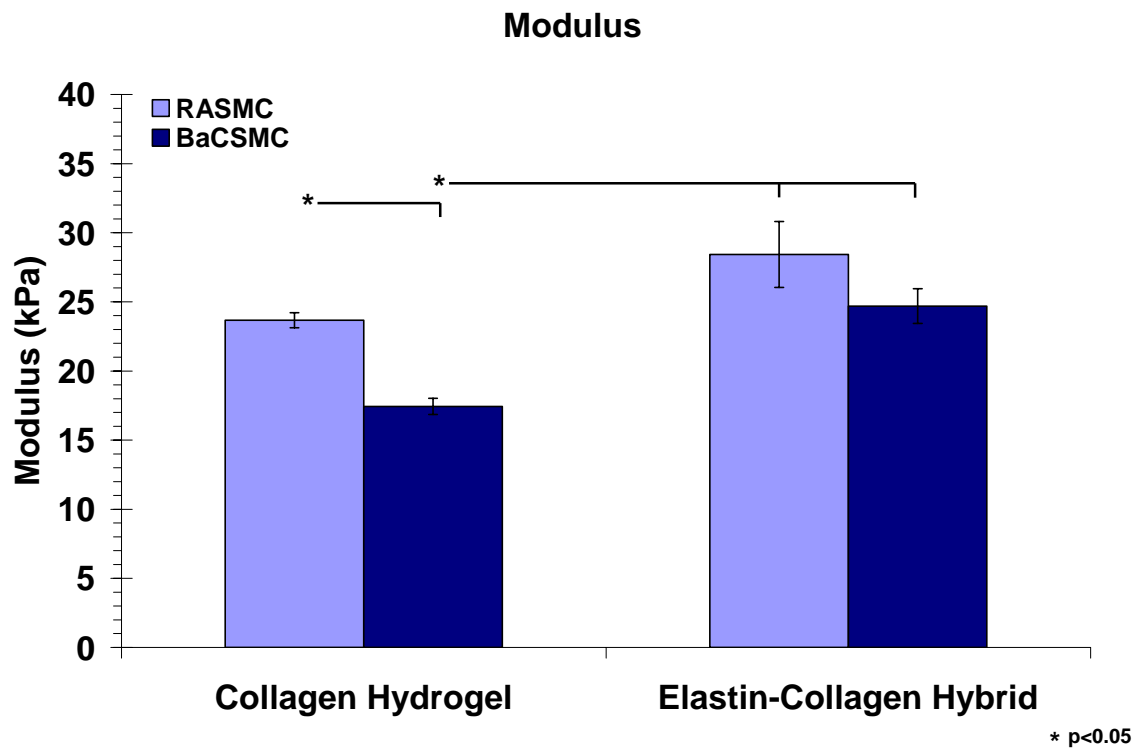
Figure 8.10: Elastin-collagen hybrid tissue material properties: linear modulus. The modulus was determined for 25-75% of the ultimate tensile stress which corresponded to the linear region of the tensile stress versus strain curve following eight days in static culture. Data presented as mean ± SEM, n=6. ANOVA showed differences in groups (p<0.0001). Pairwise comparisons: *(p<0.05).

The linear modulus was determined from the stress versus strain relationship for each material. In these studies, the linear modulus was defined as 25-75% of the ultimate tensile stress. Modulus data are shown in Figure 8.10. In BaCSMC fabricated tissues, the incorporation of elastin resulted in a significant increase in the linear stiffness modulus ($p<0.05$). In contrast, collagen hydrogel constructs fabricated with RASMCs had significantly higher linear moduli than BaCSMC collagen hydrogels ($p<0.05$) and the addition of elastin did not significantly increase the modulus further ($p>0.05$).

Endothelial Progenitor Cells as a Vascular Lining

Endothelial progenitor cells (EPCs) derived from baboon peripheral blood were investigated as a vascular lining on elastin-collagen hybrid tissues fabricated with baboon SMCs. Elastin-collagen hybrid tissues were secured with sutures to thin walled Teflon tubing connectors (250μm), embedded in an agar matrix and encased with heat shrinkable Teflon tubing. The apparatus was connected to a perfusion loop with silicon rubber tubing and the ends were sealed by heating, avoiding direct heat to the tissue segments. This aseptically sealed individual construct bioreactor was then used for EPC seeding, shear stress preconditioning and interposition in the baboon AV shunt. A side view schematic of the apparatus is shown in Figure 8.11.

EPCs were expanded *in vitro* and seeded onto elastin hybrid constructs. EPCs readily attached and spread on the surface of elastin hybrid constructs as shown in Figure 8.12A and C, 24 hours after initial seeding. EPCs were labeled with a fluorescent cell tracker (Orange CMTMR, Molecular Probes, Carlsbad, CA) prior to seeding onto the

engineered tissue to identity EPCs from underlying SMCs within the wall of the engineered construct. EPCs formed a confluent monolayer lining the construct lumen.

Arterial Shear Preconditioning

Cell Morphology

The response of EPCs to fluid shear stress was also investigated on the elastin-collagen hybrid tissue. In preparation for functional evaluations in a baboon shunt model, EPCs were seeded onto the engineered tissue in two bolus injections (1.5 hours apart), rotated in 15 minute increments and allowed to adhere for a total of three hours. Flow was initiated through the construct gradually increasing steady laminar shear stress to 15 dynes/cm^2 (arterial shear) over the course of forty minutes. EPCs were then arterial shear preconditioned for an additional 20 hours. EPCs adhered to the matrix and responded to flow by orienting and aligning parallel to the direction of flow as shown in Figure 8.12B and D.

Functional Evaluation

Cell Retention in the Ex Vivo Shunt

Elastin hybrid constructs seeded with EPCs and exposed to *in vitro* shear preconditioning were then transitioned into a nonanticoagulated baboon arteriovenous (AV) shunt for functional evaluation. EPCs radiolabeled with Indium 111 chloride were seeded onto the elastin hybrid construct, arterial shear preconditioned for 20 hours, and then connected to the baboon AV shunt. Scintillation camera imaging was used to quantify changes in radioactivity and therefore EPCs retention on the construct surface as

a function of time in the shunt. Figure 8.13 shows a representative gamma camera image

and quantification of the change in the number of cells within the construct as a function

of time. Quantification was normalized to the number of cells measured at initiation of

shunt flow and averaged for two studies. The number of EPCs on the construct surface

remained constant within 9% of the initial cell density for up to 60 minutes of whole

blood exposure.
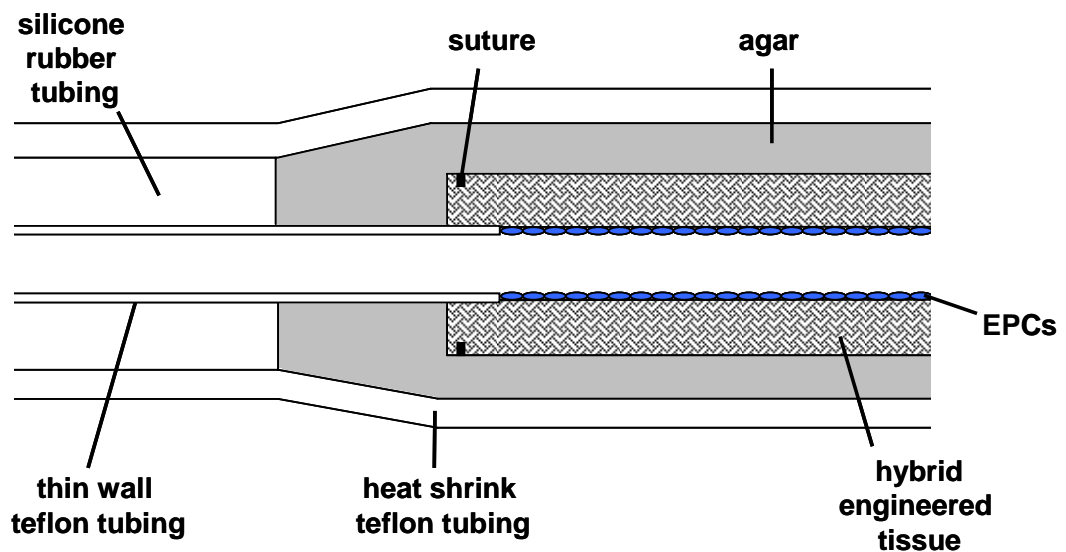
Figure 8.11: Schematic of elastin-collagen hybrid tissue bioreactor. The hybrid
tissue was cannulated at each end by thin wall Teflon tubing and secured with a suture.
The engineered tissue was embedded in agar and covered by an outer heat shrink Teflon
casing to provide external support and the possibility of blood being lost through the
device. Silicon rubber was used to connect the engineered tissue to the arteriovenous
shunt.

EPCs on Elastin-Collagen Hybrid Tissue

Static **Shear**

Flow ➡
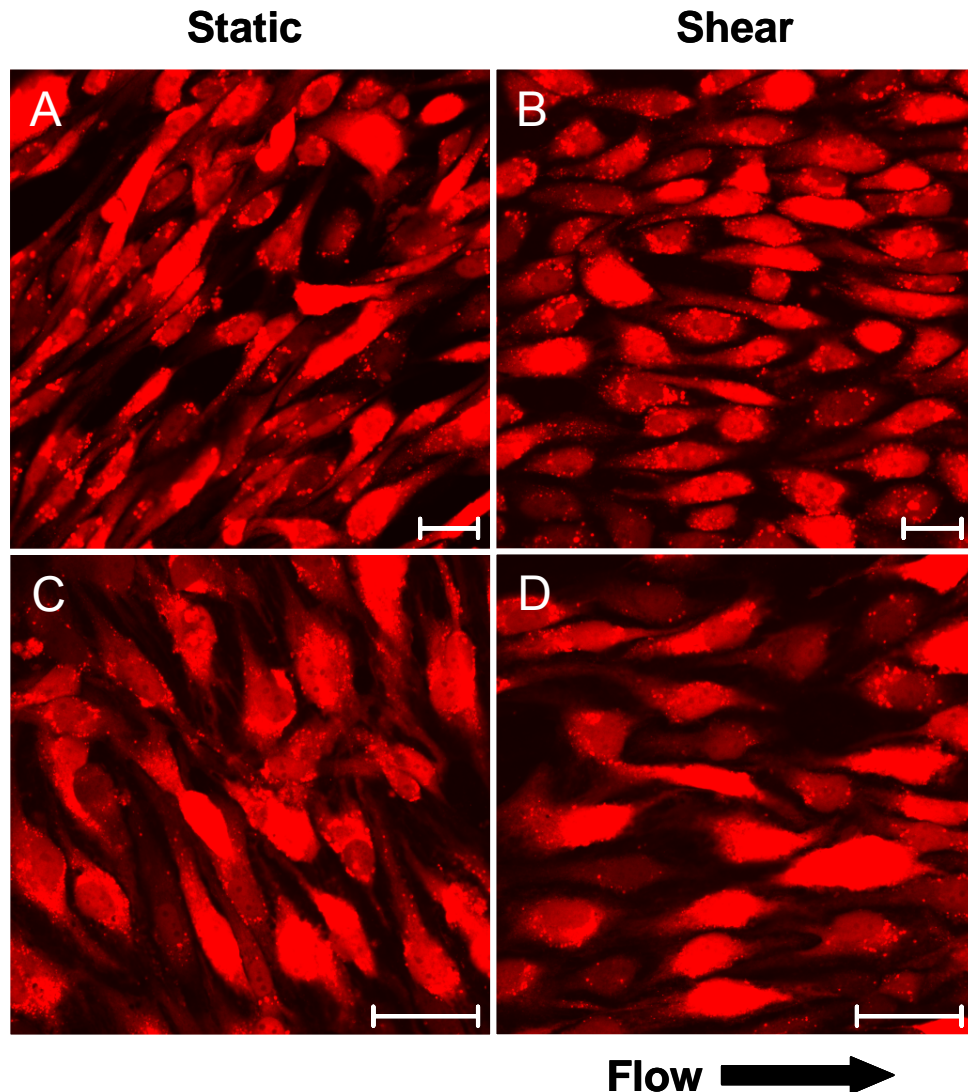
Figure 8.12: EPCs attached to the luminal surface of an elastin-collagen hybrid vascular tissue. EPCs were labeled with a fluorescent cell tracker (Orange CMTMR, Molecular Probes) and seeded onto the luminal surface of the hybrid tissue. (A, C) Confocal microscopy images of EPCs on the hybrid tissue lumen following 24 hours of static culture. (B,D) EPCs were exposed to steady laminar shear stress (15 dynes/cm^2) for 20 hours after a three hour static incubation,. Scale bar = 50μm.
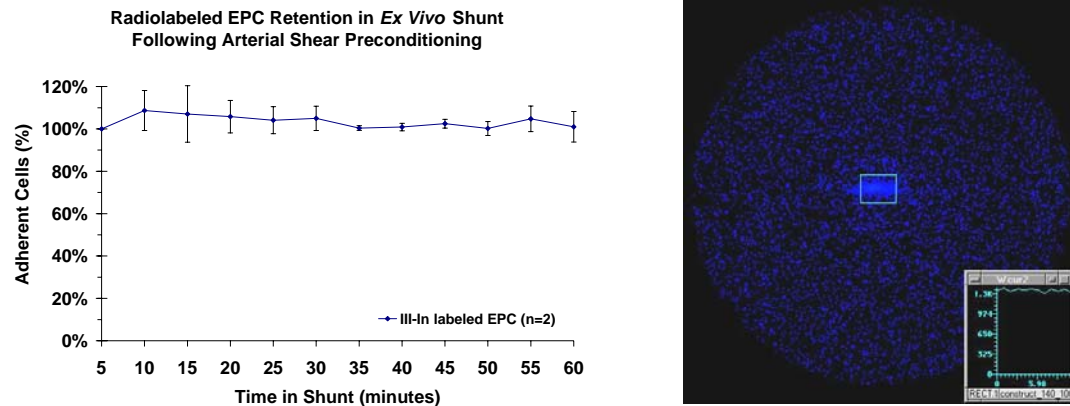
Figure 8.13: Radiolabeled EPC retention in an *ex vivo* shunt following arterial shear preconditioning. (left panel) The percentage of adherent EPCs on the elastin hybrid tissue as a function of time in a baboon *ex vivo* shunt was determined using 111In labeled EPCs and gamma camera imaging. Prior to interposition in the shunt, EPCs were exposed to *in vitro* steady laminar shear stress (15 dyne/cm^2) for 20 hours. Gamma camera imaging data was normalized to the initial five minute acquisition and are presented as mean ± standard deviation, n=2. (right panel) Representative gamma camera image of EPC seeded hybrid tissue following 45 minutes in the *ex vivo* shunt. The radioactivity from 111In labeled EPCs is shown as bright blue within the outlined construct area.

Quantification of Platelet Deposition

Using the same techniques employed to radioactively label EPCs, autologous baboon platelets were labeled with Indium 111 chloride and returned to the baboon's circulation. Unlabeled EPCs were seeded onto the elastin hybrid construct and were shear preconditioned prior to interposition in the AV shunt. Identical constructs without EPCs were preconditioned in the same manner and served as hybrid tissue controls. In the shunt, scintillation camera imaging was used to quantify platelet deposition on the construct surface. Figure 8.14 shows the experimental layout with two representative gamma camera images of EPC seeded and non-seeded constructs. Images were color-coded based on the quantity of radioactivity measured during each five minute acquisition. Constructs were positioned on the surface of the imaging system as shown (Figure 8.14A). Two region of interest (ROI) markers were used to identify the entire construct length and also to isolate the central 1cm region. The number of platelets in the central 1cm ROI were quantified and compared across all experiments.

Figure 8.15 shows the quantified platelet deposition on the surface of arterial shear preconditioned elastin-collagen hybrid constructs as a function of time in the AV shunt. Elastin hybrid tissues without EPCs show a linear and significant increase in platelet accumulation with increasing time in the shunt. In sharp contrast, EPC seeded constructs resisted platelet deposition with significantly less platelets on the surface after 25, 30, and 35 minutes of nonanticoagulated blood exposure ($p < 0.05$).

Systemic Coagulation Markers

Chronic arteriovenous shunts placed between the femoral artery and vein in juvenile baboons (*Papio anubis*) allowed for multiple studies to be conducted in the same animal. Three animals were used for the 18 studies presented as part of this dissertation. Table 8.1 lists the baseline measurements of circulating plasma fibrinogen and the average blood platelet concentration for each of the three animals. Fibrinogen concentrations were measured daily for each animal. There was no significant difference in the measured plasma fibrinogen ($p>0.05$) which ranged from 2.28 to 2.82 mg/mL for all animals. Blood platelet concentration was measured immediately prior to each study and averaged between 310,000 to 561,000/µL for each of the three animals. Animal 24565 had a significantly higher platelet concentration than either 24081 or 24567. The blood platelet concentration for 24565 was reasonably consistent, varying by less than 6.5% for the seven studies which were conducted in this animal during the course of three weeks.

Table 8.2 presents study related changes in blood platelet concentration and circulating thrombin-antithrombin III (TAT). Platelet concentration was measured immediately following each shunt study and compared to pre-study values. Circulating platelet numbers decreased in construct studies with or without EPCs an average of 34,500/µL. There was not a significant difference in the reduction in platelets between EPC seeded or non-seeded tissues ($p>0.05$). The TAT was also measured immediately prior and immediately following each shunt study. There was an increase in circulating TAT following studies with or without EPCs but no significant difference was related to the presence or absence of EPCs on the construct surface ($p>0.05$).
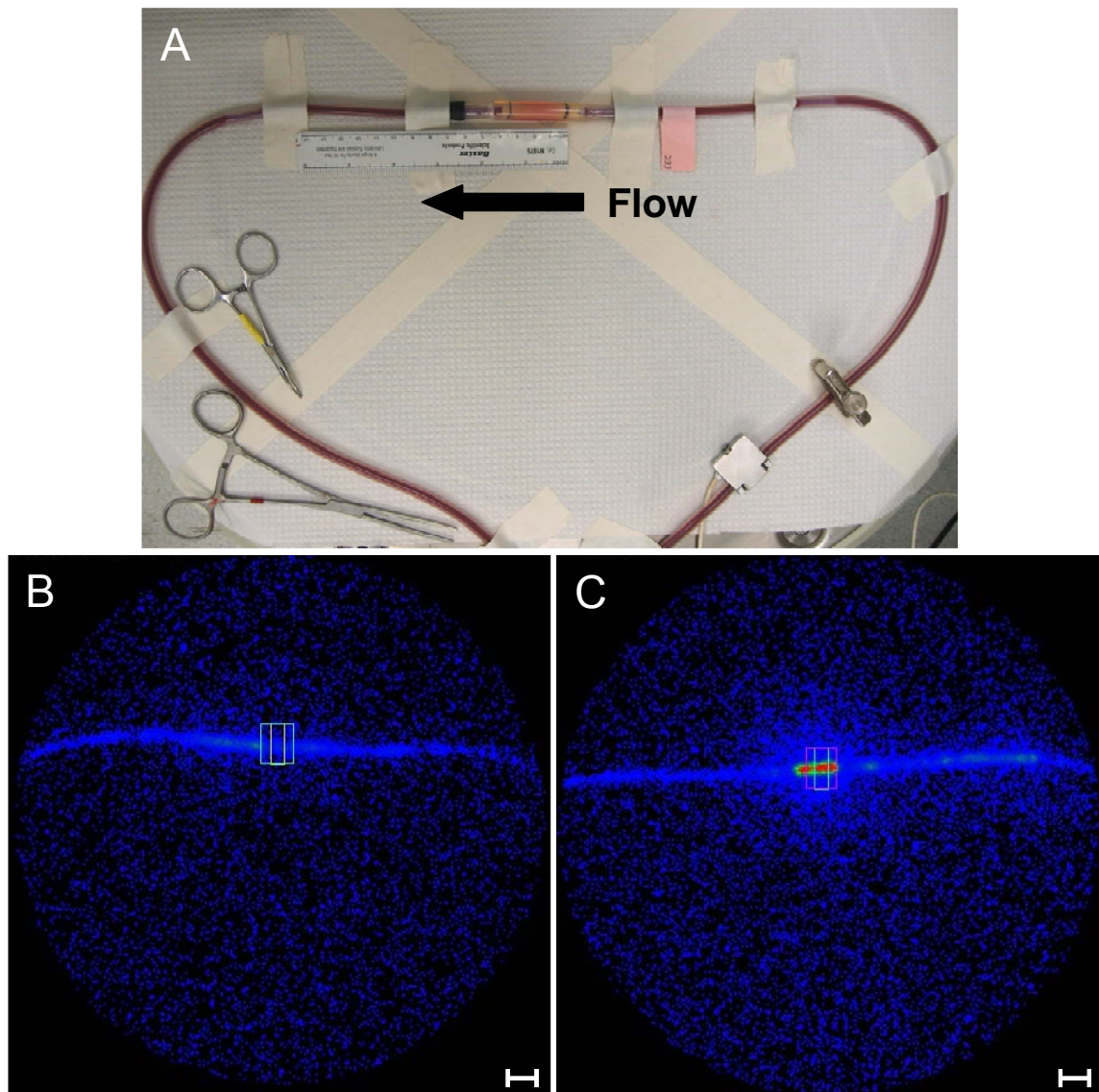
Figure 8.14: Gamma camera images of 111 Indium labeled platelet deposition in a baboon arteriovenous *ex vivo* shunt. (A) Image of experimental setup showing nonanticoagulated blood flowing through the construct sample (100ml/min). (B) Example gamma camera image of an arterial shear preconditioned EPC seeded hybrid tissue construct (40 minutes). Imaging was used to quantify 111In-labeled platelet deposition in the central 1cm region of the construct. Boxes outline the entire construct length and the central region of interest used for quantification of platelet deposition. (C) Example gamma camera image of an arterial shear preconditioned hybrid tissue construct showing significant platelet deposition on the construct surface (40 minutes). Scale bar = 2mm.

Platelet Deposition On Hybrid Engineered Tissue
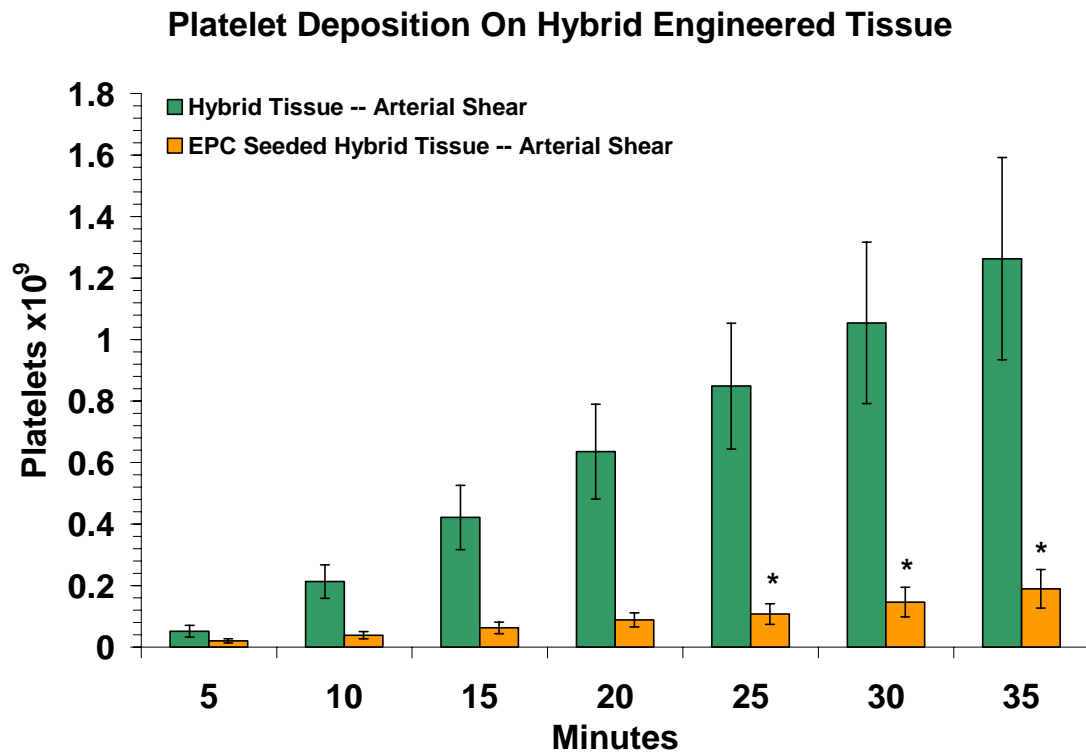
Figure 8.15: Radiolabeled platelet deposition on elastin-collagen hybrid tissues following arterial shear preconditioning. Gamma camera imaging was used to quantify autologous 111In-labeled platelet deposition on the tissue surface as a function of blood exposure time when construct samples were placed in a baboon *ex vivo* arteriovenous shunt. Prior to interposition in the shunt, hybrid tissues with and without EPCs were exposed to *in vitro* steady laminar shear stress (15 dyne/cm^2) for 20 hours. Data presented as mean ± SEM, n=6. ANOVA showed differences in groups (p<0.0001). Pairwise comparisons: *(p<0.05).

Table 8.1: Coagulation profile of normal experimental animals. Fibrinogen concentration was measured daily and blood platelet concentration was measured immediately prior and immediately following experimental studies. Data presented as mean ± standard deviation. ANOVA showed no differences in plasma fibrinogen concentration (p>0.05). *significantly different than 24081 and 24567 (ANOVA p<0.05).

Animal identification number	Number of shunt studies	Average plasma fibrinogen concentration (mg/mL)	Average platelet count prior to initiation of experiments (x10^3/μl)
24081	6	2.82 ± 0.38	369 ± 91
24565	7	2.28 ± 1.11	561 ± 36 *
24567	5	2.62 ± 0.39	310 ± 19

Table 8.2: Alterations in blood platelet concentration and TAT: arterial shear preconditioned samples. Blood platelet concentration and plasma thrombin-antithrombinIII (TAT) concentration were quantified from blood samples taken immediately prior and immediately following experimental studies. Data presented as mean ± standard deviation. ANOVA showed no significant differences (p>0.05).

Arterial Shear Preconditioning	Number of shunt studies	Average reduction in platelet count pre-study minus post-study (x10^3/μl)	Average increase in TAT post-study minus pre-study (ng/mL)
EPC Seeded Hybrid Tissue	6	32 ± 31	24 ± 11
Hybrid Tissue	6	37 ± 32	23 ± 18

Variable Shear Preconditioning

In preliminary studies (n=3) aimed at investigating the effect of low shear preconditioning on EPC functional response in the whole blood environment, EPCs were seeded onto the elastin-collagen hybrid tissue, shear preconditioned at low shear stress (1 dynes/cm^2) for 12 hours, and transitioned into the AV shunt.

Figure 8.16 shows the retention of low shear preconditioned EPCs. For up to 35 minutes, the cell number remained constant within 9% (n=2). Gamma camera imaging which allowed for quantification of platelet deposition (Figure 8.17) showed that the elastin hybrid tissue without an EPC lining was thrombogenic with linear increases in platelet accumulation over 35 minutes of nonanticoagulated blood exposure. EPCs seeded onto the hybrid tissue and exposed to low shear for 12 hours prior to functional evaluation in the shunt were also thrombogenic showing comparable platelet accumulation to hybrid tissues without EPCs (p>0.05). In the three studies conducted with low shear preconditioned EPCs on the elastin hybrid tissue, there was significant reduction in the shunt flow (<<100mL/min) requiring that the studies be terminated after 15 minutes (n=1) and 20 minutes (n=2) to ensure that the shunt and/or animal were not compromised. Blood platelet concentration measured immediate prior and immediately after each study showed an average reduction of 32,500 platelets/µL (Table 8.3) with no significant difference between EPC seeded and non-seeded construct samples (p>0.05).

Radiolabeled EPC Retention in *Ex Vivo* Shunt Following Low Shear Preconditioning
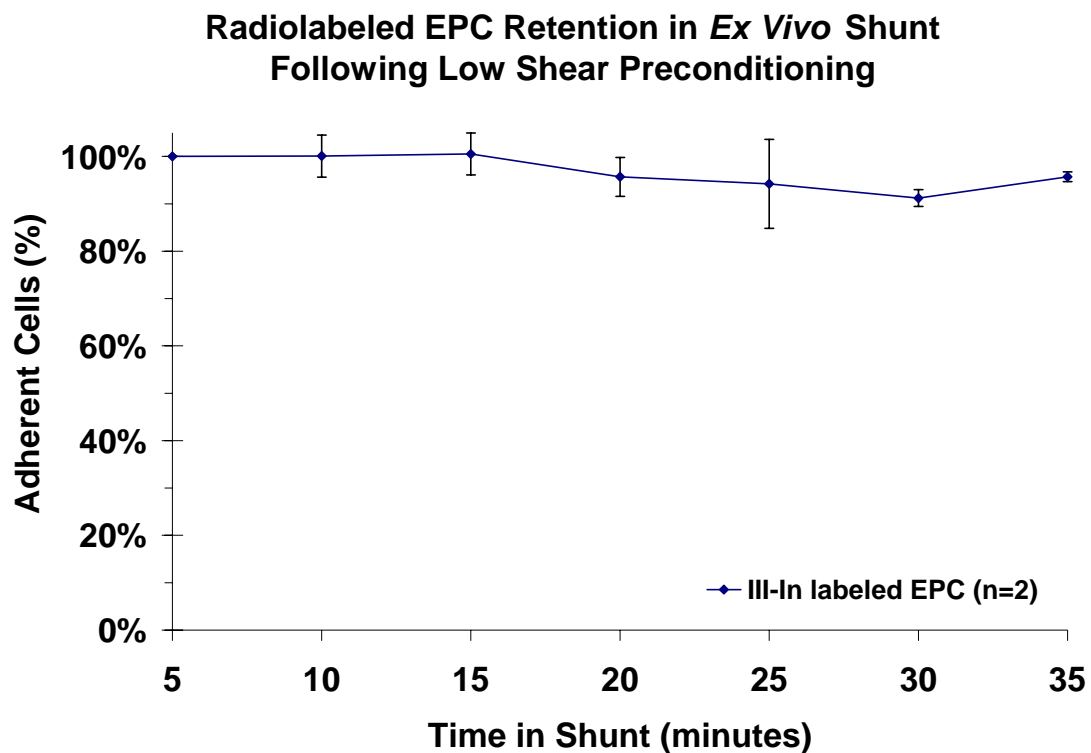
Figure 8.16: Radiolabeled EPC retention in an *ex vivo* shunt following low shear preconditioning. The percentage of adherent EPCs on the elastin hybrid tissue as a function of time in a baboon *ex vivo* shunt. Prior to interposition in the shunt, EPCs were exposed to *in vitro* steady laminar shear stress (1 dyne/cm^2) for 12 hours. Gamma camera imaging data normalized to the initial five minute acquisition and presented as mean ± standard deviation, n=2.

Platelet Deposition On Hybrid Engineered Tissue
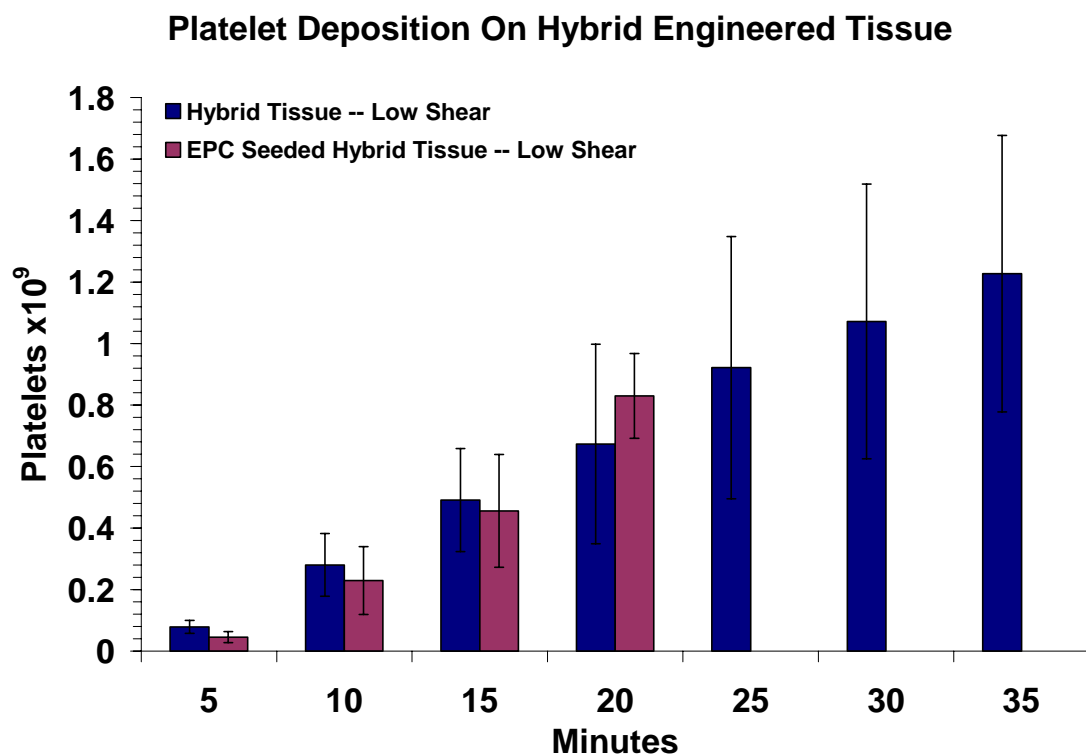
Figure 8.17: Radiolabeled platelet deposition on elastin-collagen hybrid tissues following low shear preconditioning. Gamma camera imaging was used to quantify autologous 111In-labeled platelet deposition on the tissue surface as a function of blood exposure time when construct samples were placed in a baboon *ex vivo* arteriovenous shunt. Prior to interposition in the shunt, hybrid tissues with and without EPCs were exposed to *in vitro* steady laminar shear stress (1 dyne/cm^2) for 12 hours. Data presented as mean ± SEM, n=3.

Table 8.3: Alterations in blood platelet concentration: low shear preconditioned samples. Platelet counts were quantified from blood samples taken immediately prior and immediately following experimental studies. Data presented as mean ± standard deviation. ANOVA showed no significant differences (p>0.05).

Low Shear Preconditioning	Number of shunt studies	Average reduction in platelet count pre-study minus post-study ($\times 10^3/\mu l$)
EPC Seeded Hybrid Tissue	3	32 ± 7
Hybrid Tissue	3	33 ± 7

Discussion

Limitations of the Experimental Approach

There are several limitations associated with the current work. The elastin-collagen hybrid construct displayed significantly larger ultimate tensile strengths than the more traditional collagen hydrogel tissues but did not withstand loads which would allow for an ample margin of safety upon chronic implantation. Additional research is necessary and ongoing in our laboratory to address the need for improved collagen organization and/or synthesis of appropriate extracellular matrix materials to further improve the construct strength. The overall composition of the elastin hybrid mimicked the medial layer of a native artery but the composite structure did not show significant integration and cellular infiltration between the collagen and elastin components. Without appropriate integration, the structure may be subject to possible delaminating issues when subjected to *in vivo* cyclic strains. Dynamic testing measures were not performed in these studies but have been addressed by Berglund et al. who showed that unlike the collagen hydrogels which tended to relax and creep, the elastin hybrids were able to support loads for extended periods of time and showed similar mechanical behavior as native arteries at subfailure levels [164]. Strategies to enhance integration between layers could include establishing a nutrient or growth factor gradient by culturing the constructs in a method which incorporates higher concentrations of these exogenous biochemicals inside the lumen of the tissue during maturation. Another possible strategy might be to use a pressure "sodding" technique during the fabrication of

hybrid tissues which would use a pressure gradient to force SMCs and collagen into the porous elastin matrix.

These studies were performed for up to 35 minutes of nonanticoagulated blood exposure representing the acute response to implantation which is an important determinant of graft patency. While platelet accumulation may persist for months to years after graft implantation, the maximal amount occurs immediately upon placement of the graft [169, 279]. In order to predict chronic outcomes, implantation studies would be required. While the possibility exists for autologous cell transplants, these studies were performed with allogeneic baboon SMCs and EPCs. Due to the short term nature of these studies, issues related to immune response were not considered significant. Previous work has used both xenogeneic and allogeneic cells in similar studies with success [279, 280].

We performed paired studies (± EPCs) in the same animal in morning and afternoon sessions. By performing multiple studies in the same animal in the same day, there is some risk that the first study could impact subsequent results such as causing platelets to become refractory and thus less capable of participating in thrombus formation. In order to minimize any impact of multiple studies, there was at least one hour and generally more than two hours of "rest" between studies as well as random assignment of construct types (± EPCs) to each session (morning versus afternoon). The extent, rather than the rate of blood element accumulation was measured using the scintillation camera imaging technique. Because of this, the differences in microembolization rates due to shear stress differences could have influenced the results. Different synthetic materials have been shown to produce varying platelet thrombus

embolization [172], a factor which was not investigated in this research. No gross embolization was observed from the hybrid tissues.

General Discussion

This work has built upon current tissue engineering strategies to build an engineered vascular tissue which mimics the structure of a native artery and is an appropriate model supporting acute endothelial functional studies in a baboon arteriovenous shunt. Primary baboon carotid artery SMCs were combined with an intact elastin scaffold and a reconstituted type I collagen matrix to form an engineered vascular tissue which could be cultured *in vitro* and supported a neoendothelium of peripheral blood derived endothelial progenitor cells.

In the body, elastic fibers are almost always found in close association with collagenous tissues. This is certainly the case for native blood vessels where collagen and elastin both play major roles in the mechanical performance of the tissue. In general, collagen and elastin carry out different mechanical roles in the composite tissue. In arteries, elastin is responsible for reversible extensibility while the collagen meshwork provides rigid constraints and limits the deformation of the elastic elements [277]. In this study, intact elastin scaffolds were isolated from porcine carotid arteries and retained the overall structure of elastin in the native artery. The circumferential fenestrated lamellar sheets were evident with an adventitial structure of randomly distributed elastic fibers.

The elastin scaffold was combined with type I collagen and cells to form a hybrid tissue. This newly formed extracellular matrix supported viable baboon carotid artery SMCs (>73% cell viability) which quickly remodeled and compacted the rudimentary vascular structure. This remodeling process occurred primarily in the first few days of

culture and by eight days resulted in dense tissues less than one quarter of their original

volume. A limitation of the reconstituted protein approach (i.e. collagen hydrogels) as a

tissue engineering strategy has been their limited strength. Previous investigations have

obtained similar tensile strengths for cell seeded collagen hydrogels ranging from 5kPa to

18kPa depending on the cell type and culture conditions [74, 75, 281]. In the current

studies, the stress was based on the sample dimensions of the unstressed tissue rather than

those reported by other investigators based on estimated sample dimensions at failure

[77]. While using the unstressed sample measurements results in lower ultimate stress

values, the measurements are less susceptible to subjectivity in this system. In the

engineered artery, incorporation of an elastin scaffold resulted in improved mechanical

strengths compared to collagen hydrogel controls. With BaCSMCs, the incorporation of

an elastin scaffold resulted in a greater than 2.5 fold increase in ultimate tensile stress and

a 1.4 fold increase in linear modulus. When compared to constructs fabricated with

RASMCs, BaCSMC engineered tissue had essentially equivalent ultimate tensile

strengths. RASMC remodeled tissues were modestly stiffer with an average 25.4%

higher modulus. Ultimate tensile stresses measured for elastin-collagen hybrid tissues

were slightly larger than previously reported [164]. This difference may be due to subtle

variations in cell isolates, culture conditions and testing or could be due to differences in

collagen source. The current work incorporated bovine dermal type I collagen which was

solublized in 0.02N acetic acid at a concentration of 4mg/mL. In the previous report,

investigators used commercially available acid solublized type I rat tail collagen at stock

concentrations between 3 and 4mg/mL depending on lot. Recent studies in our

laboratory have shown that collagen source contributes to differences in ultimate tensile

194

strength in other experimental constructs and that the bovine dermal type I collagen produced stronger materials [282].

Estimated burst strength can be predicted from tensile stresses using thin wall assumptions and LaPlace's relationship ($\sigma = rP/t$) [164]. Table 8.4 shows estimated burst strengths based on the ultimate tensile stress measurements for elastin hybrids and collagen controls. The estimated burst pressures for constructs containing elastin scaffolds are substantially larger than those of collagen hydrogels. While these values are significantly lower than burst pressures reported for native arteries which have been in the range of 2700 to 4500mmHg [74, 283, 284], they are in the range of physiologic blood pressures. While long term implant studies may not be achievable with this tissue, the elastin-collagen hybrid construct does provide a model of the vascular wall with sufficient strength for *ex vivo* study.

Table 8.4: Estimated burst pressures of elastin-collagen hybrid and collagen hydrogel constructs. Ultimate tensile strength was converted to an estimated burst pressure using thin wall assumptions and LaPlace's relationship ($\sigma = rP/t$) for circumferential stress. σ is stress, r is the radius, P is pressure and t is wall thickness. All values are in millimeters of mercury $\pm$ standard deviations.

	RASMC	BaCSMC
Elastin-Collagen Hybrid	159.0 ± 27.6	173.6 ± 27.4
Collagen Hydrogel	58.7 ± 5.7	43.3 ± 4.1

The success of any strategy to tissue engineer a blood vessel substitute will, in part, depend on the ability to create a nonthrombogenic lining. While large diameter (>6mm ID) artificial blood substitutes can be transplanted with clinical success, small diameter substitutes often fail due to thrombus formation. The earliest attempts at tissue engineering of blood vessel substitutes demonstrated that an endothelial lining on synthetic substrates improved patency [285, 286]. Strategies using an autologous donor vessel for primary EC harvest, have been implemented in human clinical practice but remain limited in their wide spread availability and application to small diameter grafts [9, 287]. EPCs offer a promising source of autologous cells which can be obtained minimally invasively from a peripheral blood sample. They are highly proliferative and have been shown to exhibit a number of endothelial specific markers. (see Chapter V: Cell Isolation and Characterization for a detailed analysis) In other studies, we have also shown that EPCs are responsive to the mechanical environment, altering gene and protein expression in the presence of fluid shear stress (Chapter VI and VII). In this study, we aimed to investigate the function of EPCs as a vascular lining on an elastin-collagen hybrid engineered tissue. EPCs readily attached and spread on the elastin hybrid constructs forming a confluent lining. When subjected to fluid shear stress, the EPCs elongated and aligned parallel to the direction of flow on the elastin-collagen hybrid tissue. This is consistent with our own work on absorbed collagen substrates as well as several recent observations of cytoskeleton alterations in EPCs as a function of flow exposure [145, 158]. Using a radiopharmaceutical, Indium 111 chloride, EPCs were radiolabeled and could be monitored following interposition of the engineered tissue into a baboon AV shunt. Scintillation camera imaging showed that EPCs remained adherent

to the engineered construct for up to 60 minutes of blood exposure. Using 111-In labeled cells in monolayer culture as a standard, the average EPC density on the hybrid tissue was quantified as $\approx 40,000$ cells/cm^2.

The baboon AV shunt model introduced by Hanson et al. [169] has been extensively used to study arterial and venous thrombosis as well as to investigate blood biomaterial interactions for many therapeutic applications. The baboon model has many potential advantages including its hemostatic similarity to humans, size, ease of frequent blood sampling, long-term acceptance of chronically patent AV shunts, and blood proteins which are antigenically similar to humans, permitting the use of human immunoassays [171, 288-291]. Autologous baboon platelets were labeled with 111-Indium chloride and returned to the circulation. Using scintillation camera imaging, radiolabeled platelet deposition on constructs with and without an EPC lining was quantified. EPC lined hybrid constructs which had been exposed to arterial shear preconditioning (15 dynes/cm^2) significantly resisted platelet deposition compared to construct only controls. Following 35 minutes of blood exposure, the anti-coagulant phenotype of EPCs was evident with 6.6 fold less platelets on the EPC lined tissue.

Preliminary data also suggests that the shear preconditioning regime (shear magnitude and duration) may be an important factor in EPCs pro or anticoagulant phenotype on the elastin-collagen hybrid tissue. Figure 8.18 presents a summary of platelet deposition on the hybrid constructs with and without EPCs and following both low and arterial shear preconditioning. Hybrid constructs without EPCs as well as EPCs which were low shear preconditioned resulted in a significant accumulation of platelets starting immediately following initial blood exposure. In contrast, the arterial shear

preconditioned EPCs prevented platelet deposition on the construct surface. Figure 8.19

highlights the platelet deposition quantified after 20 minutes in the AV shunt. The

positive anticoagulant effect of arterial shear preconditioning on EPCs is evident with an

average eight fold reduction in platelet deposition. Arterial shear preconditioned EPC

monolayers essentially abolished platelet deposition which is consistent with previous

studies using both HUVEC and aortic ECs seeded expanded polytetrafluoroethylene or

endarterectomized segments [279, 280].

In this study, three animals were used with varying baseline platelet

concentrations (310-561 $x10^3/\mu L$). Although, initial platelet concentration has been

reported to be correlated with total deposited platelets [170], in this study no significant

correlations could be drawn between the baseline platelet concentration and platelet

deposition on hybrid tissue with or without EPCs ($R^2<0.03$ at 20 minutes). This

demonstrates that arterial shear preconditioned EPCs provided a robust defense against

platelet deposition over a range of platelet concentrations.

Acute thrombosis in the baboon shunt has been shown to result in a reduction in

the circulating platelet concentrations [172]. In the current work, blood platelet

concentrations reduced by an average of 7.4% ± 5.6% immediately following shunt

studies but there was not a significant correlation with this reduction in platelet

concentration and construct type or shear preconditioning protocol (p>0.05). Platelet

reduction has been reported to exceed 27% in thrombogenic Dacron grafts as a result of

platelet consumption in the graft thrombus [172]. It is unclear why there was a

measurable reduction in platelet concentration in arterial shear preconditioned EPC lined

tissues

Platelet Deposition On Hybrid Engineered Tissue
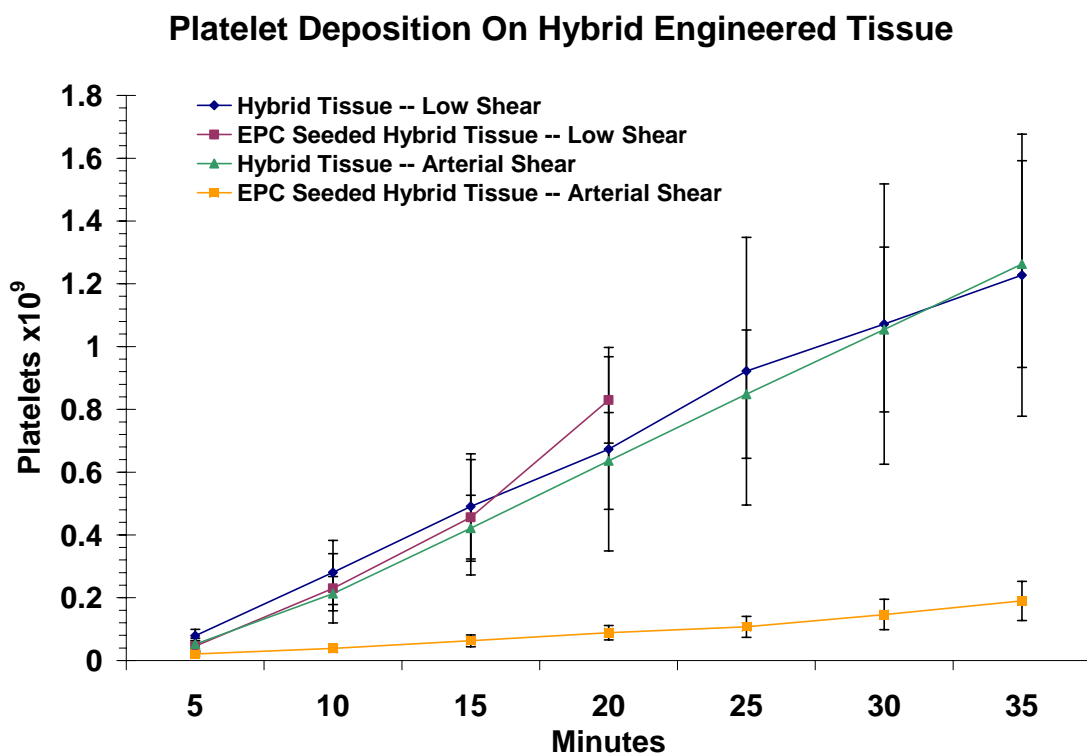
Figure 8.18: Summary of radiolabeled platelet deposition on elastin-collagen hybrid tissues. Gamma camera imaging was used to quantify autologous 111In-labeled platelet deposition on the tissue surface when construct samples were placed in a baboon *ex vivo* arteriovenous shunt. Prior to interposition in the shunt, hybrid tissues with and without EPCs were exposed to *in vitro* steady laminar shear stress (1 or 15 dyne/cm^2 for 12 and 20 hours, respectively). Data presented as mean ± SEM, n=3-6.

Platelet Deposition On Hybrid Engineered Tissue
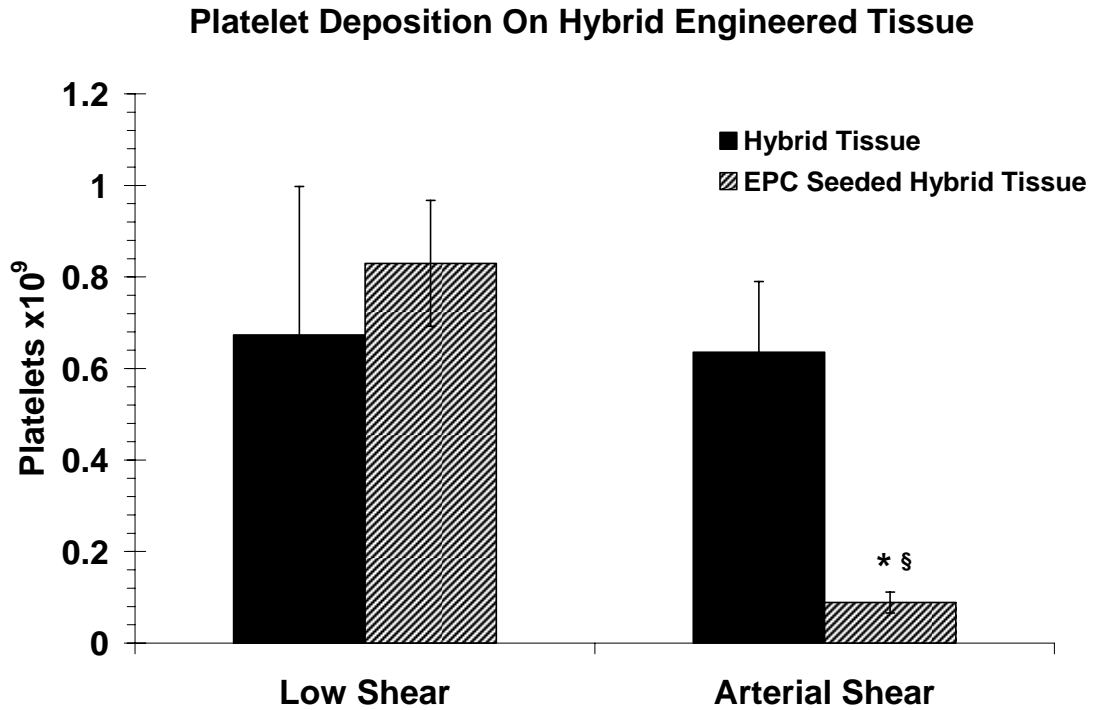
Figure 8.19: Radiolabeled platelet deposition on elastin-collagen hybrid tissues following 20 minutes in a baboon *ex vivo* arteriovenous shunt. Gamma camera imaging was used to quantify autologous 111In-labeled platelet deposition on the tissue surface as a function of blood exposure time when construct samples were placed in a baboon *ex vivo* arteriovenous shunt. Prior to interposition in the shunt, hybrid tissues with and without EPCs were exposed to *in vitro* steady laminar shear stress (1 or 15 dyne/cm^2 for 12 and 20 hours, respectively). Data presented as mean $\pm$ SEM, n=3-6. ANOVA showed differences in groups (p<0.0001). Pairwise comparisons: * different from hybrid tissue – arterial shear (p<0.05), § different from EPC seeded hybrid tissue – low shear (p<0.05).

which resisted significant platelet deposition on the construct surface. Although there was substantial effort placed on creating smooth transitions at tubing connectors within the construct and shunt apparatus, there could have been minor flow disturbances which contributed to platelet deposition (and consumption) in regions not quantified with scintillation imaging. In normal humans, approximately one-third of the total platelet mass is transiently sequestered in the spleen as part of the unique splenic circulation. The platelets within the spleen are normally in equilibrium with the peripheral circulation [292]. Another possible explanation is that the arterial shear preconditioned EPC lined constructs altered the splenic balance and caused an increase in the removal of platelets from the circulation or transient platelet sequestration, but this study provides no additional data that this occured.

In thrombus formation, circulating thrombin cleaves fibrinopeptide A from fibrinogen, producing fibrin. Thrombin complexes with antithrombin III leading to the formation of thrombin-antithrombin III (TAT) complexes. The presences of these TATs in circulation are suggestive evidence of the thromobogenic process and in certain clinical situations such as acute myocardial infarction, may be increased [293]. TAT levels were elevated following shunt studies with arterial shear preconditioned samples but we were unable to detect any significant changes in plasma TAT as a function of the construct type (with or without EPCs) or shear preconditioning (low or arterial) (P>0.05).

Plasma fibrinogen levels should directly influence fibrin formation and possibly blood cell accumulation. The fibrinogen concentration was not significantly different across all experimental animals. There were also no unusual alterations in hematocrit or

white blood cells counts during these studies (data not shown) indicating the baboons were normal and free of any obvious illness.

Concluding Remarks

The research presented as part of these studies has built upon current strategies to fabricate an engineered blood vessel substitute by creating a vascular model appropriate for *ex vivo* study in the nonhuman primate. This model which incorporates cellular and extracellular matrix components of the native artery (SMCs plus elastin and collagen) has improved material properties compared to tissues without elastin and provides sufficient strength to withstand the mechanical environment of an arteriovenous shunt for up to one hour. This research has demonstrated that peripheral blood derived EPCs can be expanded *in vitro* and provide a neointima on an engineered vascular tissue. This neointima of EPCs essentially abolishes platelet deposition on the construct surface following *in vitro* preconditioning with arterial shear stress. EPCs have been suggested as a possible autologous endothelial cell source for tissue engineering and though these studies, we have demonstrated that EPCs can provide appropriate anticoagulant function on an engineered vascular tissue.

CHAPTER IX: DISCUSSION, CONCLUSIONS AND FUTURE

RECOMMENDATIONS

The overwhelming incidence of cardiovascular disease worldwide is staggering and provides motivation for significant research in this area. Tissue engineering aims to make advances toward future clinical treatment options in the area of vascular bypass grafting and cardiac surgical reconstruction. Tissue engineering strategies to create a functional vascular tissue which could be implanted and ultimately be integrated into the host are challenging. The research presented as part of this dissertation focused on cell source, one of the core enabling technologies needed for the engineering of vascular tissues. In this work, endothelial progenitor cells (EPCs), a potential endothelial cell source for tissue engineering, were isolated from peripheral blood for evaluation. EPC phenotype was characterized in increasingly complex models which probed the cell's response to the mechanical environment and physiologic substrates. Ultimately, these studies demonstrated a functional proof of concept that EPCs can provide a non-thrombogenic lining on an engineered vascular tissue prototype.

These studies demonstrated that EPC phenotype is modulated by fluid shear stress at the gene, protein and functional level. The idea that the local mechanical environment alters vascular cell phenotype is not a new finding. Yet, with respect to EPCs, almost nothing is known about the effect of mechanical cues on their behavior. Techniques to isolate and culture circulating EPCs have only recently been described and studies of their potential role in tissue engineering remain limited. Isolation of EPC colonies from peripheral blood gave rise to cells which displayed an endothelial-like phenotype with

expression of a number of EC specific markers (VEGFR2, VEGFR1, CD31, THBD, VE-Cadherin, VWF) and functions (uptake of acLDL, intracellular eNOS and capillary tube formation) while maintaining a high proliferative capacity. When exposed to fluid shear stress, EPCs morphologically altered actin distributions within the cell and elongated and aligned parallel to the flow direction. Transcriptional profiling of EPCs and ECs in the flow environment demonstrated that the EPCs response to fluid shear stress was generally attenuated compared to vascular ECs both in the number of genes significantly regulated by shear stress and also in the overall magnitude of gene expression changes. Shear stress preconditioning of EPCs may have important positive effects including potentially priming the EPCs defense against oxidative environments or causing a shift in the coagulation balance toward anticoagulant function. *In vitro* shear stress on EPCs in a two-dimensional environment upregulated important anti-coagulant molecules transcriptionally and through cell surface protein expression without significantly altering procoagulant function. Functional assessments of EPCs on a three-dimensional engineered tissue also suggested that shear stress preconditioning enhanced anticoagulant function and resulted in an endothelial lining capable of resisting platelet deposition from the non-anticoagulated blood. Preliminary studies pointed to shear stress magnitude as an important determinant of anticoagulant function in this system. Recently, shear stress has been suggested to play a role in embryonic stem cell differentiation toward an endothelial-like phenotype [294, 295] and in maturation of EPCs [146]. Although beyond the scope of this dissertation, shear stress exposure could also be altering EPC differentiation.

Tissue engineering approaches allow a methodology to create vascular tissue *in vitro*. The extracellular matrix proteins and vascular cells are combined to recapitulate a rudimentary vascular structure. This structure can be used as an *in vitro* model system which allows for potential direct cell-cell and cell-matrix interactions as well as paracrine and autocrine signaling. Evidence continues to accumulate in the literature that simplified culture systems may not always represent a predictive model of *in vivo* function. Better *in vitro* models incorporate the use of co-culture with neighboring cell types and 3-D extracellular matrix environments which are more representative of the *in vivo* situation [296]. In our own studies, culture of EPCs on a 3-D engineered tissue composed of collagen and SMCs altered the gene expression patterns of EPCs in both the static and flow environments suggesting that more complex microenvironments may influence cellular response to a given stimulus. *In vitro* tissue engineered vascular models also provide a unique way to study potentially synergistic effects of both physical forces, such as shear stress and the complex extracellular environment including ECM proteins and neighboring cell types. These studies demonstrated that when EPCs were cultured on a 3-D engineered tissue, there was a general reduction in the expression of anticoagulant molecules and upregulation of procoagulant phenotype. It was also found that when exposed to shear on this vascular wall model, EPCs' gene expression profile was more similar to the expression pattern of mature vascular ECs.

EPCs offer several potential benefits as a cell source for tissue engineering. Although not addressed directly in the studies presented as part of this dissertation, the possibility of EPCs aiding in postnatal vasculogenesis could also benefit tissue engineering approaches. Developing vascular networks within engineered tissues is of

205

significant interest to the tissue engineering community and EPCs may be a useful cell source in this regard [152, 153]. EPCs have already been shown to improve myocardial function when injected into ischemic animal models (reviewed in [98]) and our own data suggests that EPCs express a subset of genes associated with neovascularization to a greater extent than ECs. Transcriptional profiling also identified a subset of antioxidant defense genes which were upregulated in EPCs compared to ECs in the shear environment. Ischemic tissue is known to be an environment rich in reactive oxygen species [205] and therefore shear preconditioned EPCs may be better positioned to regulate the oxidative balance in ischemic tissues.

EPCs hold a lot of promise for use in tissue engineering strategies. EPCs are a potential autologous cell source which can be isolated from peripheral blood and expanded *in vitro* to obtain favorable characteristics of endothelial cell phenotype and function. As a vascular lining, EPCs assume the role of a mature endothelial cell, responding to the shear environment both morphologically and functionally.

Future Recommendations

In each chapter, limitations of the experimental approach were discussed. As this research continues beyond the scope of the current dissertation, there are several recommendations for future studies. First, recommendations related to extensions of this research which can possibly address present limitations are discussed. Second, recommendations for complementary studies are also presented in the context of identifying viable endothelial cell sources for tissue engineering.

These studies were conducted using simplified models of human physiology. EPCs were exposed to steady laminar shear stress at a magnitude of 15 dynes/cm^2 in

206

order to mimic mean arterial shear stress. This is a simplification of the actual *in vivo* arterial environment and future studies should consider more physiologic flow regimes which incorporate unsteady effects. It is anticipated that optimization of the fluid shear environment including investigation of different shear magnitudes and duration will impact the EPCs functional response and would be worthwhile investigations. These studies could also be extended to look at markers of EPC differentiation. It has been proposed in other models that shear stress promotes differentiation of stem and progenitor cells toward a mature endothelial cell phenotype [146, 294, 295]. This hypothesis could be tested using the same methodology. In the area of coagulation, these studies should be extended to look at additional molecules important in regulation of hemostasis such as prostacyclin, CD39 and endothelial protein C receptor. *In vitro* studies of gene and protein regulation could additionally be extended to *in vitro* functional assays such as factor X activation or plasma recalcification.

Engineered vascular tissue was used as an *in vitro* model of the blood vessel wall which incorporated a more physiologic substrate for studying EPC function. Differences in gene regulation were measured when EPCs were cultured on the engineered tissue compared to an absorbed collagen substrate. Future studies should investigate the role of the extracellular matrix composition and neighboring cells in EPC phenotype and function. Studies in this area could be extended beyond thrombosis to look at markers of intimal hyperplasia, a known vascular graft failure mechanism and a condition associated with EC-SMC interaction.

An important consideration for tissue engineering applications in the replacement of diseased tissue is the age of the patient (cell donor). It has been shown that circulating

EPC numbers are reduced in older patient populations and may be inversely correlated with cardiovascular risk factors (reviewed in [297]). This could make translation of these strategies to clinical application more difficult. In the current studies we used juvenile baboons as EPC donors. Future studies using peripheral blood derived EPCs should be performed using human EPCs from older donors with known cardiovascular disease risk profiles. This research should be conducted to address species, age and donor health effects on EPC isolation potential and cellular function.

Studies presented as part of this dissertation showed encouraging results in terms of EPCs providing a non-thrombogenic vascular lining, but additional studies are needed to address the long term potential of this strategy. Implantation of engineered vascular tissues lined with EPCs should be performed to address immune and inflammatory responses as well as potential failure mechanisms such as intimal hyperplasia and graft arteriosclerosis. Implantation studies would also require engineered tissues with superior material properties. Beyond the incorporation of elastin, integration of additional extracellular matrix molecules, biochemical and mechanical stimulation, as well as promotion of matrix synthesis may be synergistic strategies which will aid in achieving tissues with material properties appropriate for implantation. Additional material property testing will also be important to predict durability in the dynamic *in vivo* environment.

A number of complementary or related studies are suggested for future consideration based on the evolving body of literature related to EPCs. In these studies, EPCs were derived from late blood outgrowth cultures as described but isolation of EPCs from peripheral blood has also been reported using specific cell selection procedures

focused on surface marker expression (e.g. CD133, c-kit, sca-1, CD34, CD14 and others [91, 106, 108, 110, 112, 114, 116, 298, 299]). It is anticipated that different cell populations could be useful for tissue engineering approaches and would be worthwhile investigating. In addition to specific selection from peripheral blood based on cell surface markers, EPCs can also be derived from umbilical cord blood [127, 300] or directly from bone marrow [92, 128]. It has also been suggested that endothelial-like cells can be derived from amniotic fluid [301]. Each of these sources may result in different isolation efficiencies in the number of endothelial-like cells that can be generated and it is anticipated that the specific cell source will impact functional outcomes. A proposed advantage of bone marrow or cord blood is that these tissues may contain larger numbers of EPCs. Depending on the therapeutic strategy (e.g. congenital applications or adult vascular replacements), these cell sources may also offer the potential for autologous application.

Recently, derivation of SMC-like cells has been reported from peripheral blood samples [136]. Complementary to the current studies, derivation of EPC and SMC-like cells from the same peripheral blood sample would allow for fabrication of an entirely autologous engineered tissue from a single blood draw and is certainly worth investigating.

Ex vivo culture of the EPCs in these studies allowed for their exponential expansion to obtain sufficient cell numbers to create a vascular lining on an *in vitro* fabricated engineered tissue. Recent reports have suggested that there may be ways to attract EPCs directly to a blood contacting surface without *ex vivo* expansion [302]. This type of approach offers significant advantage over *ex vivo* expansion methodology in

terms of potential for clinical application and cost but has yet to be proven efficacious. Initial studies using anti-CD34 coated ePTFE grafts attracted a cell population to the device surface but porcine arteriovenous implantations showed increased intimal hyperplasia in anti-CD34 coated grafts compared to uncoated controls [303]. To ultimately have an off-the-shelf available product with autologous cells, recruitment of the host's own cells to the graft would be an attractive approach and worthwhile investigating. The baboon *ex vivo* shunt model would provide an excellent mechanism to test this strategy.

In summary, these studies have provided a foundation from which additional investigations can progress. It is critical that our understanding of endothelial progenitor cell biology continue to advance in order to appropriately harness their potential for tissue engineering strategies and to bring engineered vascular substitutes one step closer to clinical application.

APPENDIX A

Select Experimental Protocols

Purpose:
To outline the steps in isolating endothelial cells (EC) and smooth muscle cells (SMC) from excised arteries. This method uses brief collagenase treatment plus gentle scraping to obtain ECs followed by enzymatic digestion of the medial tissue of the vessel to obtain SMCs. The advantages of this method include the fact that cells can be obtained quickly (within 1-2 days) and that a cross-section of SMCs from the media are isolated (i.e. the method does not preferentially select for a certain population of medial cells).

SMC have also been isolated using a non-enzymatic "migration" method involving the plating of tissue pieces onto tissue culture plastic. Over time (3-5 weeks) SMC will migrate out of the tissue and begin to proliferate. It is possible, however, that this method selects for especially "migratory" cells and therefore does not obtain a representative sample of SMC in the media. The long time required for this method also makes it less practical for some applications.

Reagents :
Hanks Balanced Saline Solution (HBSS), sterile   Invitrogen 14025-076
Collagenase CLS2   Worthington Cat# 4176
Base Medium (without supplements)
Complete Growth Medium
Antibiotic-Antimycotic solution [see Note 1]

Note: The choice of medium can be altered as appropriate for the species of interest. For baboon cells, MCDB 131 was used. For other animal species, DMEM was used.

Retrieval and Storage of Artery

1]   Transfer an appropriate amount of the HBSS to a sterile container for transporting the excised artery from the surgical suite or necroscopy (e.g. use ~40 mL in a 50 mL centrifuge tube per vessel).

2]   Add Antibiotic-Antimycotic solution to the transport HBSS to achieve a final concentration of 2X the recommended culture concentration. [see Note 1]

3]   Put the transport HBSS on ice in a cooler and bring to surgical suite where artery is to be excised.

4]   Excise artery, maintaining as high a degree of cleanliness/sterility as possible.
    Note: It is often much easier to gently dissect away adventitial and connective

tissue surrounding the vessel prior to excising the vessel from the animal. Be gentle with the tissue in order to preserve the endothelium.

5]   Place artery in transport HBSS and swirl to remove blood from lumen and outside of the artery.

6]   Place artery and transport HBSS on ice in a cooler for transport to the lab where isolation is to be performed.

7]   It is desirable to let the excised tissue cool in HBSS in order to slow the metabolism of the cells, however in general it is desirable to start the isolation procedure within 2-6 hours of excision. Successful isolations have been performed with tissue stored in HBSS for up to 24 hours. If tissue is to be stored for an extended period of time, the transport HBSS should be replaced with new HBSS after transport from the surgical suite.

Isolation Process

1]   Prepare two centrifuge tubes with 30 mL of cold HBSS with 5X concentrated antibiotic-antimycotic. Transfer the artery from the transport/storage HBSS and allow it to sit in the first tube for 15-20 minutes [Note 2], to wash off adhering debris.

2]   Autoclave a tray of instruments containing at least the following:
            dissecting scissors (small and large preferred)
            forceps (various sizes and styles)
            scalpel handle
            dissecting pins
Also prepare a sterile Petri dish containing paraffin

3]   Use a sterile Petri dish (without paraffin) as a place to manipulate the tissue. Remove the artery from the first tube of HBSS and use dissecting forceps and scissors to remove any adhering fat and connective tissue. Use two pairs of forceps to hold the artery and peel away the adventitial layer from the outside of the vessel [see Note 4]. Be gentle to prevent damage to the endothelium.

4]   Place the cleaned tissue in the second centrifuge tube containing cold HBSS with 5X concentrated antibiotic-antimycotic. Allow it to sit in the tube for 30-60 minutes [Note 3]. The collagenase solution can be prepared during this time.

5]   Collagenase solutions should be prepared fresh or frozen into single use aliquots. Two solutions should be prepared, one at 600 U/mL for EC isolation and one at 300 U/mL for medial tissue digestion [see Note 3]. Dissolve collagenase in base medium (WITHOUT FBS). You will need approximately 1 mL of 600 U/mL per 2 cm of vessel for EC isolation and approximately 20 mL of collagenase solution per 2 cm of vessel for SMC isolation. Worthington CLS 2 (Catalog #4176)

213

collagenase is the enzyme which has given the best results [see Note 3]. Enzyme is typically supplied in non-sterile form, therefore sterile filter the solution before use. For small volumes (10-60 mL), this can be done using a 0.2um syringe filter, however the filter may foul quickly and a new filter must be used for every ~10 mL of enzyme solution. Place the enzyme solution in a sealed centrifuge tube until ready for use below.

6]   Use sharp angled scissors to cut axially along one side of the artery so that the artery can be opened up and the lumen exposed. Place the artery on the floor of the Petri dish containing paraffin with the adventitial side down and gently flatten it out so that the intima is exposed (being careful to not damage the endothelium). Gently rinse the surface with HBSS+2X A/A if necessary to remove any remaining blood or debris. You may also use dissecting pins to "pin down" the tissue to the paraffin if needed [Note 5]. Using a micropipette, add a few drops of 600 U/mL collagenase (approx 300 uL / 2cm of vessel) to the surface and incubate for 5 minutes. Collagenase can be warmed to 37°C immediately prior to use to increase enzyme activity. Additional collagenase can also be added if necessary. The goal is to isolate the collagenase to the tissue surface to loosen EC attachment. Collect the collagenase solution, manually scrape the luminal surface once using a disposable cell scraper, and generously rinse the surface to detach any loose ECs, collecting all solutions [see Note 6]. Add warm culture medium (with FBS) to centrifuge tubes in order to dilute collagenase and quench digestion (approximately 2:1 by volume).

7]   Spin centrifuge tubes for 5 min at 1000 rpm.

8]   Aspirate the supernatent and reuspend cell pellet (may be too small to see) in fresh complete culture medium and plate into wells of a 6 well plate or Petri dish which has been pre-coated with 1% gelatin, 50 ug/mL collagen or 50 ug/mL fibronectin. Cels will adhere and begin to grow in small patches within 2-3 days (be patient).

9]   Rinse the de-endothelialized tissue in a clean HBSS w/ 2X A/A bath to remove any adherent cells.

10]   Discard the Petri dish used as a working surface during the cleaning of the artery, and lay out a new sterile Petri dish as a working surface.

11]   Remove the medial tissue from the HBSS bath and gently flatten it against the bottom of the Petri dish used as a working surface. The tissue should be approximately rectangular when laid out in this way.

12]   Use a scalpel (larger #20 blade works well) to cut the tissue into strips ~1-2 mm wide. Further cut these strips into pieces ~1-2 mm at a side.

13] Transfer the tissue pieces to the centrifuge tube containing the prepared 300 U/mL collagenase solution and seal the tube.

14] Place the tube in a water bath or incubator at 37°C. Agitation using a rocker table or similar device can be used, however care should be taken not the produce too much wave action which can shear and damage cells. Isolations have been successfully performed with and without agitation.

15] Allow the tissue to digest for an appropriate period of time, depending on the source and size of the vessels used. This important parameter has not been fully investigated but the following can provide some insight:

baboon carotid artery: digested an average of 16 hours with good results. Tissue pieces were visible but easily broken apart into a "slurry" by using a pipette to resuspend the solution.

canine carotid artery, porcine carotid, and rabbit aorta : digested 16 and 20 hours with good results using Worthington CLS 2 collagenase

rat aorta : digested for 12 and 16 hours with good results using Worthington CLS 2 collagenase. Tissue very digested, therefore shorter digestion times may be appropriate.

day 9 rat pups: used 4 hours digestion with good results

for canine cells, a 2 hours (n=1) and 5 hours (n=2) time point were also tested, however no cells were recovered indicating that the tissue had not been sufficiently digested at this point.

16] At end of digestion, add warm culture medium (with 10% FBS) to centrifuge tube in order to dilute collagenase and quench digestion.

17] Spin digested tissue down for 5 min at 1000 rpm and aspirate supernatant.

18] Add fresh culture medium to wash tissue, then spin digested tissue down again for 5 min at 1000 rpm (wash step can be omitted if desired).

19] Aspirate the supernatant and add fresh medium to digested tissue. The volume of medium added will depend on the number of flasks to be prepared. Generally, one T-75 flask should be prepared for each "2 cm" section of vessel. Add 20-30 mL of medium for each flask to be prepared.

20] Resuspend tissue by swirling and transfer 20-30 mL of suspension to each T-75 flask. All tissue can be plated, including larger chunks and debris.

21] Move flask(s) to incubator and allow to sit undisturbed for at least 24 hours. Generally, some cells will have attached to the flask bottom by 24 hours. Leaving the flask for a further 24-48 hours will result in more cells attaching and growing out of the loose networks of extracellular matrix that still remain (be patient).

22] Once a significant number of cells have attached and started to grow, the supernatant from the flask (containing remaining tissue) can be removed, leaving a P0 culture which can then be passaged and treated as normal. In addition, the removed supernatant from the flask (containing remaining tissue chunks) can be transferred to a new flask in order to start another culture (this can be done 2 or 3 times with canine and baboon cells, 3-4 times with porcine cells, but with rat cells there is generally not enough tissue to warrant starting further cultures).

NOTES

1] 1X concentration (of Gibco BRL Catalog #15240-062) = 100 U/mL penicillin G sodium, 100 ug/mL streptomycin sulfate and 0.25 ug/mL amphotericin B as Fungizone.

Gibco BRL Catalog #15240-062 is supplied at 100X concentration, but Sigma recommends use of 2.5 ug/mL Amphotericin B (see Antibiotics table in Sigma catalog). Can also use other antibiotics/antimycotics (e.g. Nystatin (Sigma Cat #N-1638, gentamycin, etc)).

2] Question : do antibiotics/antimycotics have any effect at this temperature for this time duration?

The antibiotic/antimycotic wash step can be modified based on the expected risk of contamination. The plated (P0) cells can also be treated with such a wash (4 hours at 37°C) to remove contamination if necessary.

3] The choice of enzyme is very important. This has not been exhaustively studied; however Worthington CLS 2 (Catalog #4176) collagenase (~230 U/mg) has been shown to work well. Collagenase products are generally relatively impure preparations and can vary considerably from lot-to-lot. 600 U/mL is used for EC isolation based on positive results from EC/SMC separation assays. Additional time/concentration optimization could be needed.

A combination of 1 mg/mL Worthington CLS1 (Catalog #4196) collagenase (~220 U/mg) and Sigma elastase (Cat # E-1250, from porcine pancreas) has also been used (n=2), however no cells were recovered using this enzyme concentration (both 5 and 16 hours digestion time attempted).

4] Peeling off of adventitia will be considerably easier for larger vessels (e.g. baboon, dog, pig), from which the adventitia will peel readily and in large pieces. For smaller arteries (e.g. mouse, rat), there may be essentially nothing that can be

removed. Remove the adventitial layer as much as possible without damaging the remaining tissue.

5]   Larger muscular vessels (e.g. baboon, canine, pig aorta) will not lay flat due to residual stress in the tissue. In this case, the dissecting pins may be very helpful. Less muscular arteries (e.g. carotids) will lay flat allowing collagenase to be added to the surface.

6]   One major challenge is to obtain ECs without SMC/fibroblast contamination. One strategy that may be worthwhile is to collect the collagnease solution and rinse prior to scraping, then in a separate collection tube, collect cells and rinse after scraping. Following centrifugation, plate each collection tube and the supernatent in separate wells of a 6 well plate to monitor for possible contaminating cells.

Acknowledgement:
Jan P. Stegemann was instrumental in development of this protocol.

Purpose:
To outline the procedure for preparing collagen hydrogels using live cells and acid solubilized Type I collagen.

Trypsin
Complete MCDB 131
5X concentrated MCDB 131
0.1 N NaOH
Type I collagen from calf skin   MP Biomedicals #15000026
     dissolved in 0.02 N acetic acid at 4 mg/mL

Note: For disk constructs, the molds to be used are the 35 mm diameter wells of a 6-well plate (non-tissue culture treated). For tubular constructs, the mold consists of a test tube and inner mandrel assembly. Tubular constructs are molded onto a silicone sleeve that is coated with collagen.

All procedures (except cell counting) should be performed in a biological safety cabinet using aseptic techniques to prevent microbial contamination.

Preparation of Silicone Sleeves (for tubular constructs only)
Note: Silicon sleeves are not required for fabrication but are helpful when constructs are cut longitudinally for embedding. Matrix and cell attachment to silicone may be enhanced by etching the silicone in sulfuric acid followed by collagen or other matrix coating. Surface modification was not required for simple embedding procedures.

1]   Tubular silicone sleeves used are 0.125" X 0.140" purchased from Vesta, Inc. (Franklin, WI).

2]   Cut sleeves into 50 mm lengths.

3]   Autoclave sleeves. Also autoclave glass mandrels, stoppers, test tubes, caps and instruments at the same time.

Preparation of Cell-Collagen Suspension

Fabrication of 2mg/mL Type I Collagen Hydrogels
Total Hydrogel Volume: 100mL

Regents	Volume	Notes
Type I Collagen (4mg/mL)	50 mL	total hydrogel volume x desired gel concentration / collagen stock concentration
0.1 N NaOH	6.25 mL	collagen volume / 8
5X MCDB 131	12.5 mL	collagen volume / 4
1X Complete MCDB 131	31.25 mL	total hydrogel volume - collagen volume - NaOH volume - 5X MCDB 131 volume

Appropriate volumes of the following reagents should be ready and kept on ice:

1] Use trypsin to detach cells to be used from their culture surface and collect cells in an appropriate tube. Wash cells once in medium and remove a sample for cell counting. Centrifuge for 5 min @ 1000 rpm to obtain a cell pellet.

2] Count cell sample using Coulter Counter or hemocytometer. Resuspend pellet of collected cells and transfer number of cells required to make constructs to a 50 mL centrifuge tube. Typical initial smooth muscle cell concentration is $1x10^6$ cells/mL.

3] Centrifuge cell suspension for 5 min @ 1000 rpm to obtain a pellet. Aspirate supernatant and place tube on ice.

4] To tube containing cell pellet, add appropriate volume of 1X complete MCDB 131 and use a pipetor to gently resuspend cells.

5] On ice, in a separate tube large enough to hold final hydrogel volume, add required volumes of Type I collagen, 5X MCDB 131 and 0.1 N NaOH and mix thoroughly. Solution is viscous, so mixing is difficult. Take care to create as few bubbles as possible. Keep solution cool to prevent gelling. The phenol red pH indicator in the MCDB 131 should indicate the pH is appropriate for addition of cells. If the pH is too low, a few additional drops of NaOH may be needed.

6] Add cell suspension to collagen solution and mix well. Cell-collagen suspension should be transferred to the appropriate mold as soon as possible.

7] Use a pipettor to transfer the required volume of cell-collagen suspension to each of the molds.
For disk constructs - Add 3.0 mL of cell-collagen suspension to 35 mm wells of a non-tissue culture treated 6-well plate. Gently swirl plate to distribute suspension evenly in the wells. Put cover on plate.

For tube constructs - First add 5.0 mL of cell-collagen suspension to glass test tubes. Then immediately insert a mandel-sleeve-stopper assembly into the test tube, ensuring that there is no air trapped in the annular space that will form the tubular construct. Cover test tubes with a cap.

8]   Immediately place mold in a cell culture incubator at 37°C. Allow to sit undisturbed for 30-60 min, until gelation is visable.

9]   For disk constructs - add warm culture media to the gelled surface
For tubular constructs - Remove molds from cell culture incubator and place in laminar flow hood. Remove caps and aspirate gelled material from lumen of glass mandrels. Be careful not to aspirate too much material (i.e. do not aspirate part of construct, only excess material in lumen of mandrel). Use ridged forceps to carefully remove mandrel assembly and gelled constructs from test tubes, and place in a 150 mm Petri dish containing ~130 ml of warm culture medium. Place constructs in cell culture incubator at 37°C.

10]   Allow constructs to incubate for 24 hours undisturbed. After this period, release constructs from mold to allow further gel compaction.

General Immunofluorescent Staining

Reagents:

Formaldehyde, 20%	Tousimis, Cat. No. #1008A
Triton X-100	Sigma X-100
Tween-20	Sigma P-7949
Hoechst 33258	Molecular Probes H-1398
Normal Goat Serum (NGS)	Sigma G-6767
Donkey Serum (DS)	Sigma D-9663
PBS	
Deionized Water (dH20)	
Mounting Medium	Dako, Cat. No. S3205

Procedure:

Fixation Buffer: 4% formaldehyde (for 50 mL final solution)
> 4% formaldehyde   10mL of 20% aqueous
> 2% sucrose (optional)   1g

> Dilute Tousimis formaldehyde (20% aqueous) to 4% in PBS. Add appropriate amount of sucrose and dissolve (optional). Solution can be stored protected from light for up to one month at 4˚C.

Blocking Buffer: 5% NGS or DS
> Add 5 mL of NGS or DS to 95 mL of PBS.

Staining Buffer: 1% NGS or DS
> Add 1 mL of NGS or DS to 99 mL of PBS.

For Intracellular Staining:
Triton X-100 Stock Solution: 10 %
> Triton X-100   10 mL

> Add Triton X-100 to 90 mL of dH20 and put on stir plate with stir bar. Will take ≈30-60 minutes to fully dissolve.

Permeabilization Buffer :
> Add 1 mL of Triton X-100 Stock to 99 mL of PBS (for final concentration of 0.1% Triton X-100) and mix well.
>> - higher concentrations of Triton can also be used (e.g. 0.2 %, 0.5 %)

Staining Cell Monolayers:

1]   Fix the cells in fixation buffer for 5 minutes.

2]   Rinse twice with PBS.

3]   For intracellular staining: permeabilize the cells in cold 0.1% triton-X 100 for 5 minutes.

4]   Rinse twice with PBS.

5]   Incubate in 5% NGS or DS Blocking Buffer for one hour at 37°C. Blocking serum should be chosen so as to not interfere with the primary or secondary antibody. Using serum from the donor species of the secondary antibody usually yields good results.

6]   Incubate in primary antibody, diluted to the proper concentration with 1% NGS or DS Staining Buffer, for 40 minutes at 37°C.

7]   Rinse twice with PBS.

8]   Incubate in secondary antibody diluted to the appropriate concentration in 1% NGS or DS Staining Buffer for 40 minutes at 37°C. Many fluorophores used in secondary antibodies are sensitive to light, so cover them with an opaque container. Note: Hoechst counterstain diluted to the appropriate concentration (usually 1:400) can be incubated together with the secondary antibody.

9]   Rinse twice with PBS.

10]   Rinse once in dH20.

11]   Place 1-2 drop(s) of mounting medium on the slide or coverslip to be sealed.

12]   Place a coverslip over the drop and press firmly but evenly on the coverslip to remove the air bubbles. Be careful not to slide the coverslip across the slide.

13]   Seal the coverslip with nail polish. (1.0 or less for higher magnification imaging)

14]   Place in the refrigerator protected from light if storage is necessary.

NOTES:

The following antibodies have been used with success. Typical primary antibody dilution 1:100 and secondary dilution 1:40 were used following manufacturer's recommendation. These may need optimization depending on the specific system.

Primary Antibody	Supplier	Description	Product Information
Acetylated LDL	Molecular Probes	acetylated low-density lipoprotein from human plasma, DiI complex (DiI AcLDL)	L3484
Alpha smooth muscle actin	Sigma	FITC conjugated monoclonal anti-alpha-smooth muscle actin (clone 1A4)	F 3777
Calponin	DakoCytomation	monoclonal mouse anti-human calponin (clone CALP)	M3556
CD14	Beckman Coulter	monoclonal mouse anti-human (clone RM052)	IMO643
Endoglin (CD105)	Research Diagnostics Inc.	FITC conjugated monoclonal mouse anti-human (clone 8E11)	RDI-CBL418FT
eNOS (NOS Type Ⅲ)	Santa Cruz Biotechnology	polyclonal rabbit anti-human (N-20)	sc-653
Flk-1 (VEGFR2)	Research Diagnostics Inc.	polyclonal rabbit anti-mouse Flk-1	RDI-MFLK1abrX
Flt-1 (VEGFR1)	Alpha Diagnostic International	polyclonal rabbit anti-human	FLT11-A
Myosin heavy chain (MHC)	Santa Cruz Biotechnology	monoclonal mouse anti-rat full length myosin heavy chain	sc-6956
Myosin heavy chain (MHC)	Santa Cruz Biotechnology	PE conjugated monoclonal mouse anti-rat full length myosin heavy chain	sc-6956 PE
PECAM-1 (CD31)	BD Pharmingen	FITC conjugated monoclonal mouse anti-human (clone WM59)	555445
Thrombomodulin (CD141)	DakoCytomation	monoclonal mouse anti-thrombomodulin (clone 1009)	M0617
Tissue Factor (CD142)	American Diagnostica Inc.	monoclonal mouse anti-human tissue factor	4508
Tissue Factor (CD142)	American Diagnostica Inc.	FITC conjugated monoclonal mouse anti-human tissue factor	CJ4508
Ulex europaeus lectin	Sigma	FITC conjugate	L 9006
VE-cadherin (CD144)	Santa Cruz Biotechnology	polyclonal goat anti-human (C-19)	sc-6458
Von Willebrand factor	DakoCytomation	polyclonal rabbit anti-human	A0082
Secondary Antibody	**Supplier**	**Description**	**Product Information**
	DakoCytomation	FITC conjugated polyclonal swine anti-rabbit	F0205
	DakoCytomation	FITC conjugated polyclonal rabbit anti-mouse	F0313
	Jackson Immuno Research	FITC conjugated polyclonal donkey anti-rabbit	711-095-152
	Jackson Immuno Research	FITC conjugated polyclonal donkey anti-goat	705-095-147

Reagents :

Glycine	Sigma G-8790
NaCl	Sigma S-7653
Normal Goat Serum (NGS)	Sigma G-6767
Formaldehyde (20% aqueous)	Tousimis Cat #1008A
Sucrose	
Triton X-100	Sigma X-100
Trizma Pre-Set Crystals	Sigma T-4753
Tween-20	
DPBS	

Solutions :

Tween-20 Stock Solution : 0.1 %
>   Tween-20   100 uL
>   Add Tween-20 to 100 mL of dH20 and mix well.

Tris-Buffered Saline with Tween (TBS-T)
>   Trizma Pre-Set Crystals   14.2 g
>   NaCl   11.7 g
>   Tween-20 Stock   10 mL
>
>   Dissolve the Trizma Crystals and NaCl in 990 mL dH20 and add 10 mL of 0.1%
>   Tween stock (to give a final concentration of 0.001 % Tween). Mix well. Adjust
>   pH to ~8.0 using Tris-Base/Tris-Cl at RT.

Glycine : 20 mM
>   Add 0.15 g of glycine to 100 mL of TBS-T and mix to dissolve. Adjust pH to 2-3
>   for use in protocol.

0.1% Sodium azide in PBS (PBS+SA)
>   Add 0.5 g sodium azide to 500 mL PBS

Blocking buffer: 5% NGS
>   Add 5 mL of NGS to 95 mL of TBS-T.

Staining buffer: 1% NGS
>   Add 1 mL of NGS to 99 mL of TBS-T.

Fixation buffer: Formaldehyde (for 50 mL final solution)
    4% formaldehyde   10mL of 20% aqueous
    2% sucrose   1g

    Dilute Tousimis formaldehyde (20% aqueous) to 4% in PBS. Add appropriate
    amount of sucrose and allow to dissolve. Solution can be stored protected from
    light for up to one month at 4°C.

Triton X-100 Stock Solution : 10 %
    Triton X-100   10 mL

    Add Triton X-100 to 90 mL of dH20 and put on stir plate with stir bar. Will take
    ~30-60 minutes to fully dissolve.

Permeabilization buffer :
    Add 1 mL of Triton X-100 Stock to 99 mL of TBS-T (for final concentration of
    0.1% Triton X-100) and mix well.
        - higher concentrations of Triton X-100 can also be used (e.g. 0.2 %, 0.5
    %)

Procedure starting with slides from flow chambers:

1]   In square dishes -- rinse slides in 20mL cold PBS+SA, aspirate.

2]   Add 2mL/slide of warm collagenase to slide and incubate for 5 minutes.

3]   Add 5mL growth media to each slide.

4]   Use cell lifter to gently remove cells from slide.

5]   Transfer media + cells to 15mL centrifuge tube.

6]   Rinse slide with 7mL cold PBS+SA and add to 15mL tube.

7]   Spin 1000rpm for 5 min, aspirate

8]   Add 1mL cold 4% formaldehyde+sucrose, vortex gently, incubate 5 minutes.

9]   Spin1000rpm for 5 min, aspirate

10]   Add 2mL cold 20 mM glycine solution for 15 min.

11]   Spin1000rpm for 5 min, aspirate

12]   Resuspend in 2mL TBS-T and save at 4°C for staining.

For intracellular staining (perform 13 & 14) otherwise skip to 15.

13]   Permeabilize cells in Permeabilization buffer for 5 min at room temperature.

14]   Wash cells gently 2 times in TBS-T. For each wash, suspend the cells in TBS-T
        and agitate gently, then spin down at 1000 rpm for 5 min and aspirate supernatant.

15]   In 15mL tubes, block nonspecific binding with 5% normal goat serum (diluted in
        TBS-T) for 1 hour at 37 °C. Choose blocking buffer volume so that following
        blocking, cells can be split into the appropriate number of microcentrifuge tubes
        with 0.5mL each. Blocking serum can be changed as needed depending on the
        source of the primary and secondary antibody.

16]   Transfer cells plus blocking buffer to microcentrifuge tubes and spin1000rpm for
        5 min, aspirate. (no wash).

17]   Dilute antibody & isotype control in 1% NGS/TBS-T (200uL/sample).

18]   Incubate samples in the following solutions at 37°C for 1 hour:
        Unstained control (or secondary only)   1% NGS
        Isotype control (optional)   isotype control antibody in 1% NGS
        Stained sample   antibody of interest in 1% NGS

19]   Add 1mL TBS-T, spin 1000rpm for 5 min, aspirate.

20]   Wash cells in 1mL TBS-T, spin 1000rpm for 5 min, aspirate.

21]   If necessary – incubate with secondary antibody at 37°C for 45min.

22]   Resuspend in 200uL TBS-T and transfer to flow cytometry tubes.

NOTES:

Others have suggested being consistent with buffers. TBS appeared harsh to cells on
slides so AEE started with PBS through fixation step then switch to TBS-T.

Optional: Low retention centrifuge tubes (VWR # 20170-650) can be used to minimize
cells sticking to sides of tubes. This prevents loss of cells during the multiple washing
steps.

Cells should be in suspension to begin protocol
- if cells are from monolayer culture they must be trypsinized to bring into suspension
- for preservation of surface receptors, cell dissociation solution or collagenase may be
needed.

- if cells are from 3D construct, the construct must be digested to bring cells into suspension

Note: This blocking time has not been optimized. JPS used 12-15 h at 4°C with alpha actin. Blocking should generally be done with source of secondary antibody.

To prepare sample for analysis using flow cytometry, force sample through a 40 um mesh filter. This ensures that the sample does not contain cell clusters or debris that could clog the flow cytometer nozzle.

Acknowledgement:
This protocol was based on the advice of Jan P. Stegemann.

Reagents & Supplies:

RNeasy Mini Isolation kit	Qiagen 74104
Qiashredders	Qiagen 79654
RNase-free DNase kit	Qiagen 79254
RNase/DNase Free Water	Sigma W-4502
Ethanol – molecular biology	Sigma E702-3
RNase/DNase free B-mercaptoethanol	Sigma M3148
RNase/DNase free tubes	
Agilent UV-Vis Quartz Cuvette (50µL)	

Solutions:

DNase stock

> Mix lyophilized DNase powder with water in kit to get DNase stock solution, then aliquot 100 µL and store at -20°C

Lysis Buffer

> Mix RLT buffer (10mL) with 100 µL B-ME; protect from light and store at room temp for up to a month (can scale down ie. 5ml RLT + 50µL B-ME)

70% Ethanol

> Mix 200 proof ethanol for molecular biology with RNase/DNase Free Water and store solution at RT

DNase mix

> Add 10 µL DNase stock to 70 µL RDD (in Qiagen kit) so there is 80 µL mix per sample. Prepare enough solution for 1 extra sample so there is plenty of DNase mix.

Procedure:

Prepare Cells

1]   Aspirate media, rinse with PBS and add trypsin.

2]   Quench trypsin with media and place cell/media/trypsin suspension into centrifuge tube; rinse flask with PBS and place in centrifuge tube.

3]   Spin 5-10 min at 1000 rpm and 4°C.

4]   Completely aspirate supernatant and place tubes with cell pellet on ice.

Prepare Cell Lysate

1]   Add 350 µL of lysis buffer to the tube and mix well; transfer mixture to qiashredder homogenizer column and spin in centrifuge at max for 2 minutes. (Alternative to qiashredder: Leave lysate mixture in tube and put 20-gauge needle on 3 mL syringe and place in tube. Pass the lysate 5-10 times through the needle)

2]   FREEZE at -70C at this point if desired

Isolate RNA

If using frozen samples, allow to warm at 37°C for 10min before adding ethanol

1]   Add 350 µL of 70% ethanol and mix well by pipetting

2]   Transfer 700 µL of the sample to the RNeasy mini column placed in a 2mL collection tube. Centrifuge at 10,000 rpm for 30 sec.

3]   Suck up supernatant with micropipette and add to top of column. Centrifuge at 10,000 rpm for 30 sec then discard effluent. (If solution remains above column, spin briefly to force through column)

4]   Add 350 µL of RW1 solution to the RNeasy column. Centrifuge at 10,000 rpm for 30 sec and discard the effluent.

5]   Add 80 µL DNase mix to the column and incubate at room temp for 15 minutes

6]   Add 350 µL of RW1 solution to the RNeasy column. Centrifuge at 10,000 rpm for 30 sec and discard the effluent.

7]   Discard the old collection tube and replace with a new collection tube. Add 500 µL of RPE Buffer; centrifuge at 10,000 rpm for 30 sec and discard the effluent

8]   Add 500 µL RPE Buffer and centrifuge at MAX speed for 2 minutes. If any solution remains above the column, spin again for 30-60 seconds to force through column and then discard the effluent.

9]   Label 1.5 mL collection tubes (in kit) and aliquot some RNase free water into a medium eppendorf tube

10]   Transfer the RNeasy column to the new collection tube; Add 25 µL (or desired volume) of RNase free water and incubate for 1 minute. Centrifuge at MAX speed for 1 minute and discard the RNeasy column. Place collection tube with RNA on ice.

Spec Samples to Determine Concentration and Purity

1]   Prepare small tubes (label for each sample)

2]   Aliquot 68ul water into each tube

3]   Put 2ul of sample (after mixing well) into corresponding tube

4]   Read at 260nm and 280nm

Determine sample concentration:

(avg spec reading at 260nm)*(dilution factor)*(RNA quantification value) = sample conc (ug/ml)

sample conc (ug/ml)*(volume of sample remaining) = quantity of sample

Determine sample purity:

(spec reading at 260nm/spec reading at 280nm) should be 1.8-2.1 for pure RNA

Samples are also now ready for Bioanalyzer analysis.

Acknowledgement:

This procedure was initially developed by Tiffany L. Johnson

<div style="border: 2px solid black; background-color: orange; text-align: center; padding: 20px;">

cDNA Synthesis for RT-PCR

</div>

Reagents:
SuperScript III First-Strand Synthesis System for RT-PCR   Invitrogen 18080-051
RNase/DNase Free Water   Sigma W-4502
RNase/DNase free tubes
RNA samples – concentrations known

Procedure:
<u>Carefully follow ALL steps as detailed in the SuperScript III procedure outline – details listed here are meant as a supplement only.</u>

Controls: Several controls are used in RT-PCR reactions. At this step, be sure to create –RT controls. These are samples which contain sample RNA and all reagents for cDNA synthesis EXCEPT the reverse transcriptase enzyme (therefore no cDNA will be created and these samples will be a control to check for genomic DNA during the PCR amplification steps)

Preparing RNA Samples
1]   Determine concentration and quality of RNA samples using spec and bioanalyzer prior to cDNA synthesis. You will need 1µg of RNA in NO MORE than 8µL of water for each tube (cDNA tube as well as –RT tube). If your RNA is more dilute than this, concentrate by precipitation (see protocol)
2]   Based on spec readings and concentration calculations, determine volume of RNA for each sample which gives 1µg.
3]   Using spreadsheet, calculate appropriate volumes of RNA and water for each sample for a total volume of 10µL. The components for the first step are in the following proportions:

Component	Amount
RNA (1µg)	n µL
Primer (50µM oligo dT)	1 µL
10mM dNTP mix	1 µL
RNase/DNase free water	10-(2+n) µL

cDNA Synthesis
Remember to use new tips when moving between reagents and between tubes!
Before preparing samples, turn on thermal cycler and load program to heat to 65°C.

Denaturation step:

1]   Mix and briefly centrifuge RNA samples, oligodT, and dNTP mix
2]   Label RNase/DNase free tubes for cDNA synthesis (remember –RT controls)
3]   Add correct volume of RNA to each tube, then add correct volume of water to each tube (total at this point should be 8µL)
4]   Add 1µL oligodT to each tube
5]   Add 1µL dNTP mix to each tube
6]   Vortex briefly and centrifuge to collect total volume
7]   Place in thermal cycler for 5 minutes at 65°C then place on ice for at least 1 minute.

Annealing and cDNA synthesis step:

1]   Mix and briefly centrifuge 10X RT buffer, 25mM MgCl2, 0.1M DTT, RNase out and Superscript III RT.
2]   Change program on thermal cycler to 50°C if using oligodT.
3]   Prepare enough cDNA mix for all tubes + 0.15 extra for pipetting error
4]   Create one tube for cDNA synthesis reactions and one tube for –RT reactions.
5]   Always mix reagents together into one tube in the following order:

Component	1 cDNA rxn	10 cDNA rxns	1 –RT rxn	10 –RT rxns
10X RT buffer	2 µL	20.3 µL	2 µL	20.3 µL
25mM MgCl$_2$	4 µL	40.6 µL	4 µL	40.6 µL
0.1 M DTT	2 µL	20.3 µL	2 µL	20.3 µL
RNase Out	1 µL	10.15 µL	1 µL	10.15 µL
SuperScript III RT	1 µL	10.15 µL	0	0
Rnase free water	0	0	1 µL	10.15 µL

6]   Vortex and centrifuge to collect total volume of mixture
7]   Add 10ul of cDNA mix or –RT mix to each tube, then mix gently and centrifuge briefly to collect
8]   If oligo dT was used, incubate at 50°C for 50 minutes.

Terminate Reaction and Remove RNA:

1]   Terminate the reactions at 85°C for 5 minutes and then chill on ice.
2]   Collect reactions by brief centrifugation and then add 1ul of RNase H to each tube.
3]   Incubate at 37°C for 20 minutes.
4]   Store cDNA samples at -20°C or use in PCR immediately

Acknowledgement:
This procedure was initially developed by Tiffany L. Johnson

REFERENCES

1.   WHO (2006) *World Health Organization Atlas of Heart Disease and Stroke (http://www.who.int/cardiovascular_diseases/resources/atlas/en/index.html accessed 3/1/06).*

2.   AHA (2006) *American Heart Association Heart Disease and Stroke Statistics – 2006 Update.*

3.   Patel, J., Kobashigawa, J.A. (2004) Cardiac transplantation: the alternate list and expansion of the donor pool. *Curr Opin Cardiol* 19, 162-5.

4.   Ahsan, T., Nerem, R.M. (2005) Bioengineered tissues: the science, the technology, and the industry. *Orthod Craniofac Res* 8, 134-40.

5.   Nerem, R.M., Ensley, A.E. (2004) The tissue engineering of blood vessels and the heart. *Am J Transplant* 4 Suppl 6, 36-42.

6.   Shin'oka, T., Matsumura, G., Hibino, N., Naito, Y., Watanabe, M., Konuma, T., Sakamoto, T., Nagatsu, M., Kurosawa, H. (2005) Midterm clinical result of tissue-engineered vascular autografts seeded with autologous bone marrow cells. *J Thorac Cardiovasc Surg* 129, 1330-8.

7.   L'Heureux, N., Dusserre, N., Konig, G., Victor, B., Keire, P., Wight, T.N., Chronos, N.A., Kyles, A.E., Gregory, C.R., Hoyt, G., Robbins, R.C., McAllister, T.N. (2006) Human tissue-engineered blood vessels for adult arterial revascularization. *Nat Med* 12, 361-5.

8.   Bos, G.W., Poot, A.A., Beugeling, T., van Aken, W.G., Feijen, J. (1998) Small-diameter vascular graft prostheses: current status. *Arch Physiol Biochem* 106, 100-15.

9.   Meinhart, J.G., Deutsch, M., Fischlein, T., Howanietz, N., Froschl, A., Zilla, P. (2001) Clinical autologous in vitro endothelialization of 153 infrainguinal ePTFE grafts. *Ann Thorac Surg* 71, S327-31.

10.   Rotmans, J.I., Pasterkamp, G., Verhagen, H.J., Pattynama, P.M., Blankestijn, P.J., Stroes, E.S. (2005) Hemodialysis access graft failure: time to revisit an unmet clinical need? *J Nephrol* 18, 9-20.

11.   Da Lio, A.L., Jones, N.F. (1998) New concepts and materials in microvascular grafting: prosthetic graft endothelial cell seeding and gene therapy. *Microsurgery* 18, 263-6.

12.   Windus, D.W. (1993) Permanent vascular access: a nephrologist's view. *Am J Kidney Dis* 21, 457-71.

13.   Hanson, S.R., Harker, L.A. (1996) Blood Coagulation and Blood-Materials Interactions. In *Biomaterials Science An Introduction to Materials in Medicine* (B. D. Ratner, A. S. Hoffman, F. J. Schoen and J. E. Lemons, eds), Academic Press, San Diego, CA 193-199.

14.   Lin, P.H., Chen, C., Bush, R.L., Yao, Q., Lumsden, A.B., Hanson, S.R. (2004) Small-caliber heparin-coated ePTFE grafts reduce platelet deposition and neointimal hyperplasia in a baboon model. *J Vasc Surg* 39, 1322-8.

15.   Chen, C., Ofenloch, J.C., Yianni, Y.P., Hanson, S.R., Lumsden, A.B. (1998) Phosphorylcholine coating of ePTFE reduces platelet deposition and neointimal hyperplasia in arteriovenous grafts. *J Surg Res* 77, 119-25.

16.   Jaffe, J.A. (1988) Endothelial Cells. In *Inflammation: basic principles and clinical correlates* (J. I. Gallin, I. M. Goldstein and R. Snyderman, eds), Raven Press, Ltd., New York.

17.   Martini, F.H. (1998) *Fundamentals of anatomy and physiology*. Prentice Hall, Inc., New Jersey.

18.   Cines, D.B., Pollak, E.S., Buck, C.A., Loscalzo, J., Zimmerman, G.A., McEver, R.P., Pober, J.S., Wick, T.M., Konkle, B.A., Schwartz, B.S., Barnathan, E.S., McCrae, K.R., Hug, B.A., Schmidt, A.M., Stern, D.M. (1998) Endothelial cells in physiology and in the pathophysiology of vascular disorders. *Blood* 91, 3527-61.

19.   van Hinsbergh, V.W. (2001) The endothelium: vascular control of haemostasis. *Eur J Obstet Gynecol Reprod Biol* 95, 198-201.

20.   Sporn, L.A., Huber, P. (2001) Endothelial Cell Biology. In *Hemostasis and thrombosis : basic principles and clinical practice* (R. W. Colman, J. Hirsh, V. J. Marder, A. W. Clowes and J. N. George, eds), Lippincott Williams & Wilkins, Philadelphia 615-623.

21.   Duda, D.G., Fukumura, D., Jain, R.K. (2004) Role of eNOS in neovascularization: NO for endothelial progenitor cells. *Trends Mol Med* 10, 143-5.

22.   Rees, D.D., Higgs, E.A., Moncado, S. (2001) Nitric oxide and the vessel wall. In *Hemostasis and thrombosis : basic principles and clinical practice* (R. W. Colman, J. Hirsh, V. J. Marder, A. W. Clowes and J. N. George, eds), Lippincott Williams & Wilkins, Philadelphia 1577.

23.   Pearson, P.J., Evora, P.R., Schaff, H.V. (1992) Bioassay of EDRF from internal mammary arteries: implications for early and late bypass graft patency. *Ann Thorac Surg* 54, 1078-84.

24. Shapira, O.M., Xu, A., Aldea, G.S., Vita, J.A., Shemin, R.J., Keaney, J.F., Jr. (1999) Enhanced nitric oxide-mediated vascular relaxation in radial artery compared with internal mammary artery or saphenous vein. *Circulation* 100, II322-7.

25. Panaro, N.J., McIntire, L.V. (1993) Flow and Shear Stress Effects on Endothelial Cell Function. In *Hemodynamic Forces and Vascular Biology* (B. E. Sumpio, ed) R.G. Landes Company, Austin, TX 119.

26. Zarins, C.K., Giddens, D.P., Bharadvaj, B.K., Sottiurai, V.S., Mabon, R.F., Glagov, S. (1983) Carotid bifurcation atherosclerosis. Quantitative correlation of plaque localization with flow velocity profiles and wall shear stress. *Circ Res* 53, 502-14.

27. Gimbrone, M.A., Cotran, R.S., Folkman, J. (1974) Human Vascular Endothelial Cells in Culture: Growth and DNA Synthesis. *The Journal of Cell Biology* 60, 673-684.

28. Jaffe, E.A., Nachman, R.L., Becker, C.G., Minick, C.R. (1973) Culture of human endothelial cells derived from umbilical veins. *J Clin Invest* 52, 2745-56.

29. Lewis, L.J., Hoak, J.C., Maca, R.D., Fry, G.L. (1973) Replication of human endothelial cells in culture. *Science* 181, 453-4.

30. Ku, D.N., Zhu, C. (1993) The Mechanical Environment of the Artery. In *Hemodynamic Forces and Vascular Biology* (B. E. Sumpio, ed) R.G. Landes Company, Austin, TX 119.

31. Eskin, S.G., Ives, C.L., McIntire, L.V., Navarro, L.T. (1984) Response of cultured endothelial cells to steady flow. *Microvasc Res* 28, 87-94.

32. Dewey, C.F., Jr., Bussolari, S.R., Gimbrone, M.A., Jr., Davies, P.F. (1981) The dynamic response of vascular endothelial cells to fluid shear stress. *J Biomech Eng* 103, 177-85.

33. Remuzzi, A., Dewey, C.F., Jr., Davies, P.F., Gimbrone, M.A., Jr. (1984) Orientation of endothelial cells in shear fields in vitro. *Biorheology* 21, 617-30.

34. Levesque, M.J., Nerem, R.M. (1985) The elongation and orientation of cultured endothelial cells in response to shear stress. *J Biomech Eng* 107, 341-7.

35. Gimbrone, M.A., Jr., Topper, J.N., Nagel, T., Anderson, K.R., Garcia-Cardena, G. (2000) Endothelial dysfunction, hemodynamic forces, and atherogenesis. *Ann N Y Acad Sci* 902, 230-9; discussion 239-40.

36. Davies, P.F. (1995) Flow-mediated endothelial mechanotransduction. *Physiol Rev* 75, 519-60.

37. Resnick, N., Gimbrone, M.A., Jr. (1995) Hemodynamic forces are complex regulators of endothelial gene expression. *FASEB J* 9, 874-82.

38. Ali, M.H., Schumacker, P.T. (2002) Endothelial responses to mechanical stress: where is the mechanosensor? *Crit Care Med* 30, S198-206.

39. Traub, O., Berk, B.C. (1998) Laminar shear stress: mechanisms by which endothelial cells transduce an atheroprotective force. *Arterioscler Thromb Vasc Biol* 18, 677-85.

40. Cunningham, K.S., Gotlieb, A.I. (2005) The role of shear stress in the pathogenesis of atherosclerosis. *Lab Invest* 85, 9-23.

41. Shyy, J.Y., Chien, S. (2002) Role of integrins in endothelial mechanosensing of shear stress. *Circ Res* 91, 769-75.

42. Fisher, A.B., Chien, S., Barakat, A.I., Nerem, R.M. (2001) Endothelial cellular response to altered shear stress. *Am J Physiol Lung Cell Mol Physiol* 281, L529-33.

43. Frangos, J.A., Eskin, S.G., McIntire, L.V., Ives, C.L. (1985) Flow effects on prostacyclin production by cultured human endothelial cells. *Science* 227, 1477-9.

44. Grabowski, E.F., Jaffe, E.A., Weksler, B.B. (1985) Prostacyclin production by cultured endothelial cell monolayers exposed to step increases in shear stress. *J Lab Clin Med* 105, 36-43.

45. Rubanyi, G.M., Romero, J.C., Vanhoutte, P.M. (1986) Flow-induced release of endothelium-derived relaxing factor. *Am J Physiol* 250, H1145-9.

46. Busse, R., Pohl, U., Luckhoff, A. (1989) Mechanisms controlling the production of endothelial autacoids. *Z Kardiol* 78 Suppl 6, 64-9.

47. Stamler, J., Mendelsohn, M.E., Amarante, P., Smick, D., Andon, N., Davies, P.F., Cooke, J.P., Loscalzo, J. (1989) N-acetylcysteine potentiates platelet inhibition by endothelium-derived relaxing factor. *Circ Res* 65, 789-95.

48. Diamond, S.L., Eskin, S.G., McIntire, L.V. (1989) Fluid flow stimulates tissue plasminogen activator secretion by cultured human endothelial cells. *Science* 243, 1483-5.

49. Diamond, S.L., Sharefkin, J.B., Dieffenbach, C., Frasier-Scott, K., McIntire, L.V., Eskin, S.G. (1990) Tissue plasminogen activator messenger RNA levels increase in cultured human endothelial cells exposed to laminar shear stress. *J Cell Physiol* 143, 364-71.

50. Westmuckett, A.D., Lupu, C., Roquefeuil, S., Krausz, T., Kakkar, V.V., Lupu, F. (2000) Fluid flow induces upregulation of synthesis and release of tissue factor pathway inhibitor in vitro. *Arterioscler Thromb Vasc Biol* 20, 2474-82.

51. Malek, A.M., Jackman, R., Rosenberg, R.D., Izumo, S. (1994) Endothelial expression of thrombomodulin is reversibly regulated by fluid shear stress. *Circ Res* 74, 852-60.

52. Takada, Y., Shinkai, F., Kondo, S., Yamamoto, S., Tsuboi, H., Korenaga, R., Ando, J. (1994) Fluid shear stress increases the expression of thrombomodulin by cultured human endothelial cells. *Biochem Biophys Res Commun* 205, 1345-52.

53. Motwani, J.G., Topol, E.J. (1998) Aortocoronary saphenous vein graft disease: pathogenesis, predisposition, and prevention. *Circulation* 97, 916-31.

54. Kim, A.Y., Walinsky, P.L., Kolodgie, F.D., Bian, C., Sperry, J.L., Deming, C.B., Peck, E.A., Shake, J.G., Ang, G.B., Sohn, R.H., Esmon, C.T., Virmani, R., Stuart, R.S., Rade, J.J. (2002) Early loss of thrombomodulin expression impairs vein graft thromboresistance: implications for vein graft failure. *Circ Res* 90, 205-12.

55. Sperry, J.L., Deming, C.B., Bian, C., Walinsky, P.L., Kass, D.A., Kolodgie, F.D., Virmani, R., Kim, A.Y., Rade, J.J. (2003) Wall tension is a potent negative regulator of in vivo thrombomodulin expression. *Circ Res* 92, 41-7.

56. Gosling, M., Golledge, J., Turner, R.J., Powell, J.T. (1999) Arterial flow conditions downregulate thrombomodulin on saphenous vein endothelium. *Circulation* 99, 1047-53.

57. Kuchan, M.J., Frangos, J.A. (1993) Shear stress regulates endothelin-1 release via protein kinase C and cGMP in cultured endothelial cells. *Am J Physiol* 264, H150-6.

58. Malek, A.M., Greene, A.L., Izumo, S. (1993) Regulation of endothelin 1 gene by fluid shear stress is transcriptionally mediated and independent of protein kinase C and cAMP. *Proc Natl Acad Sci U S A* 90, 5999-6003.

59. Mazzolai, L., Silacci, P., Bouzourene, K., Daniel, F., Brunner, H., Hayoz, D. (2002) Tissue factor activity is upregulated in human endothelial cells exposed to oscillatory shear stress. *Thromb Haemost* 87, 1062-8.

60. Grabowski, E.F., Reininger, A.J., Petteruti, P.G., Tsukurov, O., Orkin, R.W. (2001) Shear stress decreases endothelial cell tissue factor activity by augmenting secretion of tissue factor pathway inhibitor. *Arterioscler Thromb Vasc Biol* 21, 157-62.

61. Herring, M.B., Dilley, R., Jersild, R.A., Jr., Boxer, L., Gardner, A., Glover, J. (1979) Seeding arterial prostheses with vascular endothelium. The nature of the lining. *Ann Surg* 190, 84-90.

62.   Rupnick, M.A., Hubbard, F.A., Pratt, K., Jarrell, B.E., Williams, S.K. (1989) Endothelialization of vascular prosthetic surfaces after seeding or sodding with human microvascular endothelial cells. *J Vasc Surg* 9, 788-95.

63.   Wang, Z.G., Du, W., Li, G.D., Pu, L.Q., Sharefkin, J.B. (1990) Rapid cellular luminal coverage of Dacron inferior vena cava prostheses in dogs by immediate seeding of autogenous endothelial cells derived from omental tissue: results of a preliminary trial. *J Vasc Surg* 12, 168-79.

64.   Hedeman Joosten, P.P., Verhagen, H.J., Heijnen-Snyder, G.J., van Vroonhoven, T.J., Sixma, J.J., de Groot, P.G., Eikelboom, B.C. (1998) Thrombogenesis of different cell types seeded on vascular grafts and studied under blood-flow conditions. *J Vasc Surg* 28, 1094-103.

65.   Williams, S.K. (1991) Endothelial cell transplantation. *Cell Transplantation* 4, 401-410.

66.   Pasic, M., Muller-Glauser, W., von Segesser, L., Odermatt, B., Lachat, M., Turina, M. (1996) Endothelial cell seeding improves patency of synthetic vascular grafts: manual versus automatized method. *Eur J Cardiothorac Surg* 10, 372-9.

67.   Berger, K., Sauvage, L.R., Rao, A.M., Wood, S.J. (1972) Healing of arterial prostheses in man: its incompleteness. *Ann Surg* 175, 118-27.

68.   Deutsch, M., Meinhart, J., Vesely, M., Fischlein, T., Groscurth, P., von Oppell, U., Zilla, P. (1997) In vitro endothelialization of expanded polytetrafluoroethylene grafts: a clinical case report after 41 months of implantation. *J Vasc Surg* 25, 757-63.

69.   Laube, H.R., Duwe, J., Rutsch, W., Konertz, W. (2000) Clinical experience with autologous endothelial cell-seeded polytetrafluoroethylene coronary artery bypass grafts. *J Thorac Cardiovasc Surg* 120, 134-41.

70.   Karube, N., Soma, T., Noishiki, Y., Yamazaki, I., Kosuge, T., Ichikawa, Y., Takanashi, Y. (2001) Clinical long-term results of vascular prosthesis sealed with fragmented autologous adipose tissue. *Artif Organs* 25, 218-22.

71.   Weinberg, C.B., Bell, E. (1986) A blood vessel model constructed from collagen and cultured vascular cells. *Science* 231, 397-400.

72.   Barocas, V.H., Girton, T.S., Tranquillo, R.T. (1998) Engineered alignment in media equivalents: magnetic prealignment and mandrel compaction. *J Biomech Eng* 120, 660-6.

73.   Ogle, B.M., Mooradian, D.L. (2002) Manipulation of remodeling pathways to enhance the mechanical properties of a tissue engineered blood vessel. *J Biomech Eng* 124, 724-33.

74. Girton, T.S., Oegema, T.R., Tranquillo, R.T. (1999) Exploiting glycation to stiffen and strengthen tissue equivalents for tissue engineering. *J Biomed Mater Res* 46, 87-92.

75. Berglund, J.D., Mohseni, M.M., Nerem, R.M., Sambanis, A. (2003) A biological hybrid model for collagen-based tissue engineered vascular constructs. *Biomaterials* 24, 1241-54.

76. Matsuda, T., He, H. (2002) Newly designed compliant hierarchic hybrid vascular grafts wrapped with a microprocessed elastomeric film--I: Fabrication procedure and compliance matching. *Cell Transplant* 11, 67-74.

77. Seliktar, D., Black, R.A., Vito, R.P., Nerem, R.M. (2000) Dynamic mechanical conditioning of collagen-gel blood vessel constructs induces remodeling in vitro [In Process Citation]. *Ann Biomed Eng* 28, 351-62.

78. Seliktar, D., Nerem, R.M., Galis, Z.S. (2003) Mechanical Strain-Stimulated Remodeling of Tissue-Engineered Blood Vessel Constructs. *Tissue Engineering* 9, 657-666.

79. Hodde, J. (2002) Naturally occurring scaffolds for soft tissue repair and regeneration. *Tissue Eng* 8, 295-308.

80. Lantz, G.C., Badylak, S.F., Hiles, M.C., Coffey, A.C., Geddes, L.A., Kokini, K., Sandusky, G.E., Morff, R.J. (1993) Small intestinal submucosa as a vascular graft: a review. *J Invest Surg* 6, 297-310.

81. Grassl, E.D., Oegema, T.R., Tranquillo, R.T. (2002) Fibrin as an alternative biopolymer to type-I collagen for the fabrication of a media equivalent. *J Biomed Mater Res* 60, 607-12.

82. Ye, Q., Zund, G., Benedikt, P., Jockenhoevel, S., Hoerstrup, S.P., Sakyama, S., Hubbell, J.A., Turina, M. (2000) Fibrin gel as a three dimensional matrix in cardiovascular tissue engineering. *Eur J Cardiothorac Surg* 17, 587-91.

83. Niklason, L.E., Gao, J., Abbott, W.M., Hirschi, K.K., Houser, S., Marini, R., Langer, R. (1999) Functional arteries grown in vitro. *Science* 284, 489-93.

84. Agrawal, C.M., Athanasiou, K.A. (1997) Technique to control pH in vicinity of biodegrading PLA-PGA implants. *J Biomed Mater Res* 38, 105-14.

85. Athanasiou, K.A., Niederauer, G.G., Agrawal, C.M. (1996) Sterilization, toxicity, biocompatibility and clinical applications of polylactic acid/polyglycolic acid copolymers. *Biomaterials* 17, 93-102.

86. L'Heureux, N., Paquet, S., Labbe, R., Germain, L., Auger, F.A. (1998) A completely biological tissue-engineered human blood vessel. *Faseb J* 12, 47-56.

87. Campbell, J.H., Efendy, J.L., Campbell, G.R. (1999) Novel vascular graft grown within recipient's own peritoneal cavity. *Circ Res* 85, 1173-8.

88. Levenberg, S., Golub, J.S., Amit, M., Itskovitz-Eldor, J., Langer, R. (2002) Endothelial cells derived from human embryonic stem cells. *Proc Natl Acad Sci U S A* 99, 4391-6.

89. Vittet, D., Prandini, M.H., Berthier, R., Schweitzer, A., Martin-Sisteron, H., Uzan, G., Dejana, E. (1996) Embryonic stem cells differentiate in vitro to endothelial cells through successive maturation steps. *Blood* 88, 3424-31.

90. Yamashita, J., Itoh, H., Hirashima, M., Ogawa, M., Nishikawa, S., Yurugi, T., Naito, M., Nakao, K. (2000) Flk1-positive cells derived from embryonic stem cells serve as vascular progenitors. *Nature* 408, 92-6.

91. Asahara, T., Murohara, T., Sullivan, A., Silver, M., van der Zee, R., Li, T., Witzenbichler, B., Schatteman, G., Isner, J.M. (1997) Isolation of putative progenitor endothelial cells for angiogenesis. *Science* 275, 964-7.

92. Asahara, T., Masuda, H., Takahashi, T., Kalka, C., Pastore, C., Silver, M., Kearne, M., Magner, M., Isner, J.M. (1999) Bone marrow origin of endothelial progenitor cells responsible for postnatal vasculogenesis in physiological and pathological neovascularization. *Circ Res* 85, 221-8.

93. PubMed ((www.pubmed.gov)) National Library of Medicine 2/1/06.

94. Hristov, M., Weber, C. (2004) Endothelial progenitor cells: characterization, pathophysiology, and possible clinical relevance. *J Cell Mol Med* 8, 498-508.

95. Ingram, D.A., Caplice, N.M., Yoder, M.C. (2005) Unresolved questions, changing definitions, and novel paradigms for defining endothelial progenitor cells. *Blood* 106, 1525-1531.

96. Iwami, Y., Masuda, H., Asahara, T. (2004) Endothelial progenitor cells: past, state of the art, and future. *J Cell Mol Med* 8, 488-97.

97. Khakoo, A.Y., Finkel, T. (2005) Endothelial progenitor cells. *Annu Rev Med* 56, 79-101.

98. Rafii, S., Lyden, D. (2003) Therapeutic stem and progenitor cell transplantation for organ vascularization and regeneration. *Nat Med* 9, 702-12.

99. Urbich, C., Dimmeler, S. (2004) Endothelial progenitor cells - Characterization and role in vascular biology. *Circulation Research* 95, 343-353.

100. Zammaretti, P., Zisch, A.H. (2005) Adult 'endothelial progenitor cells' - Renewing vasculature. *International Journal of Biochemistry & Cell Biology* 37, 493-503.

101. Stump, M.M., Jordan, G.L., Jr., Debakey, M.E., Halpert, B. (1963) Endothelium Grown from Circulating Blood on Isolated Intravascular Dacron Hub. *Am J Pathol* 43, 361-7.

102. Scott, S.M., Barth, M.G., Gaddy, L.R., Ahl, E.T., Jr. (1994) The role of circulating cells in the healing of vascular prostheses. *J Vasc Surg* 19, 585-93.

103. Suzuki, T., Nishida, M., Futami, S., Fukino, K., Amaki, T., Aizawa, K., Chiba, S., Hirai, H., Maekawa, K., Nagai, R. (2003) Neoendothelialization after peripheral blood stem cell transplantation in humans: a case report of a Tokaimura nuclear accident victim. *Cardiovasc Res* 58, 487-92.

104. Kouchi, Y., Onuki, Y., Wu, M.H., Shi, Q., Ghali, R., Wechezak, A.R., Kaplan, S., Walker, M., Sauvage, L.R. (1998) Apparent blood stream origin of endothelial and smooth muscle cells in the neointima of long, impervious carotid-femoral grafts in the dog. *Ann Vasc Surg* 12, 46-54.

105. Rafii, S., Oz, M.C., Seldomridge, J.A., Ferris, B., Asch, A.S., Nachman, R.L., Shapiro, F., Rose, E.A., Levin, H.R. (1995) Characterization of hematopoietic cells arising on the textured surface of left ventricular assist devices. *Ann Thorac Surg* 60, 1627-32.

106. Pelosi, E., Valtieri, M., Coppola, S., Botta, R., Gabbianelli, M., Lulli, V., Marziali, G., Masella, B., Muller, R., Sgadari, C., Testa, U., Bonanno, G., Peschle, C. (2002) Identification of the hemangioblast in postnatal life. *Blood* 100, 3203-8.

107. Loges, S., Fehse, B., Brockmann, M.A., Lamszus, K., Butzal, M., Guckenbiehl, M., Schuch, G., Ergun, S., Fischer, U., Zander, A.R., Hossfeld, D.K., Fiedler, W., Gehling, U.M. (2004) Identification of the adult human hemangioblast. *Stem Cells Dev* 13, 229-42.

108. Zhang, R.X., Yang, H., Li, M., Yao, Q.Z., Chen, C.Y. (2005) Acceleration of endothelial-like cell differentiation from CD14(+) monocytes in vitro. *Experimental Hematology* 33, 1554-1563.

109. Mutin, M., Canavy, I., Blann, A., Bory, M., Sampol, J., Dignat-George, F. (1999) Direct evidence of endothelial injury in acute myocardial infarction and unstable angina by demonstration of circulating endothelial cells. *Blood* 93, 2951-8.

110. Shi, Q., Rafii, S., Wu, M.H., Wijelath, E.S., Yu, C., Ishida, A., Fujita, Y., Kothari, S., Mohle, R., Sauvage, L.R., Moore, M.A., Storb, R.F., Hammond, W.P. (1998) Evidence for circulating bone marrow-derived endothelial cells. *Blood* 92, 362-7.

111. Yin, A.H., Miraglia, S., Zanjani, E.D., Almeida-Porada, G., Ogawa, M., Leary, A.G., Olweus, J., Kearney, J., Buck, D.W. (1997) AC133, a novel marker for human hematopoietic stem and progenitor cells. *Blood* 90, 5002-12.

112. Gehling, U.M., Ergun, S., Schumacher, U., Wagener, C., Pantel, K., Otte, M., Schuch, G., Schafhausen, P., Mende, T., Kilic, N., Kluge, K., Schafer, B., Hossfeld, D.K., Fiedler, W. (2000) In vitro differentiation of endothelial cells from AC133-positive progenitor cells. *Blood* 95, 3106-12.

113. Friedrich, E.B., Walenta, K., Scharlau, J., Nickenig, G., Werner, N. (2006) A CD34-/CD133+/VEGFR-2+ Endothelial Progenitor Cell Subpopulation With Potent Vasoregenerative Capacities. *Circ Res*.

114. Peichev, M., Naiyer, A.J., Pereira, D., Zhu, Z., Lane, W.J., Williams, M., Oz, M.C., Hicklin, D.J., Witte, L., Moore, M.A., Rafii, S. (2000) Expression of VEGFR-2 and AC133 by circulating human CD34(+) cells identifies a population of functional endothelial precursors. *Blood* 95, 952-8.

115. Handgretinger, R., Gordon, P.R., Leimig, T., Chen, X., Buhring, H.J., Niethammer, D., Kuci, S. (2003) Biology and plasticity of CD133+ hematopoietic stem cells. *Ann N Y Acad Sci* 996, 141-51.

116. Reyes, M., Dudek, A., Jahagirdar, B., Koodie, L., Marker, P.H., Verfaillie, C.M. (2002) Origin of endothelial progenitors in human postnatal bone marrow. *J Clin Invest* 109, 337-46.

117. Fernandez Pujol, B., Lucibello, F.C., Gehling, U.M., Lindemann, K., Weidner, N., Zuzarte, M.L., Adamkiewicz, J., Elsasser, H.P., Muller, R., Havemann, K. (2000) Endothelial-like cells derived from human CD14 positive monocytes. *Differentiation* 65, 287-300.

118. Schmeisser, A., Garlichs, C.D., Zhang, H., Eskafi, S., Graffy, C., Ludwig, J., Strasser, R.H., Daniel, W.G. (2001) Monocytes coexpress endothelial and macrophagocytic lineage markers and form cord-like structures in Matrigel under angiogenic conditions. *Cardiovasc Res* 49, 671-80.

119. Urbich, C., Heeschen, C., Aicher, A., Dernbach, E., Zeiher, A.M., Dimmeler, S. (2003) Relevance of monocytic features for neovascularization capacity of circulating endothelial progenitor cells. *Circulation* 108, 2511-6.

120. Rehman, J., Li, J., Orschell, C.M., March, K.L. (2003) Peripheral blood "endothelial progenitor cells" are derived from monocyte/macrophages and secrete angiogenic growth factors. *Circulation* 107, 1164-9.

121. Zhao, Y., Glesne, D., Huberman, E. (2003) A human peripheral blood monocyte-derived subset acts as pluripotent stem cells. *Proc Natl Acad Sci U S A* 100, 2426-31.

122. Hill, J.M., Zalos, G., Halcox, J.P., Schenke, W.H., Waclawiw, M.A., Quyyumi, A.A., Finkel, T. (2003) Circulating endothelial progenitor cells, vascular function, and cardiovascular risk. *N Engl J Med* 348, 593-600.

123. Lin, Y., Weisdorf, D.J., Solovey, A., Hebbel, R.P. (2000) Origins of circulating endothelial cells and endothelial outgrowth from blood. *J Clin Invest* 105, 71-7.

124. Lin, Y., Chang, L., Solovey, A., Healey, J.F., Lollar, P., Hebbel, R.P. (2002) Use of blood outgrowth endothelial cells for gene therapy for hemophilia A. *Blood* 99, 457-62.

125. Swerlick, R.A., Lee, K.H., Wick, T.M., Lawley, T.J. (1992) Human dermal microvascular endothelial but not human umbilical vein endothelial cells express CD36 in vivo and in vitro. *J Immunol* 148, 78-83.

126. Dimmeler, S., Aicher, A., Vasa, M., Mildner-Rihm, C., Adler, K., Tiemann, M., Rutten, H., Fichtlscherer, S., Martin, H., Zeiher, A.M. (2001) HMG-CoA reductase inhibitors (statins) increase endothelial progenitor cells via the PI 3-kinase/Akt pathway. *J Clin Invest* 108, 391-7.

127. Eggermann, J., Kliche, S., Jarmy, G., Hoffmann, K., Mayr-Beyrle, U., Debatin, K.M., Waltenberger, J., Beltinger, C. (2003) Endothelial progenitor cell culture and differentiation in vitro: a methodological comparison using human umbilical cord blood. *Cardiovasc Res* 58, 478-86.

128. Griese, D.P., Achatz, S., Batzlsperger, C.A., Strauch, U.G., Grumbeck, B., Weil, J., Riegger, G.A. (2003) Vascular gene delivery of anticoagulants by transplantation of retrovirally-transduced endothelial progenitor cells. *Cardiovasc Res* 58, 469-77.

129. Griese, D.P., Ehsan, A., Melo, L.G., Kong, D., Zhang, L., Mann, M.J., Pratt, R.E., Mulligan, R.C., Dzau, V.J. (2003) Isolation and transplantation of autologous circulating endothelial cells into denuded vessels and prosthetic grafts: implications for cell-based vascular therapy. *Circulation* 108, 2710-5.

130. Gulati, R., Jevremovic, D., Peterson, T.E., Chatterjee, S., Shah, V., Vile, R.G., Simari, R.D. (2003) Diverse origin and function of cells with endothelial phenotype obtained from adult human blood. *Circ Res* 93, 1023-5.

131. Gulati, R., Jevremovic, D., Witt, T.A., Kleppe, L.S., Vile, R.G., Lerman, A., Simari, R.D. (2004) Modulation of the vascular response to injury by autologous blood-derived outgrowth endothelial cells. *American Journal of Physiology-Heart and Circulatory Physiology* 287, H512-H517.

132. He, T., Peterson, T.E., Holmuhamedov, E.L., Terzic, A., Caplice, N.M., Oberley, L.W., Katusic, Z.S. (2004) Human endothelial progenitor cells tolerate oxidative stress due to intrinsically high expression of manganese superoxide dismutase. *Arterioscler Thromb Vasc Biol* 24, 2021-7.

133. Hur, J., Yoon, C.H., Kim, H.S., Choi, J.H., Kang, H.J., Hwang, K.K., Oh, B.H., Lee, M.M., Park, Y.B. (2004) Characterization of two types of endothelial

progenitor cells and their different contributions to neovasculogenesis. *Arterioscler Thromb Vasc Biol* 24, 288-93.

134. Ingram, D.A., Mead, L.E., Moore, D.B., Woodard, W., Fenoglio, A., Yoder, M.C. (2005) Vessel wall-derived endothelial cells rapidly proliferate because they contain a complete hierarchy of endothelial progenitor cells. *Blood* 105, 2783-2786.

135. Ingram, D.A., Mead, L.E., Tanaka, H., Meade, V., Fenoglio, A., Mortell, K., Pollok, K., Ferkowicz, M.J., Gilley, D., Yoder, M.C. (2004) Identification of a novel hierarchy of endothelial progenitor cells using human peripheral and umbilical cord blood. *Blood* 104, 2752-2760.

136. Simper, D., Stalboerger, P.G., Panetta, C.J., Wang, S., Caplice, N.M. (2002) Smooth muscle progenitor cells in human blood. *Circulation* 106, 1199-204.

137. Tepper, O.M., Galiano, R.D., Capla, J.M., Kalka, C., Gagne, P.J., Jacobowitz, G.R., Levine, J.P., Gurtner, G.C. (2002) Human endothelial progenitor cells from type II diabetics exhibit impaired proliferation, adhesion, and incorporation into vascular structures. *Circulation* 106, 2781-6.

138. Wagner, S.J., Myrup, A.C. (2005) Toward closed-system culture of blood origin endothelial cells. *Transfusion* 45, 1201-1207.

139. Walenta, K., Friedrich, E.B., Sehnert, F., Werner, N., Nickenig, G. (2005) In vitro differentiation characteristics of cultured human mononuclear cells-implications for endothelial progenitor cell biology. *Biochem Biophys Res Commun* 333, 476-82.

140. Yoon, C.H., Hur, J., Park, K.W., Kim, J.H., Lee, C.S., Oh, I.Y., Kim, T.Y., Cho, H.J., Kang, H.J., Chae, I.H., Yang, H.K., Oh, B.H., Park, Y.B., Kim, H.S. (2005) Synergistic Neovascularization by mixed transplantation of early endothelial progenitor cells and late outgrowth endothelial cells - The role of angiogenic cytokines and matrix metalloproteinases. *Circulation* 112, 1618-1627.

141. Assmus, B., Schachinger, V., Teupe, C., Britten, M., Lehmann, R., Dobert, N., Grunwald, F., Aicher, A., Urbich, C., Martin, H., Hoelzer, D., Dimmeler, S., Zeiher, A.M. (2002) Transplantation of Progenitor Cells and Regeneration Enhancement in Acute Myocardial Infarction (TOPCARE-AMI). *Circulation* 106, 3009-17.

142. Kalka, C., Masuda, H., Takahashi, T., Kalka-Moll, W.M., Silver, M., Kearney, M., Li, T., Isner, J.M., Asahara, T. (2000) Transplantation of ex vivo expanded endothelial progenitor cells for therapeutic neovascularization. *Proc Natl Acad Sci U S A* 97, 3422-7.

143. Murasawa, S., Llevadot, J., Silver, M., Isner, J.M., Losordo, D.W., Asahara, T. (2002) Constitutive human telomerase reverse transcriptase expression enhances regenerative properties of endothelial progenitor cells. *Circulation* 106, 1133-9.

144. Gulati, R., Simari, R.D. (2005) Cell therapy for angiogenesis - Embracing diversity. *Circulation* 112, 1522-1524.

145. Yamamoto, K., Takahashi, T., Asahara, T., Ohura, N., Sokabe, T., Kamiya, A., Ando, J. (2003) Proliferation, differentiation, and tube formation by endothelial progenitor cells in response to shear stress. *J Appl Physiol* 95, 2081-8.

146. Rossig, L., Urbich, C., Bruhl, T., Dernbach, E., Heeschen, C., Chavakis, E., Sasaki, K., Aicher, D., Diehl, F., Seeger, F., Potente, M., Aicher, A., Zanetta, L., Dejana, E., Zeiher, A.M., Dimmeler, S. (2005) Histone deacetylase activity is essential for the expression of HoxA9 and for endothelial commitment of progenitor cells. *J Exp Med* 201, 1825-35.

147. Yang, Z., Tao, J., Wang, J.M., Tu, C., Xu, M.G., Wang, Y., Pan, S.R. (2006) Shear stress contributes to t-PA mRNA expression in human endothelial progenitor cells and nonthrombogenic potential of small diameter artificial vessels. *Biochem Biophys Res Commun* 342, 577-84.

148. Stachelek, S.J., Alferiev, I., Choi, H., Kronsteiner, A., Uttayarat, P., Gooch, K.J., Composto, R.J., Chen, I.W., Hebbel, R.P., Levy, R.J. (2005) Cholesterol-derivatized polyurethane: characterization and endothelial cell adhesion. *J Biomed Mater Res A* 72, 200-12.

149. Stachelek, S.J., Alferiev, I., Connolly, J.M., Sacks, M., Hebbel, R.P., Bianco, R., Levy, R.J. (2006) Cholesterol-modified polyurethane valve cusps demonstrate blood outgrowth endothelial cell adhesion post-seeding in vitro and in vivo. *Ann Thorac Surg* 81, 47-55.

150. Schmidt, D., Breymann, C., Weber, A., Guenter, C.I., Neuenschwander, S., Zund, G., Turina, M., Hoerstrup, S.P. (2004) Umbilical cord blood derived endothelial progenitor cells for tissue engineering of vascular grafts. *Ann Thorac Surg* 78, 2094-8.

151. Dvorin, E.L., Wylie-Sears, J., Kaushal, S., Martin, D.P., Bischoff, J. (2003) Quantitative evaluation of endothelial progenitors and cardiac valve endothelial cells: proliferation and differentiation on poly-glycolic acid/poly-4-hydroxybutyrate scaffold in response to vascular endothelial growth factor and transforming growth factor beta1. *Tissue Eng* 9, 487-93.

152. Wu, X., Rabkin-Aikawa, E., Guleserian, K.J., Perry, T.E., Masuda, Y., Sutherland, F.W., Schoen, F.J., Mayer, J.E., Jr., Bischoff, J. (2004) Tissue-engineered microvessels on three-dimensional biodegradable scaffolds using human endothelial progenitor cells. *Am J Physiol Heart Circ Physiol* 287, H480-7.

153. Sieminski, A.L., Hebbel, R.P., Gooch, K.J. (2005) Improved microvascular network in vitro by human blood outgrowth endothelial cells relative to vessel-derived endothelial cells. *Tissue Engineering* 11, 1332-1345.

154. Bhattacharya, V., McSweeney, P.A., Shi, Q., Bruno, B., Ishida, A., Nash, R., Storb, R.F., Sauvage, L.R., Hammond, W.P., Wu, M.H. (2000) Enhanced endothelialization and microvessel formation in polyester grafts seeded with CD34(+) bone marrow cells. *Blood* 95, 581-5.

155. Boyer, M., Townsend, L.E., Vogel, L.M., Falk, J., Reitz-Vick, D., Trevor, K.T., Villalba, M., Bendick, P.J., Glover, J.L. (2000) Isolation of endothelial cells and their progenitor cells from human peripheral blood. *J Vasc Surg* 31, 181-9.

156. He, H., Shirota, T., Yasui, H., Matsuda, T. (2003) Canine endothelial progenitor cell-lined hybrid vascular graft with nonthrombogenic potential. *J Thorac Cardiovasc Surg* 126, 455-64.

157. Kaushal, S., Amiel, G.E., Guleserian, K.J., Shapira, O.M., Perry, T., Sutherland, F.W., Rabkin, E., Moran, A.M., Schoen, F.J., Atala, A., Soker, S., Bischoff, J., Mayer, J.E., Jr. (2001) Functional small-diameter neovessels created using endothelial progenitor cells expanded ex vivo. *Nat Med* 7, 1035-40.

158. Shirota, T., He, H., Yasui, H., Matsuda, T. (2003) Human endothelial progenitor cell-seeded hybrid graft: proliferative and antithrombogenic potentials in vitro and fabrication processing. *Tissue Eng* 9, 127-36.

159. Shirota, T., Yasui, H., Shimokawa, H., Matsuda, T. (2003) Fabrication of endothelial progenitor cell (EPC)-seeded intravascular stent devices and in vitro endothelialization on hybrid vascular tissue. *Biomaterials* 24, 2295-302.

160. Shirota, T., Yasui, H., Matsuda, T. (2003) Intralumenal tissue-engineered therapeutic stent using endothelial progenitor cell-inoculated hybrid tissue and in vitro performance. *Tissue Eng* 9, 473-85.

161. Stegemann, J.P., Nerem, R.M. (2003) Altered response of vascular smooth muscle cells to exogenous biochemical stimulation in two- and three-dimensional culture. *Exp Cell Res* 283, 146-55.

162. Campbell, J.H., Campbell, G.R. (1993) Culture techniques and their applications to studies of vascular smooth muscle. *Clin Sci (Lond)* 85, 501-13.

163. McMurray, H.F., Parrott, D.P., Bowyer, D.E. (1991) A standardised method of culturing aortic explants, suitable for the study of factors affecting the phenotypic modulation, migration and proliferation of aortic smooth muscle cells. *Atherosclerosis* 86, 227-37.

164.   Berglund, J.D., Nerem, R.M., Sambanis, A. (2004) Incorporation of intact elastin scaffolds in tissue-engineered collagen-based vascular grafts. *Tissue Eng* 10, 1526-35.

165.   Freshley, R.I. (2000) *Culture of Animal Cells: A Manual of Basic Technique*. John Wiley & Sons, Inc., New York, NY.

166.   Byers, B.A., Garcia, A.J. (2004) Exogenous Runx2 expression enhances in vitro osteoblastic differentiation and mineralization in primary bone marrow stromal cells. *Tissue Eng* 10, 1623-32.

167.   Byers, B.A., Pavlath, G.K., Murphy, T.J., Karsenty, G., Garcia, A.J. (2002) Cell-type-dependent up-regulation of in vitro mineralization after overexpression of the osteoblast-specific transcription factor Runx2/Cbfal. *J Bone Miner Res* 17, 1931-44.

168.   IngenuitySystems (2006) Ingenuity Pathways Analysis www.ingenuity.com.

169.   Hanson, S.R., Kotze, H.F., Savage, B., Harker, L.A. (1985) Platelet interactions with Dacron vascular grafts. A model of acute thrombosis in baboons. *Arteriosclerosis* 5, 595-603.

170.   Cadroy, Y., Hanson, S.R. (1990) Effects of red blood cell concentration on hemostasis and thrombus formation in a primate model. *Blood* 75, 2185-93.

171.   Cadroy, Y., Horbett, T.A., Hanson, S.R. (1989) Discrimination between platelet-mediated and coagulation-mediated mechanisms in a model of complex thrombus formation in vivo. *J Lab Clin Med* 113, 436-48.

172.   Schneider, P.A., Kotze, H.F., Heyns, A.D., Hanson, S.R. (1989) Thromboembolic potential of synthetic vascular grafts in baboons. *J Vasc Surg* 10, 75-82.

173.   Torem, S., Schneider, P.A., Hanson, S.R. (1988) Monoclonal antibody-induced inhibition of platelet function: effects on hemostasis and vascular graft thrombosis in baboons. *J Vasc Surg* 7, 172-80.

174.   Jarmolych, J., Daoud, A.S., Landau, J., Fritz, K.E., McElvene, E. (1968) Aortic media explants. Cell proliferation and production of mucopolysaccharides, collagen, and elastic tissue. *Exp Mol Pathol* 9, 171-88.

175.   Campbell, G.R., Uehara, Y., Mark, G., Burnstock, G. (1971) Fine structure of smooth muscle cells grown in tissue culture. *J Cell Biol* 49, 21-34.

176.   Campbell, G.R., Campbell, J.H. (1995) Development of the vessel wall: overview. In *The vascular smooth muscle cell: molecular and biological responses to the extracellular matrix* (S. M. Schwartz and R. P. Mecham, eds), Academic Press, Inc., San Diego, CA 1-15.

177. Groschel-Stewart, U., Chamley, J.H., Campbell, G.R., Burnstock, G. (1975) Changes in myosin distribution in dedifferentiating and redifferentiating smooth muscle cells in tissue culture. *Cell Tissue Res* 165, 13-22.

178. Voyta, J.C., Via, D.P., Butterfield, C.E., Zetter, B.R. (1984) Identification and isolation of endothelial cells based on their increased uptake of acetylated-low density lipoprotein. *J Cell Biol* 99, 2034-40.

179. Kojima, H., Nakatsubo, N., Kikuchi, K., Kawahara, S., Kirino, Y., Nagoshi, H., Hirata, Y., Nagano, T. (1998) Detection and imaging of nitric oxide with novel fluorescent indicators: diaminofluoresceins. *Anal Chem* 70, 2446-53.

180. Nakatsubo, N., Kojima, H., Kikuchi, K., Nagoshi, H., Hirata, Y., Maeda, D., Imai, Y., Irimura, T., Nagano, T. (1998) Direct evidence of nitric oxide production from bovine aortic endothelial cells using new fluorescence indicators: diaminofluoresceins. *FEBS Lett* 427, 263-6.

181. Qiu, W., Kass, D.A., Hu, Q., Ziegelstein, R.C. (2001) Determinants of shear stress-stimulated endothelial nitric oxide production assessed in real-time by 4,5-diaminofluorescein fluorescence. *Biochem Biophys Res Commun* 286, 328-35.

182. Libby, P., Theroux, P. (2005) Pathophysiology of coronary artery disease. *Circulation* 111, 3481-8.

183. Blokhina, O., Virolainen, E., Fagerstedt, K.V. (2003) Antioxidants, oxidative damage and oxygen deprivation stress: a review. *Ann Bot (Lond)* 91 Spec No, 179-94.

184. Stocker, R., Keaney, J.F., Jr. (2004) Role of oxidative modifications in atherosclerosis. *Physiol Rev* 84, 1381-478.

185. Brooks, A.R., Lelkes, P.I., Rubanyi, G.M. (2002) Gene expression profiling of human aortic endothelial cells exposed to disturbed flow and steady laminar flow. *Physiol Genomics* 9, 27-41.

186. Chen, B.P., Li, Y.S., Zhao, Y., Chen, K.D., Li, S., Lao, J., Yuan, S., Shyy, J.Y., Chien, S. (2001) DNA microarray analysis of gene expression in endothelial cells in response to 24-h shear stress. *Physiol Genomics* 7, 55-63.

187. Chiu, J.J., Lee, P.L., Chang, S.F., Chen, L.J., Lee, C.I., Lin, K.M., Usami, S., Chien, S. (2005) Shear stress regulates gene expression in vascular endothelial cells in response to tumor necrosis factor-alpha: a study of the transcription profile with complementary DNA microarray. *J Biomed Sci* 12, 481-502.

188. Dai, G., Kaazempur-Mofrad, M.R., Natarajan, S., Zhang, Y., Vaughn, S., Blackman, B.R., Kamm, R.D., Garcia-Cardena, G., Gimbrone, M.A., Jr. (2004) Distinct endothelial phenotypes evoked by arterial waveforms derived from

atherosclerosis-susceptible and -resistant regions of human vasculature. *Proc Natl Acad Sci U S A* 101, 14871-6.

189. Dekker, R.J., van Soest, S., Fontijn, R.D., Salamanca, S., de Groot, P.G., VanBavel, E., Pannekoek, H., Horrevoets, A.J. (2002) Prolonged fluid shear stress induces a distinct set of endothelial cell genes, most specifically lung Kruppel-like factor (KLF2). *Blood* 100, 1689-98.

190. McCormick, S.M., Eskin, S.G., McIntire, L.V., Teng, C.L., Lu, C.M., Russell, C.G., Chittur, K.K. (2001) DNA microarray reveals changes in gene expression of shear stressed human umbilical vein endothelial cells. *Proc Natl Acad Sci U S A* 98, 8955-60.

191. Ohura, N., Yamamoto, K., Ichioka, S., Sokabe, T., Nakatsuka, H., Baba, A., Shibata, M., Nakatsuka, T., Harii, K., Wada, Y., Kohro, T., Kodama, T., Ando, J. (2003) Global analysis of shear stress-responsive genes in vascular endothelial cells. *J Atheroscler Thromb* 10, 304-13.

192. Peters, D.G., Zhang, X.C., Benos, P.V., Heidrich-O'Hare, E., Ferrell, R.E. (2002) Genomic analysis of immediate/early response to shear stress in human coronary artery endothelial cells. *Physiol Genomics* 12, 25-33.

193. Warabi, E., Wada, Y., Kajiwara, H., Kobayashi, M., Koshiba, N., Hisada, T., Shibata, M., Ando, J., Tsuchiya, M., Kodama, T., Noguchi, N. (2004) Effect on endothelial cell gene expression of shear stress, oxygen concentration, and low-density lipoprotein as studied by a novel flow cell culture system. *Free Radic Biol Med* 37, 682-94.

194. Wasserman, S.M., Mehraban, F., Komuves, L.G., Yang, R.B., Tomlinson, J.E., Zhang, Y., Spriggs, F., Topper, J.N. (2002) Gene expression profile of human endothelial cells exposed to sustained fluid shear stress. *Physiol Genomics* 12, 13-23.

195. Zhao, Y., Chen, B.P., Miao, H., Yuan, S., Li, Y.S., Hu, Y., Rocke, D.M., Chien, S. (2002) Improved significance test for DNA microarray data: temporal effects of shear stress on endothelial genes. *Physiol Genomics* 12, 1-11.

196. Chi, J.T., Chang, H.Y., Haraldsen, G., Jahnsen, F.L., Troyanskaya, O.G., Chang, D.S., Wang, Z., Rockson, S.G., van de Rijn, M., Botstein, D., Brown, P.O. (2003) Endothelial cell diversity revealed by global expression profiling. *Proc Natl Acad Sci U S A* 100, 10623-8.

197. Magness, C.L., Fellin, P.C., Thomas, M.J., Korth, M.J., Agy, M.B., Proll, S.C., Fitzgibbon, M., Scherer, C.A., Miner, D.G., Katze, M.G., Iadonato, S.P. (2005) Analysis of the Macaca mulatta transcriptome and the sequence divergence between Macaca and human. *Genome Biol* 6, R60.

198. Gomes, I., Sharma, T.T., Mahmud, N., Kapp, J.D., Edassery, S., Fulton, N., Liang, J., Hoffman, R., Westbrook, C.A. (2001) Highly abundant genes in the transcriptosome of human and baboon CD34 antigen-positive bone marrow cells. *Blood* 98, 93-9.

199. Giddens, D.P., Zarins, C.K., Glagov, S. (1993) The role of fluid mechanics in the localization and detection of atherosclerosis. *J Biomech Eng* 115, 588-94.

200. Stocker, R., Keaney, J.F., Jr. (2005) New insights on oxidative stress in the artery wall. *J Thromb Haemost* 3, 1825-34.

201. Wasserman, S.M., Topper, J.N. (2004) Adaptation of the endothelium to fluid flow: in vitro analyses of gene expression and in vivo implications. *Vasc Med* 9, 35-45.

202. Brooks, A.R., Lelkes, P.I., Rubanyi, G.M. (2004) Gene expression profiling of vascular endothelial cells exposed to fluid mechanical forces: relevance for focal susceptibility to atherosclerosis. *Endothelium* 11, 45-57.

203. Ivanova, N.B., Dimos, J.T., Schaniel, C., Hackney, J.A., Moore, K.A., Lemischka, I.R. (2002) A stem cell molecular signature. *Science* 298, 601-4.

204. Ramalho-Santos, M., Yoon, S., Matsuzaki, Y., Mulligan, R.C., Melton, D.A. (2002) "Stemness": transcriptional profiling of embryonic and adult stem cells. *Science* 298, 597-600.

205. Rossig, L., Urbich, C., Dimmeler, S. (2004) Endothelial progenitor cells at work: not mature yet, but already stress-resistant. *Arterioscler Thromb Vasc Biol* 24, 1977-9.

206. Haendeler, J., Dimmeler, S. (2006) Inseparably tied: functional and antioxidative capacity of endothelial progenitor cells. *Circ Res* 98, 157-8.

207. Dernbach, E., Urbich, C., Brandes, R.P., Hofmann, W.K., Zeiher, A.M., Dimmeler, S. (2004) Antioxidative stress-associated genes in circulating progenitor cells: evidence for enhanced resistance against oxidative stress. *Blood* 104, 3591-7.

208. Urbich, C., Aicher, A., Heeschen, C., Dernbach, E., Hofmann, W.K., Zeiher, A.M., Dimmeler, S. (2005) Soluble factors released by endothelial progenitor cells promote migration of endothelial cells and cardiac resident progenitor cells. *J Mol Cell Cardiol* 39, 733-42.

209. Urbich, C., Heeschen, C., Aicher, A., Sasaki, K., Bruhl, T., Farhadi, M.R., Vajkoczy, P., Hofmann, W.K., Peters, C., Pennacchio, L.A., Abolmaali, N.D., Chavakis, E., Reinheckel, T., Zeiher, A.M., Dimmeler, S. (2005) Cathepsin L is required for endothelial progenitor cell-induced neovascularization. *Nat Med* 11, 206-13.

210. Chiu, J.J., Chen, L.J., Chen, C.N., Lee, P.L., Lee, C.I. (2004) A model for studying the effect of shear stress on interactions between vascular endothelial cells and smooth muscle cells. *J Biomech* 37, 531-9.

211. Chiu, J.J., Chen, L.J., Lee, P.L., Lee, C.I., Lo, L.W., Usami, S., Chien, S. (2003) Shear stress inhibits adhesion molecule expression in vascular endothelial cells induced by coculture with smooth muscle cells. *Blood* 101, 2667-74.

212. Rainger, G.E., Stone, P., Morland, C.M., Nash, G.B. (2001) A novel system for investigating the ability of smooth muscle cells and fibroblasts to regulate adhesion of flowing leukocytes to endothelial cells. *J Immunol Methods* 255, 73-82.

213. Fillinger, M.F., Sampson, L.N., Cronenwett, J.L., Powell, R.J., Wagner, R.J. (1997) Coculture of endothelial cells and smooth muscle cells in bilayer and conditioned media models. *J Surg Res* 67, 169-78.

214. Nackman, G.B., Bech, F.R., Fillinger, M.F., Wagner, R.J., Cronenwett, J.L. (1996) Endothelial cells modulate smooth muscle cell morphology by inhibition of transforming growth factor-beta 1 activation. *Surgery* 120, 418-25; discussion 425-6.

215. van Buul-Wortelboer, M.F., Brinkman, H.J., Dingemans, K.P., de Groot, P.G., van Aken, W.G., van Mourik, J.A. (1986) Reconstitution of the vascular wall in vitro. *Exp Cell Res* 162, 151-8.

216. Ziegler, T., Alexander, R.W., Nerem, R.M. (1995) An endothelial cell-smooth muscle cell co-culture model for use in the investigation of flow effects on vascular biology. *Ann Biomed Eng* 23, 216-25.

217. Davies, P.F., Truskey, G.A., Warren, H.B., O'Connor, S.E., Eisenhaure, B.H. (1985) Metabolic cooperation between vascular endothelial cells and smooth muscle cells in co-culture: changes in low density lipoprotein metabolism. *J Cell Biol* 101, 871-9.

218. Korff, T., Kimmina, S., Martiny-Baron, G., Augustin, H.G. (2001) Blood vessel maturation in a 3-dimensional spheroidal coculture model: direct contact with smooth muscle cells regulates endothelial cell quiescence and abrogates VEGF responsiveness. *Faseb J* 15, 447-57.

219. Zhang, J.C., Ruan, Q., Paucz, L., Fabry, A., Binder, B.R., Wojta, J. (1999) Stimulation of tissue factor expression in human microvascular and macrovascular endothelial cells by cultured vascular smooth muscle cells in vitro. *J Vasc Res* 36, 126-32.

220. Lavender, M.D., Pang, Z., Wallace, C.S., Niklason, L.E., Truskey, G.A. (2005) A system for the direct co-culture of endothelium on smooth muscle cells. *Biomaterials* 26, 4642-53.

221. Wada, Y., Sugiyama, A., Kohro, T., Kobayashi, M., Takeya, M., Naito, M., Kodama, T. (2000) In vitro model of atherosclerosis using coculture of arterial wall cells and macrophage. *Yonsei Med J* 41, 740-55.

222. Niwa, K., Kado, T., Sakai, J., Karino, T. (2004) The effects of a shear flow on the uptake of LDL and acetylated LDL by an EC monoculture and an EC-SMC coculture. *Ann Biomed Eng* 32, 537-43.

223. Davies, P.F., Barbee, K.A., Volin, M.V., Robotewskyj, A., Chen, J., Joseph, L., Griem, M.L., Wernick, M.N., Jacobs, E., Polacek, D.C., dePaola, N., Barakat, A.I. (1997) Spatial relationships in early signaling events of flow-mediated endothelial mechanotransduction. *Annu Rev Physiol* 59, 527-49.

224. Colman, R.W., Hirsh, J., Marder, V.J., Clowes, A.W., George, J.N. (2001) *Hemostasis and thrombosis : basic principles and clinical practice*. Lippincott Williams & Wilkins, Philadelphia.

225. Esmon, C.T. (2001) Protein C, Protein S, and Thrombomodulin. In *Hemostasis and thrombosis : basic principles and clinical practice* (R. W. Colman, J. Hirsh, V. J. Marder, A. W. Clowes and J. N. George, eds), Lippincott Williams & Wilkins, Philadelphia 1577.

226. Kato, H. (2002) Regulation of functions of vascular wall cells by tissue factor pathway inhibitor: basic and clinical aspects. *Arterioscler Thromb Vasc Biol* 22, 539-48.

227. Morrissey, J.H. (2001) Tissue factor and factor VII initiation of coagulation. In *Hemostasis and thrombosis : basic principles and clinical practice* (R. W. Colman, J. Hirsh, V. J. Marder, A. W. Clowes and J. N. George, eds), Lippincott Williams & Wilkins, Philadelphia 1577.

228. Montgomery, R.R. (2001) Structure and function of von willebrand factor. In *Hemostasis and thrombosis : basic principles and clinical practice* (R. W. Colman, J. Hirsh, V. J. Marder, A. W. Clowes and J. N. George, eds), Lippincott Williams & Wilkins, Philadelphia 1577.

229. Wagner, D.D., Fay, P.J., Sporn, L.A., Sinha, S., Lawrence, S.O., Marder, V.J. (1987) Divergent fates of von Willebrand factor and its propolypeptide (von Willebrand antigen II) after secretion from endothelial cells. *Proc Natl Acad Sci U S A* 84, 1955-9.

230. Imberti, B., Seliktar, D., Nerem, R.M., Remuzzi, A. (2002) The response of endothelial cells to fluid shear stress using a co-culture model of the arterial wall. *Endothelium* 9, 11-23.

231. Dewey, C.F., Jr. (1984) Effects of fluid flow on living vascular cells. *J Biomech Eng* 106, 31-5.

232. Hirokawa, K., Aoki, N. (1990) Up-Regulation of Thrombomodulin in Human Umbilical Vein Endothelial-Cells Invitro. *Journal of Biochemistry* 108, 839-845.

233. Hirokawa, K., Aoki, N. (1991) Up-Regulation of Thrombomodulin by Activation of Histamine H-1-Receptors in Human Umbilical-Vein Endothelial-Cells Invitro. *Biochemical Journal* 276, 739-743.

234. Ohdama, S., Takano, S., Ohashi, K., Miyake, S., Aoki, N. (1991) Pentoxifylline Prevents Tumor Necrosis Factor-Induced Suppression of Endothelial-Cell Surface Thrombomodulin. *Thrombosis Research* 62, 745-755.

235. Weilerguettler, H., Yu, K., Soff, G., Gudas, L.J., Rosenberg, R.D. (1992) Thrombomodulin Gene-Regulation by Camp and Retinoic Acid in F9-Embryonal Carcinoma-Cells. *Proceedings of the National Academy of Sciences of the United States of America* 89, 2155-2159.

236. Moore, K.L., Andreoli, S.P., Esmon, N.L., Esmon, C.T., Bang, N.U. (1987) Endotoxin Enhances Tissue Factor and Suppresses Thrombomodulin Expression of Human Vascular Endothelium Invitro. *Journal of Clinical Investigation* 79, 124-130.

237. Nawroth, P.P., Handley, D.A., Esmon, C.T., Stern, D.M. (1986) Interleukin-1 Induces Endothelial-Cell Procoagulant While Suppressing Cell-Surface Anticoagulant Activity. *Proceedings of the National Academy of Sciences of the United States of America* 83, 3460-3464.

238. Nawroth, P.P., Stern, D.M. (1986) Modulation of Endothelial-Cell Hemostatic Properties by Tumor-Necrosis-Factor. *Journal of Experimental Medicine* 163, 740-745.

239. Edelberg, J.M., Christie, P.D., Rosenberg, R.D. (2001) Regulation of vascular bed-specific prothrombotic potential. *Circ Res* 89, 117-24.

240. Suzuki, K., Nishioka, J., Hayashi, T., Kosaka, Y. (1988) Functionally Active Thrombomodulin Is Present in Human-Platelets. *Journal of Biochemistry* 104, 628-632.

241. Soff, G.A., Jackman, R.W., Rosenberg, R.D. (1991) Expression of Thrombomodulin by Smooth-Muscle Cells in Culture - Different Effects of Tumor-Necrosis-Factor and Cyclic Adenosine-Monophosphate on Thrombomodulin Expression by Endothelial-Cells and Smooth-Muscle Cells in Culture. *Blood* 77, 515-518.

242. McCachren, S.S., Diggs, J., Weinberg, J.B., Dittman, W.A. (1991) Thrombomodulin Expression by Human Blood Monocytes and by Human Synovial Tissue Lining Macrophages. *Blood* 78, 3128-3132.

243. Satta, N., Freyssinet, J.M., Toti, F. (1997) The significance of human monocyte thrombomodulin during membrane vesiculation and after stimulation by lipopolysaccharide. *British Journal of Haematology* 96, 534-542.

244. Healy, A.M., Rayburn, H.B., Rosenberg, R.D., Weiler, H. (1995) Absence of the Blood-Clotting Regulator Thrombomodulin Causes Embryonic Lethality in Mice before Development of a Functional Cardiovascular-System. *Proceedings of the National Academy of Sciences of the United States of America* 92, 850-854.

245. Weiler-Guettler, H., Aird, W.C., Rayburn, H., Husain, M., Rosenberg, R.D. (1996) Developmentally regulated gene expression of thrombomodulin in postimplantation mouse embryos. *Development* 122, 2271-81.

246. Bagley, R.G., Walter-Yohrling, J., Cao, X., Weber, W., Simons, B., Cook, B.P., Chartrand, S.D., Wang, C., Madden, S.L., Teicher, B.A. (2003) Endothelial precursor cells as a model of tumor endothelium: characterization and comparison with mature endothelial cells. *Cancer Res* 63, 5866-73.

247. Grabowski, E.F., Zuckerman, D.B., Nemerson, Y. (1993) The functional expression of tissue factor by fibroblasts and endothelial cells under flow conditions. *Blood* 81, 3265-70.

248. Aicher, A., Brenner, W., Zuhayra, M., Badorff, C., Massoudi, S., Assmus, B., Eckey, T., Henze, E., Zeiher, A.M., Dimmeler, S. (2003) Assessment of the tissue distribution of transplanted human endothelial progenitor cells by radioactive labeling. *Circulation* 107, 2134-9.

249. Ozuyaman, B., Ebner, P., Niesler, U., Ziemann, J., Kleinbongard, P., Jax, T., Godecke, A., Kelm, M., Kalka, C. (2005) Nitric oxide differentially regulates proliferation and mobilization of endothelial progenitor cells but not of hematopoietic stem cells. *Thromb Haemost* 94, 770-2.

250. Asahara, T., Takahashi, T., Masuda, H., Kalka, C., Chen, D., Iwaguro, H., Inai, Y., Silver, M., Isner, J.M. (1999) VEGF contributes to postnatal neovascularization by mobilizing bone marrow-derived endothelial progenitor cells. *Embo J* 18, 3964-72.

251. Takahashi, T., Kalka, C., Masuda, H., Chen, D., Silver, M., Kearney, M., Magner, M., Isner, J.M., Asahara, T. (1999) Ischemia- and cytokine-induced mobilization of bone marrow-derived endothelial progenitor cells for neovascularization. *Nat Med* 5, 434-8.

252. Ii, M., Nishimura, H., Iwakura, A., Wecker, A., Eaton, E., Asahara, T., Losordo, D.W. (2005) Endothelial progenitor cells are rapidly recruited to myocardium and mediate protective effect of ischemic preconditioning via "imported" nitric oxide synthase activity. *Circulation* 111, 1114-20.

253. Boo, Y.C., Jo, H. (2003) Flow-dependent regulation of endothelial nitric oxide synthase: role of protein kinases. *Am J Physiol Cell Physiol* 285, C499-508.

254. Chiu, J.J., Chen, L.J., Chang, S.F., Lee, P.L., Lee, C.I., Tsai, M.C., Lee, D.Y., Hsieh, H.P., Usami, S., Chien, S. (2005) Shear stress inhibits smooth muscle cell-induced inflammatory gene expression in endothelial cells: role of NF-kappaB. *Arterioscler Thromb Vasc Biol* 25, 963-9.

255. de Frutos, T., de Miguel, L.S., Garcia-Duran, M., Gonzalez-Fernandez, F., Rodriguez-Feo, J.A., Monton, M., Guerra, J., Farre, J., Casado, S., Lopez-Farre, A. (1999) NO from smooth muscle cells decreases NOS expression in endothelial cells: role of TNF-alpha. *Am J Physiol* 277, H1317-25.

256. Tsai, H.M. (2003) Shear stress and von Willebrand factor in health and disease. *Semin Thromb Hemost* 29, 479-88.

257. Galbusera, M., Zoja, C., Donadelli, R., Paris, S., Morigi, M., Benigni, A., Figliuzzi, M., Remuzzi, G., Remuzzi, A. (1997) Fluid shear stress modulates von Willebrand factor release from human vascular endothelium. *Blood* 90, 1558-64.

258. Matsumoto, Y., Kawai, Y., Watanabe, K., Sakai, K., Murata, M., Handa, M., Nakamura, S., Ikeda, Y. (1998) Fluid shear stress attenuates tumor necrosis factor-alpha-induced tissue factor expression in cultured human endothelial cells. *Blood* 91, 4164-72.

259. Grabowski, E.F., Lam, F.P. (1995) Endothelial cell function, including tissue factor expression, under flow conditions. *Thromb Haemost* 74, 123-8.

260. Houston, P., Dickson, M.C., Ludbrook, V., White, B., Schwachtgen, J.L., McVey, J.H., Mackman, N., Reese, J.M., Gorman, D.G., Campbell, C., Braddock, M. (1999) Fluid shear stress induction of the tissue factor promoter in vitro and in vivo is mediated by Egr-1. *Arterioscler Thromb Vasc Biol* 19, 281-9.

261. Lin, M.C., Almus-Jacobs, F., Chen, H.H., Parry, G.C., Mackman, N., Shyy, J.Y., Chien, S. (1997) Shear stress induction of the tissue factor gene. *J Clin Invest* 99, 737-44.

262. Silverman, M.D., Waters, C.R., Hayman, G.T., Wigboldus, J., Samet, M.M., Lelkes, P.I. (1999) Tissue factor activity is increased in human endothelial cells cultured under elevated static pressure. *Am J Physiol* 277, C233-42.

263. Silverman, M.D., Manolopoulos, V.G., Unsworth, B.R., Lelkes, P.I. (1996) Tissue factor expression is differentially modulated by cyclic mechanical strain in various human endothelial cells. *Blood Coagul Fibrinolysis* 7, 281-8.

264. Mackman, N. (1997) Regulation of the tissue factor gene. *Thromb Haemost* 78, 747-54.

265. Nemerson, Y. (1988) Tissue factor and hemostasis. *Blood* 71, 1-8.

266. Osterud, B. (1997) Tissue factor: a complex biological role. *Thromb Haemost* 78, 755-8.

267. Crossman, D.C., Carr, D.P., Tuddenham, E.G., Pearson, J.D., McVey, J.H. (1990) The regulation of tissue factor mRNA in human endothelial cells in response to endotoxin or phorbol ester. *J Biol Chem* 265, 9782-7.

268. Fisher, K.L., Gorman, C.M., Vehar, G.A., O'Brien, D.P., Lawn, R.M. (1987) Cloning and expression of human tissue factor cDNA. *Thromb Res* 48, 89-99.

269. Helenius, G., Heydarkhan-Hagvall, S., Siegbahn, A., Risberg, B. (2004) Expression of fibrinolytic and coagulation factors in cocultured human endothelial and smooth muscle cells. *Tissue Eng* 10, 353-60.

270. Dora, K.A. (2001) Cell-cell communication in the vessel wall. *Vasc Med* 6, 43-50.

271. Isakson, B.E., Duling, B.R. (2005) Heterocellular contact at the myoendothelial junction influences gap junction organization. *Circ Res* 97, 44-51.

272. Sandow, S.L., Hill, C.E. (2000) Incidence of myoendothelial gap junctions in the proximal and distal mesenteric arteries of the rat is suggestive of a role in endothelium-derived hyperpolarizing factor-mediated responses. *Circ Res* 86, 341-6.

273. Chaytor, A.T., Martin, P.E., Edwards, D.H., Griffith, T.M. (2001) Gap junctional communication underpins EDHF-type relaxations evoked by ACh in the rat hepatic artery. *Am J Physiol Heart Circ Physiol* 280, H2441-50.

274. Conte, M.S. (1998) The ideal small arterial substitute: a search for the Holy Grail? *Faseb J* 12, 43-5.

275. Cummings, C.L., Gawlitta, D., Nerem, R.M., Stegemann, J.P. (2004) Properties of engineered vascular constructs made from collagen, fibrin, and collagen-fibrin mixtures. *Biomaterials* 25, 3699-706.

276. Girton, T.S., Oegema, T.R., Grassl, E.D., Isenberg, B.C., Tranquillo, R.T. (2000) Mechanisms of stiffening and strengthening in media-equivalents fabricated using glycation. *J Biomech Eng* 122, 216-23.

277. Gosline, J. (1977) The physical properties of elastic tissue. In *International review of connective tissue research*, Volume 7 (D. Hall, ed) Academic Press, New York 211-249.

278. MolecularProbes (2003) LIVE/DEAD viability/cytotoxicity kit for animal cells product information.

279. Schneider, P.A., Hanson, S.R., Price, T.M., Harker, L.A. (1988) Preformed confluent endothelial cell monolayers prevent early platelet deposition on vascular prostheses in baboons. *J Vasc Surg* 8, 229-35.

280. Schneider, P.A., Hanson, S.R., Price, T.M., Harker, L.A. (1990) Confluent durable endothelialization of endarterectomized baboon aorta by early attachment of cultured endothelial cells. *J Vasc Surg* 11, 365-72.

281. Seliktar, D., Nerem, R.M., Galis, Z.S. (2001) The role of matrix metalloproteinase-2 in the remodeling of cell-seeded vascular constructs subjected to cyclic strain. *Ann Biomed Eng* 29, 923-34.

282. Guerra, P.C. (2001) Effect of the cell and collagen source on tissue engineered vascular grafts. Chemical engineering masters thesis, Georgia Institute of Technology, Atlanta, GA.

283. Cohuet, G., Challande, P., Osborne-Pellegrin, M., Arribas, S.M., Dominiczak, A., Louis, H., Laurent, S., Lacolley, P. (2001) Mechanical strength of the isolated carotid artery in SHR. *Hypertension* 38, 1167-71.

284. Conklin, B.S., Richter, E.R., Kreutziger, K.L., Zhong, D.S., Chen, C. (2002) Development and evaluation of a novel decellularized vascular xenograft. *Med Eng Phys* 24, 173-83.

285. Clagett, G.P., Burkel, W.E., Sharefkin, J.B., Ford, J.W., Hufnagel, H., Vinter, D.W., Kahn, R.H., Graham, L.M., Stanley, J.C., Ramwell, P.W. (1984) Platelet reactivity in vivo in dogs with arterial prostheses seeded with endothelial cells. *Circulation* 69, 632-9.

286. Graham, L.M., Burkel, W.E., Ford, J.W., Vinter, D.W., Kahn, R.H., Stanley, J.C. (1982) Expanded polytetrafluoroethylene vascular prostheses seeded with enzymatically derived and cultured canine endothelial cells. *Surgery* 91, 550-9.

287. Meinhart, J., Deutsch, M., Zilla, P. (1997) Eight years of clinical endothelial cell transplantation. Closing the gap between prosthetic grafts and vein grafts. *Asaio J* 43, M515-21.

288. Hampton, J.W., Matthews, C. (1966) Similarities between baboon and human blood clotting. *J Appl Physiol* 21, 1713-6.

289. Todd, M.E., McDevitt, E., Goldsmith, E.I. (1972) Blood-clotting mechanisms of nonhuman primates. Choice of the baboon model to simulate man. *J Med Primatol* 1, 132-41.

290. Hanson, S.R., Harker, L.A. (1987) Baboon models of acute arterial thrombosis. *Thromb Haemost* 58, 801-5.

291.   Hanson, S.R., Harker, L.A. (1987) Vascular graft thrombus formation. *Ann N Y Acad Sci* 516, 653-61.

292.   George, J.N. (2001) Platelet Kinetics and Pathophysiology of Thrombocytopenia. In *Hemostasis and thrombosis : basic principles and clinical practice* (R. W. Colman, J. Hirsh, V. J. Marder, A. W. Clowes and J. N. George, eds), Lippincott Williams & Wilkins, Philadelphia 447-460.

293.   Fareed, J., Hoppensteadt, D.A., Leya, F., Iqbal, O., Wolf, H., Bick, R. (1998) Useful laboratory tests for studying thrombogenesis in acute cardiac syndromes. *Clin Chem* 44, 1845-53.

294.   Yamamoto, K., Sokabe, T., Watabe, T., Miyazono, K., Yamashita, J.K., Obi, S., Ohura, N., Matsushita, A., Kamiya, A., Ando, J. (2005) Fluid shear stress induces differentiation of Flk-1-positive embryonic stem cells into vascular endothelial cells in vitro. *Am J Physiol Heart Circ Physiol* 288, H1915-24.

295.   Huang, H., Nakayama, Y., Qin, K., Yamamoto, K., Ando, J., Yamashita, J., Itoh, H., Kanda, K., Yaku, H., Okamoto, Y., Nemoto, Y. (2005) Differentiation from embryonic stem cells to vascular wall cells under in vitro pulsatile flow loading. *J Artif Organs* 8, 110-8.

296.   Dora, K.A. (2001) Cell-cell communication in the vessel wall. *Vasc Med* 6, 43-50.

297.   Dzau, V.J., Gnecchi, M., Pachori, A.S., Morello, F., Melo, L.G. (2005) Therapeutic potential of endothelial progenitor cells in cardiovascular diseases. *Hypertension* 46, 7-18.

298.   Awad, O., Dedkov, E., Jiao, C., Bloomer, S., Tomanek, R.J., Schatteman, G.C. (2006) Differential Healing Activities of CD34+ and CD14+ Endothelial Cell Progenitors. *Arterioscler Thromb Vasc Biol*.

299.   Friedrich, E.B., Walenta, K., Scharlau, J., Nickenig, G., Werner, N. (2006) CD34-/CD133+/VEGFR-2+ endothelial progenitor cell subpopulation with potent vasoregenerative capacities. *Circ Res* 98, e20-5.

300.   Murohara, T., Ikeda, H., Duan, J., Shintani, S., Sasaki, K., Eguchi, H., Onitsuka, I., Matsui, K., Imaizumi, T. (2000) Transplanted cord blood-derived endothelial precursor cells augment postnatal neovascularization. *J Clin Invest* 105, 1527-36.

301.   Soker, S. (2006) Personal Communication with Dr. Soker. Wake Forest Institute for Regenerative Medicine, Winston-Salem, NC.

302.   Aoki, J., Serruys, P.W., van Beusekom, H., Ong, A.T., McFadden, E.P., Sianos, G., van der Giessen, W.J., Regar, E., de Feyter, P.J., Davis, H.R., Rowland, S., Kutryk, M.J. (2005) Endothelial progenitor cell capture by stents coated with antibody against CD34: the HEALING-FIM (Healthy Endothelial Accelerated

Lining Inhibits Neointimal Growth-First In Man) Registry. *J Am Coll Cardiol* 45, 1574-9.

303.   Rotmans, J.I., Heyligers, J.M., Verhagen, H.J., Velema, E., Nagtegaal, M.M., de Kleijn, D.P., de Groot, F.G., Stroes, E.S., Pasterkamp, G. (2005) In vivo cell seeding with anti-CD34 antibodies successfully accelerates endothelialization but stimulates intimal hyperplasia in porcine arteriovenous expanded polytetrafluoroethylene grafts. *Circulation* 112, 12-8.